IN VITRO AND *IN VIVO* STUDIES OF PROATHEROGENIC EFFECTS INDUCED BY END-PRODUCTS OF CHOLESTERYL ESTERS OXIDATION

NEUZA LUISA DA SILVA DOMINGUES

Tese para obtenção do grau de Doutor em Envelhecimento e Doenças Crónicas

Doutoramento em associação entre:
Universidade NOVA de Lisboa (Faculdade de Ciências Médicas - NMS|FCM/UNL)
Universidade de Coimbra (Faculdade de Medicina - FM/UC)
Universidade do Minho (Escola de Medicina - EMed/UM)

dezembro, 2017

IN VITRO AND *IN VIVO* STUDIES OF PROATHEROGENIC EFFECTS INDUCED BY END-PRODUCTS OF CHOLESTERYL ESTERS OXIDATION

Neuza Luisa da Silva Domingues
Otília Vieira, Investigadora Principal e Prof. auxiliar contratada, NMS-FCM
Margarida Saraiva, Investigadora Principal, I3S - Universidade do Porto
Gil Castro, Prof. Associado, Escola de Medicina - Universidade do Minho

---

Tese para obtenção do grau de Doutor em Envelhecimento e Doenças Crónicas

Doutoramento em associação entre:
Universidade NOVA de Lisboa (Faculdade de Ciências Médicas - NMS|FCM/UNL)
Universidade de Coimbra (Faculdade de Medicina - FM/UC)
Universidade do Minho (Escola de Medicina - EMed/UM)

dezembro, 2017

This work was performed at the Center for Chronic Diseases (CEDOC), NOVA Medical School - Faculdade de Ciências Médicas. Its execution was supported by a PhD fellowship from the Portuguese Foundation for Science and Technology (SFRH/BD/52293/2013), attributed by the Doctoral Programme in Ageing and Chronic Diseases (PhDOC).

Este trabalho foi realizado no Centro de Doenças Crónicas (CEDOC) da NOVA Medical School - Faculdade de Ciências Médicas, ao abrigo de uma bolsa de Doutoramento, financiada pela Fundação para a Ciência e a Tecnologia (SFRH/BD/52293/2013) e atribuída pelo Programa Doutoral em Envelhecimento e Doenças Crónicas (PhDOC).

INTER-UNIVERSITY DOCTORAL PROGRAMME IN
AGEING AND CHRONIC DISEASE

FCT
Fundação para a Ciência e a Tecnologia
MINISTÉRIO DA CIÊNCIA, TECNOLOGIA E ENSINO SUPERIOR

CEDOC
CHRONIC DISEASES | NOVA MEDICAL SCHOOL

AGRADECIMENTOS

À Doutora Otília Vieira, minha orientadora, deixo um especial agradecimento por me ter recebido no grupo e ter apoiado e incentivado a minha candidatura ao PhD. Fico imensamente grata pela sapiente orientação ao longo destes anos de aprendizagem e no derradeiro último esforço envolvido na elaboração do presente manuscrito. Agradeço ainda todo demais apoio e a confiança depositada no meu trabalho intelectual e experimental. Por fim, espero que a nossa interacção extremamente dinâmica tenha contribuído para a evolução de ambas, a nível pessoal e profissional.

Ao Professor Doutor Winchil Vaz pelas discussões químicas, moleculares e analíticas que muito contribuíram para o meu enriquecimento científico.

À Professora Doutora Margarida Castro por todo o apoio incondicional desde a minha iniciação como Bioquímica e incentivo durante toda a minha progressão académica. Para além de me ter iniciado nesta vida científica, tornou-se um pilar importantíssimo de apoio durante o doutoramento.

À Doutora Margarida Saraiva por todo o inquestionável apoio e conhecimento científico que prontamente me transmitiu em cada oportunidade que tivemos de discussão do projecto, pelas produtivas sugestões científicas e pelo incansável apoio nesta última fase de escrita. Desde o primeiro dia, durante a rotação laboratorial no ICVS, que a Margarida me abriu as portas para qualquer tipo de colaboração e ajuda a nível experimental, merecendo um obrigada muito especial.

A todos os antigos colegas do grupo "Infection and Pathogens", no CNC: à Ângela Inácio, que foi um exemplo para mim de determinação e perspicácia para enfrentar as dificuldades no PhD; ao Luís Estronca pela transmissão de conhecimento técnico essencial para a iniciação do meu projecto.

Aos membros do meu grupo "Lysosomes in Chronical Human Pathologies and Infection Group": ao Mark Gibson, que me transmitiu todos seus conhecimentos técnicos de biologia molecular e esforçou-se na correcção desta dissertação; à Inês Santarino, que por toda a ajuda a nível técnico e pessoal, desde o meu primeiro ano em Bioquímica até agora; à Liliana Alves, o membro mais recente do grupo, mas também o mais carinhoso e paciente, tentando sempre aliviar o meu stress e fazendo com que o "botão se desligasse" nos momentos certos; à nossa ex-Pos-doc Marisa Encarnação, a ti não há como te agradecer, foste o meu pilar em Lisboa, ajudaste me durante na minha difícil adaptação ao ambiente da capital e a nível cientifico foste incrível. Agradeço-te Marisa por todas

as discussões científicas e pessoais que tivemos, por toda a sabedoria que me transmitiste e agora a mais de 300 Km de distância, foste incansável a ajudar me na tese. Acreditas em mim como futura cientista e isso nesta fase tão cansativa transmitiu muita força e confiança. Por isso, Obrigada!

Aos membros do grupo do "Membrane Traffic in Infection and Disease": ao Duarte Barral, à Liliana Lopes, ao Hugo Moreiras e à Matilde, por todo o apoio técnico e boa disposição. À Cristiana Escrevente um agradecimento especial por todo o tempo disponibilizado e discussões técnicas que tivemos.

Ao grupo do António Jacinto que me iniciou nas experiências com "zebrafish", principalmente à Raquel Lourenço que se tornou a minha tutora nas experiências *in vivo*.

Ao Diogo Bitoque, sempre disponível a ajudar a nível técnico e pessoal. Por toda a motivação que me deste e por todas as nossas sessões de escrita naquela pequena sala que tanto me ajudaram a iniciar a escrita da tese.

A todos os colegas e amigos do CEDOC, com um especial agradecimento: ao José Vicente que tanto me ajudou a nível técnico nos últimos tempos e pela companhia em tantos serões naquele terceiro piso; ao Manuel Vicente, por todas as nossas discussões científicas e todo o apoio a nível analítico; à Ana Soares que esteve sempre pronta a ouvir e dar uma palavra positiva de apoio, assim como toda a ajuda técnica; à Catarina pela a amizade e força matinal.

Aos técnicos do CEDOC, Cláudia Andrade e Telmo Pereira, por tanta dedicação e profissionalismo.

À Doutora Helena Soares e à Sofia Almeida pelo apoio técnico e científico prestado.

À Joana Gaifem que foi incansável e muito profissional em todo o trabalho desenvolvido no ICVS.

Ao Paulo Oliveira e à Drª Vilma do grupo "MITOX" do UC-BIOTECH – CNC, por toda a ajuda na construção do meu "puzzle metabólico".

Aos membros da direcção do meu programa doutoral em envelhecimento e doenças crónicas – PhDOC por terem confiado em mim como aluna de doutoramento e à FCT por ter financiado a minha bolsa.

À minha família: à minha avó Virgínia e à Lúcia que tanto me ajudaram; aos meus avós pelo brilho no olhar a cada (infelizmente) rara visita minha; ao Cardoso e à Diana.

À Tilena que gentilmente me cedeu o seu ninho durante estes 3 anos em Lisboa e tanto carinho me deu nas suas visitas a Cascais.

À minha mãe por ter sido o meu exemplo de força e luta. Sozinha conseguiu proporcionar me condições à minha formação e com o seu apoio me ajudou a chegar aqui hoje. Sempre me ofereceu a liberdade necessária para fazer as minhas próprias escolhas, ajudando-me a crescer como pessoa.

Ao meu pai (o meu anjinho da guarda) que quero acreditar que lá de cima me apoia e me dá e deu toda a força necessária para ultrapassar todos os momentos difíceis causados principalmente pela distância nestes últimos anos.

À minha irmã, a minha eterna amiga, por todos os telefonemas, todas as palavras, todos os sorrisos, todos os abraços, toda a ajuda no design em inúmeras trabalhos que lhe pedi, etc. Agradeço-te do fundo do meu coração e desculpa toda a sobrecarga e exigência que te coloquei em cima dos ombros. Apesar de tudo, nunca desististe de mim e estiveste sempre aqui para mim. Obrigada Samanta!

Ao Hugo, pelo apoio incondicional nos bons e maus momentos, por todos os Km que tiveste que percorrer para me acompanhares, por toda a paciência, pela espera que nunca mais termina, pelo carinho e força, pelo companheirismo. Obrigada por não desistires. Agradeço do fundo do coração por sempre apoiares a minha ambição profissional e desculpa todos os problemas originados pela distância, que tão bem soubeste lidar. Muito obrigada por tudo!

“It is not enough to have a good mind;
the main thing is to use it well.“

Rene Descartes

TABLE OF CONTENTS

ABBREVIATIONS AND ACRONYMS

15-LOX	15-Lipoxygenases
4-HNE	4-hydroxynonenal
5'-TOP	5'-terminal oligopyrimidine
ABC	ATP-binding cassette transporter
ACAT	Acyl CoA:cholesterol acyltransferase
Acetyl CoA	Acetyl coenzyme A
Acsl	Acyl-CoA synthetase
AggLDL	Aggregated LDL
AL	Autophagosomes
ALX	Lipoxin A4 receptor
AMPK	AMP-activated protein kinase
AP	Adaptor protein
Apo	Apolipoproteins
ASC	Apoptosis-associated speck-like protein containing CARD
ASCVD	Atherosclerotic cardiovascular diseases
ATF1	Activating transcription factor 1
BMDM	Bone marrow derived macrophages
BRCC	BRCA (breast cancer)1-BRCA2–containing complex
CCL	Chemokine C-C motif ligand
CCR	C¬C chemokine receptor
CE	Cholesteryl esters
CETP	Cholesterol ester transfer protein
CGDs	Granulomatosus diseases
ChA	The most abundant cholesteryl hemiester identified in our study, which the name must be protected
ChE	Cholesteryl hemiesters
ChS	Cholesteryl hemisuccinate
CKD	Chronic kidney disease
ClC	Chloride channel
CMRs	Chylomicrons remnants
CMs	Chylomicrons
COX-2	Cyclooxygenase 2
CSF1R	Colony-stimulating factor 1 receptor
CVD	Cardiovascular diseases
CVDs	Cardiovascular diseases
CX3CL	C-X-C3 motif chemokine ligand
CX3CR	C-X-C3 motif chemokine receptor
DALYs	Disability-adjusted life years
DAMPs	Damage Associated Molecular Patters
DCs	Dendritic cells
Dpf	Days post fertilization
EC	Endothelial cells
ECAR	Extracellular acidification rate
ED_{50}	Effective dose

EE	Early endosomes
Eef1al1	Eukaryotic elongation factor 1 alpha like 1
EL	Endolysossomes
ER	Endoplasmic reticulum
ERC	Endocytic recycling compartment
F-2,6-BP	Fructose-2,6-bisphosphate
FA	Fatty acid
FABPs	Fatty acid–binding proteins
FACS	Fluorescence-activated cell sorting
FAO	Fatty acid oxidation
FC	Free Cholesterol
FPN	Ferroportin
FPR2	Formyl peptide receptor 2
GAS	Growth arrest-specific
GEF	Nucleotide exchange factor
GlycoPER	Glycolytic proton efflux rate
GRASP55	Golgi reassembly stacking protein 55
Gsr	Glutathione reductase
GTPase	Guanosine triphosphatases
HDL	High density lipoproteins
HIF-α	Hypoxia-inducible factor -1α
HL	Hepatic lipase
HLA-DR	Human leukocyte antigen DR
HMGCR	3-hydroxy-3-methylglutaryl coenzyme A reductase
Hmox-1	Heme oxygenase 1
HSCs	Hematopoietic stem cells
ICAM-1	Intercellular adhesion molecule 1
IFN-γ	Interferon-γ
IL	Interleukin
iNOS	Inducible nitric oxide synthase
Jmjd3	JmjC-domain protein 3
KLF	Kruppel-like factor
LacCer	Lactosylceramide
LAL	Lysosomal acid lipase
LAMP	Lysosome-associated membrane glycoproteins
LCAT	Lecithin cholesterol acyltransferase
LCCM	L929-cells conditioned medium
LDL	Low density lipoprotein
LDLr	LDL receptor
LE	Late endosomes
LIMP2	Lysosome integral membrane protein-2
LIPA	Lysosomal acid lipase A
LOX-1	Lectin-like oxLDL receptor-1
LPL	Lipoprotein lipase
Lp-PLA2	Lipoprotein-associated phospholipase A2
LPS	Lipopolysaccharide
LRP-1	LDL receptor-related protein 1
LSD	lysosomal storage disease
LUVs	Large Unilamelar Vesicles

LXR-β	Liver X receptor β
LYNUS	Lysosomal nutrient sensing machinery
Mac	Macrophages antigen
MAPK	Mitogen-activated protein kinase
MCP-1	Monocyte chemoattractant protein-1
M-CSF	Macrophage-colony stimulating factor
MDA	Malondialdehyde
MDM	Monocyte-derivated macrophages
MER-TK	c-Mer tyrosine kinase
MFG-E8	Milk fat globule-EGF factor 8
MFI	Median fluorescence intensity
MHC	Major histocompatibility complex
MitoOCR	Mitochondrial oxygen consumption rate
MMPs	Metalloproteinases
MMR	Macrophage mannose receptor
MPO	Myeloperoxidase
mTOR	Mechanistic target of rapamycin
mTORC1	mTOR complex 1
MTP	Microsomal triglyceride transfer protein - MTP
MYD88	Myeloid differentiation primary response protein 88
NADPH	Nicotinamide adenine dinucleotide phosphate
Nat-LDL	Native LDL
NETs	Neutrophil extracellular traps
NF-κB	Factor nuclear kappa B
NK	Natural killer cells
NKT	Natural killer T
NLRP3	NOD-like receptor family Pyrin domain containing 3
NLRs	NOD-like receptors
NO	Nitric oxide
NOXs	NADPH oxidases
NPC	Niemann-Pick C1-like protein
Nrf2	Nuclear factor erythroid 2-related factor 2
OCR	Oxygen consumption rate
OSTM1	Osteopetrosis-associated transmembrane protein 1
Ox-LDL	Oxidized low density lipoprotein
Ox-LDL	Oxidized low density lipoprotein
Ox-Lp	Oxidized lipid
OxPAPC	Oxidized 1-palmitoyl-2-arachidonyl-*sn*-3-glycero-phosphorylcholine
OXPHOS	Oxidative phosphorylation
PAMPs	Pathogen-associated molecular patterns
PC	Phosphocholine
PCSK9	Proprotein convertase subtilisin/kexin type 9
PFK-2/FB	6-phosphofructo-2-kinase/fructose-2,6-bisphosphatase
PFKFB	6 phosphofructo 2 kinase/fructose 2, 6 bisphosphatase
PGN	Polymeric peptidoglycan
PI(3)K	Phosphatidylinositol 3-kinase
PI(3,5)P_2	Phosphatidylinositol 3,5-bisphopsphate
PI3P	Phosphatidylinositol 3-phopsphate
PON	Paraoxonases

POPC	(1-palmitoyl-2-oleoyl-sn-glycero-3-phosphocholine)
PPAR	Peroxisome proliferator-activated receptor-γ
PPP	Phosphorylation pathway
Pro-IL-1β	IL-1β precursor
PRRs	Pattern Recognition Receptors
PS	Phosphatidilyserine (PS)
PUFA	Polyunsaturated fatty acids
Rab	Ras-related in brain
RBCs	Red blood cells
Rheb	Ras homolog enriched in brain
ROS	Reactive oxygen species
Rpl13a	Ribosomal protein L13a were
SKIP	SifA and kinesin-interacting protein
Slc27a	Fatty Acid transport protein
Slc3a2	Glutamine transporter
SMase	Sphingomyelinase
SMCs	Smooth muscle cells
SNAREs	Soluble NSF attachment receptor
SNX	Sorting nexin
sPLA2	Secretory phospholipase 2
SR-A1	Scavenger receptor A1
SREBP	Sterol regulatory element-binding proteins
Srxn1	Sulfiredoxin
Syk	Spleen tyrosine kinase
Syt VII	Synaptotagmin VII
TBA	Thiobarbituric acid
TBARS	Thiobarbituric acid reactive substances
TCA	Tricarboxylic acid
TFEB	Transcription factor EB
TG	Triglycerides
TGN	Trans-Golgi network
Th	T helper cells
TIM	T-cell immunoglobulin
TIP47	tail-interacting protein
TL1A	TNF-like protein 1A
TLR	Toll like receptor
TMEM9B	Transmembrane protein 9B
TNF-α	Tumor necrosis factor-α
Treg	regulatory T cells
TRPMLs	Transient receptor potential mucolipins
Txnrd1	Thioredoxin reductase 1
ULK1	Uncoordinated 51-like kinases 1
VAMP	Vesicle-associated membrane protein
VCAM-1	Vascular adhesion molecule 1
V-H$^+$ATPase	Vacuolar H^+-ATPase
vLDL	Very low-density lipoprotein
VPS	Vacuolar protein sorting
WT	Wild-type
XO	Xanthine oxidase

ABSTRACT

Atherosclerosis is a chronic inflammatory disease and the major worldwide cause of human death. It is initiated by the constitutive uptake of modified low density lipoproteins trapped in the arterial intima by monocyte-derived macrophages, leading to the formation of foam cells. The oxidation levels and the quantity of lipid loading in macrophages influence their inflammatory phenotype and function. With time, atherosclerotic macrophages become dysfunctional and a clear trigger for this process relies on lysosomal malfunction. Eventually this process leads to apoptotic cells and toxic lipid accumulation in arterial intima, culminating in the formation of an irreversible advanced atheroma. Thus, the establishment of a correlation between the composition of lipid species and the irreversibility/instability of atherosclerotic lesions can contribute to the development of powerful tools for the diagnosis and treatment of the cardiovascular disease burden. The main objective of this work was the study of cholesteryl hemiesters (ChE), an oxidized product of cholesteryl esters, as an atherogenic compound. Here, using the shotgun lipidomics technique, we showed that these lipids are increased in the plasma of cardiovascular disease patients. We subsequently evaluated the *in vitro* and *in vivo* atherogenic relevance of these oxidized lipids. Monocytes and macrophages exposed to ChE presented an unusual inflammatory profile, presenting both pro- and anti-inflammatory markers. ChE-loaded macrophages revealed endocytic trafficking delays and dysfunctional enlarged lysosomes. The sub cellular location of the observed enlarged stressed lysosomes was more peripheral than lysosomes from control macrophages. Furthermore, these lysosomes from ChE-loaded macrophages displayed an increase in their exocytic capacity. In addition, macrophages stimulated with ChE revealed a metabolic shift, which, as with the inflammatory response, was dependent on toll-like receptor 4 signaling. These foamy macrophages also presented an increased proliferative capacity as compared to the control macrophages. Finally, using zebrafish larvae, several of the *in vitro* atherogenic properties of ChE were confirmed *in vivo*, namely lipid accumulation, inflammation and macrophage lysosomal dysfunction. Altogether, the work presented here contributes to the identification of new etiologic compounds in human atherosclerotic lesions and advances our mechanistic understanding of the alterations observed in atherosclerotic macrophages.

RESUMO

A aterosclerose é uma doença inflamatória crónica e a principal causa de morte no mundo inteiro. Caracteriza-se pela internalização contínua de lipoproteínas de baixa densidade, que sofreram modificações por macrófagos derivados de monócitos, levando à formação de "células espumosas". O nível de oxidação lipídica e a quantidade de lípido internalizada pelos macrófagos influencia o seu fenótipo e a sua função inflamatória. Com o tempo, os macrófagos presentes na lesão tornam-se disfuncionais e um dos principais responsáveis por este processo é o mau funcionamento dos lisossomas. Eventualmente, esta disfunção lisossomal leva à formação de células apoptóticas e à acumulação de lípidos tóxicos na íntima arterial, culminando na formação de um ateroma de estado avançado e irreversível. Deste modo, o estabelecimento de uma correlação entre a composição das espécies lipídicas e a irreversibilidade/instabilidade da lesão pode contribuir para o desenvolvimento de ferramentas fundamentais no diagnóstico e tratamento de doenças cardiovasculares. O objetivo principal deste trabalho foi o estudo de hemiesteres de colesterol (ChE), produtos resultantes da oxidação de ésteres de colesterol, como compostos aterogénicos. Neste trabalho, através da utilização da técnica de lipidómica "shotgun", demonstramos que os ChE estão aumentados no plasma de pacientes com doenças cardiovasculares. De seguida, avaliamos a relevância aterogénica destes lípidos oxidados, através de estudos *in vitro* e *in vivo*. Monócitos e macrófagos expostos a ChE apresentaram um perfil inflamatório incomum, exibindo marcadores pró- e anti-inflamatórios. Os macrófagos carregados de ChE revelaram atrasos no tráfego endocítico e um aumento do tamanho dos seus lisossomas, assim como uma perda da sua função. Observou-se, também, uma alteração da localização dos lisossomas stressados nas células tratadas com ChE, verificando-se uma distribuição mais periférica, enquanto as células controlo apresentam uma distribuição mais homogénea dos lisossomas. Estes lisossomas de macrófagos carregados com ChE demonstraram um aumento adicional da sua capacidade exocítica. Além disso, os macrófagos estimulados com ChE revelaram uma alteração metabólica, que juntamente com a resposta inflamatória, foi dependente da sinalização através do receptor "toll like receptor-4". Os macrófagos "espumosos" apresentaram, ainda, um aumento da capacidade proliferativa em relação aos macrófagos controlo. Finalmente, usando larvas de peixe-zebra, várias propriedades aterogénicas dos ChE observadas *in vitro* foram confirmadas *in vivo*, nomeadamente, a acumulação de lípidos, a propriedade inflamatória e a disfunção lisossomal em macrófagos. Em suma, o trabalho aqui apresentado contribui para a identificação de novos compostos etiológicos nas lesões de aterosclerose humana e contribui para o avanço da nossa compreensão mecanística das alterações celulares nos macrófagos das lesões.

AUTHOR'S CONTRIBUTION

Contribution to the paper and chapters in this thesis are:

Chapter 3

Luís Estronca (former postdoc at Otília's lab) and João Silva, a master student, contributed for the technical performance of the Figure 3.1, Figure 3.2 A-G, Figure 3.3A-L, Figure 3.4B-F and Supplementary Figure 3.1. The work by this authors was executed at the Center for Neuroscience and Cell Biology (CNC), University of Coimbra. Marisa Encarnação (former postdoc at Otília's lab) contributed with technical support in Figure 3.2H.

Chapter 4

Human data was quantified and analyzed by Lipotype (Figure 4.1), a spin-off company in Dresden, and Prof. Dr. Winchil Vaz. Figure 4.2 and 4.3 were performed by Joana Gaifem from Life and Health Sciences Research Institute (ICVS), at University of Braga. Mark Gibson, a postdoc of Otília's lab, executed the experiments from Figure 4.4 and Figure 4.5 A-C. Clare Futter of University College London obtained the transmission electron microscopy images (Figure 4.6B).

Chapter 5

Images of transmission electron microscopy were obtained by Clare Futter of University College London (Figure 5.2). The software used to quantify the distribution of lysosomes in cytoplasm was developed by Telmo Pereira, a technician at CEDOC (Figure 5.4A-B). Figure 5.5B and F, Supplementary Figure 3.2B was performed by Inês Simões, a former member of our group. José Vicente, from Vasco Barreto's group from CEDOC, optimized Rab7a, Tfeb Arl8b primers and prepared the mRNA for qRT-PCR.

Chapter 6

José Vicente performed the technical work on mRNA extraction and cDNA synthesis from zebrafish for qRT-PCR.

01 INTRODUCTION

1.1 ATHEROSCLEROSIS

The word atherosclerosis derives from Greek: *skleros* meaning hardening of the arterial walls and *athere* meaning gruel, deposition of fatty substances, fibrous material, and immune cells to form plaques with gruel-like consistency. Atherosclerosis is a slowly progressive disease of the large and medium-sized arteries, characterized by the accumulation of lipids that may ultimately trigger myocardial infarction or stroke, the leading causes of death worldwide. The phenomenon beyond lipid accumulation is characterized by infiltration of leukocytes, proliferation of smooth muscle cells (SMCs), accumulation of connective tissue components and thrombus formation. Lipids are derived from low-density lipoproteins (LDL), the major carriers of lipids in the circulation, and when trapped in arterial walls are susceptible to oxidation. Then, LDL, or '*bad cholesterol*' in layman's terms, has a central role in plaque development. However, more recently, researchers have increasingly acknowledged about atherogenesis, putting inflammatory reactions as a pivotal step in the disease development (Gisterå & Hansson, 2017a; Göran K. Hansson, 2005a; Libby, Bornfeldt, & Tall, 2016).

Before becoming clinically evident, atherosclerotic development progresses silently for years until rupture or erosion of the plaque elicits thrombus formation that occludes the blood flow through the artery, interrupting the oxygen and nutrients supply to the tissues.

1.1.1 Incidence and risk factors

The burden of ischemic cardiovascular conditions is the main cause of morbidity, and mortality worldwide (Mozaffarian et al., 2015). According to published data by the Worth Health Organization, cardiovascular diseases (CVDs) take the lives of 17.7 million people every year, 31% of all global deaths. A Global Burden of Disease study in 2010, which measured disability-adjusted life years (DALYs), reveal that communicable diseases have receded, and chronic diseases, notably those caused by atherosclerosis and hypertension, have become dominant public health problems in developing countries (C. J. L. Murray et al., 2012). Atherosclerosis manifests early in life, and some studies have shown that maternal hypercholesterolemia during pregnancy is associated with a marked increase in the formation of fatty streaks in the human fetus (Palinski & Napoli, 1999). In most children, atherosclerotic vascular changes are minor and can be minimized or prevented with a healthy lifestyle (Hong, 2010). These early lesions appear in the aorta (during fetal life), while they appear in the coronary arteries in the follow decades and later in the cerebral arteries (Singh, Mengi, Xu, Arneja, & Dhalla, 2002). Some lesions regress while others become complicated, with the exact localization one important factor. Focal development of the lesions is seen at predisposed sites such as the branch points, whereas the proximal parts and the curvatures of smaller vessels have a higher predilection (Smedby, 1996; Smedby et al., 1995).

Epidemiological studies over the past years have revealed numerous risk factors for atherosclerosis. These can be grouped into factors with an important genetic component, and those that are largely environmental. Dyslipidaemia, diabetes *mellitus*, obesity, smoking, hypertension, lack of exercise and positive family history are some of the classic risk factors for atherosclerosis. Age and gender are also factors involved in disease prevalence. Below age 60, men develop CVDs at more than twice the rate of women. In addition, several psychosocial factors, such as depression and stress, have been also linked to atherosclerosis prevalence (Lusis, 2000). Thus, atherosclerosis is probably one of the most complex diseases, with a large variety of risk factors. Genetics components are associated with multiple risk factors, such as plasma lipid levels and blood pressure, HDL levels, and exhibit smooth population distributions characteristic of polygenic traits (Lusis, Fogelman, & Fonarow, 2004), being far from completely identified (Lusis, 2012). However, any of these factors alone is sufficient to produce an atherosclerotic lesion. The interplay among the consequences associated to these risk processes is a key event in the increased cardiovascular disease risk (Libby et al., 2016). Frequently, the interactions between risk factors are not simply additive; for example, the effects of hypertension on CVDs are considerably amplified if cholesterol levels are high. The importance of genetics and environment in human CVDs has been examined in many family and twin studies (Marenberg, 1994). Within a population, the heritability of atherosclerosis (the fraction of disease explained by genetics) has been high in most studies, frequently exceeding 50%. Thus, the common forms of CVDs result from the combination of an unhealthy environment, genetic susceptibility and our increased lifespan (Lusis, 2012). Atherosclerotic risk factors are abundant in number and each day more is understood as results of the research in the mechanisms thereby risk factors act at systemic and local level. Due to the complexity of atherosclerosis disease, the interplaying between inflammation and systemic risk factors such as diabetes, lipid accumulation and shear stress, justifies the need for inter-disciplinary research that ties these different risk factors together.

1.1.2 Arteries haemodynamic and endothelial injury

As briefly mentioned above, early atherosclerosis lesions in the human carotid artery develop in the area of a major curvature (carotid sinus) or branch-points such as bifurcations of the arteries (Figure 1.1A) (DeBakey, Lawrie et al. 1985; Nakazawa, Yazdani et al. 2010). These regions are exposed to low time-average shear stress, a high oscillatory shear index, and steep temporal and spatial gradients (Figure 1.1B). Thus, shear stress is a key haemodynamic factor in atherosclerosis development. The levels of shear stress have been correlated with atherogenic gene expression by endothelial cells: arterial-level shear stress (>15 dyne/cm^2) leads to the expression of protective genes, while low shear stress (<4 dyne/cm^2) induces an atherogenic phenotype (Malek, 1999), increasing the probability of molecules and cells retention. In endothelial cells with an atheroprone phenotype, there is the stimulation of a proinflammatory milieu driven the priming of the factor nuclear kappa B (NF-κB) signaling pathway, which it is then amplified in response to subendothelial LDL (Figure 1.1C). NF-κB pathway activation leads to the recruitment of neutrophils and monocytes.

In contrast, endothelial region that are exposed to uniform laminar flow present an increase in transcriptional integrators Kruppel-like factor (KLF) 2 and KLF4, which drive an atheroprotective endothelial cell phenotype (Atkins & Simon, 2013). This atheroprotective endothelial phenotype, together with a decrease in lipoprotein retention, promotes an anti-inflammatory and anti-thrombotic environment that affords relative protection from atherosclerotic lesion development (Ira Tabas, García-Cardeña, & Owens, 2015).

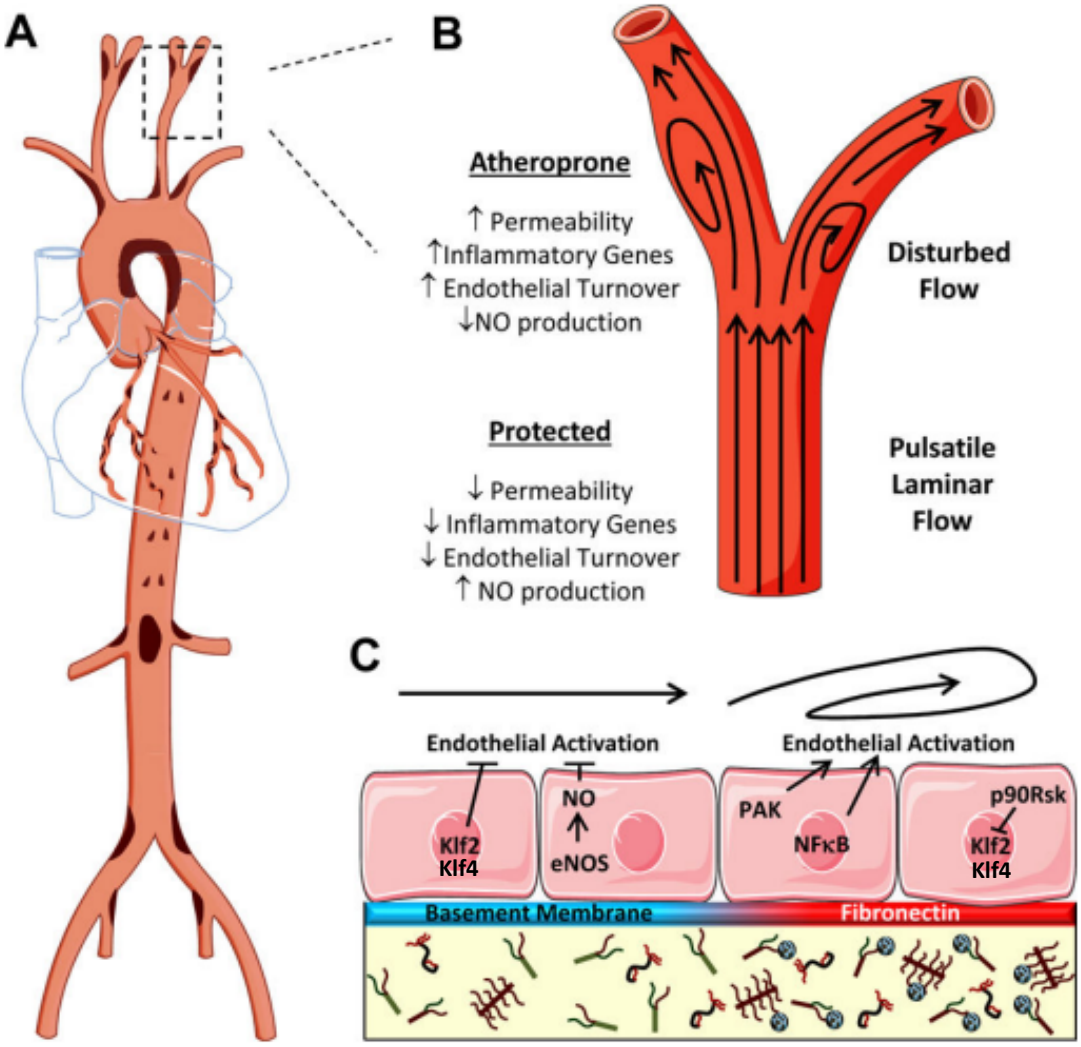

Figure 1.1 | Vascular endothelial cells and the development of areas prone to develop early atherosclerotic lesions.

A. Schematic representation for the prevalence of atherosclerotic plaque formation throughout the arterial tree. Plaque-prone areas are indicated in brown. **B.** Early lesions of atherosclerosis in the human carotid artery develop in the area of a major curvature (carotid sinus) exposed to low time-average shear stress, a high oscillatory shear index, and steep temporal and spatial gradients. **C.** Arterial geometries that are exposed to uniform laminar flow evoke an atheroprotective endothelial cell phenotype driven by Kruppel-like family of transcription factors (KLF) 2 and KLF4. This atheroprotective endothelial phenotype, together with a decrease in LDL retention, promotes an anti-inflammatory and -thrombotic environment that affords relative protection from atherosclerotic lesion development. In contrast, endothelial cells at this site display an atheroprone phenotype, which promotes a proinflammatory milieu driven by the priming of the NF-κB signaling pathway. Adapted from (Yurdagul et al., 2016).

1.1.3 Artery anatomy and physiological alterations in atherosclerosis

Arteries and veins are constituted by three primary layers: the intima, media, and adventitia (Figure 1.2A and B), involved embedded in a complex extracellular matrix. The intima layer

is lined with endothelial cells, which are in direct contact with blood and by the internal elastic lamina. Moreover, the media is composed of multiple layers of SMCs, which present the capacity for contracting or relaxing in response to neural and chemical signals. The outermost layer is the adventia, which consists of connective tissue and also contains nerves and small blood vessels supplying the artery itself.

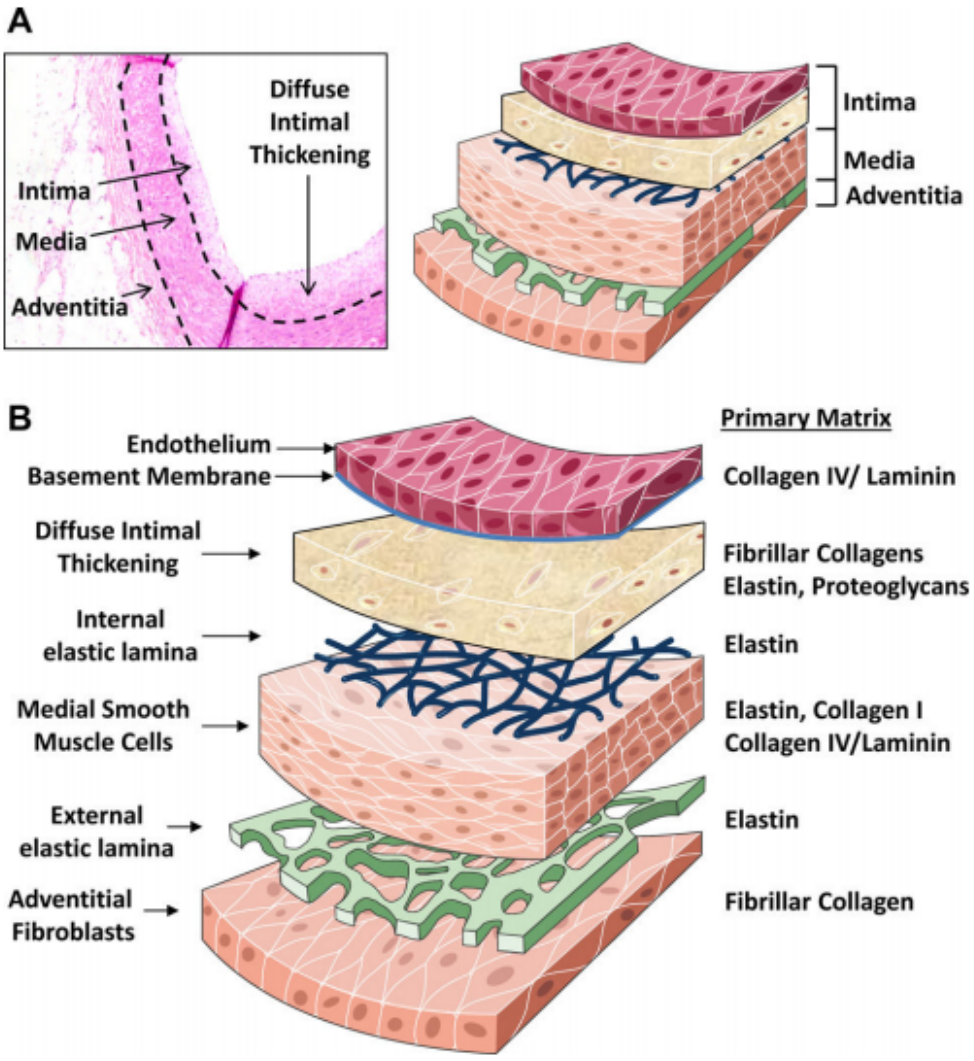

Figure 1.2 | Cross-sectional diagram of the aortic vessel matrix.

A. Histological (left) and representative (right) images of the arterial intima, media, and adventitia in a human coronary artery. Dashed lines represent the internal and external elastic lamina. **B.** Primary vascular matrix components in the different arterial layers. Adapted from (Yurdagul et al., 2016).

Extracellular matrix composition differs significantly between the arterial layers. The basement membrane, where endothelial cells are normally connected, is a thin layer of collagen IV, laminin-8/10, nidogen, and heparan sulfate proteoglycans (Figure 1.2B) (Stratman & Davis, 2012). The smooth muscle-rich medial layer consists of fibers of elastin, providing elasticity to the vessel, and fibrillar type I and type III collagens that provide tensile strength. SMCs interact with both fibrillar collagens and a thin collagen IV/laminin-rich basal laminae (Barnes & Farndale, 1999). In the atheroma plaque neointima, the composition of the extracellular matrix changes considerably. Intimal thickening precedes atherosclerotic plaque development and consists of non-proliferative SMCs, proteoglycans, and elastin fibers (Nakashima, Wight, & Sueishi, 2008). In atheroma the degradation of internal elastic laminae, a barrier for SMCs

recruitment from the media, through elastases produced by invading macrophages and activated SMCs, was observed (Yasuda et al., 2004). The neointimal SMCs are responsible for the atherosclerotic matrix production, primarily involving in collagen synthesis, with 60% of total plaque protein composed of type I collagen (Yurdagul, Finney, Woolard, & Orr, 2016).

1.1.4 Lipoprotein particles and their oxidation

1.1.4.1 Composition and structure of lipoproteins

Lipoproteins are complex particles that have a central hydrophobic core of non-polar lipids, primarily cholesterol esters (CE) and triglycerides (TG). This hydrophobic core is surrounded by a hydrophilic monolayer consisting of phospholipids, free cholesterol, and apolipoproteins (Apo). Plasma lipoproteins are divided in to different classes based on size, lipid composition, and apolipoproteins, which can be either structural or exchangeable among different lipoprotein classes. Thus, lipoproteins can be classified as: chylomicrons (CM), very low density lipoproteins (VLDL), LDL and high density lipoproteins (HDL), from the lowest to the highest density (Vance & Vance, 2008). Besides the crucial role in lipids transport through lymphatic and circulatory systems, Apo also regulate the interactions with cellular receptors and are involved in inflammatory and immune processes as well as in lipid metabolism by modulating enzymes implicated in these metabolic pathways (Bolanos-Garcia & Miguel, 2003). Here, we will focus on LDL due to its central role in atherogenesis.

LDL particles (d = 1.019 – 1.063 g/mL; diameter ≈ 20 nm) are the end products of VLDL catabolism and represent the principal plasma carriers of cholesterol. In each LDL particle there is an Apo molecule B-100, playing an important role in both lipoprotein structural stabilization and their removal from the circulation (Segrest, Jones, De Loof, & Dashti, 2001). The LDL particle contains on average 600 molecules of free cholesterol, 1600 molecules of CE, 700 molecules of phospholipids, 170 molecules of TG, and 1 molecule of ApoB, with varying amounts of antioxidants such as α- and γ-tocopherol, coenzyme Q10, and β-carotene (Levitan, Volkov, & Subbaiah, 2010; Niki, 2014). The fatty acid composition varies between LDL particles and depends on the diet. The main fatty acids identified in LDL were linoleic (18:2), palmitic (16:0), and oleic acid (18:1) comprising about 85% of the total fatty acids, followed by stearic (18:0), arachidonic (20:4), myristic (14:0), and pamitoleic (16:1) acid (H Esterbauer, Jürgens, Quehenberger, & Koller, 1987). Cholesteryl esters are 40-50% of the total lipids in LDL and cholesteryl linoleate and arachidonate are the most abundant. LDL contain on average 1300 molecules of polyunsaturated fatty acids (PUFAs) bound in the different lipid classes, which are susceptible to oxidation (Hermann Esterbauer, Puhl, Martina, Waeg, & Rabl, 1991). Oxidation is protected by the antioxidant components of LDL. The predominant antioxidant in LDL is vitamin E - α-tocopherol, with an average of 6 molecules in each LDL particle. The other components with potential antioxidant activity are: ϒ-tocopherol, β-carotene, α-carotene, lycopene, cryptoxanthin, cantaxanthin, phytofluene and ubiquinol-10 (Hermann Esterbauer et al., 1991). Additionally, a study showed that the

oxidative degradation of the PUFAs in LDL only starts when vitamin E is largely consumed (H Esterbauer et al., 1987).

1.1.4.2 Mechanisms of lipoprotein oxidation *in vitro* and *in vivo* and detection methodologies

The precise mechanisms that generate oxidized lipoproteins *in vivo* are still only partially understood. Under normal circumstances, antioxidants help to prevent oxidation of LDL in the circulation. However, in pathological condition they become oxidized. LDL circulating in the plasma appears to be protected from oxidation, both by dietary antioxidants (such as vitamin E) and by protective enzymes including glutathione peroxidases, peroxiredoxins, lipoprotein-associated phospholipase A2 (Lp-PLA2) and paraoxonases (PON) from HDL (Linton et al., 2015). Retention of LDL in the intima, due to interactions with the extracellular matrix, such as chondroitin sulfate-rich proteoglycans, sequesters LDL away from the antioxidant environment of the plasma. The high oxygen pressure observed in arterial intima contribute to further increase LDL susceptibility to suffer oxidation. The oxidation hypothesis of LDL in atherosclerosis suggests that oxidative modification of LDL plays a crucial role in the disease development. In addiction, its suggests that the resulting oxidized LDL (ox-LDL) promote the immune and inflammatory reactions that characterize atherosclerosis (Steinberg, Parthasarathy, Carew, Khoo, & Witztum, 1989). A variety of oxidases and peroxidases generate strong oxidants that can readily oxidize LDL in a complex process, which apparently involves macrophages, SMCs and endothelial cells (EC) action (Linton et al., 2015). Some oxidative enzymes were already described as having a role in LDL oxidation by increasing reactive oxygen species (ROS): myeloperoxidase (MPO), xanthine oxidase (XO), NADPH oxidases (NOXs), and inducible nitric oxide synthase (iNOS) (Elahi, Kong, & Matata, 2009; Madamanchi, Vendrov, & Runge, 2005). Oxygenases such as lipoxygenases (LOX) have also been shown to oxidize LDL *in vitro* (Upston, Neuzil, & Stocker, 1996). However, the complete role of each enzymes in lipoprotein oxidation *in vivo* and therefore their impact on to atherosclerosis remains to be fully elucidated.

MPO, one of the main enzymes found in neutrophilic granules, is released when these cells are activated (and to a lesser extent from monocytes/macrophages) and can accumulate in the intimal space of the artery wall (Lacy, 2006; Noguchi et al., 2000). Neutrophil activation indirectly increases the chance of lipoprotein oxidation. Several studies have already demonstrated that increased levels of MPO are correlated with higher levels of ox-LDL, increasing atherosclerosis risk (Ferrante et al., 2010; Karakas et al., 2012; Pignatelli et al., 2009; Puntoni et al., 2011). Another enzyme studied in the context of atherosclerosis is LOX, which catalyze the oxygenation of PUFAs such as arachidonic acid and linoleic acid. Although the primary substrates for lipoxygenases are non-esterified fatty acids, exposure of LDL to 15-LOX also leads to oxidation of phospholipids and CE (Mashima & Okuyama, 2015; Upston et al., 1996). In mice, the deletion of the gene analogous to the human 15-LOX, the 12/15-LOX gene, on an *ApoE*$^{-/-}$ background reduced atherosclerosis compared to *ApoE*$^{-/-}$ mice (Cyrus et al., 1999). Interestingly, lower levels of autoantibodies against ox-LDL and malondialdehyde (a product of PUFAs oxidation) (MDA)-LDL were also observed.

As described, above the exact process of LDL oxidation *in vivo* is controversial. Since the discovery of the impact of LDL oxidation in atherosclerosis, metal ion-dependent oxidation of LDL has been extensively used for *in vitro* experiments. Iron (Fe^{3+}) and copper (Cu^{2+}) are the two major metal ions described to catalyze LDL oxidation (Delporte, Van Antwerpen, Vanhamme, Roumeguère, & Zouaoui Boudjeltia, 2013; Lynch & Frei, 1993). Metal ion-dependent oxidation mechanisms assume a high concentration of cations at the oxidation site, which is controversial from a physiological perspective (Yoshida & Kisugi, 2010). Nevertheless, Cu^{2+} and Fe^{3+}-free intimal contents were measured and an increase in the levels of both cations was demonstrated in the intima of lesions compared with healthy controls, with the levels of Fe^{3+} correlated with cholesterol levels (Stadler, Lindner, & Davies, 2004). Despite the detection of these cations in atheromata, their roles in atherosclerosis remain a point of contention. Indeed, some studies have positively correlated metal ion levels with cardiovascular risk, whereas others have negatively correlated them (Delporte et al., 2013; Gaut & Heinecke, 2001). Nevertheless, epidemiological studies as well as *in vitro* experiments with Fe^{3+} agree on its potential impact on atherogenesis, whereas Cu^{2+} might be ambiguous (Sullivan, 2009).

Others studies defend the non-oxidative modification of LDL as a crucial step in atherogenesis. LDL aggregation and glycosylation have also been identified in atheroma (I Tabas, 1999). Diabetes is a well-known risk factor for atherosclerosis, and investigators had correlated specific modifications of lipoproteins by glycation with this susceptibility (Basta, Schmidt, & De Caterina, 2004; Lopes-Virella & Virella, 1996). Thus, it is critical to keep in mind that modified LDL are in fact highly heterogeneous and complex particles and the mechanism that mediates their pathology is far from completely defined. Nevertheless, oxidation of LDL *in vitro* has been used extensively to study the biological activities of ox-LDL, but, even here, the actual species resultant vary significantly with the oxidation method (for example Cu^{2+} and oxidases treatment, or other methods, such as air and ultraviolet irradiation exposure) and the length of oxidation (Linton et al., 2015).

Several methods commonly used to detect and measure the ox-LDL concentration *in vivo* only measure general characteristics of these particles. For instance, one of the methodologies used to measure ox-LDL is agarose gel electrophoresis. Reactive lipid species react with lysine residues of ApoB converting native positively charged LDL to a negatively charged particle, increasing electrophoretic mobility (Parthasarathy, Raghavamenon, Garelnabi, & Santanam, 2010). Moreover, ox-LDL can also be detected using the most prominent assay, as an index of lipid peroxidation, the measurement of thiobarbituric acid reactive substances (TBARS) through the thiobarbituric acid (TBA) test (Walter et al., 2004). Alternatively, ox-LDL in plasma and other tissues can be quantified by the immunoreactivity of the natural IgM autoantibody E06 which binds to the oxidized group of phosphocholine (PC) (Tsimikas et al., 2011). While modification of LDL with MDA-LDL or others lipid peroxidation products, such as 4-hydroxynonenal (HNE), which affects mainly ApoB structure, are often used as a model of ox-LDL and can be detected with IK17 antibody (Linton et al., 2015; Tsimikas et al., 2011). Therefore, *in vivo* ox-LDL is a mixture of many different compounds

and ox-LDL atherogenic activities represent multiple cellular responses to the full range of oxidized compounds.

1.1.4.3 LDL oxidation products

Literally hundreds of products have been identified in the ox-LDL and it is impossible to identify and quantify all of them (Y. I. Miller & Shyy, 2017; Niki, 2014; Parthasarathy et al., 2010). Interestingly, the oxidation of lipids can have both adverse and protective effects in different tissue and pathophysiological contexts (Y. I. Miller & Shyy, 2017). Nevertheless, a summary of lipid/protein oxidation products generated during the oxidation of LDL is shown in Table 1.1. As already mentioned, considering the heterogeneity of LDL, it is difficult to define, characterize and quantify "ox-LDL" and "minimally modified LDL"(Niki, 2014). In this section we will focus on the lipid peroxidation products due to its relevance in the objective of this thesis.

Table 1.1 | Summary of the main reported lipid and protein oxidation products generated during the oxidation of LDL. Adapted from (Parthasarathy et al., 2012).

List of main reported lipid/protein oxidation products generated during the oxidation of LDL
Fatty acid oxidation products
Free and esterified fatty acid peroxides, such as 13-hydroperoxylinoleic acid (13-HPODE)
Free and esterified fatty acid hydroxides, such as 13-hydroxylinoleic acid (13-HODE)
Prostaglandin-like products, such as isoprostanes in free and esterified form
Aldehydes, such as malondialdehyde (MDA), 4-hydroxy nonenal (HNE) and hexanal
Pentane and other hydrocarbons
Lipid derived products
Lysophosphatidylcholine
Cholesterol and cholesteryl esters oxidation products, such as 7-keto-cholesterol and 9−oxononanoyl-cholesterol
Internally modified phosphatidyl ethanolamine/serine products
Protein oxidation products
Protein carbonyls
Non-enzymatic proteolyzed fragments
Modified cysteine, cystine, histidine, methionine, lysine, arginine, tryptophan, and tyrosine
Protein cross-links due to tyrosine cross-links as well as due to bifunctional aldehydes
Lipid–protein adducts which could be classified as ceroids (lipofuscins)
Other changes
Increased buoyant density
Increased negative charge
Loss of characteristic yellow color (human)
Loss of enzyme activities associated with LDL

The mechanisms and products of lipid peroxidation have been studied extensively and are now well understood (Niki, 2009; Yin, Xu, & Porter, 2011). One of the characteristics of lipid peroxidation is that it proceeds by a non-specific mode. The oxidation vulnerability of PUFAs and their esters results from the relatively low energy required for free radicals generations, particularly hydroxyl radicals (●OH), to abstract hydrogen atoms located between two adjacent double bonds (bis-allelic hydrogens) (Figure 1.3). The major PUFAs present *in vivo* are linoleic (18:2), linolenic (18:3), arachidonic (20:4), eicosapentaenoic acid (20:5, EPA), and docosahexaenoic acid (22:6, DHA), which have one, two, three, four, and five bis-allylic methylene groups respectively (Niki, 2014). As stated above, cholesteryl linoleate and cholesteryl arachidonate are the predominant CE in LDL particles. When oxygen radicals reacts with bis-allylic hydrogens there is the formation of a lipid radical that reacts instantaneously with any molecular oxygen present in the environment, producing lipid hydroperoxides as major primary products. The lipid peroxide radical (LOO●) can then propagate the radical reaction by abstracting hydrogens from neighbouring phospholipids or can react with itself to create a large number of secondary peroxidation products. Secondary products that may be relevant to atherogenesis can be organized in two broad classes: oxidized lipids (primarily oxidized phospholipids but also oxidized CE) and reactive lipid aldehydes that exert their effects by modifying proteins and other macromolecules (Linton et al., 2015). Some of these aldehyde products, such as HNE and MDA, are hydrophilic while others are less polar, presenting a variable degree of partitioning capacity between lipid and aqueous phases (H Esterbauer et al., 1987). Cholesterol/CE or its oxidized derivatives are present in this latter group of aldehyde products, which have be known as ‘‘core-aldehydes’’, are present in atherosclerotic lesions and resist hydrolysis upon internalization by macrophages (Hoppe, Ravandi, Herrera, Kuksis, & Hoff, 1997). Due to their amphiphilic properties, aldehyde oxidized products are in constant equilibrium with all the lipidic structures, cell membranes, the (intra- and extracellular) aqueous phase, and translocate readily across cellular membranes. Over time the increasingly in oxidative environment or via the action of intracellular aldehyde oxidizing systems, aldehydes from CE will be oxidized to stable cholesteryl hemiesters of the corresponding bi-acids as shown in Figure 1.3 (Estronca et al., 2012).

1.1.5 Principles of atherosclerosis – a molecular and cellular view

Atherogenesis is initiated by the entry and retention of LDL into the subendothelial space, or intima, at regions of disturbed blood flow in arteries (Figure 1.4A). The LDL retention level is determined by its concentration in the blood, the age and metabolic state of the individual, genetic and environmental factors, as described above. These considerations affect arterial wall biology, including variations in subendothelial proteoglycans that retain LDL and factors that alter endothelial permeability. LDL molecules accumulate in the intima where they undergo oxidation. Then, the oxidized lipid and protein components of LDL take on properties of damage-associated molecular patterns (DAMPs) and thereby trigger an inflammatory response (Lusis, 2000). Ox-LDL- activited EC synthesize proinflammatory molecules, cellular adhesion complexes- vascular cell adhesion molecule 1 (VCAM-1), intercellular adhesion

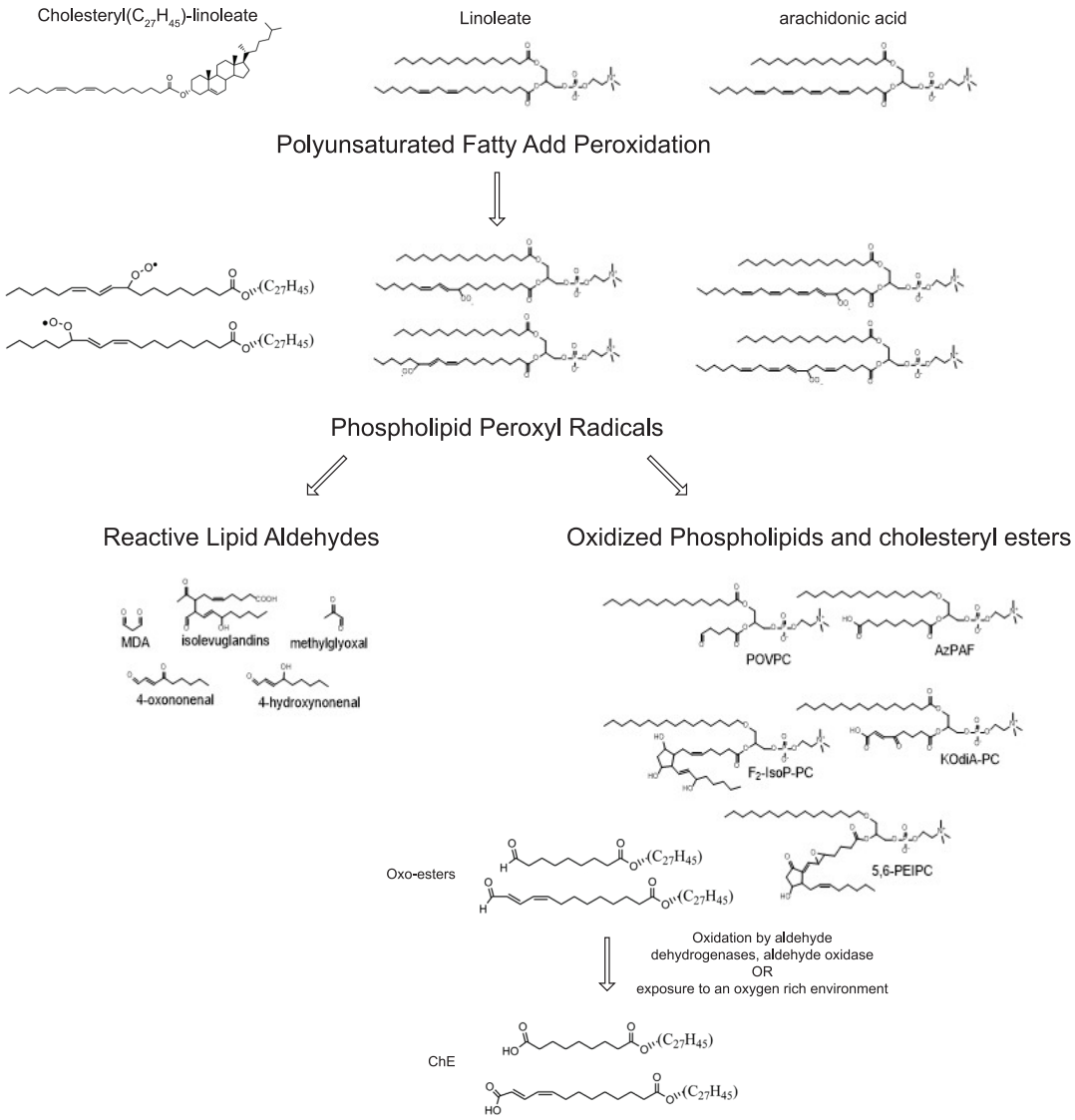

Figure 1.3 | Oxidation of polyunsaturated fatty acids in phospholipids and cholesteryl ester.

Oxidation of polyunsaturated fatty acid present in plasma lipoproteins components results in formation of a variety of reactive lipid aldehydes and the resulting oxidized lipids, converting these lipoproteins to atherogenic particles. Reactive lipid species include malondialdehyde (**MDA**), isolevuglandins (**IsoLG**), methyglyoxal (**MGO**), 4-oxononenal (**ONE**), and 4-hydroxynonenal (**HNE**). Oxidized phospholipids include 1-palmitoyl-2-oxovaleroyl-sn-glycero-3-phosphorylcholine (**POVPC**), 1-O-alkyl-2-azelaoyl-sn-glycero-3-phophorylcholine (**azPAF**), 1-(Palmitoyl)-2-(5-keto-6-octene-dioyl) phosphatidylcholine (**KOdiA-PC**), 1-palmitoyl-2-F2-isoprostane-sn-glycero-3-phosphocholine (**F2IsoP-PC**), 1-palmitoyl-2-(5,6)-epoxyisoprostane E2-sn-glycero-3-phosphocholine (**PEIPC**) and cholesteryl hemiesters (**ChE**). Adapted from (Linton et al., 2015; Estronca et al., 2012).

molecules (ICAM-1), P- and E-selectins and growth factors (macrophage-colony stimulating factor (M-CSF)). This inflammatory response, together with flow-mediated changes in EC (Gimbrone & García-Cardeña, 2013; Ira Tabas et al., 2015), promotes the entry into the intima of bone-marrow-derived neutrophils and monocytes (Rotzius et al., 2010; Swirski et al., 2007). Driven by M-CSF and probably other differentiation factors, the majority of monocytes in early atherosclerotic lesions become cells with macrophage and/or dendritic cell-like features (Jason L Johnson & Newby, 2009; Moore & Tabas, 2011). Neutrophils in the presence of ox-LDL increase the secretion of neutrophilic extracellular traps (NETs), that can have a role in monocyte/macrophage priming (Warnatsch, Ioannou, Wang, & Papayannopoulos, 2015). As soon as monocytes differentiate into macrophages, together with EC, they

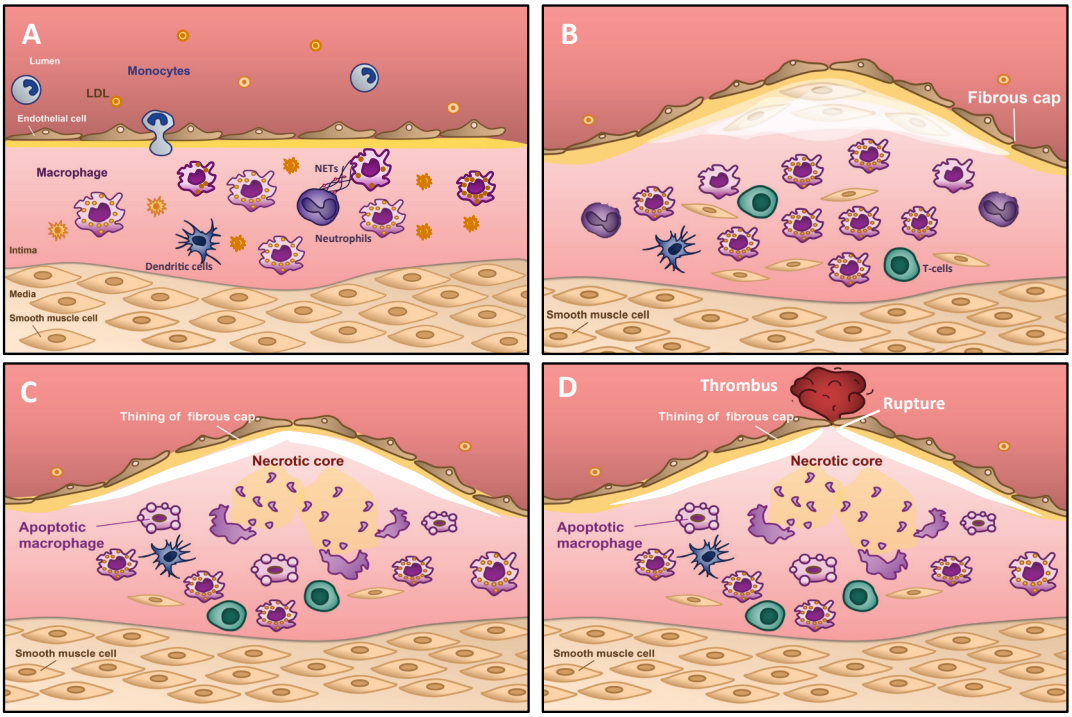

Figure 1.4 | Progression of an atherosclerotic lesion.

Early fatty streak lesions are characterized by the accumulation of LDL in the subendothelial space. The complex environment generated through the trapping and oxidation lipid in the vessel wall initiates a response to injury, beginning with the recruitment of neutrophils, which have a role in macrophages priming through release of neutrophils extracellular traps (NETs), and monocytes. Consequently, maturation into dendritic cells and macrophages, which becoming foam cells, are an important step in the initiation of fatty steak **(A)**. As the atherosclerotic lesion progresses, smooth muscle and T cells also infiltrate the intima. Smooth muscle cells synthesize collagen under normal conditions, originating the fibrous cap **(B)**. Vulnerable plaques are characterized by the accumulation of apoptotic cells and defective phagocytic clearance (efferocytosis), resulting in the lipid-filled necrotic core and the thinning of fibrous cap **(C)**. A thinning fibrous cap decreases lesion stability, making these atherosclerotic plaques susceptible to rupture and the formation of a thrombus **(D)**.

produce ROS, the enzymes sphingomyelinase (SMase), secretory phospholipase 2 (sPLA2), MPO and other lipases that have an effect on ox-LDL, which can aggregate and become highly oxidized (Lusis, 2000). Ox-LDL are taken up by macrophages via scavenger receptor (SR-A) and CD36, in an uncontrolled manner. The expression of these receptores is promoted by peroxisome proliferator-activated receptor-γ (PPAR), a transcription factor whose ligands include oxidized fatty acids, or by cytokines such as tumour necrosis factor-α (TNF-α) and interferon-γ (IFN-γ) (Ashraf & Gupta, 2011; Tontonoz, Nagy, Alvarez, Thomazy, & Evans, 1998). These immune cells ingest modified lipoproteins and become foam cells, cells enriched in lipid depositis, the hallmark of atherosclerotic lesions (Kruth 2001; Collot- Teixeira, Martin et al. 2007). When macrophages are activated by oxidized components of LDL, they initiate a strong inflammatory program. Macrophage increase the production of proinflammatory cytokines, as interleukin-1β (IL-1β), IL-6, IL-12, and TNF-α, chemokines, such as monocyte chemoattractant protein-1 (MCP-1) or chemokines to attract more monocytes (Ira Tabas & Bornfeldt, 2016), amplifying the inflammatory process with in atheroma. In part as a result of this accumulation of inflammatory macrophages, an inflammatory adaptive immune response involving primarily T helper 1 (Th1) cells, but also Th17 and Th2 cells and B cells, develops in conjunction with a progressive decrease in regulatory T (Treg) cells (Figure 1.4B) (Witztum & Lichtman, 2014). Other immune cells, including natural killer cells (NK), mast

cells, and eosinophils, are present in human atheroma and have been shown to promote atherosclerosis via additional mechanisms in mouse models (Witztum & Lichtman, 2014) .

Later as the lesion progresses, cytokines as MCP-1, C-X-C motif ligand-8 (CXCL8) and IFN-γ as well as growth factors, stimulate SMCs proliferation and migration from the tunica media into the intima, where they produce and stimulate the synthesis of new extracellular matrix to form a collagenous fibrous cap (composed of collagen type I and III), as a response to the inflammatory environment (Figure 1.4B) (Newby & Zaltsman, 1999; Wight, 1989). A fibrous cap is generally considered to be a protective layer of fibrous tissue separating the necrotic core from the arterial lumen (Göran K. Hansson, 2005b). Necrotic cores in advanced plaques arise from the combination of lesional macrophages and defective phagocytic clearance (or efferocytosis) of the apoptotic macrophages in advanced plaques (Figure 1.4C) (Tabas, 2010a). Macrophage death also occurs in early atherosclerotic lesions, but here the efferocytic clearance of macrophages is efficient, decreasing lesion cellularity, inflammation, and plaque progression rather than an increase in plaque necrosis. Macrophages undergo apoptosis due to intracellular undigested ox-LDL accumulation and one of the well accepted pathway it is through induced endoplasmic reticulum (ER) stress (Tabas, 2010b). In a physiological post-inflammatory response, macrophages and other inflammatory cells secrete molecules and carry out functions that dampen the inflammatory response and promote tissue repair (Serhan, Chiang, & Van Dyke, 2008). However, this so-called resolution response can be not efficient in the setting of atherosclerosis. Impaired resolution in atherosclerotic lesions leads to sustained, non-resolving, and maladaptive inflammation that promotes plaque progression (Merched, Ko, Gotlinger, Serhan, & Chan, 2008; Viola et al., 2016). The pathological features of clinically dangerous plaques include large areas of necrosis and thinning of the fibrous cap. When a breach forms in the fibrous cap, blood is exposed to thrombogenic material in the lesion, and acute occlusive thrombosis with tissue infarction can ensue (Figure 1.4D) (Libby, 2013). With the obstruction of the blood supply to the surrounding tissues of the lesion, there is a decrease in oxygen and nutrient supply, resulting in sudden cardiac death.

1.1.6 Diagnostic – serum biomarkers

Basic research over the last two decades has identified a large number of molecules critical to the atherosclerotic process. Current cardiovascular risk prediction models incorporate traditional risk factors to estimate cardiovascular risk as mentioned in section 1.1.1. Numerous blood-based biomarkers have been identified which are associated with increased cardiovascular risk after adjusting for traditional risk factors. Many of these biomarkers, either alone or in combination, have been incorporated into risk prediction models to determine whether the addition of these markers increases their predictive capacity (T. M. Brown & Bittner, 2009; J. Wang et al., 2017). The biomarkers associated with various pathophysiological processes underlying cardiovascular disease were summarized in Table 1.2.

Table 1.2 Risk biomarkers used for diagnosis of cardiovascular disease.

Adapted from (Upadhyay, 2015)

Serum biomarker	Overview
Metabolic dysfunction	
Total cholesterol to HDL-Cholesterol ratio	Total cholesterol to HDL cholesterol ratio and low ankle brachial index in an elderly population can predict risks of CVDs. Thus, total cholesterol to HDLc ratio and low ankle brachial index (ABI) are important biomarkers which predict CVDs (Zhan, Yu, Ding, Sun, & Hu, 2014).
Levels of ApoB and ApoAI or ratio of ApoB : ApoAI	ApoA1/ApoB ratios are considered as good biomarkers for prediction of CVDs in human (Shah & Arneja, 2013).
Triglyceride to HDL cholesterol ration	Increasing evidence suggests that both fasting and nonfasting triglyceride levels predict prospective cardiovascular risk. Therefore, triglyceride HDL cholesterol ratio has become increasingly important, providing mixed dyslipidemic patterns in the setting of obesity and the metabolic syndrome. A triglyceride: HDL cholesterol ratio >3.5 appears to be associated with increased cardiovascular risk (Zhan et al., 2014).
Biomarkers of lipid peroxidation	
Hydroxyoctadecadienoic acid (HODE)	HODEs are one of the most abundant lipid oxidation products found in human plasma. They are produced by reduction of hydroperoxides and also directly by oxidation with cytochrome P450. hydroperoxides are chemically and thermally unstable (Niki, 2014).
Oxysterols	7-Hydroperoxycholesterol, 7-ketocholesterol and 7-Hydroxylated cholesterol (7-OH CH) are the major oxysterols formed via cholesterol oxidation. Increased levels of 7β-OH CH have been associated with a high risk of developing cardiovascular disease and coronary atherosclerotic plaques(Khatib & Vaya, 2014).
Malondialdehyde (MDA) and thiobarbituric acid reactive substances (TBARS)	MDA and TBARS have been used frequently as a standard biomarker of lipid peroxidation *in vivo*. Further, many other biological materials may react with TBA, resulting in high TBARS levels and reduced specificity. Although increased circulating levels of MDA-LDL are associated with coronary artery disease, there is no direct evidence that increased MDA-LDL is a prognostic factor for CVDs (Kotani et al., 2015; Tsimikas, 2006).
Myocardial necrosis	
High-sensitivity cardiac troponin (hs-cTn)	Cardiac troponin I (cTnI) and T (cTnT) are proteins that are unique to the heart and are specific and sensitive biomarkers of myocardial damage. Hs-cTn assay has an increase in the accuracy of AMI diagnosis, and it might be an excellent tool for risk stratification (Agewall, Olsson, & Löwbeer, 2007).
Heart-type fatty acid binding protein (H-FABP)	Cytoplasmic FABP is a family of transport of fatty acids through the membranes. H-FABP is rapidly released into the cytosol early in AMI. Data has shown that H-FABP is either superior to or adds incremental value to cTn in the early diagnosis of ACS. H-FABP could be a useful indicator for the early identification of high risk patients (Furuhashi & Hotamisligil, 2008).
Inflammation	
High-sensitivity C-reactive protein (HsCRP)	CRP is an innate immune response protein, a nonspecific inflammatory marker that has been extensively studied in CVD. CRP itself mediates atherothrombosis. HsCRP that detects lower levels of CRP (< 5mg/L) could help detect high risk patients more early and accurately. However, the causal association is unknown (Boekholdt et al., 2006; Koenig & Khuseyinova, 2007).
Growth-differentiation factor-15 (GDF-15)	GDF-15, previously referred to as macrophage-inhibitory cytokine-1, is expressed by activated macrophages. GDF-15 is a strong predictor of cardiovascular events and clinical trials suggest that GDF-15 is a potential tool for risk stratification (Ho et al., 2013; Upadhyay, 2015).

Fibrinogen	Fibrinogen is an acute phase protein synthesized in the liver. Elevated fibrinogen levels are associated to thrombotic disease. ESC guidelines allow fibrinogen measurement as a part of the risk assessment in patients with an unusual or moderate cardiovascular risk (Raut, Hamill, Daniels, & Heath, 2014; Upadhyay, 2015).
Uric acid (UA)	UA is the end product of purine metabolism. Elevated serum UA increases oxidative stress, promotes endothelial dysfunction, and enhances inflammation, showing an independent positive association with cardiovascular mortality. However, there is still conflicting evidence for the results (J. Wang et al., 2017).
Plaque instability	
Pregnancy-associated plasma protein-A (PAPP-A)	PAPP-A is a metalloproteinases which, by activation of insulin-derived growth factor-1, induces inflammation and lipid uptake. Circulating PAPP-A is a promising biomarker for risk stratification of ACS (J. Wang et al., 2017).
Myeloperoxidase (MPO)	MPO is produced by leukocytes and released in inflammatory conditions. MPO is capable of activating metalloproteinases, inducing LDL and ApoA-I oxidation and reduces cholesterol efflux capacity. Prospective and cross-sectional studies addressed the role of MPO as a circulating inflammatory marker in CVD. However, its routine measurement is not recommended in clinical settings (Cavusoglu et al., 2007; J. Wang et al., 2017).
Platelet activation	
Lipoprotein-associated phospholipase A2 (Lp-PLA2) and secretory phospholipase A2 (s-PLA2)	Lp-PLA2 and s-PL2 are mainly produced by monocytes and macrophages and by modifying the surface of LDL particles in the phospholipid hydrolysis process, increases their susceptibility to oxidation. Although elevated PLA2 levels have been shown to be associated with an increased cardiovascular risk, the overall incremental clinical utility of this biomarker remains unclear (J. Wang et al., 2017).
Soluble CD40 ligand (sCD40L)	CD40L belongs to the tumor necrosis factor superfamily and is expressed in various cell types. The surface-expressed CD40L is subsequently cleaved, generating a soluble fragment (sCD40L) that is associated with atherosclerosis and plaque instability. Apart from binding to CD40 and thus leading to its activation, sCD40L can also bind to receptors in the platelet surface. However, the results of some investigations are controversial (Heeschen et al., 2003; J. Wang et al., 2017).
Neurohormonal activation	
Copeptin	Copeptin, a glycosylated peptide, is a C-terminal part of the precursor pre-provasopressin. Copeptin could predict CAD development and cardiovascular mortality, while whether the heart contributes to its release is unknown.
Mid-regional-pro-adrenomedullin (MR-proADM)	ADM, a peptide with C-terminal amidation, is a potent vasodilator synthesized in response to physical stretch and specific cytokines. This peptide can be indirectly quantified by measuring MR-proADM, which is more stable. ADM is a promising biomarker for risk prediction in patients with HF and for early atherosclerotic plaque development and subclinical CVDs (Valenzuela-Sánchez, Valenzuela-Méndez, Rodríguez-Gutiérrez, Estella-García, & González-García, 2016).
Myocardial stress	
Natriuretic peptides (NPs)	NPs are peptides involved in sodium and water balance. In conditions of myocardial stretch, the induction of the B-type natriuretic peptide (BNP) gene results in the production and secretion of prohormone, which is cleaved into the biologically more stable N-terminal pro–B-type natriuretic peptide (NT-proBNP). In the current European guidelines, the NT-proBNP and MR-proANP are regarded as equal for the diagnosis of HF (Villacorta & Maisel, 2015; J. Wang et al., 2017).
ST2	ST2 is a member of the interleukin-1 receptor family. Its downstream effects include activation of T-helper type 2 (Th2) cells and production of Th2-associated cytokines. The studies have confirmed the role of ST2 in cardiovascular risk stratification (Upadhyay, 2015; Villacorta & Maisel, 2015).

Endothelin-1 (ET-1)	ET1 is a potent vasoconstrictor and pro-fibrotic hormone that is secreted by vascular endothelial cells, with levels that correlate to shear stress and pulmonary artery pressure. Studies have shown C-terminal portion of pro-Endothelin-1 was associated with cardiovascular death and HF independent of clinical variables (J. Wang et al., 2017).
Galectin-3 (Gal3)	Gal-3 is a glycoprotein-binding protein that is secreted by activated cardiac macrophages. It has a pivotal role in atherogenesis through its enhancement of phagocytosis, and it displays a reversal of the inducible-nitric oxide synthase to arginase switch within plaques. Gal-3 was approved by FDA in 2010 as a new biomarker in the risk stratification of HF (Lisowska et al., 2016; J. Wang et al., 2017).
Neuregulin-1 (NRG-1)	NRG-1 is a paracrine growth factor that is released from endothelial cells and binds to a family of ErbB receptors on nearby cardiac myocytes. Various cardiovascular stimuli, such as oxidative stress, ischemia, and exercise, activate the expression of NRG-1. Thus, NRG-1/ErbB4 paracrine signaling is involved in cardiac adaptation to various forms of physiologic stress. However, its use in clinical set as a risk factor needs further studies (J. Wang et al., 2017).
MicroRNAs	Several cardiac miRNAs are increased early after MI. However, their detection techniques are time consuming and their clinical benefits beside current diagnostic tools remain unclear (Lovren et al., 2012; J. Wang et al., 2017).

ACS: acute coronary syndrome; AMI: acute myocardial infarction; CAD: coronary artery disease CVD: cardiovascular disease; cTn: cardiac troponin; ET-1: Endothelin-1; H-FABP: heart-type fatty acid binding protein; hs-cTn: high-sensitivity cardiac troponin; hsCRP: high-sensitivity C-reactive Protein; Gal3: galectin-3; GDF-15: growth-differentiation factor-15; Lp-PLA2: lipoprotein-associated phospholipase A2; miRNAs: microRNAs; MMPs: matrix metalloproteinases; MPO: myeloperoxidase; MR-proADM: mid-regional-pro-adrenomedullin; NPs: natriuretic peptides; NRG-1: Neuregulin-1; PAPP-A: pregnancy-associated plasma protein-A; sCD40L: soluble CD40 ligand; sPLA2: secretory phospholipase A2; UA: uric acid.

1.1.7 Animal models

The manipulation of animal models of atherosclerosis is a crucial tool for an improve understanding of the knowledge of the molecular mechanisms behind atherosclerotic plaque formation and progression, as well as the occurrence of plaque rupture and its association with cardiovascular events. An ideal animal model of atherosclerosis resembles human anatomy and pathophysiology. Moreover, animal models allow the assessment of novel pharmacological treatments and must be easy to acquire, with a reasonable cost and easy to handle. Summarily, animal models for atherosclerosis are based on accelerated plaque formation due to: (i) a cholesterol-rich/Western-type diet, (ii) manipulation of genes involved in cholesterol metabolism, and (iii) the introduction of additional risk factors for atherosclerosis, such as diabetes (Emini Veseli et al., 2016).

Mouse and rabbit models have been extensively used, followed by pigs and non-human primates, and more recently zebrafish. Each of these models has its advantages and limitations. The mouse animal models has become the predominant species to study experimental atherosclerosis because of its rapid reproduction, ease of genetic manipulation and its ability to monitor atherogenesis in a reasonable time frame (Emini Veseli et al., 2016). Murine atherosclerotic models depend on generating a non-HDL based hypercholesterolemia (Getz, Reardon, Getz, & Reardon, 2012). Both *ApoE*$^{-/-}$ and LDL-receptor (LDLr) knockout mice (*Ldlr*$^{-/-}$) have been frequently used, but also *ApoE*$^{-/-}$/*Ldlr*$^{-/-}$, ApoE3-Leiden and pro-protein convertase subtilisin/kexin type 9 (PCSK9) - adeno associated virus (AAV) (PCSK9-AAV) mice are valuable

tools in atherosclerosis research (Emini Veseli et al., 2016). *ApoE*$^{-/-}$ and *ApoE*$^{-/-}$*/Ldlr*$^{-/-}$ mice have the advantage of developing atherosclerosis on a normal diet. *Ldlr*$^{-/-}$ mice show a human-like lipid profile and a functional ApoE, without an observed impact on inflammation. This feature is also prominent in ApoE3-Leiden mice. However, for the development of the atheroma lesion, these two animal models need to be fed with a Western-type diet. PCSK9-AAV animals are not genetically manipulated, but a fat-enriched diet is also required for atherosclerotic plaque development (Emini Veseli et al., 2016). All these mice models develop a stable fibrous plaque, which it is not susceptible to rupture, thus are not a good models to study thrombosis or other complications (Getz et al., 2012). Nevertheless, great efforts have been made to develop a model in which intra-plaque microvessels, haemorrhages, spontaneous atherosclerotic plaque ruptures, myocardial infarction and sudden death occur consistently. These features are present in *ApoE*$^{-/-}$ fibrillin-1 mutant (*ApoE*$^{-/-}$*Fbn1*$^{C1039G+/-}$) mice, presenting significantly larger plaques with a highly unstable phenotype, characterized by a large necrotic core, and a strongly diminished collagen content. Accelerated atherogenesis in these mice is likely to be the result of enhanced vascular inflammation, leading to increased monocyte attraction, oxidation and accumulation of lipids (Gargiulo, Gramanzini, & Mancini, 2016). Thus, the *ApoE*$^{-/-}$*Fbn1*$^{C1039G+/-}$ mouse is a suitable model for validation of pre-clinical studies to evaluate novel plaque-stabilizing drugs.

Through a combination of modern genome editing tools, developmental and physiological advantages, the zebrafish has emerged as a major model for studying dyslipidemia and atherosclerosis. The general strengths of zebrafish for biomedical research reside in their facile husbandry, low cost of housing and maintenance, rapid development and well described nutrient requirement (Kaushik, Georga, & Koumoundouros, 2011; Schlegel, 2016). These advances have been combined to progress in working in zebrafish larvae, juveniles, and adults, where numerous aspects of physiology pertinent to atherosclerosis emerge (Schlegel, 2016). Feeding zebrafish larvae or adults with a high cholesterol diet, without any genetic intervention, results in significant hypercholesterolemia and robust lipoprotein oxidation, making zebrafish an attractive animal model to study mechanisms relevant to early development of human atherosclerosis (Stoletov et al., 2009). These studies are facilitated by the optical transparency of zebrafish larvae and the availability of transgenic zebrafish expressing fluorescent proteins in endothelial cells and macrophages. Thus, vascular and inflammatory processes can be monitored in live animals (Fang, Liu, & Miller, 2014). Zebrafish cholesterol metabolism is very similar to humans. They express all the major classes of apolipoproteins, ApoA, ApoB, ApoC and ApoE, which share high homology with human Apo (Avraham-Davidi et al., 2012; Babin et al., 1997; Schlegel, 2016). HDL dominates the lipoprotein profile in zebrafish fed with a normal diet, as described by mouse models, being considered a “HDL” animal (i.e. HDL is the primary lipoprotein) (Getz et al., 2012; Stoletov et al., 2009). However, feeding zebrafish with a high cholesterol diet (HCD) increases the proportion of VLDL and LDL fractions in plasma and results in a lipoprotein profile, closely resembling human plasma, and presenting extremely high levels of ox-LDL (Stoletov et al., 2009). As in mouse models, oxidized lipids in the homogenates of zebrafish larvae fed with a HCD were already

characterized using liquid chromatography (LC)-mass spectromety (MS)/MS, showing an increase of 10–70-fold oxidized CE. These findings suggest that hypercholesteromia in larvae leads to profound lipoprotein oxidation (Fang et al., 2010).

1.2 CHOLESTEROL METABOLISM

For decades, it is known that sterols are found in cells of the body owing to their essential role in membrane synthesis and function. Whereas all cells express enzymes for cholesterol biosynthesis, there is no biological pathway for its degradation. Thus, cholesterol must be excreted intact. Cholesterol dynamics have been studied intensively over many decades and therapeutic advances in the field have been built upon a detailed understanding of how sterols are transported and metabolized, particularly within the arteries of the liver, heart and brain (Hajjar & Hajjar, 2016).

1.2.1 Lipoprotein metabolism – Cholesterol efflux and reverse cholesterol transport

As mentioned in section 1.1.4.1, the main lipids in lipoproteins are free- and esterified-cholesterol and TG. Hydrolysed dietary fats enter intestinal cells (enterocytes) via fatty acid (FA) transporters and sterols enter via the Niemann-Pick C1-like 1 (NPC1) transporter and some are resecreted by heterodimeric ATP-binding cassette transporter G5/G8 (ABCG5/G8) (Figure 1.5). In enterocytes, the majority of the cholesterol absorbed is esterified to CE by acyl CoA:cholesterol acyltransferase (ACAT). The TG and CE are packaged into CM in the ER. Reconstituted TG is packaged with CE and transferred to the ApoB isoform B48 into CM by microsomal TG-transfer protein (MTP) through a vesicular pathway. CM, containing ApoA5 (A5), ApoC2 (C2) and ApoC3 (C3), are secreted via the lymphatic system, enter the vena cava and circulate until they interact with lipoprotein lipase (LPL) (Hegele, 2009; Hussain, Fatma, Pan, & Iqbal, 2005). LPL is synthesized in muscle, heart, and adipose tissue, then secreted and attached to the endothelium of the adjacent blood capillaries. This enzyme hydrolyzes the TG carried in CM to FA, which can be taken up by cells (Feingold & Grunfeld, 2015). CM remnants (CMRs) are internalized by hepatic LDLr or in the absence of LDLr they are taken up by LDLr-related protein-1 (LRP1) (Hegele, 2009). In hepatocytes, TG and CE are transferred in the ER to newly synthesized ApoB100 and, similar to the intestine, this transfer is mediated by MTP. This assembly forms the VLDL. In a pathway analogous to the removal of CMR these VLDL remnants (IDL) particles can be removed from the circulation by the liver via binding of ApoE to LDL and LRP receptors. The remaining TG in the IDL particles are hydrolyzed by hepatic lipase (HL) leading to a further decrease in TG content, thereby yielding LDL. These LDL particles predominantly contain CE and ApoB (Feingold & Grunfeld, 2015). LDL is endocytosed by peripheral cells and hepatocytes by LDLr, assisted by an adaptor protein and controlled by the availability of cholesterol in the cells. After internalization the lipoprotein particle is degraded

in lysosomes and free cholesterol is released, being metabolized or stored in lipid droplets as CE. The LDLr can be recycled back to the plasma membrane or degraded when is complexed with PCSK9 (Horton, Cohen, & Hobbs, 2007).

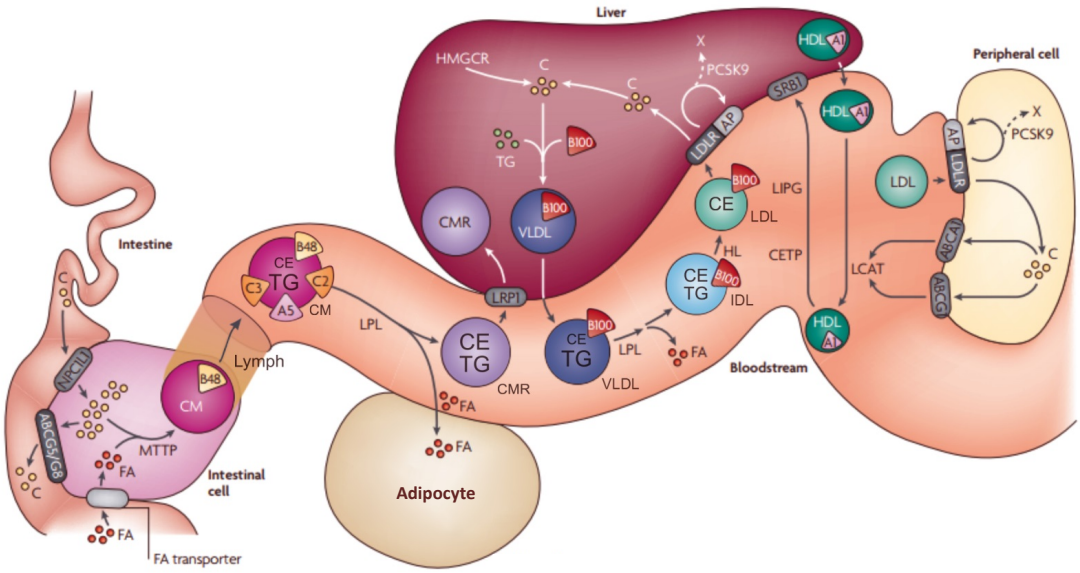

Figure 1.5 | Lipoprotein metabolism.

The main lipids in lipoproteins are free and esterified cholesterol (CE) and triglyceride (TG). In intestinal cells (enterocytes), sterols and hydrolyzed dietary TG enter into enterocytes via the Niemann-Pick C1-like 1 (NPC1L1) and fatty acid (FA) transporters, respectively. Sterols in the intestinal lumen can be resecreted by heterodimeric ATP-binding cassette transporter G5/G8 (ABCG5/G8). Reconstituted TG is packaged with CE and the apolipoprotein B (ApoB) isoform B48 into chylomicrons (CMs) by microsomal TG-transfer protein (MTP) through a vesicular pathway. CMs, secreted via the lymphatic system, enter the vena cava and circulate until they interact with lipoprotein lipase (LPL). CMs contain apoliproteins, including ApoA5 (A5), ApoC2 (C2) and ApoC3 (C3). Released free FAs incompletely enter peripheral cells, being storage in adipocyte tissue. CM remnants (CMRs) are taken up by hepatic LDL receptor (LDLr), in the absence of LDLr they are taken up by LDLr-related protein-1 (LRP1). In liver cells (hepatocytes), cholesterol is recycled or synthesized de novo, with 3-hydroxy-3-methylglutaryl coenzyme A reductase (HMGCR) being rate-limiting. Then, esterified cholesterol is packaged with TG and the ApoB isoform B100 into very low-density lipoprotein (VLDL); the TG contained in plasmatic VLDL is hydrolyzed by LPL, releasing FAs and VLDL remnants (IDL) that are hydrolyzed by hepatic lipase (HL), thereby yielding LDL. LDL transports cholesterol from the liver to the periphery. LDL is endocytosed by peripheral cells and hepatocytes by LDLr, assisted by an adaptor protein (AP). Proprotein convertase subtilisin/kexin type 9 (PCSK9), when complexed to LDLr, short-circuits recycling of LDLr from the endosome, leading to its degradation (X). In HDL cholesterol metabolism, HDL, via ApoA-I (A1), mediates reverse cholesterol transport by interacting with ATP-binding cassette A1 (ABCA1) and ABCG1 transporters on non-hepatic cells. Lecithincholesterol acyltransferase (LCAT) esterifies cholesterol so it can be used in HDL cholesterol. After HDL remodeling by cholesterol ester transfer protein (CETP), which transfer CE to LDL, and by endothelial lipase (LIPG), enters hepatocytes via scavenger receptor class B type I (SRB1) and can be secreted trough liver biliary excretion. Adapted from (Hegele, 2009).

In HDL cholesterol metabolism, HDL, via ApoA-1, mediates reverse cholesterol transport via cellular efflux pumps ATP-binding cassette A1 (ABCA1) and ABCG1 transporters on non-hepatic cells. The serum enzyme lecithin-cholesterol acyltransferase (LCAT) associates to discoid HDL and esterifies cholesterol to CE, with CE accumulation in the middle core in HDL. Then they become more spherical and are taken up by the liver for excretion or recirculation of their constituents. CE can also be transfered from HDL to VLDL in exchange with TG to HDL by cholesteryl ester transfer protein (CETP). In addition, when cholesterol is transferred to the liver, HDL can transfer cholesterol via interaction with SR-BI, associated to the

HL, where can be eliminated through the biliary secretion into the feces (Anastasius et al., 2016; Rigotti, Miettinen, & Krieger, 2003).

With aging, approximately half of our cholesterol is derived from *de novo* biosynthesis (Michael W King, 2013). Acetyl coenzyme A (acetyl CoA) arises from the oxidation of amino acids, fatty acids, and pyruvic acid is metabolized to hydroxyl methyl glutaryl coenzyme A (HMG-CoA). In a rate-limiting step inhibited by the statin class of drugs, such as, pravastatin, HMG-CoA is converted to mevalonate, which, in turn, is converted to cholesterol through a series of enzyme-catalyzed reactions. A detailed understanding of this pathway led to the development of statins, which have revolutionized the treatment of hypercholesterolemia (Hajjar & Hajjar, 2016; Michael W King, 2013). Since, in healthy adults can synthesize ± 1 g per day of cholesterol and, on a Western diet, we can consume approximately 0.4 g (Michael W King, 2013), total serum cholesterol levels (<200 mg/dL) can usually be maintained by controlling cholesterol synthesis. Thus, inhibition of HMG-CoA reductase by statins can reduce deposition of cholesterol in blood vessels. However, unacceptable side-effects associated with statins administration underscore the need for new therapies. In addition, excessive reduction of serum cholesterol can be also deleterious due to its role in multiple biosynthetic reactions (Hajjar & Hajjar, 2016). Therefore, maintaining cholesterol homeostasis is vital.

1.2.2 Macrophage cholesterol metabolism

During the initial fatty streak phase of atherogenesis, the monocyte-derived macrophages internalize the retained ApoB-containing lipoproteins, which are degraded in lysosomes, where excess free cholesterol is trafficked to the ER. Oxidative modification of LDL particles enhances their uptake through a number of receptors not down-regulated by cholesterol levels including CD36, SR-A, and lectin-like receptor family (LOX-1) (Figure 1.6) (Ashraf & Gupta, 2011; Moore & Freeman, 2006). However, *in vitro* studies have proved evidences of alternative mechanisms, including phagocytosis of matrix-retained LDL and fluid phase pinocytosis of native LDL and aggregated LDL (Moore et al., 2005). Once ingested, LDL are degraded and CE are hydrolyzed in late endosomes/lysosomes in to cholesterol, often referred as free cholesterol, and fatty acid. Free cholesterol is trafficked to peripheral cellular sites by a mechanism involving the late endosomal proteins NPC1 and NPC2 (Ouimet et al., 2011). Delivery of free cholesterol to the ER has important roles in downregulating both LDL receptors and endogenous cholesterol synthesis by suppressing the sterol-regulatory element binding pathway (SREBP) (Michael S. Brown & Goldstein, 1997). In ER free cholesterol is esterified by acyl CoA:cholesterol acyltransferase (ACAT), and the resulting CE is packaged into cytoplasmic lipid droplets, which are characteristic of foam cells (Figure 1.6) (M. S. Brown, Ho, & Goldstein, 1980).

Cytoplasmic CE is cleared by two major pathways. The first route described involves the hydrolysis of cytoplasmic CE by cholesterol ester hydrolase (NCEH) and the resulting free

cholesterol is mobilized away from the ACAT pool (M. S. Brown et al., 1980) and made available for efflux via ABCA1, ABCG1, SR-BI, and aqueous diffusion. Alternatively, cytoplasmic CE in lipid droplets are packaged into autophagosomes, which are trafficked to lysosomes, where the CE is hydrolyzed by lysosomal acid lipase generating free cholesterol mainly for ABCA1-dependent efflux (Ouimet et al., 2011). This process is specifically induced upon macrophage cholesterol loading, being the lysosomal hydrolysis a crucial process in the mobilization of lipid droplets-associated cholesterol for reverse cholesterol transport (Ouimet & Marcel, 2012).

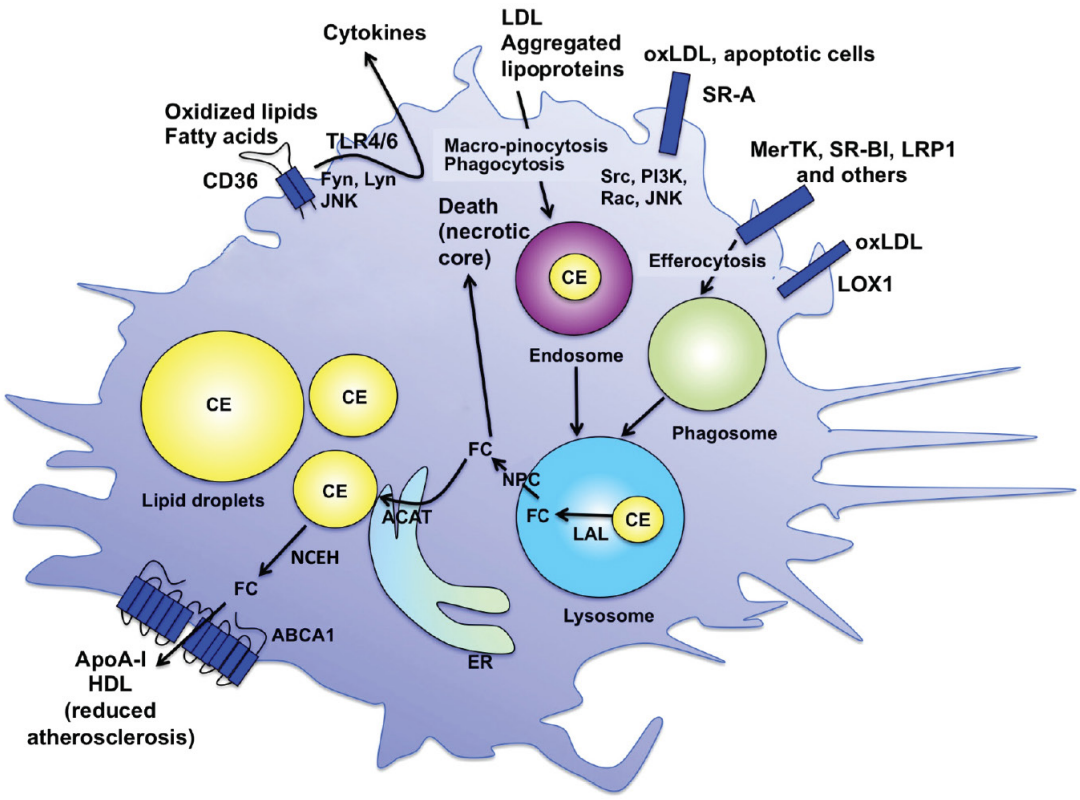

Figure 1.6 | Macrophage lipid metabolism and its effect on macrophage phenotype

Lipoproteins are taken up by macrophages through macropinocytosis, phagocytosis, and scavenger receptors (SRs), including SR-A, CD36, SR-BI and LOX1. The SRs also have signaling capacities. Because the lipoproteins are degraded in endosomes–lysosomes, cholesteryl ester (CE) is converted to free cholesterol (FC) and fatty acids by lysosomal acid lipase (LAL). Most of the FC partitions into, and is removed as vesicles form, from the lysosome membrane. The bulk of the lysosomal FC is delivered to the plasma membrane where it plays a critical role in modulating plasma membrane function. Other FC portion is redistributed to other cellular compartments through Niemann–Pick disease, type C (NPC) proteins. FC is converted back to CE by acyl-CoA cholesterol acyltransferase (ACAT) in the endoplasmatic reticulum (ER) and the excess is stored as CE droplets in the cytoplasm. CE within these cytoplasmic lipid droplets can be hydrolyzed back to FC by the enzyme neutral cholesterol ester hydrolase (NCEH) and then FC is effluxed from the cell through the cholesterol exporters ATP-binding cassette, sub-family A, member 1 (ABCA1) and ATP-binding cassette, sub-family G, member 1 (ABCG1) to apolipoprotein A-I (ApoA-I) or high-density lipoprotein (HDL). FC can exert detrimental effects if it is not re-esterified to CE in lipid droplets or effluxed through ABCA1 and ABCG1. For example, cholesterol crystal formation leads to inflammasome activation, and FC accumulation causes ER stress and cell death. These processes promote progression of lesions of atherosclerosis and necrotic core expansion. Adapted from (Tabas & Bornfeldt, 2016).

1.3 INFLAMMATION

Although the presence of inflammatory cells in lesioned arteries was described as early as the 1800s by Rudolph Virchow and others, it took decades for the role of inflammation in the pathophysiology of atherosclerosis progression to be fully appreciated. Evidence has emerged from various studies about the inflammatory etiology of atherosclerosis – both innate and adaptive immune-mediated inflammation (Göran K. Hansson, 2005b; Libby, 2012; Libby, Ridker, & Maseri, 2002). Nowadays, although it is well established that inflammation plays an essential role in the initiation, progression, and destabilization of atherosclerotic plaques, the mechanisms that drive the persistent non-resolving inflammation in the vessel wall remain incompletely understood (Ira Tabas & Bornfeldt, 2016). The major immune cell present in atherosclerotic lesions is the macrophage. Cells of the adaptive immune system such as T and B lymphocytes are also present, but in lower numbers. Several lines of evidence have demonstrated that innate immune cells can adopt a persistent proinflammatory phenotype, known as trained immunity, after brief exposure to a variety of stimuli (Christ, Bekkering, Latz, & Riksen, 2016).

1.3.1 Immune response

A dynamic population of innate and adaptive immune cells exists in the arterial wall throughout the different stages of atherosclerotic lesion development. The activation of innate immune cells occurs in the absence of any contribution by adaptive immune cells. The ensuing release of inflammatory mediators by resident tissue macrophages and neutrophils alerts the local tissue cells. Consequently, it initiates continued recruitment of immune cells to the developing lesion, which greatly amplifies the initial inflammatory response and profoundly alters the metabolism of resident arterial wall cells. The adaptive immune responses mounted by T and B lymphocytes arriving later at the inflamed site and are shaped by the ongoing innate response (Gisterå & Hansson, 2017b; Witztum & Lichtman, 2014). Conversely, monocyte-derived macrophages are a major cell population in atherosclerotic plaques and, in this section these cells will receive more attention due to their relevance to the work of this thesis.

1.3.1.1 Innate immune response

In atherosclerotic plaques, a key component of the inflammatory process is the persistence of different innate immune cell types including mast cells, neutrophils, NK cells, monocytes, macrophages and dendritic cells (DCs) (Chávez-Sánchez et al., 2014). In response to tissue damage or infection, neutrophils infiltrate in response to CXCL8 release by EC, followed by monocytes. Recently, neutrophils were demonstrated to have a crucial role in the initiation and progression of atheromatous plaque (Döring, Soehnlein, & Weber, 2017). Stimulated

neutrophils release granules which instruct the recruitment and activation of monocyte, macrophages and DCs (Soehnlein, 2012). Besides the release of granule proteins, proteases, and reactive oxygen metabolites, neutrophils also respond to infectious challenges via the formation of NETs. NET formation may occur at all stages of atherosclerosis progression, is responsible for macrophage priming, as briefly mentioned before (Warnatsch et al., 2015) and also exacerbates endothelial dysfunction (Qi, Yang, & Zhang, 2017). In advanced plaques, neutrophil-derived proteases (such as, MPO) and ROS increase the degree of plaque destabilization (Döring et al., 2017) through the induction of EC apoptosis in humans (Denny et al., 2010). The lifespan of neutrophils is short and they eventually undergo apoptosis, which is, *per se*, an anti-inflammatory process since clearance of apoptotic neutrophils by macrophages unleashes signals for the resolution of inflammation. However, if the engulfment capacity of macrophages is exceeded, then neutrophils became necrotic, perpetuating the inflammation (Soehnlein, 2012).

Monocytes and macrophages effectively promote the initiation, progression, and destabilization of atherosclerotic plaques by several mechanisms (Boring, Gosling, Cleary, & Charo, 1998; Potteaux et al., 2011). Monocytes are another type of leukocyte recruited during atherosclerosis; these myeloid lineage cells are of great interest in atherosclerotic disease due to their phenotypic and functional heterogeneity. In mice, two monocyte subsets, Ly-6C^{high} and Ly6C^{low}, have been described as fundamental drivers of inflammatory responses and the resolution of inflammation, respectively (C. Shi & Pamer, 2014). In contrast, three monocyte subsets have been identified in humans based on their CD14 and CD16 surface expression: CD14^{+}/CD16^{-} “classical” monocytes, CD14^{+}/CD16^{+} “intermediate” monocytes and “nonclassical” CD14^{-}/CD16^{+} (Chávez-Sánchez et al., 2014; R. Mukherjee et al., 2015). Several studies have shown that hypercholesterolemia considerably increases the number of circulating Ly6C^{high} proinflammatory monocytes in mice (or the CD14^{+}CD16^{-}/CD14^{+}CD16^{+} equivalent in humans), thereby accelerating atherosclerosis (Swirski et al., 2007; Wildgruber et al., 2016). Additionally, hypercholesterolaemia and cardiovascular events, such as, acute myocardial infarction, stroke or sepsis have been associated with an increase in monocytosis (Dutta et al., 2012; Murphy et al., 2011; Rahman et al., 2017). Interestingly, hypercholesterolaemia-mediated monocytosis in the bone marrow and blood compartments might be dependent on chemokine signaling, specifically mediated by C¬C motif chemokine 2 (CCL2), C¬C chemokine receptor type 5 (CCR5), CCR2 and CX3CR1 (Rahman et al., 2017). However, myeloid priming and reprogramming under hypercholesterolaemic conditions can occur within the bone marrow, due to an overload of cholesterol and defective efflux pathways in hematopoietic stem and myeloid precursor cells (Jia, Gao, & Zhao, 2017). Through bone marrow transplantation experiments, it was showed that bone marrow from Western type diet fed animals in *Ldlr*$^{-/-}$ mice fed with a chow diet markedly increased myeloid progenitor proliferation compared to donor bone marrow from chow fed animals (van Kampen, Jaminon, van Berkel, & Van Eck, 2014). Thus, it has been highlighted the relationship between hypercholesterolemia, altered epigenetic patterning in hematopoietic stem cells and myeloid progenitors, and increased susceptibility to atherosclerosis (Jia et al., 2017).

Within atherosclerotic plaques, during the early stages of atherogenesis, the population of macrophages resulting from recruitment of Ly6C^{high} monocytes; and in advanced lesions, arterial plaque macrophages, are sustained by local proliferation (Robbins et al., 2013a) (a more detailed description is in section 1.3.2.1). During the early stages of atherosclerosis, macrophages contribute to the clearance of reactive lesional ox-LDL particles and apoptotic cells. In later stages, macrophages are impaired in their phagocytic functionality due to intracellular accumulation and defective efflux of ox-LDL. Foam cell macrophages undergo apoptosis due to cellular stress and inflammatory responses, a process, which ultimately contributes to the formation of the pro-thrombotic necrotic core that characterizes unstable atherosclerotic plaques. Multiple triggers could hence cause an inflammatory milieu in the plaque through the increase of proinflammatory molecules release, as IL-1β (Duewell et al., 2010). Finally, lesional macrophages contribute to the remodeling of atherosclerotic plaques into a rupture-prone unstable phenotype by the production of proteases, such as matrix metalloproteinases (Shah, 2003). Overall, plaque macrophages display a marked phenotypic heterogeneity (Colin, Chinetti-Gbaguidi, & Staels, 2014), which is dictated by the composition of the local DAMPs that are present in the specific environment during different stages of plaque development.

Mast cells express a variety of pattern recognition receptors (PRRs) and Fc receptors, which are susceptible to activation by the crosslinking of Fc receptors and IgE, as well as, by other mechanisms, such as cytokines (IL-1β and TNF-α), leading to the release of various inflammatory mediators that can affect lesion development (Kumar & Sharma, 2010). These inflammatory cells are found in the intima of healthy carotid arteries and in early and advanced atherosclerotic lesions. *In vivo* studies have showed that a specific mast cells deficiency significantly reduced atherogenesis in mice (J L Johnson, Jackson, Angelini, & George, 1998; Sun et al., 2007). After activation mast cells present an important function in plaque activation and acute coronary syndromes because they produce a host of proteases (including some produced by macrophages), and numerous vasoactive chemoattractants which accumulate in the perivascular tissue surrounding atherosclerotic arteries (Conti et al., 2017). Factors released from mast cells may degrade the extracellular matrix and could also influence the functions of surrounding cells and modify locally deposited lipoproteins (G. K. Hansson, 2002).

The role of NK cells in response to microbial pathogens and inflammatory disorders such as atherosclerosis has received increasing attention in recent years. The natural killer T (NKT) cells are a specialized subset of CD4^{+} T cells, representing a link between the innate and adaptive immune systems (Chávez-Sánchez et al., 2014). Endogenous self-lipid antigens and exogenous lipid antigens, including those on microorganisms can activate NKT cells. CD1d molecules on antigen-presenting cells - DCs, macrophages, and B cells, presented glycolipids or phospholipids to the T-cell receptor on NKT cells, which results in the rapid production of cytokines and cytotoxic proteins (Getz & Reardon, 2017). Numerous studies have shown that NKT cells can promote atherogenesis (Martin-Murphy et al., 2014; VanderLaan et al.,

2007), with the release of inflammatory cytokines such as IFN-γ a key component in the role of NKT cells in the atherogenic process (Major et al., 2004; Tupin et al., 2004). Then, NKT cells can promote atherosclerosis also by the induction of apoptosis by cytotoxic proteins (Getz & Reardon, 2017).

DCs, which are antigen-presenting cells, exhibit a variety of antigens to T cells in addition to initiating and sustaining immune responses, as well as, inhibiting the activation of T cells. DCs are transformed by activated innate immune receptors, such as the Toll-Like Receptors (TLR), into antigen-presenting cells that activate T effector cells, whereas, immunological tolerance is produced by antigen presentation which develops when TLR activation is not present (Ilhan & Kalkanli, 2015). Therefore, DCs also play a critical role in bridging innate and adaptive immune responses (Wigren, Nilsson, & Kolbus, 2012). In the lesion, DC precursors or monocytes are recruited to the arterial intima where they differentiate into DCs. $CD11c^+$ DCs, a DC subset, have been found in atherosclerotic lesions and can exert different proatherogenic and protective functions (A Zernecke, 2015). DCs can engulf ox-LDL, adopting a foam cell-like appearance, inducing costimulatory molecules and cytokine expression (Perrin-Cocon et al., 2001; A Zernecke, 2015). The interactions between DCs and NKT cells induce IL-12 production by DCs which increases IFN-γ secretion in T cells and NKT cells. In macrophages, IFN-γ induces metalloproteinase secretion and inhibits the secretion of extracellular matrix proteins derived from SMCs, inducing atherosclerotic plaque destabilization. Additionally, DCs secret TNF-α, which induces an increase in adhesion molecule expression on the endothelium (Chávez-Sánchez et al., 2014), promoting the recruitment of inflammatory cells.

1.3.1.2 Adaptive immune response

Accumulating evidence supports a key regulatory role for adaptive immunity in atherosclerosis and its complications. The adaptive immune responses mounted by T and B lymphocytes arriving later at the inflamed site are shaped by the ongoing innate response. Despite their minority status, lymphocytes — particularly T lymphocytes — appear to function decisively in the regulation of inflammation during atherogenesis, regulating the innate inflammatory response in atherosclerosis (Libby, 2012). A key unresolved question is the identity of the relevant activating antigens of T cells in atherosclerotic plaques. However, some reports have identified potential endogenous antigens, including LDL and heat shock protein, which may stimulate adaptive immunity (Witztum & Lichtman, 2014). Modified LDL are processed by DCs and presented as peptide/major histocompatibility complex (MHC) molecules to naive T cells in secondary lymphoid tissues, leading to clonal T cell expansion and differentiation into effector T cells, such as Th1 or Th17 cells. The effector T cells migrate into arterial lesions, where resident macrophages or DCs present the same peptide-MHC antigens. This process leads to effector T cell activation and expression of proinflammatory effector molecules, such as secreted IFN-γ and IL-17 and membrane-bound CD40 ligand. These molecules promote lesion growth and/or destabilization (Lichtman, Binder, Tsimikas, & Witztum, 2013). Thus, like mononuclear phagocytes, T lymphocytes exhibit functional diversity. The Th1 lympho-

cytes appear to accelerate atherogenesis response. Th17 cells may also exert particularly proinflammatory actions, while Th2 cells release cytokines that may modulate inflammation such as IL-4 that can promote humoral immunity. However the role of Th2 in atherosclerosis is controversial (Libby, Ridker, & Hansson, 2009). Regulatory T cells, through the secretion of transforming growth factor beta (TGF-β) and in some cases IL-10, appear to limit atherosclerosis. Thus, the balance between these T-cell subsets with CD4 surface markers may influence the formation and character of lesions (Andersson, Libby, & Hansson, 2010).

The main role of B cells in immunity is to mount antibody responses and act as antigen presenting cells for T cells (Ketelhuth & Hansson, 2016). B cells play important roles in both innate and adaptive immunity through both antibody production and cytokine release. B cells are divided into two sub types: B1 and B2 cells. B cells also populate plaques and it has been shown that the elimination of B cell populations increases plaque formation, whereas adoptive transfer of B cells protected mice from developing disease (Caligiuri, Nicoletti, Poirierand, & Hansson, 2002). Humoral immunity, appears to mitigate atherogenesis (Libby, 2012). B1 cells that give rise to natural IgM antibody have been associated with a protective function against atherosclerosis (Ketelhuth & Hansson, 2016; Kyaw et al., 2011). Vaccination with putative antigens, such as modified LDL, appears to protect against atherosclerosis (Libby, 2012). In contrast, B2 lymphocytes may aggravate atheroma lesions development (Binder et al., 2008). Indeed, depletion of B cells with anti-CD20 antibody treatment limits lesion size in mice in an IL-17-dependent manner (Ait-Oufella et al., 2010). However, it was also demonstrated that resident adventitial B cells mediated protection from early atherosclerosis in part through inhibiting intimal macrophage accumulation (Doran et al., 2012). Indeed subsets of regulatory B cells, including B cells that secrete IL-10, are well known (Mauri & Bosma, 2012). These data indicate a complex role for B cells and B cell subsets in atherogenesis. Thus, it was suggested that B cells affect lesion formation both systemically via secretion of antibodies and locally within the aorta, by affecting macrophage and T cell biology (Lichtman et al., 2013).

1.3.2 Macrophages

Macrophages are integral cells of the innate immune system that perform both immune surveillance and homeostatic functions. Resident macrophages are found in almost all healthy human tissues, comprising ≈10 % of total cells in many tissues (Sasmono et al., 2003). Macrophages are stellate cells typically occupying a niche in close contact with endothelial or epithelial cells. As described by Elie Metchnikoff in the 19th century (Metschnikoff, 1893), the key function of macrophages is continuous phagocytosis of material, both host-derived and microbial, from their surroundings (from Greek: *makros*, “large”, and *phagein*, “eat”). However, resident tissue macrophages develop highly specialized functions related to their niche. Heterogeneity and plasticity are, indeed, the defining features of macrophages and present a crucial role in all stage of atheroma development (Ira Tabas & Lichtman, 2017). In the following sections, some of the key aspects of macrophage biology and their role in the atherogenesis process will be discussed.

1.3.2.1 Mechanism of macrophages accumulation in atheroma

According to the traditional view, resident tissue macrophages differentiate from circulating bone marrow-derived monocytes that infiltrate peripheral tissues (Hume 2008, van Furth 1968). The circulating monocytes recruitment to the arterial intima is fundamental in the initiation and progression of atherosclerotic lesions. In plaque, Ly6C^{high}CCR2^{+} monocytes have been identified as the major precursors of plaque macrophages. Their recruitment to plaques depends on expression of the chemokine receptors CCR2, CCR5, and CX3CR1 (Swirski et al., 2007; Tacke et al., 2007). Bone marrow hematopoiesis has long been considered the major, source of monocytes in atherosclerosis (Nagareddy et al., 2013; Soehnlein & Swirski, 2013). However, it is now well established that also extramedullary hematopoiesis in the spleen significantly contributes to atherosclerosis associated monocytosis and that monocytes originating from the spleen participate in macrophage accumulation within lesions. Mechanistically, hematopoietic stem cells migrate from the bone marrow to the spleen, where the microenvironment supports their progressive differentiation towards mature monocytes (Robbins et al., 2012). Moreover, a study based on a model of parabiosis, where the blood circulation of two mice is joined, shed new light on macrophage proliferation as a source of atherogenic macrophages. Through the discrimination of the cell origin in tissue from either recruited, circulating or locally expanded cells, macrophage accumulation in established lesions was predominantly dependent on macrophage proliferation. In other hand, recruitment of circulating monocytes was only instrumental in the early phases of the disease (Robbins et al., 2013b). In contrast to this finding, a recent report suggested that macrophage proliferative activity was higher in early rather than in advanced lesions (Lhoták et al., 2016). In addition, it was also found that a substantial proportion of macrophages in established lesions are senescent (B. G. Childs et al., 2016), thus providing a contrasting picture of the role of macrophage proliferation in atherosclerosis. The fact that highly proliferative and plastic vascular SMCs can adopt a macrophage-like phenotype and express classical macrophage markers, such as Mac3 or Mac2, in lesions further complicates interpretation of studies investigating macrophage proliferation in atherosclerosis (Feil et al., 2014). It was shown that cells co-expressing macrophages and vascular SMC markers make up to 50% of the cells identified as macrophage (Allahverdian, Chehroudi, McManus, Abraham, & Francis, 2014).

Early colonialization of bone marrow-derived monocytes during embryonic development has also been implicated in atheroma initiation and development. In the absence of hypercholesterolemia and atherosclerotic disease, healthy arteries already contain resident macrophages and DCs. This was recently demonstrated with the help of genetic fate mapping models, and it reveals that murine arteries contain a resident population of macrophages derived from two distinct sources: bone marrow-derived monocytes that colonize arterial tissue during embryonic development and in the colonization during the first few days after birth (Ensan et al., 2015). The role of this resident macrophage population in atherosclerosis remains to be determined, but it is conceivable that they may impact disease initiation in a similar fashion

to vascular resident DCs that take up lipids and form foam cells at very early stages of lesion formation (Paulson et al., 2010). Their proliferative ability also suggests that they may contribute to macrophage accumulation during lesion progression. Regardless of their origin, the differentiation, survival, and proliferation of all tissue macrophages is maintained by constant secretion of M-CSF by stromal cells and signaling via its receptor, CSF1R (Jenkins & Hume, 2014). The balance between M-CSF secretion and consumption defines the size of a tissue macrophage population at any given time (Hume, 2008).

1.3.2.2 The role of macrophages in atherosclerosis

As stated before, macrophages are the most abundant immune cell types in atherosclerotic lesions and have an essential role during all stages of the disease, from lesion initiation to plaque rupture. One of the key features of macrophages is their high degree of plasticity that allows them to produce a fine-tuned response to various microenvironmental stimuli (Bobryshev, et al., 2016). In general, inflammatory macrophages carry out processes that promote atherosclerosis progression, whereas resolving macrophages carry out functions that can suppress plaque progression and promote their regression (Peled & Fisher, 2014). By secreting cytokines, proteases, and other factors, inflammatory macrophages increase the cellular expansion of lesions and cause plaque morphological changes that can trigger plaque rupture and acute luminal thrombosis. Some of the cytokines which have been assigned a proatherogenic role are IL-1β, TNFα, IL-6, IL-18, and IL-12 (Cochain & Zernecke, 2017; Tabas & Lichtman, 2017). Additionally, inflammatory macrophages are known to have a strong proteolytic activity (Quillard, et al., 2011). *In vivo* studies have providing evidences of macrophage-derived metalloproteinases (MMP), namely MMP-9 and 14 (Gough, et al., 2006; Schneider et al., 2008) which are important in collagen fibrous cap thinning, demonstrating the critical role of macrophage-mediated proteolysis in plaque destabilization. In contrast, resolving macrophages carry out functions that are associated with plaque stabilization. These macrophages also produce anti-inflammatory cytokines, and leukocyte-specific deficiency of IL-10 or IL-13 increased plaque inflammation and lesion formation (Cardilo-Reis et al., 2012). These functions include: i) efferocytosis, which stabilize plaques by preventing post-apoptotic cellular necrosis; ii) secreting collagen that can form a protective cap over the lesion; and iii) producing proteins and lipids that suppress inflammation and promote tissue repair (Tabas & Lichtman, 2017).

Formation of macrophage foam cells in the vascular intima is a hallmark of atherosclerosis. The extent to which macrophages accumulate intracellular lipids represents the balance between extracellular lipid uptake and reverse lipid transport from the intracellular compartment to extracellular lipid acceptors (Cochain & Zernecke, 2017). As discussed previously, macrophages take up modified LDL through scavenger receptors among others (Tabas & Bornfeldt, 2016). Therefore, several experimental studies in mice deficient in scavenger receptors have confirmed their role in foam cell formation and atherogenesis progression (Lillis et al., 2015; Mehta et al., 2007; Moore et al., 2005; Robbins et al., 2013a). Recent research

demonstrated that the adhesion receptor CD146, which is expressed on human and murine plaque macrophages, also has a role in foam cell formation, mediating the accumulation of ox-LDL and macrophage activation by driving CD36 internalization (Luo et al., 2017).

The proliferative capacity of macrophages can also be considered an important functional trait of lesional macrophages (Cochain & Zernecke, 2017; Robbins et al., 2013a). In contrast to proliferating macrophages, lesions also contain cells with terminal loss of proliferative ability, namely senescent cells. It has been reported that senescent macrophage foam cells were pathogenic during the whole atherogenic process (B. G. Childs et al., 2016; Bennett, et al., 2015; J. C. Wang & Bennett, 2012) and the clearance of these cells from established lesions halted lesion progression and was associated with features of plaque stability (B. G. Childs et al., 2016). Thus, senescence can be considered as a novel deleterious dysfunctional state of macrophages in lesions. Moreover, survival and apoptosis in plaques represent critical aspects of macrophage biology in atherosclerosis. Both processes contribute, not only to necrotic core formation, but can also underlie plaque regression and resolution of inflammation upon normalization of blood lipid levels (Potteaux et al., 2011). However, it is still unclear how modulation of macrophage survival impacts atherosclerosis, since contradictory results have been reported regarding its beneficial or deleterious effect (Babaev et al., 2016; Bouchareychas et al., 2015; Cochain & Zernecke, 2017). Whether increased macrophage survival or apoptosis ultimately determines plaque progression or regression most likely depends on the plaque stage and total efferocytotic ability of surrounding viable macrophages (Cochain & Zernecke, 2017).

Finally, macrophage efferocytotic ability has a critical impact on atherosclerotic lesion formation and progression (E. Thorp & Tabas, 2009; Van Vré, et al., 2012). Apoptotic cells can be recognized by phosphatidilyserine (PS) binding protein milk fat globule-EGF factor 8 (MFG-E8) and growth arrest-specific 6 (GAS6) which bind to αvβ3/β5 integrins and c-Mer tyrosine kinase (MER-TK), respectively, on macrophages. The deletion of these PS-binding proteins have been associated with increased atherosclerosis and necrotic core formation (Ait-Oufella et al., 2007, 2008; Edward Thorp, et al., 2008). Blockade of T-cell immunoglobulin and mucin domain protein (TIM)-1 or TIM-4, which also recognize PS on apoptotic cells (Foks et al., 2016), or genetic deficiency in the complement C1q, in macrophages (involved in apoptotic cell clearance) also increased lesion formation in *Ldlr*$^{-/-}$ mice (Bhatia et al., 2007). Thus, efferocytosis is a crucial and therapeutically targetable function of atherosclerotic lesional macrophages.

1.3.2.3 Macrophage subsets in atheroma

Several classes of macrophages have been described based on their marker expression, the production of specific factors, and their biological functions in response to a specific environmental stimulus (Martinez, 2008; P. J. Murray et al., 2014). Such plasticity and heterogeneity made it challenging to achieve a comprehensive macrophage classification. Moreover, *in vitro* studies of macrophage activation and differentiation may not reflect the

in vivo situation accurately enough. These processes are well regulated by various factors present in the organism's blood and tissues and *in vitro* they can be only modelled roughly (Bobryshev et al., 2016). Atherosclerotic lesion site provides a specific microenvironment, enriched with activated cells, modified lipoproteins, and proinflammatory factors, as well as with dying and apoptotic cells. Consequently, the macrophage population of atherosclerotic plaques is heterogeneous (De Paoli, Staels, & Chinetti-Gbaguidi, 2014).

The identification of pro- and anti-inflammatory macrophages led to the establishment of the classical model of macrophage activation. This model defined two main phenotypes of macrophages: proinflammatory M1 and alternative or resolving M2. M1 macrophages differentiate in response to TLR and IFN-γ signaling and can be induced by the presence of pathogen-associated molecular complexes (PAMPs), lipopolysaccharides (LPS), and lipoproteins. These cells secrete proinflammatory factors, such as TNF-α, IL-1β, IL-12, and IL-23, and chemokines CXCL9, CXCL10, and CXCL11, as well as, ROS and nitric oxide (NO) (Table 1.3) (Chistiakov et al., 2015). On the other hand, M2 macrophages that have anti-inflammatory properties are induced in response to Th2-type cytokines IL-4 and IL-13 and secrete anti-inflammatory factors, such as IL-1 receptor agonist and IL-10 (Chistiakov et al., 2015). In atherosclerosis, lesion progression is associated with an increase of both macrophages populations, with cells expressing proinflammatory markers, such as TNF-α, preferentially distributed in shoulder regions that are more susceptible to rupture and cells bearing markers of alternative activation located in the adventitia (Kadl et al., 2010; Stöger et al., 2012). Identification of different types of macrophages in human tissues remains challenging because of the lack of specific and reliable markers (Orekhov et al., 2015). Thus, several *in vitro* experiments have revealed the effect of oxidized lipids in macrophages subsets. For instance, macrophages exposed to minimally ox-LDL, cholesterol crystals or oxidized cholesterol products (including 7 ketocholesterol) are polarized towards the proinflammatory M1 phenotype (Emanuel et al., 2014; Larrayoz, Huang, Lee, Pascual, & Rodríguez, 2010; Van Tits et al., 2011). Moreover, it has been also demonstrated that anti-inflammatory, alternatively activated macrophages (M2-like) are present in more stable regions of plaques and are more resistant to foam cell formation (Chinetti-Gbaguidi et al., 2011; Kadl et al., 2010). Lipids such as 9 oxononanoyl-cholesterol (a major CE oxidation product), sphingolipid metabolites (sphingosine 1-phosphate), ω3-PUFA derivatives and conjugated linoleic acid were found to switch macrophage polarization towards an M2-like phenotype (Hughes et al., 2008; McCarthy et al., 2013; Mitchell & McLeod, 2008; Serhan et al., 2009; Sottero et al., 2005; Titos et al., 2011). Therefore, the pro- and anti-inflammatory macrophage subtypes are directly related to the oxidation degree of the lipid composition of an atheroma and may reflect the plaque progression/instability or regression correspondingly.

Apart from the typical pro- and anti-inflammatory macrophages that can be classified into M1 and M2 types, human atherosclerotic lesions contain other specific macrophage phenotypes with pro- or anti-atherogenic properties (Table 1.3). In the haemorrhagic zones of human atherosclerotic lesions, macrophages present the M(Hb) phenotype. This subpopulation

Table 1.3 Human and mice macrophage phenotypes detected in atherosclerosis.

Adapted from (Bobryshev et al., 2016; Murray et al., 2014; Chinetti-Gbaguidi et al., 2014).

Phenotype	Induction	Markers	Secreted molecules	Functions	Role in atherosclerosis
M1 (human, mouse)	Th1 cytokines (IFN-γ, TNF-α, IL-1β), LPS, and other TRL-mediated stimuli	IL-1β, IL-6, IL-12, IL-23, TNF-α, CXCL9, CXCL10, and CXCL11	IL-6, IL-10 low, IL-12high, TNF-α, nitrites and ROS	Th1 response, antitumor	Plaque progression, maintaining inflammatory response
M2a (human, mouse)	Th2 cytokines (IL-4, IL-13)	Human: MMR, IL1RA, CCL18, CD163, stabilin-1 Mouse: Arg-1, FIZZ1, Ym1/2 and CD163	IL-10, TGF-β, CCL17, and CCL22	Tissue repair and remodelling	
M2b (human, mouse)	IL-1β, LPS	IL-10^{high}, IL-12^{low}	IL-6, IL-10^{high}, IL-12^{low}, and TNF-α	Immune regulatory functions	Enriched in regressing plaques in humans and mice
M2c (human, mouse)	IL-10, TGF-β, and glucocorticoids	Human: MMR Mouse: Arg-1	IL-10, TGF-β, and PTX3	Phagocytosis, apoptotic cell clearance	
M2d (mouse)	TLR + A_2R ligands	IL-12 (low), TNF-α (low)	IL-10, VEGF, and nitrites	Angiogenesis	Present in murine plaques
M4 (human)	CXCL4	MMR, MMP7 and S100-A8	IL-6, TNF-α, and MMP12	Weak phagocytosis	Minimal foam cell formation, potentially proatherogenic
Mox	Oxidized phospholipids	HO-1, Nrf2, Srxn1, and TR	IL-1β, COX-2	Weak phagocytosis	Proatherogenic properties in mice
HA-mac (human)	HA-mac (human)	CD163^{high}, HLA-DR^{low}	HO-1	Haemoglobin clearance	Atheroprotective
M(Hb) (human)	Haemoglobin-haptoglobin complex	MR, CD163	IL-10	Haemoglobin clearance	Cholesterol efflux atheroprotective
Mhem (human, mouse)	Heme	ATF-1, CD163, LXR	IL-10 and HO-1	Erythrocyte phagocytosis	Atheroprotective

of CD68^{+} macrophages express both macrophage mannose receptor 1 (MMR, also known as CD206) and scavenger receptor cysteine-rich type 1 protein M130 (CD163) (Boyle et al., 2009). These cells are responsible for haemoglobin endocytosis and clearance, playing a protective role in atherosclerotic lesions. Another atheroprotective macrophage subtype present in humans is Mhem. These cells also express CD163, as well as heme-dependent activating transcription factor 1 (ATF1), which induces expression of heme oxygenase-1 (Hmox-1) and liver X receptor- (LXR-) β. Mhem macrophages participate in haemoglobin clearance via erythrocyte phagocytosis and have increased cholesterol efflux due to expres-

sion of LXR-β-dependent genes LXR-α and ABCA1 (Boyle et al., 2012). These cells produce anti-inflammatory IL-10 and ApoE (Boyle, 2012). Functionally, the macrophages described above seem to be resistant to lipid accumulation and foam cell formation and have reduced levels of oxidative stress (Chinetti-Gbaguidi, Colin, & Staels, 2014).

Platelet factor 4 or CXCL4 is abundantly expressed in macrophages and the neovascular endothelium of human atherosclerotic plaques (Pitsilos et al., 2003). In humans, CXCL4 induces the M4 macrophage phenotype, which completely lacks the capacity for phagocytosis (Gleissner, Shaked, Little, & Ley, 2010). M4 macrophages play a role in the formation of unstable plaques by producing MMP 7 and MMP12 and promoting destabilization of the plaque fibrous cap (Chistiakov et al., 2015; Erbel, Wolf, et al., 2015). In addition, macrophages exposed to oxidized phospholipids differentiate into the Mox phenotype, which is triggered by the activation of the nuclear factor erythroid 2-related factor 2 (Nrf2), expressing typically Nrf2-mediated redox-regulatory genes, such as *hmox-1*, *sulfiredoxin* (*srxn1*), *thioredoxin reductase 1*(*txnrd1*), *glutathione reductase* (*gsr*) and *ferroportin* (*fpn*) (Kadl et al., 2010; Marques, Negre-Salvayre, Costa, & Canonne-Hergaux, 2016). Compared with M1 and M2 macrophages, Mox macrophages display reduced phagocytic and chemotactic capacities (Kadl et al., 2010). Recently, it was also found that the Mox phenotype presents a compromised FPN mediated iron export, suggesting iron retention in lipid-loaded macrophages (Marques et al., 2016). Moreover, in response to oxidized phospholipids, Mox macrophages express some proinflammatory markers, such as IL-1β and cyclooxygenase-2 (COX-2). In advanced atherosclerotic lesions of mice, Mox macrophages comprise approximately 34% of the total number of macrophages (Kadl et al., 2010). This macrophages phenotype were found only in mouse models of atherosclerosis, so whether Mox macrophages are also present in human atherosclerotic lesions remains to be determined.

1.3.2.4 Macrophages receptors involved in lipid signaling

The resulting endogenous danger ligands that accumulate in atherosclerotic plaques, such as modified LDL and its oxidized lipids, trigger PRRs that are expressed by macrophages, including NOD-like receptors (NLRs), scavenger receptors and TLRs, thereby activating the inflammatory response. Several studies have been performed to define and characterize the participating TLR signaling pathways or its adaptor proteins, such as myeloid differentiation primary response protein 88 (MYD88) (Björkbacka et al., 2004; Michelsen et al., 2004) in the promotion of atherosclerosis (Ding et al., 2012; Duewell et al., 2010; Michelsen et al., 2004; Mullick, Tobias, & Curtiss, 2005; Stewart et al., 2010). The extent of LDL oxidation influences their recognition by TLRs: i) minimally ox-LDL is recognized by CD14-TLR4- associated protein MD2 and initiates cytoskeletal rearrangements, as well as TNF-α, IL-6 and IL-10 production; ii) moderately ox-LDL sequestered by CD36 induces intracellular CD36-TLR4-TLR6 heteromerization, which results in NF-κB activation and chemokine expression (Stewart et al., 2010) that promote monocyte recruitment to atherosclerotic lesions; iii) finally, oxidized phospholipids and saturated fatty acids induce cooperative signaling of

CD36 and TLR2-TLR6 that promotes continuous ER stress and consequently apoptosis in human or mouse lesional macrophages (Seimon et al., 2010) (Figure 1.7). Controversially, *in vitro*, oxidized 1-palmitoyl-2-arachidonyl-sn-3-glycero-phosphorylcholine (OxPAPC) induced TLR2-dependent inflammatory gene expression and JNK and p38 signaling in macrophages, independently of CD36 (Kadl et al., 2011). In addition to these ligand-initiated signaling pathways, the enrichment of macrophage plasma membranes with free cholesterol can also lead to the sustained activation of various TLRs, including TLR3 and TLR4 (Yvan-Charvet et al., 2008; Zhu et al., 2008). Miller *et al.* also found that oxidized CE use TLR4 and spleen tyrosine kinase (Syk) to induce a proinflammatory response in macrophages (Choi et al., 2013). Thus, numerous pathways may contribute to the initiation and maintenance of TLR-induced macrophage inflammation in atherosclerotic plaques and are specifically dependent on oxidative molecule presented.

Although SR-A and CD36 mediate the majority of modified LDL uptake by macrophages *in vitro*, their genetic deletion has yielded varying effects on mouse atherosclerosis (Greaves & Gordon, 2009). It was observed that combined deficiency of SR-A and CD36 in *ApoE*$^{-/-}$

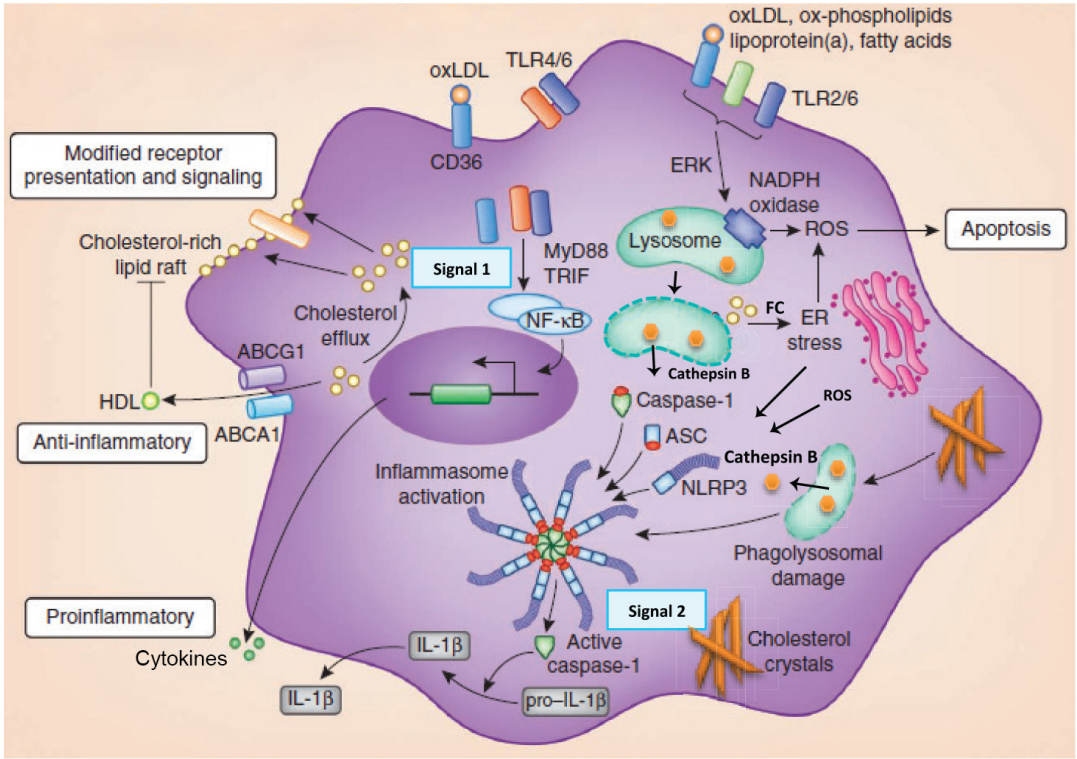

Figure 1.7 | Pathways involved in lipid signaling and inflammatory response in atherogenic macrophages.

Oxidized (ox)-LDL binds CD36, inducing intracellular CD36-TLR4-TLR6 heterotrimerization, which activates NF-κB and chemokine expression by lesional macrophages. Atherogenic lipid mediators, such as OxLDL, oxidized lipids, as weel as, fatty acids and lipoproteins, trigger NADPH oxidase activation through a CD36-TLR2-TLR6 pathway, resulting in a sustained oxidative burst and apoptosis of endoplasmic reticulum (ER)-stressed cholesterol-overloaded foam cells. Furthermore, an intracellular excess of free cholesterol, for example due to defective cholesterol efflux by ATP-binding cassette (ABC) transporters, can modify receptor presentation and signaling by increasing lipid raft formation, which in hematopoietic stem cells induces myeloproliferation due to enhanced IL-3 and GM-CSF-signaling. Also, intracellular cholesterol crystals can exert proatherogenic effects by stimulating IL-1β production by macrophages through NLRP3 inflammasome activation induced by cathepsin B lysosomal release. Lipids can also affect endothelial cell functions—the phospholipase Lipoprotein-associated phospholipase A2 (Lp-PLA2) hydrolyzes ox-LDL-associated phospholipids into oxidized fatty acids and lysophosphatidylcholine (LPC), and the derivative lysophosphatidic acid (LPA) triggers endothelial cells to secrete and present CXCL1 for monocyte adhesion. Thus, oxLDL and associated lipids act on diverse cell types to instigate inflammation and proatherogenic processes. FC, free cholesterol. Adapted from (Weber& Noels, 2011).

mice reduced progression to more advanced necrotic lesions, implicating these receptors in atheroprogression (Manning-Tobin et al., 2009). CD36 has a crucial role in the accumulation and the nucleation of cholesterol crystals within macrophages that have been treated with ox-LDL, as well as in the ensuing lysosomal disruption and NLR pyrin domain containing 3 (NLRP3) inflammasome activation (Kummer et al., 2007). Consequently, it was observed that macrophages lacking CD36 failed to induce IL-1β production in response to ox-LDL, and this result was also confirmed *in vivo*. By targeting CD36 in atherosclerotic mice, decreased serum IL-1β levels and plaque cholesterol crystal accumulation were observed (Kummer et al., 2007). Moreover, cholesterol crystals, present in early and advanced atherosclerotic plaques, are found in both extracellular spaces and within plaque macrophages, where they are known to induce the NLRP3 inflammasome (Duewell et al., 2010; R. S. Lim et al., 2011) (Figure 1.7). It has been shown that two signals are required for NLRP3 inflammasome activation: i) the first signal is NLRP3 transcription through NF-κB activation (mainly considered a TLR activated pathway) or breast cancer 1 (BRCA1)–BRCA2-containing complex (BRCC) 3 activation, a deubiquitinating enzyme; ii) the second signal is NLRP3 activation and apoptosis-associated speck-like protein containing CARD (ASC) phosphorylation, which lead to the formation of the NLRP3 inflammasome complex (Figure 1.7). When NLRP3 is activated, it interacts with ASC. ASC, in the form of speck-like cytoplasmic aggregation in cooperation with NLRP3, causes procaspase-1 to be cleaved, resulting in caspase-1 activation. Many examples of cellular dysfunction deliver the second signal required for inflammasome activation, such as K^+ efflux, ROS overproduction, ER stress, mitochondrial dysfunction, Ca^{2+} signaling and lysosome rupture (Guo, Callaway, & Ting, 2015; Hoseini et al., 2017). Consequently, activated caspase-1 cleaves pro-IL-1β into IL-1β. In atheroma lesions, uptake of pre-formed crystals by human and mouse macrophages induces lysosomal destabilization as well as the release of proteases, such as cathepsin B, and/or increase ROS production that activate NLRP3, leading to the processing and release of IL-1β (Baldrighi, Mallat, Li, & al., 2017; Hoseini et al., 2017). Patients with coronary atherosclerosis show high levels of NLRP3 expression in the aorta, with NLRP3 expression correlating with the severity of coronary artery stenosis (Paramel Varghese et al., 2016; Zheng, Xing, Gong, & Xing, 2013). The crucial role of this pathway has also been largely studied using rodent atherosclerosis models, where high NLRP3 levels were observed in macrophages (Kummer et al., 2007; Peng et al., 2015) and the deletion of its components led to reduced plaque formation (Yuan He, et al., 2016).

1.3.2.5 Cytokines profile of atheroma macrophages

More refined analysis of local vascular inflammation and the cytokines expressed in atherosclerotic plaques revealed that there is a balance between proinflammatory and anti-inflammatory cytokines and this balance is crucial for lesion development (Figure 1.8A). In general, cytokines can be classified broadly as pro- or anti-atherogenic, depending on their effects on the formation and progression of the atherosclerotic plaque.

1.3.2.5.1 Proatherosclerotic cytokines

Cytokines and chemokines, a sub-group of cytokines, play a fundamental role in the early stages of lesion formation. IFN-γ and TNF-α are proatherogenic cytokines that induce reorganization of the actin and tubulin cytoskeletons of ECs during the initial formation of an atherosclerotic lesion. This alterations lead to ECs shape changes and consequent increase in the endothelial layer permeability (Ramji & Davies, 2015). Therefore, ECs activated by ox-LDL release a variety of cytokines and chemokines, such as CCL2, which play an important role in the recruitment of circulating monocytes and other immune cells to the site of ox-LDL retention (McLaren, et al., 2011; Moore & Tabas, 2011; Soehnlein et al., 2013; Woollard & Geissmann, 2010). For circulating monocytes to enter into the arterial intima they must reduce their speed by rolling along the endothelium (Moore & Tabas, 2011; Soehnlein et al., 2013) and C-X3-C motif ligand (CX3CL)1 and chemokine CCL5 play here an important role. The rolling monocytes come to rest when adhesion molecules such as VCAM-1 and ICAM-1 bind to their receptors on the monocytes, allowing monocytes to migrate into the intima (Moore & Tabas, 2011; Ramji & Davies, 2015; Soehnlein et al., 2013). Interestingly, a deficiency of CCL2, CX3CL1 and CCL5, three of the major chemokines, and their corresponding receptors completely abrogates the development of atherosclerosis in mouse model systems (Combadière et al., 2008; Ingersoll, Platt, Potteaux, & Randolph, 2011; Ramji & Davies, 2015; Alma Zernecke & Weber, 2010), representing a promising therapeutic avenues to attenuate the development and progression of atherosclerosis (Moss & Ramji, 2016).

Once in the intima of the arteries, the monocytes are exposed to several cytokines, including M-CSF, and differentiate into macrophages (McLaren et al., 2011). As briefly discussed above, the local microenvironment together with signaling from additional cytokines will affect whether the macrophages will be proinflammatory, induced by the proinflammatory cytokines IFN-γ, IL-1β and TNF-α, or adopt an anti-inflammatory phenotype, induced by IL-4 and IL-13 (Chinetti-Gbaguidi et al., 2014; Leitinger & Schulman, 2013; McLaren et al., 2011; Wolfs, Donners, & de Winther, 2011). These proatherogenic macrophages are able to exert their deleterious actions by releasing the proinflammatory cytokines IL-1β, IL-6, IL-12, IL-15, IL-18 and TNF-α (Ramji & Davies, 2015; Ira Tabas & Bornfeldt, 2016). The cytokine CXCL4 has been identified as being able to differentiate macrophages into a proinflammatory phenotype (M4) in human atherosclerotic plaques (Erbel, Tyka, et al., 2015).

Foam cells begin to form when the balance of cholesterol uptake and efflux is in favour of uptake and retention (McLaren et al., 2011; Ramji & Davies, 2015). Cytokines have an important role in maintaining this balance since they are able to affect the expression of several key genes involved in cholesterol uptake and efflux (McLaren et al., 2011). IFN-γ can induce foam cell formation by increasing the expression of scavenger receptor, attenuating the expression of ABCA1, as well as inducing the expression of ACAT (Canton, Neculai, & Grinstein, 2013; Kzhyshkowska, Neyen, & Gordon, 2012; Ramji & Davies, 2015).

As referred before, proinflammatory macrophages also secrete IL-1α, IL-1β, IL-18 cytokines and TNF-α which play a major role in atherosclerosis progression (Moss & Ramji, 2016; Ramji & Davies, 2015) (Figure 1.8B). *ApoE*$^{-/-}$ mice which were also deficient for IL-1α and IL-β or IL-1 receptor type-1 were found to develop smaller atherosclerotic lesions compared to

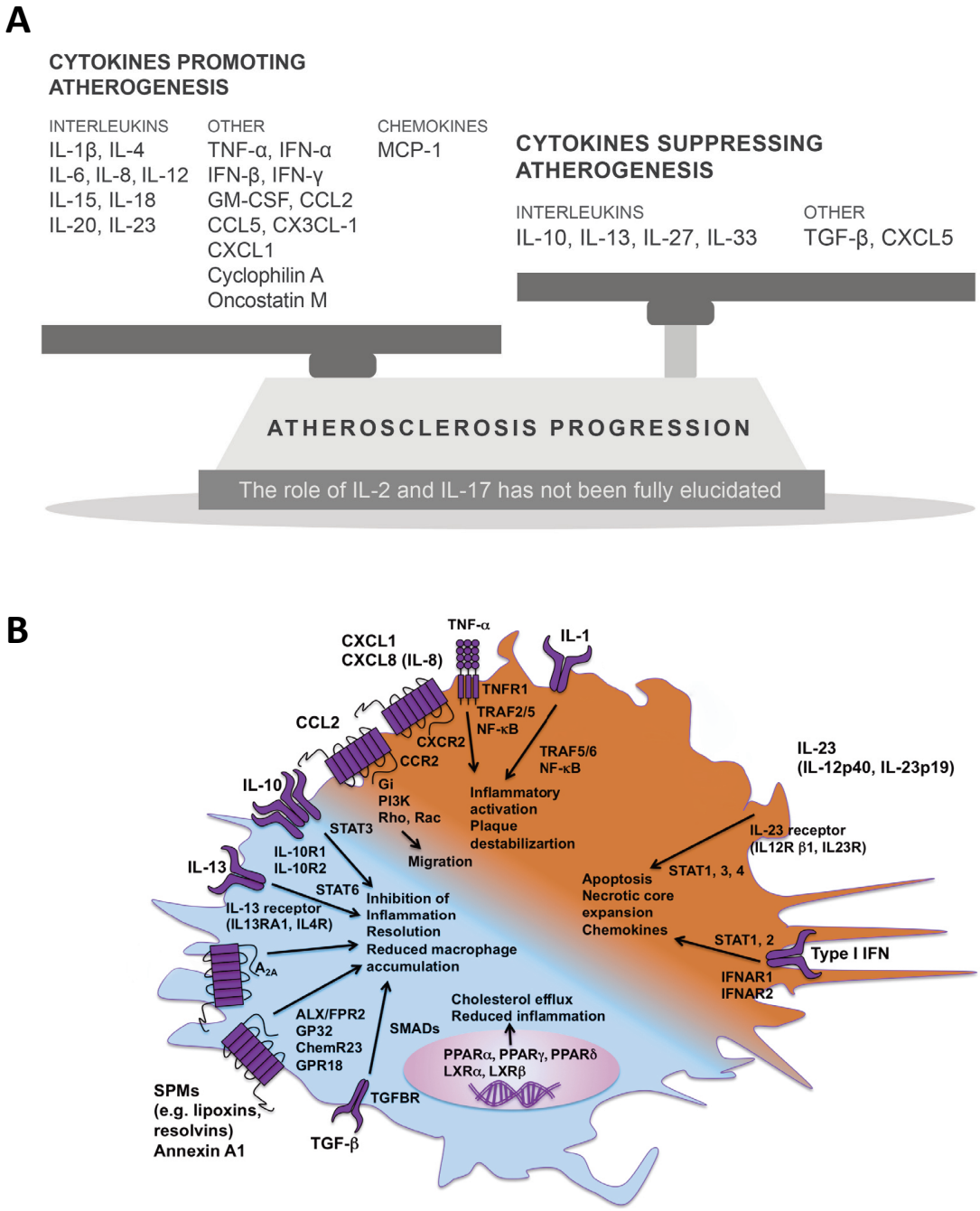

Figure 1.8 | Proatherogenic and anti-atherogenic cytokines based on their effects in mouse atherosclerosis models.

A. The balance between proinflammatory and anti-inflammatory cytokines is crucial for lesion development and imbalance is colloquially referred to exacerbate atherosclerotic disease. Pro- and anti-atherogenic cytokines. Cytokines can be divided into two groups depending on whether they promote or suppress atherogenesis. Notably, there are also cytokines such as interleukin-2 and interleukin-17 whose exact role in atherogenesis has not been fully elucidated. **B.** Receptors involved in inflammatory mediators in macrophage phenotype. Proinflammatory and proresolving mediators act on macrophages through binding to specific receptors and activation of intracellular signaling pathways. The balance between proinflammatory mediators (indicated by light brown) and proresolving mediators (indicated by blue) determines the macrophage phenotype. Effects on atherosclerosis are indicated by arrows. BLT1 indicates leukotriene B4 receptor; CCL, chemokine (C–C motif) ligand; IFN, interferon; IL, interleukin; LTB4, leukotriene B4; NF-κB, nuclear factor kappa; SPM, specialized proresolving mediators; STAT, signal transducer and activator of transcription; TGF, transforming growth factor; and TNFR1, TNF receptor 1; GM-CSF, granulocyte-macrophage colony-stimulating factor; MCP-1, monocyte chemoattractant protein. Adapted from (Tousoulis et al., 2016; Tabas & Bornfeldt, 2016).

the control mice (Kamari et al., 2011; Shemesh et al., 2012). This correlated with reduced expression of monocyte recruitment genes including CCL2, ICAM-1 and VCAM-1 in the vascular wall when IL-1β is depleted (Shemesh et al., 2012), demonstrating the proinflammatory effects of IL-1 during atherosclerosis development. Studies using *ApoE*$^{-/-}$ mice have tried to characterize the role of IL-18 in atherosclerosis development, however its exact function is still not clear. Increasing recombinant IL-18 in *ApoE*$^{-/-}$ mice amplified the development of larger and more unstable lesions (Bhat et al., 2015) and the same results were obtained in *ApoE*$^{-/-}$*IL-18*$^{-/-}$ mice (Pejnovic et al., 2009), indicating that IL-18 may actually attenuate atherosclerosis development. Other proinflammatory cytokines that promote foam cell formation include IL-6 (Schuett et al., 2012), IL-15 (van Es et al., 2011), TNF-related weak inducer of apoptosis (Sastre et al., 2014) and TNF-like protein 1A (TL1A) (McLaren, Calder, et al., 2010). IL-23 is another proatherogenic cytokine recently demonstrated to have important effects on lesions: IL-23 promotes necrotic core expansion by mediating macrophage apoptosis (Subramanian, Thorp, & Tabas, 2015; Ira Tabas & Bornfeldt, 2016).

1.3.2.5.2 Anti-atherosclerotic cytokines

The majority of anti-atherogenic cytokines, such as the classical IL- 10 and TGF-β are secreted by anti-inflammatory macrophages (Leitinger & Schulman, 2013), but it has also been shown in mouse models that IL-13 and IL-27 also retain atheroprotective function (Tabas & Bornfeldt, 2016) (Figure 1.8B). The overexpression of TGF-β in *ApoE*$^{-/-}$ mice leads to smaller and more stable plaques compared to controls after receiving a high fat diet (Reifenberg et al., 2012). Inhibition of TGF-β signaling in *ApoE*$^{-/-}$ and *Ldlr*$^{-/-}$ mice resulted in an increase in atherosclerotic lesion size, as well as increasing in inflammatory markers IFN-γ and IL-6, respectively (Gisterå & Hansson, 2017b; Lievens et al., 2013). Therefore targeting TGF-β signaling may represent a promising therapeutic avenue to reduce early lesion formation. TGF-β as well as IL-33, another anti-inflammatory cytokine, were found to be capable of attenuating macrophage foam cell formation by intefering with the expression of key genes implicated cholesterol metabolism promoting its efflux (McLaren, Michael, et al., 2010; Michael, Salter, & Ramji, 2012). In addition, studies in *ApoE*$^{-/-}$ mice in which the action of IL-33 was inhibited by injection of ST2, a soluble decoy receptor or augmented by injection of the cytokine revealed its protective role in atherosclerosis (A. M. Miller et al., 2008). Other cytokines such as IL-10 and IL-13 have also shown cardiovascular protective effects. Overexpressing IL-10 in *Ldlr*$^{-/-}$ mice resulted in an increase in cholesterol efflux, reduced apoptosis as well as a reduction in the expression of proinflammatory molecules including TNF-α and CCL2 (Han, Kitamoto, Wang, & Boisvert, 2010). Moreover, IL-13 injection in *Ldlr*$^{-/-}$ mice fed with high fat diet showed a reduced in total number of macrophages, decreasing the ratio of M1:M2. IL-13 depletion in *Ldlr*$^{-/-}$ mice induced the development of larger atherosclerotic plaques, which confirmed the anti-atherogenic properties of IL-13 (Cardilo-Reis et al., 2012). Finally, annexin A1, acting through the receptor lipoxin ALX/FPR2 (formyl peptide receptor 2), has emerged as another proresolving protein with the ability to prevent myeloid cell recruitment into atherosclerotic lesions in mice (Drechsler et al., 2015).

The cytokine role in macrophage polarization makes them a promising therapeutic target. By switching the balance of M1:M2 formation in favour of the M2 phenotype, in order to change the atherosclerotic plaque environment from a proinflammatory to an anti-inflammatory one, it will to attenuate disease progression.

1.3.2.6 Metabolic shift in the presence of an inflammatory stimulus

Immunometabolism is an evolving field, which determines the metabolic machinery of immune cells correlating how changes in metabolic phenotype affects immune cell function. The environmental signals which are involved in metabolic regulation are cytokines, growth factors, oxygen levels, and nutrient availability. As consequence to a specific microenvironment, macrophages reprogram their metabolic phenotype to fulfill cellular needs, such as survival and proliferation or to carry out specific effector functions, such as phagocytosis and cytokine production (Geeraerts, Bolli, Fendt, & Van Ginderachter, 2017).

1.3.2.6.1 Metabolic shift in classically activated macrophages

A simplistic view of proinflammatory macrophage activation (M1) with a range of stimuli, including LPS and IFN-γ (Krawczyk et al., 2010; Langston, Shibata, & Horng, 2017; Pantel et al., 2014), induces a metabolic switch from oxidative phosphorylation (OXPHOS) to glycolysis, in a phenomenon similar to the Warburg effect (Krawczyk et al., 2010). The Warburg effect was described as the metabolic profile of tumors in normoxic conditions, in which glycolysis predominates even though there is oxygen available for oxidative metabolism (Warburg, 1927). Thus, TCA cycle activity in activated macrophages and flux through the electron transport chain is diminished (Krawczyk et al., 2010; Tannahill, et al., 2013), leading to the accumulation of citrate and succinate (Jha et al., 2015), while lactate production and flux through the pentose phosphorylation pathway (PPP) are increased (Figure 1.9A) (Freemerman et al., 2014; Haschemi et al., 2012). Additionally, accumulation of succinate and citrate metabolites has been associated with a truncated TCA cycle at the level of isocitrate dehydrogenase (IDH) and succinate dehydrogenase (SDH). Accumulated citrate is exported from the mitochondria into the cytosol, where it is converted to acetyl-CoA. This metabolic intermediate is essential for several biosynthetic pathways such as the synthesis of fatty acids and the production of antimicrobial and proinflammatory molecules (including itaconic acid, NO, ROS and prostaglandins) (Gaber, Strehl, & Buttgereit, 2017). It was also shown that upon LPS stimulation and in the presence of succinate, macrophages increased mitochondrial oxidation resulting in an elevation in mitochondrial membrane potential and a mitochondrial ROS production. Together with succinate oxidation by product, these metabolic changes lead to the stabilization and increased activity of hypoxia-inducible factor-1α (HIF-1α) (Mills et al., 2016). HIF-1α in turn increases the expression of glycolytic genes, as well as inflammatory genes (Huo et al., 2012). To ensure carbon entry into the truncated TCA cycle, LPS-activated macrophages repress pyruvate dehydrogenase kinase 1, which in turn leads to sustained conversion of pyruvate into acetyl-CoA via pyruvate dehydrogenase and

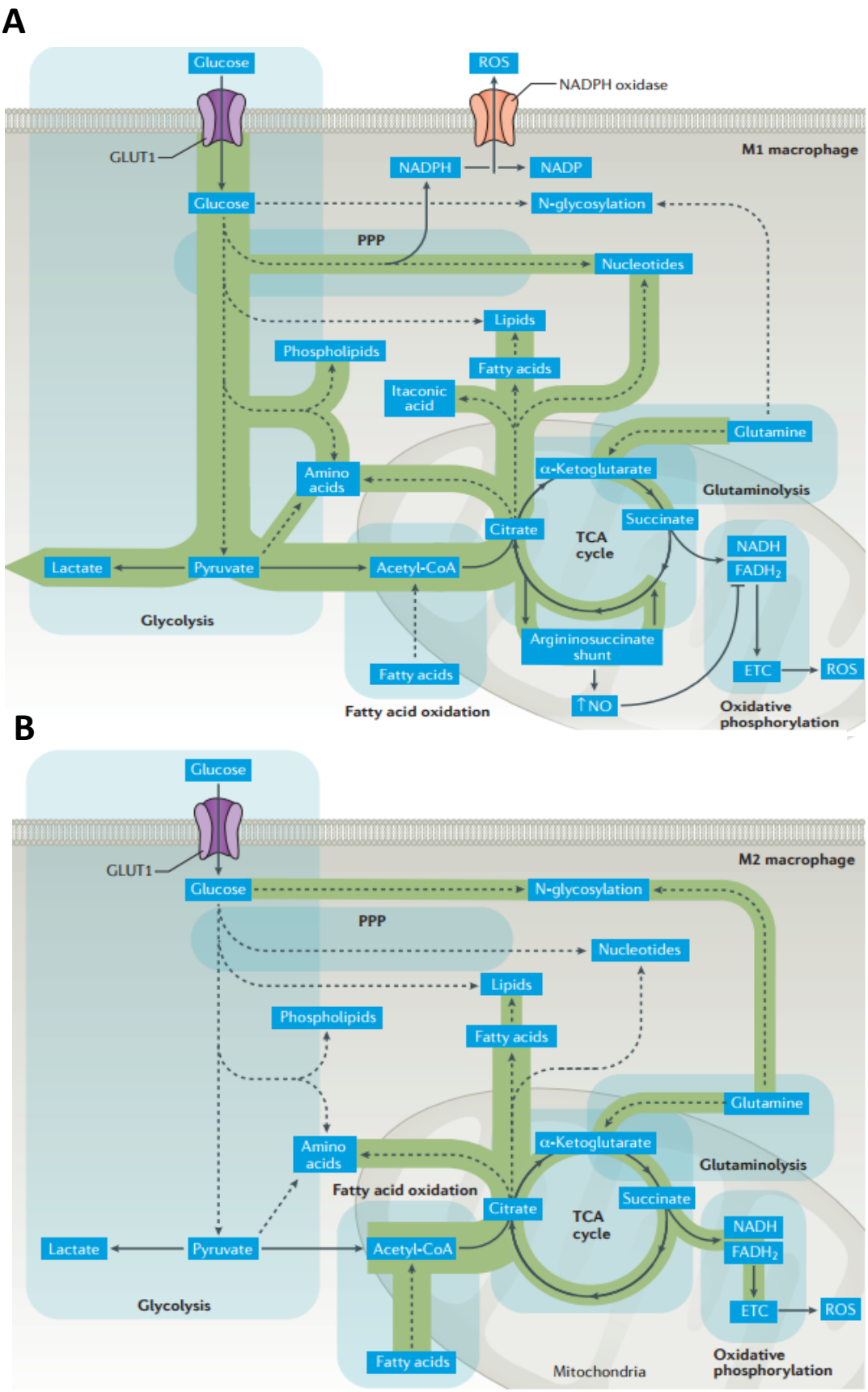

Figure 1.9 | Metabolic reprogramming of canonical activated M1 and M2 macrophages.

A. Classically LPS activated M1 macrophages primarily use aerobic glycolysis to generate energy and molecules for biosynthetic processes, thereby increasing flux through the pentose phosphate pathway (PPP), leading to an increase in NADPH. NADPH is an energy substrate for redox homeostasis and for the production of reactive oxygen species (ROS) and nitric oxide by NADPH oxidases. ROS are also produced by mitochondria. Although the tricarboxylic acid (TCA) cycle is mainly fueled by pyruvate from

glycolysis and acetyl-CoA or succinyl-CoA from fatty acid oxidation, TCA intermediates removed from the mitochondria for use in biosynthetic pathways have to be replenished by glutamine in M1 macrophages due to the interruption of the TCA cycle at two positions. The first break at isocitrate dehydrogenase 1 (IDH1) results in the accumulation of citrate, which is used for synthesis of itaconic acid and fatty acid synthesis, membrane biosynthesis, and prostaglandin production. Anabolic synthesis of fatty acids generates NADPH and, subsequently, ROS via NADPH oxidases. The argininosuccinate shunt replenishes levels of fumarate and malate, required for citrate production, thereby generating nitric oxide (NO), which together with itaconic acid, inhibits succinate dehydrogenase activity. This inibition induces a second break that causes succinate accumulation, which activates hypoxia-inducible factor (HIF)-1α induced inflammatory gene expression and increases glycolysis. LPS induces mitochondrial hyperpolarization (Δψ), SDH-mediated succinate oxidation, and reverse electron transport (RET), which together drive mitochondrial ROS production and IL-1β expression. This is accompanied by mitochondrial supercomplex destabilization. **B.** Alternatively activated M2 macrophages are characterized by increased fatty acid oxidation, low glycolysis activity and reduced flux through the PPP. Acetyl-CoA generated by fatty acid oxidation enters the intact TCA cycle for oxidative metabolism. Glutamine is mainly used for the synthesis of amino-sugars and nucleotide sugars, but also fuels the TCA cycle. ETC, electron transport chain; GLUT1, glucose transporter type 1. Adapted from (Gaber et al., 2017).

activates glutaminolysis (Meiser et al., 2016). A dysfunctional TCA cycle in LPS-stimulated macrophages triggers the expression of the glutamine transporter (Slc3a2). Glutamine can be oxidized to succinate through anaplerosis via α-ketoglutarate, being an alternative source of succinate to restore the TCA (Tannahill, Curtis, Adamik, Palsson-Mcdermott, et al., 2013). Moreover, with the increase in PPP activity in activated macrophages, there is an increase in purine and pyrimidine production, which can be used for biosynthesis, as well as, in NADPH, which produces ROS (Bedard & Krause, 2007). NADPH is also used by M1 macrophages for phagocytosis and for the production of the antioxidant glutathione, which protects the cell against ROS-mediated damage (Haschemi et al., 2012). Glycolytic ATP production induces a mitochondrial metabolism shift away from ATP production and towards ROS production by the electron transport chain, helping the increase in ROS levels (Kelly & O'Neill, 2015; Palsson-Mcdermott & O'Neill, 2013). Thus, an increase in glycolysis, truncated TCA, inhibition of fatty acid oxidation and induction of fatty acid synthesis act together to facilitate the differentiation of proinflammatory macrophages (Gaber et al., 2017) (Figure 1.9A).

The mechanism behind the glycolytic activity observed in activated macrophages have been performed through the activation of TLR4 with LPS and the pathways involved in this metabolic shift are summarized in Figure 1.10. There are at least four main processes leading to Warburg metabolism in LPS-activated macrophages. Activated macrophages present an increase in inducible nitric oxide synthase (iNOS) expression, which generates NO, which can inhibit mitochondrial respiration (Kelly & O'Neill, 2015). In addition, TLR4 stimulation leads to the activation of a serine/threonine protein kinase, i. e., mechanistic target of rapamycin (mTOR), leading to an increase in HIF-1α expression. mTOR mediates the increase in HIF-1α expression by promoting translation of mRNAs containing 5'-terminal oligopyrimidine (5'-TOP) signals, motifs that are present in HIF-1α mRNA (Huo et al., 2012). Another TLR4-regulated target involved in the switch to glycolysis is an isoform of 6-phosphofructo-2-kinase/fructose-2,6-bisphosphatase (PFK-2/FB). Proinflammatory macrophages present higher levels of the rate-limiting glycolytic activator 6 phosphofructo 2 kinase/fructose 2, 6 bisphosphatase 3 (PFKFB3) (Chesney et al., 1999; Jha et al., 2015; Rodriguez-Prados et al., 2010). This phosphatase present a kinase and bisphosphatase activities, controling intracellular levels of the glycolytic intermediate fructose-2,6-bisphosphate (F-2,6-BP). F-2,6-BP is an allosteric activator of 6-phosphofructo-1-kinase, increasing then the flux through the glycolytic pathway (Pilkis, El-Maghrabi, McGrane, Pilkis, & Claus, 1982). Finally, the activation of TLR4 by LPS also decreases activation of the

energy-sensing enzyme AMP-activated protein kinase (AMPK) in macrophages. AMPK induces the expression of proteins involved in OXPHOS (Vats et al., 2006) and upregulates enzymes involved in fatty acid metabolism (Winder et al., 2000). Consistent with its role in decreasing anabolism, AMPK can inhibit mTOR, represent another means by which LPS promotes mTOR activity and consequently HIF-1α signaling (Kelly & O'Neill, 2015).

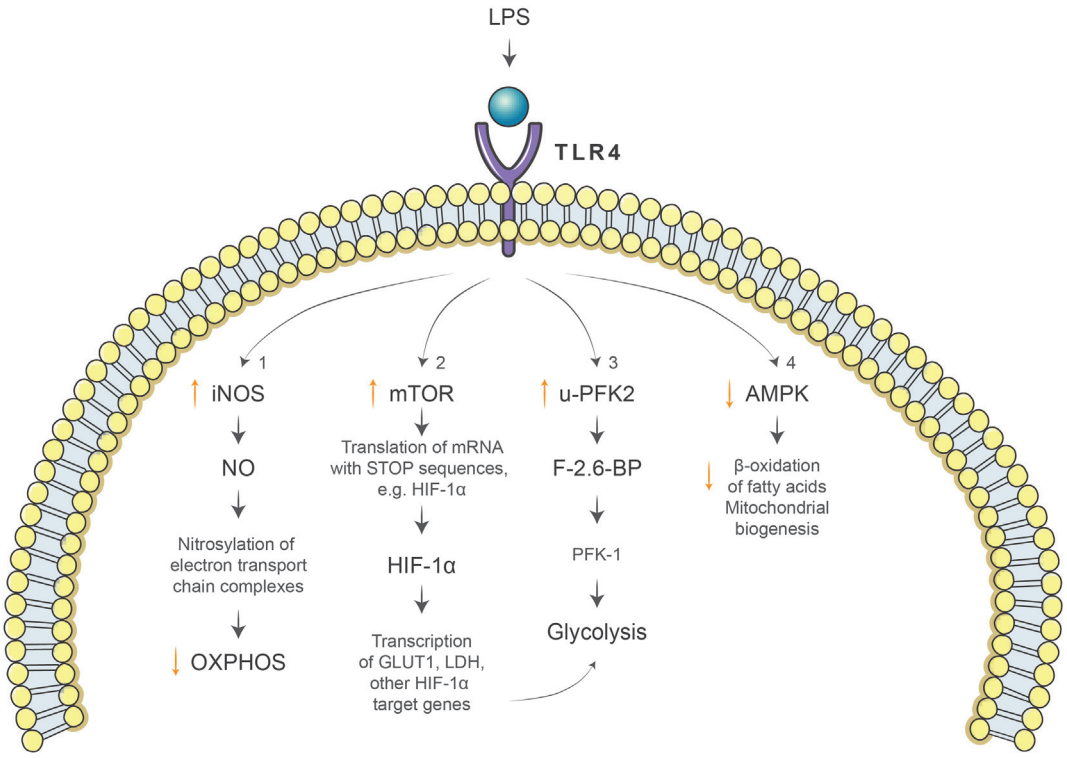

Figure 1.10 | Mechanisms of LPS-induced glycolytic metabolism in macrophages.

Upon LPS stimulation of toll-like receptors 4 (TLR4), a range of metabolic changes occur in macrophages. **1.** LPS activation upregulates inducible nitric oxide synthase (iNOS) expression, increasing the production of nitric oxide (NO), which nitrosylates and thus inhibits target proteins in the mitochondrial electron transport chain, thereby dampening oxidative phosphorilation (OXPHOS). **2.** LPS activates mechanistic target of rapamycin (mTOR), increasing the translation of mRNA with 5'-terminal oligopyrimidine (5'-TOP) sequences, including hypoxia-inducible factor (HIF)-1α mRNA. HIF-1α then increases expression of its target genes. **3.** LPS increases expression of u-PFK2 (PFKFB3), an isoform of 6-phosphofructo-2-kinase/fructose-2,6-bisphosphatase (PFK-2), thereby increasing levels of the metabolite fructose-2,6-bisphosphate (F-2,6-BP). F-2,6-BP activates the glycolytic enzyme 6-phosphofructo-1-kinase. **4.** Finally, LPS inhibits AMPK, resulting in decreased β-oxidation of fatty acids and mitochondrial biogenesis. Adapted from (Kelly & O'Neil, 2015)

1.3.2.6.2 Metabolic shift in alternatively activated macrophages

In contrast with proinflammatory macrophages, alternatively activated (M2) macrophages have sustained OXPHOS, expressing low levels of PFKFB3 and high levels of PFKFB1, PFK2 isoforms, which has less kinase activity than PFKFB3, thereby reducing glycolytic flux (Rodriguez-Prados et al., 2010). Stimulation of macrophages with anti-inflammatory cytokines resulted in the rapid phosphorylation/activation of AMPK (Sag, Carling, Stout, & Suttles, 2008). Furthermore, anti-inflammatory macrophages have high levels of arginase 1 activity, which is needed to metabolize arginine to proline, a component of collagen (Gordon & Martinez, 2010; Mantovani, et al., 2013). Polarization of cells to an M2 like macrophage phenotype by IL-4 stimulates mitochondrial biogenesis and fatty acid oxidation, providing

fuel for the intact TCA cycle as well as for OXPHOS. M2 macrophages utilize glutamine to generate TCA cycle intermediates (Figure 1.9B), but also for protein glycosylation. Recently, it was shown that production of α-ketoglutarate via glutaminolysis is crucial for alternative macrophage activation, including engagement of fatty acid oxidation and JmjC-domain protein 3 (Jmjd3)-dependent epigenetic reprogramming of M2 genes (Liu et al., 2017). However, it was also recognized that glucose can fuel OXPHOS in alternatively activated macrophages (Van den Bossche et al., 2016; Van den Bossche, O'Neill, & Menon, 2017). A complex model was proposed in which glucose fuels fatty acid synthesis for increased fatty acid oxidation in alternatively activated macrophages, thereby linking the three metabolic pathways (Huang et al., 2016). Furthermore, M2 macrophages downregulate flux through the PPP by inducing carbohydrate kinase-like protein, which inhibits this pathway. Besides both LPS-induced and IL-4-induced macrophages show increased glycolysis, this metabolic pathway is accompanied by activation of the PPP only in the former (Haschemi et al., 2012).

1.3.2.6.3 Metabolic shift in atherosclerotic macrophages

Taking into account the above metabolic description in response to inflammatory mediators, it is expected that lesional macrophages also exhibit altered metabolism. Furthermore, hypoxic conditions are believed to occur in advanced atherosclerotic lesions and are a well characterized HIF-1α inductor, which has been identified in both human and mouse atherosclerotic lesions (Parathath et al., 2011; Vink et al., 2007). The hypoxic environment in atheroma promotes an inflammatory macrophage phenotype associated with increased glucose uptake and metabolism, in a manner that is dependent on both HIF-1α and PFKFB3 (Tawakol et al., 2015). Moreover, like with cholesterol cellular homeostasis, the balance between uptake and cellular metabolism of fatty acids has important effects on macrophage phenotype (Tabas & Bornfeldt, 2016). Internalization of free fatty acid is mediated by CD36 and fatty acid transport proteins, or by flip-flopping across the plasma membrane. Inside cells, they quickly bind to intracellular fatty acid–binding proteins (FABPs) or are esterified into their acyl-CoA derivatives (Figure 1.11). Therefore, deletion of FABP4 and FABP5 in macrophages was sufficient to reduce inflammatory activation and consenquently, reduced atherosclerotic lesion (Babaev et al., 2011; Furuhashi & Hotamisligil, 2008; Makowski et al., 2001). Additionally, acyl-CoA synthetase expressed in macrophages, acyl-CoA synthetases 1, which catalyzes the reaction of acyl-CoA synthesis from free fatty acids and CoA, is markedly upregulated by inflammatory mediators and is required for atherosclerosis in diabetic mice (Kanter et al., 2012). Moreover, macrophages deficient in serine palmitoyl-transferase subunit 2 exhibit reduced levels of sphingomyelin in lipid rafts, which results in reduced TLR4 activity and reduced atherosclerosis (Chakraborty et al., 2013). A similar mechanism has been proposed for how free cholesterol promotes TLR4 activation (Yvan-Charvet et al., 2008). Finally, the role of mitochondrial oxidative stress, which it has been associated with the proinflammatory macrophage phenotype, in atherosclerosis, was already addressed. It was revealed that fat-fed *Ldlr*$^{-/-}$ mice have increased mitochondrial oxidative stress in lesional macrophages and that quelling mitochondrial oxidative stress in hematopoietic

cells suppresses atherosclerosis and cytokine production by decreasing the activation of NF-κB (Ying Wang, Wang, Rabinovitch, & Tabas, 2014). Recently, it was observed that inhibiting glutaminolysis reduced lipid induced lysosome dysfunction, inflammasome activation, and macrophages death, by decreasing the mTORC1 activation, enhancing autophagy and preventing the suppressive effect of palmitate on mitochondrial respiration (L. He, Weber, 2016). Together, these studies demonstrate a tight relationship in macrophage metabolism, phenotype, inflammation and atherosclerosis, but more metabolic studies are needed to better understand the effect of oxidized lipid on the metabolic shift in macrophages.

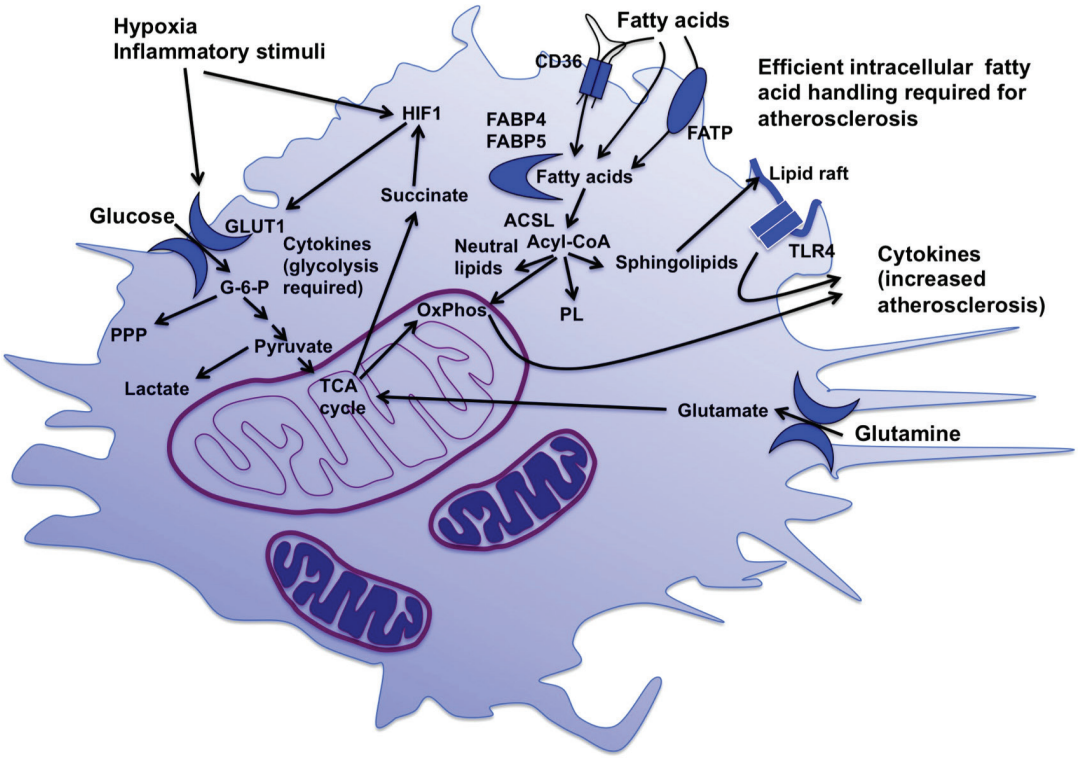

Figure 1.11 | Metabolic modulators in macrophages from atheroma lesion

Hypoxia and inflammatory stimuli originated by oxidized lipids increase glycolysis in order to suply the cell energy demands under anaerobic conditions and to generate an inflammatory response. Increased glycolysis initiated by glucose entry into the cell through glucose transporters, such as glucose transporter 1 (GLUT1). Tricarboxylic acid (TCA) cycle intermediates also play important roles in inflammatory activation of macrophages and a truncated cycle can originate an increase in succinate production, through glutamine oxidation to replenishes the TCA cycle. In addition to the increased succinate levels there is the stabilization of the hypoxia-inducible factor (HIF)-1α complex. In atheroma lipid rich environment, fatty acids are taken up by the cell through CD36 and fatty acid transport proteins (FATP) or by transport across the plasma membrane. In cytoplasm, lipids are quickly bound to intracellular fatty acid–binding proteins (FABPs) or are esterified into their acyl-CoA derivatives by a group of enzymes with acyl-CoA synthetase (ACSL) activity. Acyl-CoAs present different fates in the cell, including oxidative phosphorylation (OXPHOS), neutral lipids, phospholipids (PL), sphingolipids, or they are used for protein modification or signaling. Sphingolipids are found in lipid rafts and are believed to promote inflammatory activation by toll-like receptors (TLRs) present in these rafts. Reduced levels of intracellular fatty acids or acyl-CoAs or reduced OXPHOS lead to reduced inflammatory activation and atherosclerosis. From (Tabas & Bornfeldt, 2016).

1.4 LYSOSOMES ARE KEY ORGANELLES IN ATHEROSCLEROSIS

It has been reported that dyslipidemia, which is a common finding in patients with genetic deficiency in lysosomal acid lipase (LAL), responsible for CE hydrolysis, is associated with accelerated development of atherosclerosis, cardiovascular disease and premature mortality (Bernstein, Hülkova, Bialer, & Desnick, 2013; Elleder et al., 2000). In addition, *in vitro* LAL depletion induces a substantial accumulations of cholesterol and CE within the lysosomes of foam cells (W G Jerome & Yancey, 2003; Yancey & Jerome, 2001). The relationship between LAL deficiency and atherosclerosis has also been reported in animal models (S. Fowler, et al., 1980; Goldfischer, Schiller, & Wolinsky, 1975; Lewis, Taylor, & Jerome, 1985; Peters, Müller, & De Duve, 1972). Atherosclerosis progression has been characterized by an initially increasing amount of cholesterol retained in lysosomes, and at later disease stages there is also retention of CE (W Gray Jerome, 2006). This phenomenon can indicate that there is a general loss of lysosomal function due to cholesterol overload following unregulated cellular uptake of modified forms of LDL within artery wall cells (Dubland & Francis, 2015). The loss of LAL function due to excess cholesterol within the lysosome contributes to the formation of foam cells and the altered distribution of lipid stores within these cells. Therefore, atherosclerosis has been proposed as a type of lysosomal storage disorder (LSD) (Dubland & Francis, 2015; Lewis et al., 1985).

1.4.1 Lysosome: a multitask organelle

Lysosomes are membrane-enclosed cytoplasmic organelles that have been viewed as a cellular degradation and recycling center. Lysosomes receive material for degradation from different pathways such as: biosynthetic transport, endocytosis, phagocytosis and autophagy (Luzio, Pryor, & Bright, 2007; Pu, Guardia, Keren-Kaplan, & Bonifacino, 2016). However, in the past decade, it has become evident that lysosomes are not only the “waste bag” of the cell, but also a signaling center (C. Y. Lim & Zoncu, 2016). Lysosomes participate in many other cellular processes, including plasma membrane repair, stress resistance, programmed cell death, cell differentiation, killing of intracellular pathogens, antigen presentation, exosome release, cell adhesion and migration, tumor invasion and metastasis, metabolic signaling and gene regulation (Ballabio, 2016; Bhatia et al., 2007; Boya, 2012; Braun et al., 2015; Encarnação et al., 2016; Reddy, Caler, & Andrews, 2001). To fulfill all their functions, lysosomes are heterogeneous and dynamic with high diversity in pH, activity, localization, shape, size, and number (Bright, Davis, & Luzio, 2016; D. E. Johnson, Ostrowski, Jaumouillé, & Grinstein, 2016; Korolchuk et al., 2011). Dysfunction of lysosomes contributes to various diseases, including inherited LSDs, neurodegenerative disorders, cancer, immune diseases, and cardiovascular diseases, particularly atherosclerosis. Thus, as central and dynamic organelles, the regulation of lysosomes is of great interest to researchers in both basic science and clinical fields.

1.4.1.1 Basic properties of lysosomes

In 1955, Christian de Duve discovered and named lysosomes as a result of studying the intracellular distribution of enzymes using centrifugal fractionation (Christian de Duve, 2005). The name derives from the Greek for "digestive body", since they were initially discovered as the main digestive organelles of eukaryotic cells (Christian de Duve, 2005). Lysosomes present peculiar features: acid hydrolases, an internal acidic pH, and lysosomal specific membrane proteins (Vellodi, 2005). These acidic organelles have different types of acid hydrolases, which break down macromolecules such as, proteins, polysaccharides, and lipids into amino acids, monosaccharides, and fatty acids respectively (Xu & Ren, 2015). For optimal activities, most lysosomal hydrolases require an acidic environment, between 4.5 and 5.0, which it is conferred by vacuolar proton ATPase (V-H^+ATPase) (Figure 1.12, lysosome zoom in). This characteristic ensures that degradation by acid hydrolases only takes place in lysosomes (Mindell, 2012). Interestingly, recent studies demonstrate that not all lysosomes have an acidic pH: the range in each lysosome can vary 4.5-7 (Bright et al., 2016; D. E. Johnson et al., 2016). A population of terminal storage lysosomes were identified, in which pH is neutral and acid hydrolases are inactivated. This population has been associated with the cellular response to altered extracellular conditions or cellular stress by decreased degradative activity (Bright et al., 2016).

Moreover, lysosomes present a complete transport system facilitating the exit of degradation products (amino acids, sugars, heavy metals, lipids) from the lysosomes to the cytosol for reutilization (Pisoni & Thoene, 1991). These organelles also have multiple ion channels and transporters which are responsible for the regulation of ions influx and efflux. In particular, the V-H^+ATPase localizes to the lysosomal membrane, pumping protons into the lysosome lumen against its electrochemical gradient using free energy generated from ATP hydrolysis (Finbow & Harrison, 1997; Ohkuma, Moriyama, & Takano, 1982). In addition, lysosome membranes are composed of specific highly glycosylated membrane-associated proteins, which protect them from the lysosomal hydrolases in the lumen. Lysosomal-associated membrane proteins (LAMP-1 and LAMP-2, that together account for ~50% of lysosomal membrane protein content), lysosome integral membrane protein-2 (LIMP2) and CD63, are example of glycosylated proteins which have been commonly used as lysosomal markers (Luzio et al., 2007; Wartosch, Bright, & Luzio, 2015). These organelles can also present variable shapes, sizes and numbers depending on cell types and environmental conditions in order to adapt different functions (Bright et al., 2016; D. E. Johnson et al., 2016; Korolchuk & Rubinsztein, 2011). Even though lysosomes are spherical in most cell types, they appear as long, tubular structures, which interconnect as a network in macrophages (Swanson, Bushnell, & Silverstein, 1987). In response to environmental features, lysosomes undergo dynamic morphological changes: nutrient deprivation induces changes in lysosomal morphology and number due to biogenesis and autophagic lysosome reformation (Yu et al., 2010).

Each organelle presents a specific ionic composition. To adequately carry out their physiological functions, lysosomes maintain specific ion compositions, including high concentrations of H^+, Cl^-, Ca^{2+}, Na^+, but low K^+ (Xu & Ren, 2015). Besides the well described V-H^+ATPase role in H^+ lysosomal concentration, the chloride channel CIC-7 H^+/Cl^- exchanger has also been implicated as a modulator of endosomal pH via transporting two Cl^- into the cytosol for one H^+ into the lysosomal lumen, generating a counter-ion flux and dissipating an opposing voltage (Graves, Curran, Smith, & Mindell, 2008). Thus, both unspecified cation channels and the lysosomal Cl^-/H^+ antiporter ClC-7/Ostm1 (osteopetrosis-associated transmembrane protein 1) are partially responsible for the necessary charge compensation. These proteins

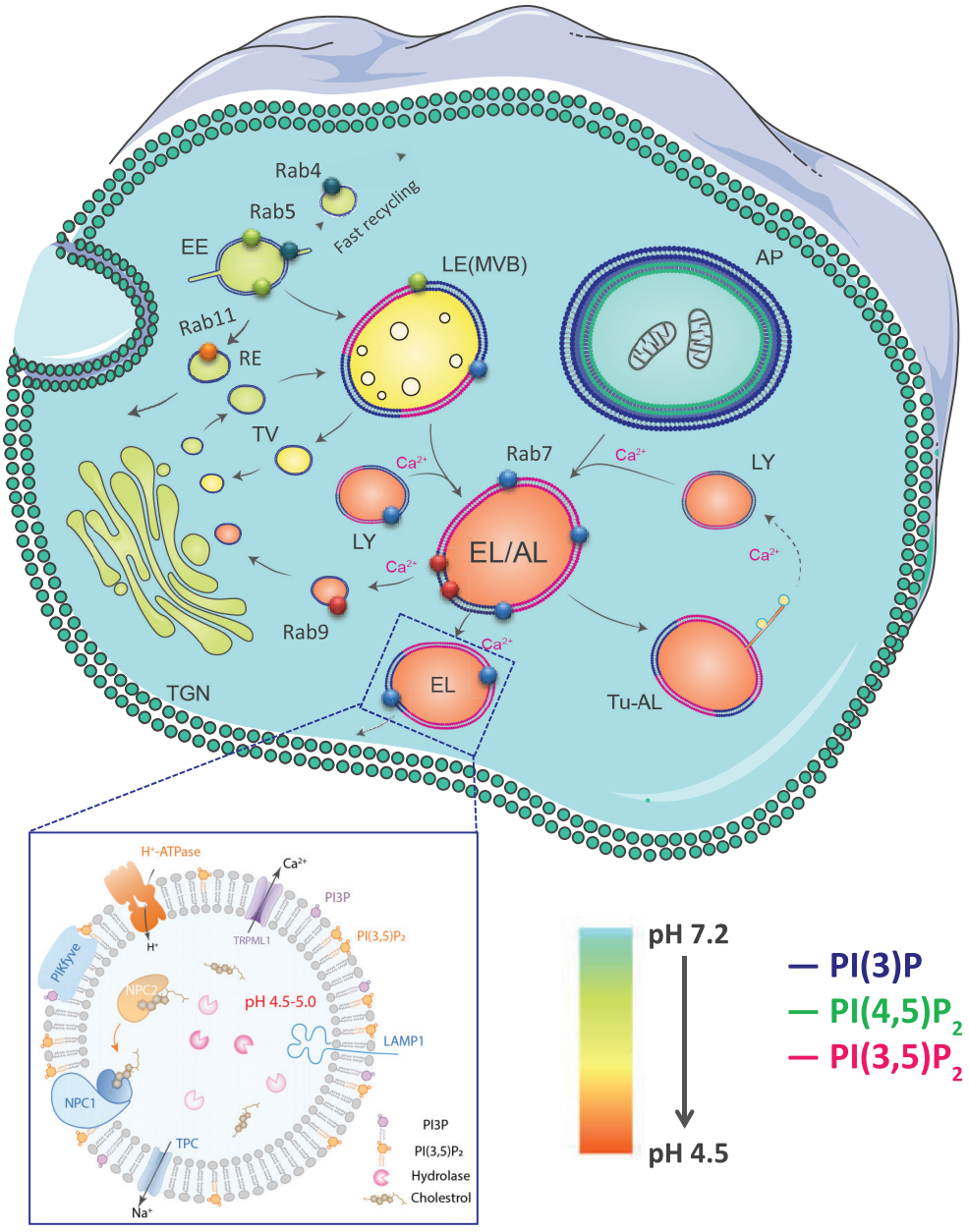

Figure 1.12 | Intracellular endocytic trafficking.

Lysosomes receive substrates from two major pathways for degradation: endocytosis for extracellular content degradation and autophagy for intracellular contents degradation. Endocytic cargos are delivery first to early endosome (EE) and routed to late endosomes (LEs), form endolysosome (EL) hybrids, and then lysosomes (LY) for degradation. Along the endocytic pathway, the intravesical pH drops from 6.0-6.5 in the early endosomes to 4.5-5.5 in the late endosomes and lysosomes, being represented with the gradient from blue (pH 7.2-7.4) to orange (pH 4.5). Upon initiation of autophagy, a phagophore with an isolated

membrane is formed around the targeted cargo, such as, intracellular damaged organelles and forms a double-membraned autophagosome (AP). The loaded autophagosome then fuses with the lysosome (LY), and contents in the autophagosome are degraded by lysosome-resident hydrolases in the newly formed autolysosome (AL)/endolysosome (EL). Endocytic and autophagic substrates are degraded in ELs and ALs by lysosomal hydrolases. Upon degradation, insoluble catabolites, such as lipids, can be transported to the Trans-Golgi Network (TGN) for reutilization via transport vesicles (TVs) in the retrograde trafficking pathway or can be released into the extracellular medium via lysosomal exocytosis. Upon completion of lysosomal degradation, ALs undergo extensive tubulation to become tubular ALs (Tu-ALs), from which protolysosomes are regenerated via a fission-based budding-off mechanism. Several trafficking steps are Ca^{2+} sensitive as indicated and depending on the recruitment of speficic Rabs as indicated in each vesicle. The plasma membrane, early endosomes (EEs), LEs, and lysosomes contain compartment-specific phosphoinositides: phosphatidylinositol 3-bisphosphate (PI(3)P, dark blue), phosphatidylinositol 4,5-bisphosphate (PI,(4,5)P_2, water green) and phosphatidylinositol 3,5-bisphosphate (PI(3,5)P_2,violet), to regulate membrane trafficking and activity of ion channels in a compartment-specific manner. Its composition is repensented by the differente colors in the membranes. In zoom in endolysossome there is a more detailed representation of the main components of this organelle. Lysosomes are maintained at acidified pH, by a proton pump vacuolar H^+-ATPase, which is required for optimal lysosomal hydrolase activity. Lysosomes are identified by the localization of lysosome-specific structural proteins, such as LAMP1/2. Lysosomal membranes are present higher levels of PI(3,5)P_2, being a lysosomal-specific phosphoinositide. Transient receptor potential mucolipin1 (TRPML1) is the major lysosomal Ca^{2+} channel, which mediates Ca^{2+} release from the lysosome lumen to the cytosol. Two-pore channels (TPCs) are lysosomal Na^+ channels. Niemann-Pick type C proteins (NPC1&2) bind with free cholesterol and mediate the export of cholesterol from the lysosomes to diverse cellular compartments. Dysfunctions in NPCs result in cholesterol accumulation inside lysosomes and a lipid storage disorder, Niemann-Pick type C. Images were adapted from (Xu and Ren 2015; Grant & Donaldson, 2011).

play a important role in lysosomal ion homeostasis and modulating the voltage across the lysosomal membrane (Wartosch et al., 2015). Ion movements across the lysosomal membrane are important for lysosomal functions and are regulated by a set of ion channels and transporters (Morgan, Platt, Lloyd-Evans, & Galione, 2011); for example, lysosomal Ca^{2+} release, which is important for lysosomal membrane trafficking and cellular signaling, is mainly mediated by transient receptor potential mucolipins (TRPMLs) (Cheng, Shen, Samie, & Xu, 2010; Dong et al., 2010). Moreover, the lysosomal membrane also has a specific fingerprint. Lysosomes are enclosed by a lipid-bilayer, composed of sphingomyelins, phosphatidylcholines, cholesterol and low abundant phosphatidylinositols (van Meer, Voelker, & Feigenson, 2008). These lysosomal lipids, especially phosphatidylinositols, provide lysosomal identity and regulate lysosomal functions. In the endocytic pathway, phosphatidylinositol 3,5-bisphosphate [PI(3,5)P_2] is produced on lysosomes from phosphatidylinositol 3-phosphate (PI3P) by phosphatidylinositol 3-phosphate 5- kinase (Jin, Lang, & Weisman, 2016). PI(3,5)P_2 provides the identity for lysosomes and mediates specific protein recruitment to ensure proper lysosomal trafficking (Di Paolo & De Camilli, 2006). The amount and distribution of cholesterol in the lysosomes are regulated by the lysosomal targeting proteins NPC1 and NPC2, which mediate cholesterol export to diverse cellular compartments. Mutations in NPC proteins result in accumulation of cholesterol in lysosomes and NPC disease, a lysosomal storage disorder (S. Mukherjee & Maxfield, 2004).

1.4.1.2 Lysosomel function

For a long time, lysosomes were simply classified as an endpoint organelle, a degradatively active compartment. The morphological heterogeneity of lysosomes was recognized early, but their dynamic, functional interactions with other organelles of the secretory, endocytic, and autophagic pathways have only been recognized in the past two decades. Moreover, as already referred, lysosomes have also been shown to play an important role in endocytic, phagocytic and autophagic degradation, antigen presentation, killing of target cells by cytotoxic T-cells and NK cells, metabolic signaling, cell adhesion and migration, tumor invasion

and metastasis, as well as plasma membrane repair (Bright, Davis, & Luzio, 2016; Pu, et al., 2016; Sardiello et al., 2009; Settembre et al., 2012).

1.4.1.2.1 Degradation

Lysosomal function and trafficking (fusion and fission) are interconnected: lysosomal trafficking supplies autophagic and endocytic substrates for degradation. Lysosomal trafficking is responsible for exporting lipid catabolites and to regulate consumption and biogenesis of lysosomes during lysosomal adaptation (Xu & Ren, 2015). The biomaterials destined for degradation are delivered to lysosomes through endocytic/phagocytic and autophagic pathways (Figure 1.12). Endocytosis or phagocytosis of extracellular or cell surface cargo begins with the fission of the plasma membrane to form vesicles that then fuse with early endosomes (EE). Association of proteins from the cytosol to the cytosolic surface of the EE membrane defines many of its functional attributes: Rab5 is a key component together with its effector the vacuolar protein-sorting (VPS) 34/p150, a phosphatidylinositol 3-kinase (PI(3)K) complex that generates the PI3P and then contributes to the identity of the organelle (Behnia & Munro, 2005; Zerial & McBride, 2001). EEs communicate with the Trans Golgi Network (TGN) through bidirectional vesicle exchange and the arrival of hydrolases gives them an initial degradative identity further reinforced during maturation to late endosomes (LEs). Endosome maturation involves the conversion from Rab5 to Rab7 (Poteryaev, et al., 2010; Rink, et al., 2005; Vonderheit & Helenius, 2005) and the conversion of PI3P to $PI(3,5)P_2$, (Nakamura & Yoshimori, 2017). This conversion can be blocked by expressing a constitutively active mutant of Rab5, and by depletion of VPS39, a subunit of the homotypic fusion and protein sorting (HOPS) complex (Rink et al., 2005). This results in the formation of hybrid endosomal compartments with markers for both EEs and LEs. In the LEs, the destined-to-be-degraded endocytic cargos are sorted into intraluminal vesicles (Xu & Ren, 2015). Mature LEs, also termed multivesicular bodies, fuse with lysosomes to become endolysosomes (EL) these latter organelles then become lysosomes for degradation (Figure 1.12). In addition, before cargo delivery to LE, several endocytic components can be recycled. Recycling can occur at the early and late stages. Vesicular components recycling can occur at the level of EEs/sorting endosomes (fast recycling), that is Rab4 and Rab35 dependent while the slow recycling is Rab11 dependent. In the latter type of recycling endocytic cargo move from the EE to the endocytic recycling compartment (ERC) by a process requiring Snx4, dynein, EHD3, Rab10, Rab22a and the Rab11 effectors FIP-2, -3 and -5 (Grant & Donaldson, 2009; Huotari & Helenius, 2011). Finally, in lysosomes, macromolecules such as complex lipids, oligosaccharides, nucleic acids and proteins are digested by the acidic lysosomal hydrolases and the monomeric molecules are integrated in cellular metabolism or are stored.

Damaged or aged intracellular organelles and protein aggregates are delivered to lysosomes through autophagy for degradation (Figure 1.12). Autophagosomes fuse directly or indirectly through LEs, with lysosomes to form autophagolysosomes (Lieberman et al., 2012; Mizushima, Levine, Cuervo, & Klionsky, 2008) in which the autophagic substrates are broken down.

Thus, the autophagy pathway can be simplified into three steps: autophagosome formation, autophagosome-lysosome fusion, and lysosomal degradation (Kaur & Debnath, 2015).

1.4.1.2.2 Secretion

Although conventional lysosomes are not secretory organelles, there are now many lines of evidence that supports the idea that lysosomes are also involved in an "unconventional" secretory pathway known as lysosomal exocytosis (Ballabio, 2016). Lysosomal secretion has been implicated in important roles in various physiological processes such as plasma membrane repair, defense against parasites, immune responses and bone resorption (Andrews, 2002; Jaiswal, Andrews, & Simon, 2002; Pu et al., 2016; Reddy et al., 2001). Secretion of conventional lysosomes appears to involve the release of a relatively small fraction of lysosomes, which are likely close to the plasma membrane. Thus, in the first step of lysosomal exocytosis, lysosomes are recruited to the close proximity of the cell surface in a Ca^{2+}-independent manner (Jaiswal et al., 2002). A key component in this process is the multisubunit complex BORC (Pu et al., 2015), which by recruiting the small GTPase Arl8b to the lysosomal membrane, enables coupling to the SifA and kinesin-interacting protein (SKIP)-kinesin-1 complex. This complex drives microtubule-guided movement of lysosomes toward the cell periphery (Pu et al., 2015; Rosa-Ferreira & Munro, 2011). Consequently, in a Ca^{2+}-dependent process, the pool of predocked/tethered lysosomes fuses with the plasma membrane in response to Ca^{2+} elevation sensed by synaptotagmin VII (Syt VII), a Ca^{2+}-sensor localized to lysosomes (Andrews, 2002; Luzio et al., 2007; Pu et al., 2015, 2016). Indeed, the increase in Ca^{2+} levels, which may be mediated by $PI(3,5)P_2$ activation of lysosomal Ca^{2+}-channel TRPML1, causes a conformational change in Syt VII, enabling its interaction with vesicle-associated membrane protein (VAMP)-7 in lysosomes and the SNAP-23 and syntaxin-4 in the plasma membrane (PM) (Rao, et al., 2004; Samie & Xu, 2014). The same mechanism is also triggered by plasma membrane damage/disruptions which leads to Ca^{2+} influx. Additionally, lysosomal docking and fusion is also regulated by transcription factor EB (TFEB), a transcription factor for lysosome biogenesis and autophagy. Recent studies have shown that TFEB controls docking and fusion of lysosomes with the PM in a process that requires the TRPML1 (Medina et al., 2011).

Besides, lysosomal exocytosis, there are at least two more distinct output pathways in lysosomal trafficking, based in membrane fission events in the lysosome and important in the recycling of cellular components. Firstly, retrograde trafficking transports the free insoluble lipids out and mannose-6-P receptor of LE to the TGN (Figure 1.12) for reutilization in biosynthetic pathways (Saftig & Klumperman, 2009). This process is controlled by Rab7b and Rab9, being localized both to the TGN and to LE. Activation of Rab7 and sequential activation of Rab5, interacts directly with the cargo recognition complex of the retromer, a heterotrimer cargo recognition complex, composed by VPS26, VPS29, and VPS35; and a sorting nexin (SNX) complex (SNX1 or SNX2 combined with SNX5 or SNX6) (Guerra & Bucci, 2016; Saftig & Klumperman, 2009). Second, lysosomal reformation from the autophagosomes

or endolysosome hybrid organelles is essential for lysosomal biogenesis and homeostasis. Upon mTOR reactivation after prolonged starvation, autophagosomes undergo extensive tubulation. Lysosomes are then regenerated from these lysosomal tubules via a poorly-understood fission-based budding-off mechanism (Figure 1.12) (Xu & Ren, 2015; Yu et al., 2010).

1.4.1.2.3 Signaling

In addition to the role of lysosomes in degradation, exocytosis and recycling of cellular waste, recent evidence indicates that lysosomes are also an important signaling center for cell metabolism and regulate metabolic homeostasis in response to nutrient availability, hypoxia and stress (C. Y. Lim & Zoncu, 2016). The lysosome membrane presents the lysosomal nutrient sensing machinery (LYNUS), consisting of the mTORC1 complex, V-H^+ATPase complex, Rag GTPases, Rag GTPase-activating proteins (GAPs) and Ragulator complex. LYNUS controls the activation of mTORC1 and integrates metabolic signals with intracellular changes (Carmine Settembre, Fraldi, Medina, & Ballabio, 2013). mTOR is a master regulator of cell growth in response to nutrient levels and exists in mTOR complex 1 (mTORC1) and mTOR complex 2 (mTORC2). mTORC1 plays a fundamental role in the integration of metabolic (lipogenesis, glycolysis and mitochondrial biogenesis), energy, hormonal and nutritional signals to promote biosynthetic pathways and suppress the catabolic process of autophagy. It exerts its effects by phosphorylating and controlling the activity of key proteins such as ribosomal protein S6 and TFEB (Carroll & Dunlop, 2017). mTORC1 is recruited to lysosomal membrane and mediates cell response at the amino acid level. Its lysosomal localization is dependent on Rag GTPases, and ragulator (Carroll & Dunlop, 2017). The Ragulator complex recruits Rag GTPases to the lysosomal surface and functions as guanine nucleotide exchange factor (GEF) for these GTPases (Liron Bar-Peled, et al., 2012; Yasemin Sancak et al., 2010). Moreover, Rag GAPs proteins activate Rag GTPases (L. Bar-Peled et al., 2013). The V-H^+ATPase complex is proposed to sense the amino acids from the lysosomal lumen by an incompletely understood mechanism and relays the signal to the Rag GTPases via Ragulator and possibly Rag GAPs (L. Bar-Peled et al., 2013; Zoncu et al., 2011). When amino acids are present, the active form Rag GTPases recruits mTORC1 to the lysosomal surface and facilitates its activation by small Ras-related GTPase Rheb (Ras homolog enriched in brain), which is controlled by growth factor (Kim, Goraksha-Hicks, Li, Neufeld, & Guan, 2008; Y. Sancak et al., 2008). On other hand, nutrient starvation, which was shown to trigger perinuclear clustering of lysosomes (Korolchuk & Rubinsztein, 2011), causes mTORC1 to be released from lysosomes, resulting in decreased phosphorylation of two key substrates: the autophagy-initiating uncoordinated 51-like kinases 1 (ULK1) and the TFEB. Dephosphorylation activates ULK1, promoting the formation of the phagophore, a precursor of the autophagosome (Itakura, et al., 2012; Russell, Yuan, & Guan, 2014), whereas dephosphorylated TFEB translocates from lysosomes to the nucleus to upregulate the expression of autophagy-associated genes (Martina, Chen, Gucek, & Puertollano, 2012; Palmieri et al., 2017; C. Settembre et al., 2011). Thus, not only are lysosomes required for mTORC1 activation, but mTOR also affects lysosomal function and positioning (Puertollano, 2014). In addition, lysosomal localization at the periphery was cor-

related with increased mTOR activity, whereas the inhibition of lysosomal scattering resulted in diminished mTOR activity and, consequently, an increased number of autophagosomes. Finally, mTOR is a key component in lysosomes and, by mediating the phosphorylation of TFEB, the important regulator of lysosome biogenesis, positioning and exocytosis, present a power effect in all the functionalities of lysosomes (Medina et al., 2011; Carmine Settembre et al., 2012).

Furthermore, in a very recent study, increased cholesterol triggers mTORC1 recruitment and activation at the lysosomal surface through a component of the Rag-Ragulator complex, SLC38A9. This lysosomal transmembrane protein is required for mTORC1 activation by cholesterol through conserved cholesterol-responsive motifs. Moreover, SLC38A9 enables mTORC1 activation by cholesterol independently from its arginine-sensing function. Conversely, the NPC1 protein binds to SLC38A9 and inhibits mTORC1 signaling through its sterol transport function. Thus, lysosomal cholesterol drives mTORC1 activation and growth signaling through the SLC38A9-NPC1 complex (Castellano et al., 2017).

1.4.2 The role of Lysosomes in inflammation

Further insights into the role of lysosomes and inflammation have come from the study of autoimmune diseases. Recent evidence suggests that lysosomal enzyme activities may contribute to the generation of autoantigens, such as, the lysosomal enzyme α-galactosidase A (Simonaro, 2016). This enzyme has a crucial role in the degradation of lipid antigens to prevent their accumulation and activation of CD1d-restricted NKT cells. Deficiency of this enzyme in Fabry disease, an inherited LSD, causes aberrant accumulation of lipid antigens and activation of immature NKT cells, resulting in autoimmunity (Mauhin et al., 2015). Additionally, the first major autoinflammatory disease in which lysosome was suggested to play a role was Crohn's disease (Spalinger, Rogler, & Scharl, 2014). Crohn's disease is a chronic inflammatory disorder of the intestine and associated to genetic variants of several important autophagy genes, such as *ATG16L1,* which have been implicated in the susceptibility and clinical severity of the pathology. Mutated form of *ATG16L1* gene has been strongly associated with defective bacterial defense, aberrant antigen presentation, and increased production of proinflammatory cytokines, including IL-1β and IL-18 (Murthy et al., 2014; C.-S. Shi et al., 2012). Thus, healthy lysosomes are required to maintain a normal autoimmune response, and lysosome dysfunction may lead to a range of autoimmune-related pathologies.

A transmembrane protein 9B (TMEM9B) was identified as an important component of TNF-α signaling and also a component shared with IL-1β and TLR pathways. TMEM9B is a glycosylated protein localized in membranes of the lysosome and partially in EEs. The expression of TMEM9B is required for the production of proinflammatory cytokines induced by TNF-α and IL-1β, through NF-κB and mitogen-activated protein kinase (MAPK) pathways (Dodeller, Gottar, Huesken, Iourgenko, & Cenni, 2008). Moreover, it was reported that Rab7b can negatively regulate LPS-induced production of TNF-α, IL-6, NO and IFN-β, by activating MAPK,

NF-κB and IFN regulatory factor 3 (IRF3) signaling pathways in macrophages by promoting the degradation of TLR4. Uncontrolled TLR4 activation may contribute to the pathogenesis of autoimmune and inflammatory diseases. Its transport to lysosomes for degradation is crucial for the negative regulation of TLR4 signaling. Rab7b, localized in LAMP-1–positive subcellular compartments, colocalizes with TLR4 after LPS treatment and can downregulate TLR4, being essential in the control of its inflammatory response (Yuzhen Wang et al., 2007). Similar experiments were performed looking at the role of LE/lysosome-localized Rab7b in TLR9 signaling. It was also observed that lysosomes can down-regulate TLR9-triggered proinflammatory cytokine and type I IFN production by promoting of TLR9 degradation (Yao et al., 2009). Thus, the involvement of a lysosomal membrane protein (such as TMEM9B) in the activation of the NF-κB and MAPK pathways and Rab-GTPase in controlling TLR responses, suggests that lysosomal compartments may play a central role in inflammatory signaling network.

1.4.2.1 Regulation of cytokine secretion by lysosomes

Cytokine secretion pathways are often adapted to suit specific cytokines and their function, depending on the cell type. Several immune cells store cytokines in distinct compartments – namely, secretory granules or lysosome-related organelles (LROs) – that enable rapid release of the cytokines upon cell activation (Marks, Heijnen, & Raposo, 2013; Rachael Zoe Murray & Stow, 2014). However, macrophages do not contain these types of granules and, instead, cytokines are synthesized after cell activation and secreted via the constitutive secretory pathway or via non-conventional secretion. The majority of cytokines in macrophages are processed and transported through the constitutive pathway, through upregulation of cellular machinery and carriers involved in expression and secretion of cytokines (Manderson,et al., 2007; R. Z. Murray, 2005; Rachael Zoe Murray & Stow, 2014). Thus, there are three major transport pathways for cytokine secretion: i) direct transport to the cell surface (IL-10) from the TGN; ii) via the recycling endosome to the extracellular site (TNF-α, IL-6, and IL-10); iii) and the last pathway occurs during phagocytosis where cytokine (TNF-α) is routed from the recycling endosome to the phagocytic cup. Nevertheless, some cytokines require non-conventional secretion for cellular release, and here, secretory lysosomes have a crucial role in the secretion or even degradation of inflammatory cytokines to regulate the immune response under an external stimulus, such as LPS and ATP (Rachael Zoe Murray & Stow, 2014). In Table 1.4, there is a quick summary of the cytokines release by the secretory pathway.

There is little evidence of the role of lysosomes in cytokine release (Table 1.4), but here, due its fundamental role in atherogenesis, their role in the secretion of IL-1β will be explored. Members of the IL-1 cytokine family, particularly IL-1β and IL-18 are key inflammatory cytokines which use non-classical or unconventional secretory pathways for their release (Dinarello, 2009). As explained above (Section 1.3.2.4), in macrophages activated through a TLR, the precursor pro-IL-1β is synthesized but to fully achieve cytokine release, a second danger signal, is necessary to activate the multisubunit signaling complex of the NLRP3/caspase-1

inflammasome, which cleaves pro-IL-1β to produce the mature, active form of the cytokine that is release. IL-1β does not traffic through the ER or Golgi and the precise mechanisms of its secretion are poorly defined (Dinarello, 2009; Martín-Sánchez et al., 2016). Potential secretory mechanisms involved in IL-1β release include: (i) exocytosis of IL-1β-containing secretory lysosomes; (ii) release of IL-1β from shed plasma membrane microvesicles; (iii) fusion of multivesicular bodies with the plasma membrane and subsequent release of IL-1β -containing exosomes; (iv) export of IL-1β through the plasma membrane using specific membrane transporters, such as ABCA-1, and (v) release of IL-1β upon cell lysis through pyroptosis and other mechanisms (Eder, 2009; Martín-Sánchez et al., 2016).

Table 1.4 | Lysosomal interaction with cytokines associated pathways. Adapted from (Ge et al, 2014).

Cytokines	Interactions between lysosome and cytokines
IL-1β	Pro-IL-1β is transformed into IL-1β by caspase-1 by interacting with Rab39a in lysosomes. Active IL-1β is secreted by lysosome exocytosis (C Andrei et al., 1999; Cristina Andrei et al., 2004)
IL-18	Similarly to IL-1β, IL-18 can reach the extracellular space via secretory lysosomes. This process is regulated by extracellular Ca^{2+} influx along the microtubular cytoskeleton (Gardella, Andrei, Poggi, Zocchi, & Rubartelli, 2000; Semino, Angelini, Poggi, & Rubartelli, 2005).
IL-6 IFN-β TNF-α	Lysosome-associated small RabGTPase Rab7b mediates inhibition of TLR4 and TLR 9 signaling, which down-regulate LPS-induced production of TNF-α, IL-6 and IFN-β (Y. Wang et al., 2007; Yao et al., 2009).
	IL-6 stimulation induces lysosome-dependent degradation of gp130, which is critical for the cessation of IL-6-mediated signaling (German, Sauer, & Howe, 2011).
	Hypoxia enhances lysosomal TNF-α degradation. Secretion of TNF-α may be localized to secretory lysosomes; TNF-α cytotoxic signaling induces lysosomal permeabilization (Lahat et al., 2008; Werneburg, Guicciardi, Yin, & Gores, 2004).
IL-8	Lysosomal polymeric peptidoglycan (PGN) processing is required for production of TNF-α in monocytes and for IL-8 production in neutrophils. LDL modified by lysosomal hydrolase can trigger the expression of IL-8 in macrophages (Hakala, Lindstedt, Kovanen, & Pentikäinen, 2006; Iyer et al., 2010).
TGF-β	SNX25 negatively regulates TGF-β signaling by enhancing the degradation of TGF-β receptor I. TGF-β1 increases its cellular expression of the receptor (integrin α5β1) by preventing integrin α5β1 degradation (Hao et al., 2011; Tian, Mythreye, Golzio, Katsanis, & Blobe, 2012).

Secretory lysosomes can either promote or suppress inflammation, depending on the stage of the inflammatory response. The first evidence demonstrating the role of lysosomes in IL-1β secretion were performed through immunoelectron microscopy analyses which revealed that in a fraction of endolysosomes intracellular pro-IL-1β and procaspase-1 colocalized with the lysosomal membrane protein LAMP-1 and the endolysosomal hydrolase cathepsin D. Furthermore, release of IL-1β from monocytes was accompanied by the secretion of cathepsin D (C Andrei et al., 1999).

The precise location of IL-1β maturation in macrophage is controversial. It has been described that an inflammatory signal (such as LPS) promotes the synthesis and cytoplasmic accumulation of the pro-IL-1β which then it is translocated into secretory lysosomes together with caspase-1. The mature form of IL-1β is produced within the lysosome by caspase-1 cleavage, after which the lysosomes fuse with the plasma membrane and their contents are released into

the extracellular space (Becker, & O'Neill, 2009; Ge, Li, Gao, & Cao, 2015). However, Brough and Rothwell clearly demonstrated that IL-1β is processed in the cytosol of ATP-stimulated peritoneal macrophages (Brough & Rothwell, 2007). Therefore, it was also found that for caspase-1 cleavage of pro-IL-1β, an interaction between caspase-1 and Rab39a is required. Proinflammatory stimuli induce Rab39a expression and IL-1β release, while Rab39a knockdown reduced IL-1β secretion (though pro-IL-1β mRNA levels are unchanged). Moreover, overexpression of Rab39a results in an increase in IL-1β secretion, showing that Rab39a functions as a trafficking adaptor linking caspase-1 to IL-1β lysosomal secretion (Becker et al., 2009). Then, the molecular mechanism of lysosome-mediated IL-1β secretion has been associated with an increase in intracellular Ca^{2+} during the release process, which mobilizes secretory lysosomes. This change occurs along microtubules close to the microtubule organizing center (Cristina Andrei et al., 2004; Carta et al., 2006), and is proceeded by actin-based movement at the cell periphery, towards the docking site at the plasma membrane. After docking to the plasma membrane, secretory lysosomes fuse with the plasma membrane and release their soluble contents into the extracellular space (Ge et al., 2015).

Finally, lysosomal related organelles: autophagosomes or autophagolysosomes, have also been implicated in IL-1β release. While autophagy is primarily a degradative process in the cytoplasm, secretory autophagy is proposed as a parallel function for unconventional secretion, in yeast and mammalian cells (Bruns, Mccaffery, Curwin, Duran, & Malhotra, 2011; Farhan, Kundu, & Ferro-Novick, 2017; Jiang, Dupont, Castillo, & Deretic, 2013). This secretory autophagy may contribute transiently to acute release of IL-1β in activated macrophages. Interestingly, it was found that this pathway is mediated by Atg5, inflammasome, the Golgi reassembly stacking protein 55 (GRASP55) and Rab8a. In addition, Rab8a knockdown reduced the secretion but not the synthesis of IL-1β (Dupont et al., 2011). Further studies are likely to reveal more of the machinery associated with these lysosomal related-unconventional secretory routes, predictably more Rabs, and also possibly SNAREs for vesicular routes.

1.4.3 Lysosome and atherosclerosis

In atherosclerosis, cellular events in lipid-loaded cells have received wide attention in last years, mainly the cellular alteration in macrophage-loaded cells (S. D. Fowler, Mayer, & Greenspan, 1985; Lewis et al., 1985). The intimal foam cells undergo extensive cytoplasmic and enzymatic alterations, which include changes in the enzymatic activity and ultrastructure of lysosomes. Beginning in the mid-1960s, evidence suggested that specific aspects of atherosclerosis have features consistent with an acquired LCD (C. de Duve, 1974). Lysosomal storage disorders are characterized by excess accumulation of material in lysosomes due to innate or acquired defects in the process of lysosomal hydrolysis. Moreover, using atherosclerotic rhesus monkeys and rabbit arteries, Fowler and collaborators successfully separated cells into two classes, which differed in density, lipid content, and lysosome character (S. Fowler et al., 1980). They found that lysosomes in the cell population described as low density and having foam cell morphology, accounted for 23-40% of the cellular volume, whereas the high density

population comprised 2-8%. It has been suggested that the increase in lysosomal volume and the shift of lipid to a lysosomal location reflect the transition of the high density to the low density cellular phenotype (S. Fowler et al., 1980; Shio, Haley, & Fowler, 1979). These findings implied that foam cell formation is accompanied by increases in the number and complexity of lysosomes. In addition, through hypercholesterolemic white Carneau pigeon experiments, it was reported the relationship among complex lysosome, lipid accumulation and cytoplasmic reorganization during lesion progression (Lewis et al., 1985; Lewis, Taylor, & Ohta, 1988). Although lysosome alteration has been suggested in foam cell formation, and complex lysosomes have been described from atherosclerotic arteries of several animal species, direct correlation of lesion progression with lysosomal alteration has not been clearly documented, as well as the underlying molecular mechanism.

As previously described in section 1.2.1 and 1.2.2, macrophages have two key sites for regulating intracellular sterol levels: the lysosome and lipid droplets. During the initial fatty streak phase of lesion development, CE accumulate mainly in cytoplasmic inclusions of atherosclerotic macrophages, indicating that lysosomal hydrolysis and sterol clearance is effective (Lewis et al., 1985). However, with the progression of atherosclerotic lesions in humans, nonhuman primates, rabbits and pigeons, a substantial accumulation of CE and cholesterol occurs in the lysosomes of macrophages and SMCs (S. Fowler et al., 1980; W. Gray Jerome & Lewis, 1990; B. F. Miller & Kothari, 1969), indicating a failure of lysosomal hydrolysis of CE and an inadequate clearance of sterols. These findings suggest that lysosome dysfunction is a key event in late-stages of the disease. In addition, *in vivo* experiments using pigeons showed that cholesterol trapped in the lysosomes of lesional foam cells remains trapped even when total plasma cholesterol returns to normal, while cytoplasmic CE droplets are rapidly cleared (W. Gray Jerome & Lewis, 1990). Treatment of THP-1 macrophages in culture with mildly ox-LDL or aggLDL shows similar trends in loss of lysosomal hydrolysis. Initially, lysosomal accumulation of free cholesterol and inhibition of CE hydrolysis is not observed. After prolonged exposure to mildly ox-LDL or aggLDL (48 h or more) increasing inhibition of CE hydrolysis occurs and lysosomes show an accumulation of CE (Griffin, Ullery, Cox, & Jerome, 2005; Yancey & Jerome, 2001). These findings suggested that lysosomal sterol accumulation is resistant to treatment and causes functional defects in lysosomes, being a key organelle in the initiation of atherosclerosis development.

1.4.3.1 Loss of lysosomal function: a crucial key in atherosclerosis

The loss of lysosomal function, including reduction in LAL-dependent CE hydrolysis over time, was verified using macrophages loaded with mildly ox-LDL or aggLDL (Cox, Griffin, Ullery, & Jerome, 2007). It was shown that increasing levels of lysosomal membrane cholesterol inhibited lysosomal acidification as a result of V-H^+ATPase inhibition. Consequently, lysosomal hydrolytic activity was diminished, corresponding to a time-dependent inhibition of CE hydrolysis and accumulation of ApoB. As LAL is only active at acidic pH, with maximal activity between pH=4-4.5 (Burton, Emery, & Mueller, 1980; Haley, Fowler, & de Duve, 1980), this

loss of V-H$^+$ATPase activity in response to cholesterol loading of the lysosomal membrane may be the main cause of loss of hydrolytic activity of LAL, and hence lead to lysosomal lipid accumulation. In addition, it was demonstrated that this lysosomal dysfunction in ox-LDL loaded macrophages was irreversible (W Gray Jerome, Cox, Griffin, & Ullery, 2008). This data indicates that inhibition of LAL activity, as well as other lysosomal enzymes such as cathepsins (O'Neil, Hoppe, & Hoff, 2003), is the result of a long-lived alteration in lysosomal function under excess lipid loading, resulting in lysosomal cargo accumulation. These findings are in agreement with our group data using a member of the cholesteryl hemiesters (ChE) family – cholesteryl hemisuccinate (ChS). Through the incubation of macrophages with LDL enriched in ChS an irreversible accumulation of undigested lipid was observed in enlarged lysosomes, which have ChS in their membranes (Domingues et al., 2017; Estronca et al., 2012). Furthermore, these enlarged lysosomes showed a decrease in hydrolytic capacity due to an increase in lysosomal pH (Domingues et al., 2017) – Chapter 3. Lysosomal dysfunction was also reported by Razani's group (Emanuel et al., 2014). They showed that ox-LDL and cholesterol crystals led to profound lysosomal dysfunction in cultured macrophages inducing: alteration in morphology, increase in lysosomal pH, decrease in proteolytic capacity and loss of lysosomal membrane integrity. Some of these results were also observed *in vivo*. Using flow cytometry, it was demonstrated that macrophages isolated from atherosclerotic plaques also display features of lysosome dysfunction. This group also reported that overexpression of TFEB in mouse peritoneal macrophages was able to preserve lysosomal acidity (Emanuel et al., 2014).

Lysosomal sterol-loaded membranes can present an increase in permeability, leading to lysosomal leakiness. This effect can be an additional reason for the increase in lysosomal pH due to a loss of the proton gradient. Furthermore, it was shown that macrophages incubated with ox-LDL or with a mixture of cholesterol oxidation products or with cholesterol crystals resulted in leakage of lysosomal enzymes into the cytosol (Emanuel et al., 2014; Li, Yuan, Olsson, & Brunk, 1998; Yuan et al., 2000). In addition, lysosomal pH increase was correlated with an increase in extracellular secretion of lysosomal enzymes, which may contribute to the extracellular LAL observed in atherosclerotic lesions (Hakala et al., 2003; Tapper & Sundler, 1992). Overall it appears that an increase in lysosomal sterols induce both defects in lysosome acidification and leakiness of the lysosomal membrane.

1.4.3.2 Lysosomol gene expression and gene mutation in atherosclerosis

In several LSDs is known the link between the loss of a given enzyme activity and lysosome cargo accumulation (W Gray Jerome, 2010). However, in other diseases, lysosomal cargo accumulation appears to be a secondary effect which creates imbalances in the cell homeostasis or metabolism (Vellodi, 2005). As detailed above, the lysosomal sterol accumulation accompanying atherosclerosis appears to represent this latter type of defect, not being identified a specific gene associated with the progression of the disease. However, some reports using animal models have associated LAL loss and atherosclerosis (S. Fowler et al., 1980; Goldfis-

cher et al., 1975; Lewis et al., 1985; Peters et al., 1972). In humans, LAL deficiency is a rare autosomal recessive LSD characterized by progressive accumulation of CE and TG in the liver, spleen and other organs (Reiner et al., 2014). Moreover, patients with LAL commonly suffer from dyslipidemia with elevated LDL-cholesterol, low HDL-cholesterol, and develop premature atherosclerosis, indicating the critical role of LAL. Thus, an increase in atherosclerosis and other cardiovascular disease prevalence was observed in these patients, along with a premature mortality (Bernstein et al., 2013; Elleder et al., 2000). In addition, the lysosomal acid lipase A (LIPA) gene has also been identified as a susceptibility gene for coronary artery disease by several genome-wide association studies (Ibc & Consortium, 2011; Wild et al., 2011). The understanding of the transcriptional regulation of LIPA in the artery wall during the progression of atherosclerosis is far from clear.

1.4.3.3 The role of Lysosomes in the inflammatory response of lipid-loaded macrophages

Among the numerous danger signals that activate NLRP3 inflammasomes, crystals and particulate matter, as silica, share similar molecular mechanisms to activate NLRP3 inflammasomes, where lysosomes execute a pivotal role. When macrophages, as well as other innate immune cells, engulf an excess of particles in lysosome, this causes an indigestion, which in turn induces lysosome destabilization and dysfunction (Karasawa & Takahashi, 2017). As described above, lysosomal destabilization can present an increase in membrane permeability and the leakage of cathepsin B into the cytosol, can occur through an unclear mechanism, which triggers NLRP3 inflammasome activation (Chen et al., 2015; Chu et al., 2009; Hornung et al., 2008). In addition to lysosomal protein release, particulate matter also trigger a K^+ efflux essential for the activation of NLRP3 inflammasomes induced by lysosomal destabilization (Yuan He, Hara, & Núñez, 2016; Muñoz-Planillo et al., 2013). However, the mechanism linking particulate matter-induced lysosomal rupture to K^+ efflux remains to be determined.

In the advanced atherosclerotic lesion, the deposition of cholesterol and calcium phosphate crystals was already identified (Small, 1988). It was found that cholesterol crystals are deposited even in the early stage of atherosclerotic lesion development and they activate NLRP3 inflammasomes via lysosomal destabilization (Duewell et al., 2010). Interestingly, it was showed that ox-LDL or cholesterol crystals not only induce cholesterol crystallization but also provide priming signals to induce NLRP3 and pro-IL-1β expression, providing signals 1 and 2 to induce IL-1β release, with induced lysosomal dysfunction being the second signal (Duewell et al., 2010; Emanuel et al., 2014) (Figure 1.7). On the other hand, calcium phosphate is also particulate matter, which becomes accumulated in atherosclerotic lesions and is associated with vascular calcification (Hirsch, Azoury, & Sarig, 1990). It was observed that calcium phosphate crystals, including hydroxyl apatite and tricalcium phosphate, activate NLRP3 inflammasomes through lysosomal rupture and subsequent cathepsin B release. Interestedly, it was also shown that calcium phosphate crystals induced caspase-1 activation and secretion of IL-1 family cytokines: IL-1β and IL-1α in macrophages (Usui et al., 2012).

Our group also observed that in macrophages incubated with ChS, which induced lysosome dysfunction, have an increased proinflammatory capacity, with elevated levels of IL-1β release, among other inflammatory cytokines (Domingues et al., 2017). However, in contrast with cholesterol crystals, ChS did not provide both signals necessary for IL-1β secretion. Furthermore, lysosome biogenesis was suggested as being protective against lysosomal destabilization-induced NLRP3 inflammasome activation. Activation of lysosome biogenesis by overexpression of TFEB inhibits NLRP3 inflammasome activation induced by cholesterol crystals and attenuates the progression of atherosclerosis, *in vitro* and *in vivo* (Emanuel et al., 2014). Since it is suggested that autophagy promotes destruction of the NLRP3 inflammasome complex in an ubiquitin-dependent manner (C.-S. Shi et al., 2012), this could explain the loss of NLRP3 upon TFEB overexpression. However, the regulatory mechanism to ubiquitinate the inflammasome complex is not fully elucidated. Further studies are required before the NLRP3 inflammasome can be considered a therapeutic target in inflammatory diseases.

1.5 CENTRAL GOALS OF THIS WORK

ChE are stable end-products resulting from CE oxidation and their precursors have been detected in human atheromata, as core-aldheydes (Hutchins & Murphy, 2011) and ox-LDL (Kamido & Myher, 1995). Macrophages exposed to LDL enriched in ChS demonstrated an irreversible accumulation of undigested lipid in lysosomes (Estronca et al., 2012). The major objective of this thesis was to define the proatherogenic properties of ChE found in human atherosclerosis lesions. Through *in vitro* and *in vivo* techniques, we aimed to define the biological activity of ChE towards primary and macrophages cell lines and zebrafish larvae. Firstly, the main focus was to demonstrate the atherogenic relevance of ChE on macrophages homeostasis and inflammation, using the only ChE commercial available - ChS, as a proof of concept. To further define ChE as proatherogenic compounds, we aimed to identify these compounds in human plasma and to correlate their levels with the pathological conditions of CVD. Then, we meant to address the activity of the main ChE found in human plasma– ChA, on monocytes inflammatory response, as well as the inflammatory and metabolic effect on macrophages. Through different approaches, we proposed to investigate the ChA effect on macrophages functionality. Finally, using zebrafish larvae, an animal model suitable to study the early stages of atheroma formation, we aimed to evaluate the proatherogenic activity of ChA. Our ultimately goal will be to contribute for the the development of an analytical tool that will permit an early diagnostic of instable atheroma plaques. Thus, in the end of this work, we aim to demonstrate the etiological relevance of ChE on the development of atherosclerotic plaque.

1.6 REFERENCES

Ait-Oufella, H., Herbin, O., Bouaziz, J.-D., Binder, C. J., Uyttenhove, C., Laurans, L., … Mallat, Z. (2010). B cell depletion reduces the development of atherosclerosis in mice. The Journal of Experimental Medicine, 207(8), 1579–1587. https://doi.org/10.1084/jem.20100155

Ait-Oufella, H., Kinugawa, K., Zoll, J., Simon, T., Boddaert, J., Heeneman, S., … Mallat, Z. (2007). Lactadherin deficiency leads to apoptotic cell accumulation and accelerated atherosclerosis in mice. Circulation, 115(16), 2168–2177. https://doi.org/10.1161/CIRCULATIONAHA.106.662080

Ait-Oufella, H., Pouresmail, V., Simon, T., Blanc-Brude, O., Kinugawa, K., Merval, R., … Mallat, Z. (2008). Defective mer receptor tyrosine kinase signaling in bone marrow cells promotes apoptotic cell accumulation and accelerates atherosclerosis. Arteriosclerosis, Thrombosis, and Vascular Biology, 28(8), 1429–1431. https://doi.org/10.1161/ATVBAHA.108.169078

Allahverdian, S., Chehroudi, A. C., McManus, B. M., Abraham, T., & Francis, G. A. (2014). Contribution of intimal smooth muscle cells to cholesterol accumulation and macrophage-like cells in human atherosclerosis. Circulation, 129(15), 1551–1559. https://doi.org/10.1161/CIRCULATIONAHA.113.005015

Anastasius, M., Kockx, M., Jessup, W., Sullivan, D., Rye, K. A., & Kritharides, L. (2016). Cholesterol efflux capacity: An introduction for clinicians. American Heart Journal. https://doi.org/10.1016/j.ahj.2016.07.005

Andersson, J., Libby, P., & Hansson, G. K. (2010). Adaptive immunity and atherosclerosis. Clinical Immunology. https://doi.org/10.1016/j.clim.2009.07.002

Andrei, C., Dazzi, C., Lotti, L., Torrisi, M. R., Chimini, G., & Rubartelli, A. (1999). The secretory route of the leaderless protein interleukin 1beta involves exocytosis of endolysosome-related vesicles. Mol Biol Cell, 10(5), 1463–1475. https://doi.org/10.1091/mbc.10.5.1463

Andrei, C., Margiocco, P., Poggi, A., Lotti, L. V, Torrisi, M. R., & Rubartelli, A. (2004). Phospholipases C and A2 control lysosome-mediated IL-1 beta secretion: Implications for inflammatory processes. Proceedings of the National Academy of Sciences of the United States of America, 101(26), 9745–50. https://doi.org/10.1073/pnas.0308558101

Andrews, N. W. (2002). Lysosomes and the plasma membrane: Trypanosomes reveal a secret relationship. Journal of Cell Biology. https://doi.org/10.1083/jcb.200205110

Ashraf, M. Z., & Gupta, N. (2011). Scavenger receptors: Implications in atherothrombotic disorders. International Journal of Biochemistry and Cell Biology, 43(5), 697–700. https://doi.org/10.1016/j.biocel.2011.01.019

Atkins, G. B., & Simon, D. I. (2013). Interplay between NF-kB and Kruppel-like factors in vascular inflammation and atherosclerosis: location, location, location. Journal of the American Heart Association, 2, e000290. https://doi.org/10.1161/JAHA.113.000290

Avraham-Davidi, I., Ely, Y., Pham, V. N., Castranova, D., Grunspan, M., Malkinson, G., … Yaniv, K. (2012). ApoB-containing lipoproteins regulate angiogenesis by modulating expression of VEGF receptor 1. Nature Medicine, 18(6), 967–973. https://doi.org/10.1038/nm.2759

Babaev, V. R., Ding, L., Zhang, Y., May, J. M., Lin, P. C., Fazio, S., & Linton, M. F. (2016). Macrophage IKKalpha Deficiency Suppresses Akt Phosphorylation, Reduces Cell Survival, and Decreases Early Atherosclerosis. Arteriosclerosis, Thrombosis, and Vascular Biology, 36(4), 598–607. https://doi.org/10.1161/ATVBAHA.115.306931

Babaev, V. R., Runner, R. P., Fan, D., Ding, L., Zhang, Y., Tao, H., … Linton, M. F. (2011). Macrophage mal1 deficiency suppresses atherosclerosis in low-density lipoprotein receptor-null mice by activating peroxisome proliferator-activated receptor-γ-regulated genes. Arteriosclerosis, Thrombosis, and Vascular Biology, 31(6), 1283–1290. https://doi.org/10.1161/ATVBAHA.111.225839

Babin, P. J., Thisse, C., Durliat, M., Andre, M., Akimenko, M. a, & Thisse, B. (1997). Both apolipoprotein E and A-I genes are present in a nonmammalian vertebrate and are highly expressed during embryonic development. Proceedings of the National Academy of Sciences of the United States of America, 94(16), 8622–8627. https://doi.org/10.1073/pnas.94.16.8622

Baldrighi, M., Mallat, Z., Li, X., & al., et. (2017). NLRP3 inflammasome pathways in atherosclerosis. Atherosclerosis, 32(0), 291. https://doi.org/10.1016/j.atherosclerosis.2017.10.027

Ballabio, A. (2016). The awesome lysosome. EMBO Molecular Medicine, 8(2), 73–76. https://doi.org/10.15252/emmm.201505966

Bar-Peled, L., Chantranupong, L., Cherniack, A. D., Chen, W. W., Ottina, K. A., Grabiner, B. C., … Sabatini, D. M. (2013). A Tumor Suppressor Complex with GAP Activity for the Rag GTPases That Signal Amino Acid Sufficiency to mTORC1. Science, 340(6136), 1100–1106. https://doi.org/10.1126/science.1232044

Bar-Peled, L., Schweitzer, L. D., Zoncu, R., & Sabatini, D. M. (2012). Ragulator is a GEF for the rag GTPases that signal amino acid levels to mTORC1. Cell, 150(6), 1196–1208. https://doi.org/10.1016/j.cell.2012.07.032

Barnes, M. J., & Farndale, R. W. (1999). Collagens and atherosclerosis. Experimental Gerontology. https://doi.org/10.1016/S0531-5565(99)00038-8

Basta, G., Schmidt, A. M., & De Caterina, R. (2004). Advanced glycation end products and vascular inflammation: Implications for accelerated atherosclerosis in diabetes. Cardiovascular Research. https://doi.org/10.1016/j.cardiores.2004.05.001

Becker, C. E., Creagh, E. M., & O'Neill, L. A. J. (2009). Rab39a binds caspase-1 and is required for caspase-1-dependent interleukin-1B secretion. Journal of Biological Chemistry, 284(50), 34531–34537. https://doi.org/10.1074/jbc.M109.046102

Bedard, K., & Krause, K.-H. (2007). The NOX Family of ROS-Generating NADPH Oxidases: Physiology and Pathophysiology. Physiological Reviews, 87(1), 245–313. https://doi.org/10.1152/physrev.00044.2005

Behnia, R., & Munro, S. (2005). Organelle identity and the signposts for membrane traffic. Nature, 438(7068), 597–604. https://doi.org/10.1038/nature04397

Bernstein, D. L., Hülkova, H., Bialer, M. G., & Desnick, R. J. (2013). Cholesteryl ester storage disease: Review of the findings in 135 reported patients with an underdiagnosed disease. Journal of Hepatology. https://doi.org/10.1016/j.jhep.2013.02.014

Bhat, O. M., Kumar, P. U., Giridharan, N. V., Kaul, D., Kumar, M. J. M., & Dhawan, V. (2015). Interleukin-18-induced atherosclerosis involves CD36 and NF-??B crosstalk in Apo E-/- mice. Journal of Cardiology, 66(1), 28–35. https://doi.org/10.1016/j.jjcc.2014.10.012

Bhatia, V. K., Yun, S., Leung, V., Grimsditch, D. C., Benson, G. M., Botto, M. B., … Haskard, D. O. (2007). Complement C1q Reduces Early Atherosclerosis in Low-Density Lipoprotein Receptor-Deficient Mice. The American Journal of Pathology, 170(1), 416–426. https://doi.org/10.2353/ajpath.2007.060406

Binder, C. J., Chou, M.-Y., Fogelstrand, L., Hartvigsen, K., Shaw, P. X., Boullier, A., & Witztum, J. L. (2008). Natural antibodies in murine atherosclerosis. Current Drug Targets, 9(3), 190–5. https://doi.org/10.2174/138945008783755520

Björkbacka, H., Kunjathoor, V. V, Moore, K. J., Koehn, S., Ordija, C. M., Lee, M. A., … Freeman, M. W. (2004). Reduced atherosclerosis in MyD88-null mice links elevated serum cholesterol levels to activation of innate immunity signaling pathways. Nature Medicine, 10(4), 416–421. https://doi.org/10.1038/nm1008

Bobryshev, Y. V., Ivanova, E. A., Chistiakov, D. A., Nikiforov, N. G., & Orekhov, A. N. (2016). Macrophages and Their Role in Atherosclerosis: Pathophysiology and Transcriptome Analysis. BioMed Research International, 2016. https://doi.org/10.1155/2016/9582430

Bolanos-Garcia, V. M., & Miguel, R. N. (2003). On the structure and function of apolipoproteins: More than a family of lipid-binding proteins. Progress in Biophysics and Molecular Biology. https://doi.org/10.1016/S0079-6107(03)00028-2

Boring, L., Gosling, J., Cleary, M., & Charo, I. F. (1998). Decreased lesion formation in CCR2-/- mice reveals a role for chemokines in the initiation of atherosclerosis. Nature, 394(6696), 894–897. https://doi.org/10.1038/29788

Bouchareychas, L., Pirault, J., Saint-Charles, F., Deswaerte, V., Le Roy, T., Jessup, W., … Lesnik, P. (2015). Promoting macrophage survival delays progression of pre-existing atherosclerotic lesions through macrophage-derived apoE. Cardiovascular Research, 108(1), 111–123. https://doi.org/10.1093/cvr/cvv177

Boya, P. (2012). Lysosomal Function and Dysfunction: Mechanism and Disease. Antioxidants & Redox Signaling, 17(5), 766–774. https://doi.org/10.1089/ars.2011.4405

Boyle, J. J. (2012). Heme and haemoglobin direct macrophage Mhem phenotype and counter foam cell formation in areas of intraplaque haemorrhage. Current Opinion in Lipidology, 23(5), 453–61. https://doi.org/10.1097/MOL.0b013e328356b145

Boyle, J. J., Harrington, H. A., Piper, E., Elderfield, K., Stark, J., Landis, R. C., & Haskard, D. O. (2009). Coronary Intraplaque Hemorrhage Evokes a Novel Atheroprotective Macrophage Phenotype. The American Journal of Pathology, 174(3), 1097–1108. https://doi.org/10.2353/ajpath.2009.080431

Boyle, J. J., Johns, M., Kampfer, T., Nguyen, A. T., Game, L., Schaer, D. J., … Haskard, D. O. (2012). Activating transcription factor 1 directs Mhem atheroprotective macrophages through coordinated iron handling and foam cell protection. Circulation Research, 110(1), 20–33. https://doi.org/10.1161/CIRCRESAHA.111.247577

Braun, R. J., Sommer, C., Leibiger, C., Gentier, R. J. G., Dumit, V. I., Paduch, K., … Madeo, F. (2015). Accumulation of basic amino acids at mitochondria dictates the cytotoxicity of aberrant ubiquitin. Cell Reports, 10(9), 1557–1571. https://doi.org/10.1016/j.celrep.2015.02.009

Bright, N. A., Davis, L. J., & Luzio, J. P. (2016). Endolysosomes Are the Principal Intracellular Sites of Acid Hydrolase Activity. Current Biology, 26(17), 2233–2245. https://doi.org/10.1016/j.cub.2016.06.046

Brough, D., & Rothwell, N. J. (2007). Caspase-1-dependent processing of pro-interleukin-1beta is cytosolic and precedes cell death. Journal of Cell Science, 120(5), 772–781. https://doi.org/10.1242/jcs.03377

Brown, M. S., & Goldstein, J. L. (1997). The SREBP pathway: Regulation of cholesterol metabolism by proteolysis of a membrane-bound transcription factor. Cell. https://doi.org/10.1016/S0092-8674(00)80213-5

Brown, M. S., Ho, Y. K., & Goldstein, J. L. (1980). The cholesteryl ester cycle in macrophage foam cells. Continual hydrolysis and re-esterification of cytoplasmic cholesteryl esters. Journal of Biological Chemistry, 255(19), 9344–9352.

Brown, T. M., & Bittner, V. (2009). Biomarkers of atherosclerosis: Clinical applications. Current Cardiovascular Risk Reports, 3(1), 23–30. https://doi.org/10.1007/s12170-009-0005-z

Bruns, C., Mccaffery, J. M., Curwin, A. J., Duran, J. M., & Malhotra, V. (2011). Biogenesis of a novel compartment for autophagosome-mediated unconventional protein secretion. Journal of Cell Biology, 195(6), 979–992. https://doi.org/10.1083/jcb.201106098

Burton, B. K., Emery, D., & Mueller, H. W. (1980). Lysosomal acid lipase in cultivated fibroblasts: Characterization of enzyme activity in normal and enzymatically deficient cell lines. Clinica Chimica Acta, 101(1), 25–32. https://doi.org/10.1016/0009-8981(80)90052-2

Caligiuri, G., Nicoletti, A., Poirierand, B., & Hansson, G. K. (2002). Protective immunity against atherosclerosis carried by B cells of hypercholesterolemic mice. Journal of Clinical Investigation, 109(6), 745–753. https://doi.org/10.1172/JCI200207272

Canton, J., Neculai, D., & Grinstein, S. (2013). Scavenger receptors in homeostasis and immunity. Nature Reviews Immunology, 13(9), 621–634. https://doi.org/10.1038/nri3515

Cardilo-Reis, L., Gruber, S., Schreier, S. M., Drechsler, M., Papac-Milicevic, N., Weber, C., … Binder, C. J. (2012). Interleukin-13 protects from atherosclerosis and modulates plaque composition by skewing the macrophage phenotype. EMBO Molecular Medicine, 4(10), 1072–1086. https://doi.org/10.1002/emmm.201201374

Carroll, B., & Dunlop, E. A. (2017). The lysosome: a crucial hub for AMPK and mTORC1 signaling. Biochemical Journal, 474(9), 1453–1466. https://doi.org/10.1042/BCJ20160780

Carta, S., Tassi, S., Semino, C., Fossati, G., Mascagni, P., Dinarello, C. A., & Rubartelli, A. (2006). Histone deacetylase inhibitors prevent exocytosis of interleukin-1beta-containing secretory lysosomes: role of microtubules. Blood, 108(5), 1618–26. https://doi.org/10.1182/blood-2006-03-014126

Castellano, B. M., Thelen, A. M., Moldavski, O., Feltes, M., van der Welle, R. E. N., Mydock-McGrane, L., … Zoncu, R. (2017). Lysosomal cholesterol activates mTORC1 via an SLC38A9–Niemann-Pick C1 signaling complex. Science, 355(6331), 1306–1311. https://doi.org/10.1126/science.aag1417

Chakraborty, M., Lou, C., Huan, C., Kuo, M. S., Park, T. S., Cao, G., & Jiang, X. C. (2013). Myeloid cell-specific serine palmitoyltransferase subunit 2 haploinsufficiency reduces murine atherosclerosis. Journal of Clinical Investigation, 123(4), 1784–1797. https://doi.org/10.1172/JCI60415

Chávez-Sánchez, L., Espinosa-Luna, J. E., Chávez-Rueda, K., Legorreta-Haquet, M. V., Montoya-Díaz, E., & Blanco-Favela, F. (2014). Innate Immune System Cells in Atherosclerosis. Archives of Medical Research. https://doi.org/10.1016/j.arcmed.2013.11.007

Chen, Y., Li, X., Boini, K. M., Pitzer, A. L., Gulbins, E., Zhang, Y., & Li, P. L. (2015). Endothelial Nlrp3 inflammasome activation associated with lysosomal destabilization during coronary arteritis. Biochimica et Biophysica Acta - Molecular Cell Research, 1853(2), 396–408. https://doi.org/10.1016/j.bbamcr.2014.11.012

Cheng, X., Shen, D., Samie, M., & Xu, H. (2010). Mucolipins: Intracellular TRPML1-3 channels. FEBS Letters. https://doi.org/10.1016/j.febslet.2009.12.056

Chesney, J., Mitchell, R., Benigni, F., Bacher, M., Spiegel, L., Al-Abed, Y., … Bucala, R. (1999). An inducible gene product for 6-phosphofructo-2-kinase with an AU-rich instability element: role in tumor cell glycolysis and the Warburg effect. Proceedings of the National Academy of Sciences of the United States of America, 96(6), 3047–52. https://doi.org/10.1073/PNAS.96.6.3047

Chi, H., Messas, E., Levine, R. A., Graves, D. T., & Amar, S. (2004). Interleukin-1 receptor signaling mediates atherosclerosis associated with bacterial exposure and/or a high-fat diet in a murine apolipoprotein E heterozygote model: Pharmacotherapeutic implications. Circulation, 110(12), 1678–1685. https://doi.org/10.1161/01.CIR.0000142085.39015.31

Childs, B. G., Baker, D. J., Wijshake, T., Conover, C. A., Campisi, J., & van Deursen, J. M. (2016). Senescent intimal foam cells are deleterious at all stages of atherosclerosis. Science, 354(6311), 472–477. https://doi.org/10.1126/science.aaf6659

Childs, B. G., Durik, M., Baker, D. J., & van Deursen, J. M. (2015). Cellular senescence in aging and age-related disease: from mechanisms to therapy. Nature Medicine, 21(12), 1424–1435. https://doi.org/10.1038/nm.4000

Chinetti-Gbaguidi, G., Baron, M., Bouhlel, M. A., Vanhoutte, J., Copin, C., Sebti, Y., … Staels, B. (2011). Human atherosclerotic plaque alternative macrophages display low cholesterol handling but high phagocytosis because of distinct activities of the PPARγ and LXRα pathways. Circulation Research, 108(8), 985–995. https://doi.org/10.1161/CIRCRESAHA.110.233775

Chinetti-Gbaguidi, G., Colin, S., & Staels, B. (2014). Macrophage subsets in atherosclerosis. Nature Reviews Cardiology, 12(1), 10–17. https://doi.org/10.1038/nrcardio.2014.173

Chistiakov, D. A., Bobryshev, Y. V., Nikiforov, N. G., Elizova, N. V., Sobenin, I. A., & Orekhov, A. N. (2015). Macrophage phenotypic plasticity in atherosclerosis: The associated features and the peculiarities of the expression of inflammatory genes. International Journal of Cardiology, 184(1), 436–445. https://doi.org/10.1016/j.ijcard.2015.03.055

Choi, S. H., Yin, H., Ravandi, A., Armando, A., Dumlao, D., Kim, J., … Miller, Y. I. (2013). Polyoxygenated cholesterol ester hydroperoxide activates TLR4 and SYK dependent signaling in macrophages. PLoS ONE, 8(12). https://doi.org/10.1371/journal.pone.0083145

Christ, A., Bekkering, S., Latz, E., & Riksen, N. P. (2016). Long-term activation of the innate immune system in atherosclerosis. Seminars in Immunology. https://doi.org/10.1016/j.smim.2016.04.004

Chu, J., Thomas, L. M., Watkins, S. C., Franchi, L., Nunez, G., & Salter, R. D. (2009). Cholesterol-dependent cytolysins induce rapid release of mature IL-1 from murine macrophages in a NLRP3 inflammasome and cathepsin B-dependent manner. Journal of Leukocyte Biology, 86(5), 1227–1238. https://doi.org/10.1189/jlb.0309164

Cochain, C., & Zernecke, A. (2017). Macrophages in vascular inflammation and atherosclerosis. Pflugers Archiv European Journal of Physiology, 469(3–4), 485–499. https://doi.org/10.1007/s00424-017-1941-y

Colin, S., Chinetti-Gbaguidi, G., & Staels, B. (2014). Macrophage phenotypes in atherosclerosis. Immunological Reviews, 262(1), 153–166. https://doi.org/10.1111/imr.12218

Combadière, C., Potteaux, S., Rodero, M., Simon, T., Pezard, A., Esposito, B., … Mallat, Z. (2008). Combined inhibition of CCL2, CX3CR1, and CCR5 abrogates Ly6Chi and Ly6Clo monocytosis and almost abolishes atherosclerosis in hypercholesterolemic mice. Circulation, 117(13), 1649–1657. https://doi.org/10.1161/CIRCULATIONAHA.107.745091

Conti, P., Lessiani, G., Kritas, S. K., Ronconi, G., Caraffa, A., & Theoharides, T. C. (2017). Mast cells emerge as mediators of atherosclerosis: Special emphasis on IL-37 inhibition. Tissue and Cell. https://doi.org/10.1016/j.tice.2017.04.002

Cox, B. E., Griffin, E. E., Ullery, J. C., & Jerome, W. G. (2007). Effects of cellular cholesterol loading on macrophage foam cell lysosome acidification. Journal of Lipid Research, 48(5), 1012–21. https://doi.org/10.1194/jlr.M600390-JLR200

Cyrus, T., Witztum, J. L., Rader, D. J., Tangirala, R., Fazio, S., Linton, M. F., & Funk, C. D. (1999). Disruption of the 12/15-lipoxygenase gene diminishes atherosclerosis in apo E-deficient mice. Journal of Clinical Investigation, 103(11), 1597–1604. https://doi.org/10.1172/JCI5897

de Duve, C. (1974). The participation of lysosomes in the transformation of smooth muscle cells to foamy cells in the aorta of cholesterol-fed rabbits. Acta Cardiologica, Suppl 20, 9–25.

de Duve, C. (2005). The lysosome turns fifty. Nature Cell Biology, 7(9), 847–9. https://doi.org/10.1038/ncb0905-847

De Paoli, F., Staels, B., & Chinetti-Gbaguidi, G. (2014). Macrophage Phenotypes and Their Modulation in Atherosclerosis. Circulation Journal, 78(8), 1775–1781. https://doi.org/10.1253/circj.CJ-14-0621

Delporte, C., Van Antwerpen, P., Vanhamme, L., Roumeguère, T., & Zouaoui Boudjeltia, K. (2013). Low-density lipoprotein modified by myeloperoxidase in inflammatory pathways and clinical studies. Mediators of Inflammation. https://doi.org/10.1155/2013/971579

Denny, M. F., Yalavarthi, S., Zhao, W., Thacker, S. G., Anderson, M., Sandy, A. R., … Kaplan, M. J. (2010). A Distinct Subset of Proinflammatory Neutrophils Isolated from Patients with Systemic Lupus Erythematosus Induces Vascular Damage and Synthesizes Type I IFNs. The Journal of Immunology, 184(6), 3284–3297. https://doi.org/10.4049/jimmunol.0902199

Di Paolo, G., & De Camilli, P. (2006). Phosphoinositides in cell regulation and membrane dynamics. Nature, 443(7112), 651–657. https://doi.org/10.1038/nature05185

Dinarello, C. A. (2009). Immunological and Inflammatory Functions of the Interleukin-1 Family. Annual Review of Immunology, 27(1), 519–550. https://doi.org/10.1146/annurev.immunol.021908.132612

Ding, Y., Subramanian, S., Montes, V. N., Goodspeed, L., Wang, S., Han, C. Y., … Chait, A. (2012). Toll-like receptor 4 deficiency decreases atherosclerosis but does not protect against inflammation in obese low-density lipoprotein receptor-deficient mice. Arteriosclerosis, Thrombosis, and Vascular Biology, 32(7), 1596–1604. https://doi.org/10.1161/ATVBAHA.112.249847

Dodeller, F., Gottar, M., Huesken, D., Iourgenko, V., & Cenni, B. (2008). The lysosomal transmembrane protein 9B regulates the activity of inflammatory signaling pathways. The Journal of Biological Chemistry, 283(31), 21487–94. https://doi.org/10.1074/jbc.M801908200

Domingues, N., Estronca, L. M. B. B., Silva, J., Encarnação, M. R., Mateus, R., Silva, D., … Vieira, O. V. (2017). Cholesteryl hemiesters alter lysosome structure and function and induce proinflammatory cytokine production in macrophages. Biochimica et Biophysica Acta - Molecular and Cell Biology of Lipids, 1862(2), 210–220. https://doi.org/10.1016/j.bbalip.2016.10.009

Dong, X., Shen, D., Wang, X., Dawson, T., Li, X., Zhang, Q., … Xu, H. (2010). PI(3,5)P2 controls membrane trafficking by direct activation of mucolipin Ca2+ release channels in the endolysosome. Nature Communications, 1(4), 1–11. https://doi.org/10.1038/ncomms1037

Doran, A. C., Lipinski, M. J., Oldham, S. N., Garmey, J. C., Campbell, K. A., Skaflen, M. D., … McNamara, C. A. (2012). B-cell aortic homing and atheroprotection depend on Id3. Circulation Research, 110(1). https://doi.org/10.1161/CIRCRESAHA.111.256438

Döring, Y., Soehnlein, O., & Weber, C. (2017). Neutrophil extracellular traps in atherosclerosis and atherothrombosis. Circulation Research. https://doi.org/10.1161/CIRCRESAHA.116.309692

Drechsler, M., De Jong, R., Rossaint, J., Viola, J. R., Leoni, G., Wang, J. M., … Soehnlein, O. (2015). Annexin A1 counteracts chemokine-induced arterial myeloid cell recruitment. Circulation Research, 116(5), 827–835. https://doi.org/10.1161/CIRCRESAHA.116.305825

Dubland, J. A., & Francis, G. A. (2015). Lysosomal acid lipase: at the crossroads of normal and atherogenic cholesterol metabolism. Frontiers in Cell and Developmental Biology, 3, 3. https://doi.org/10.3389/fcell.2015.00003

Duewell, P., Kono, H., Rayner, K. J., Sirois, C. M., Vladimer, G., Bauernfeind, F. G., … Latz, E. (2010). NLRP3 inflammasomes are required for atherogenesis and activated by cholesterol crystals. Nature, 466(7306), 652–652. https://doi.org/10.1038/nature09316

Dupont, N., Jiang, S., Pilli, M., Ornatowski, W., Bhattacharya, D., & Deretic, V. (2011). Autophagy-based unconventional secretory pathway for extracellular delivery of IL-1β. The EMBO Journal, 30(23), 4701–4711. https://doi.org/10.1038/emboj.2011.398

Dutta, P., Courties, G., Wei, Y., Leuschner, F., Gorbatov, R., Robbins, C. S., … Nahrendorf, M. (2012). Myocardial infarction accelerates atherosclerosis. Nature, 487(7407), 325–329. https://doi.org/10.1038/nature11260

Eder, C. (2009). Mechanisms of interleukin-1beta release. Immunobiology, 214(7), 543–53. https://doi.org/10.1016/j.imbio.2008.11.007

Elahi, M. M., Kong, Y. X., & Matata, B. M. (2009). Oxidative Stress as a Mediator of Cardiovascular Disease. Oxidative Medicine and Cellular Longevity, 2(5), 259–269. https://doi.org/10.4161/oxim.2.5.9441

Elleder, M., Chlumská, A., Hyánek, J., Poupětová, H., Ledvinová, J., Maas, S., & Lohse, P. (2000). Subclinical course of cholesteryl ester storage disease in an adult with hypercholesterolemia, accelerated atherosclerosis, and liver cancer. Journal of Hepatology, 32(3), 528–534. https://doi.org/10.1016/S0168-8278(00)80407-9

Emanuel, R., Sergin, I., Bhattacharya, S., Turner, J. N., Epelman, S., Settembre, C., … Razani, B. (2014). Induction of lysosomal biogenesis in atherosclerotic macrophages can rescue lipid-induced lysosomal dysfunction and downstream sequelae. Arteriosclerosis, Thrombosis, and Vascular Biology, 34(9), 1942–1952. https://doi.org/10.1161/ATVBAHA.114.303342

Emini Veseli, B., Perrotta, P., De Meyer, G. R. A., Roth, L., Van der Donckt, C., Martinet, W., & De Meyer, G. R. Y. (2016). Animal models of atherosclerosis. European Journal of Pharmacology. https://doi.org/10.1016/j.ejphar.2017.05.010

Encarnação, M., Espada, L., Escrevente, C., Mateus, D., Ramalho, J., Michelet, X., … Vieira, O. V. (2016). A Rab3a-dependent complex essential for lysosome positioning and plasma membrane repair. Journal of Cell Biology, 213(6), 631–640. https://doi.org/10.1083/jcb.201511093

Ensan, S., Li, A., Besla, R., Degousee, N., Cosme, J., Roufaiel, M., … Robbins, C. S. (2015). Self-renewing resident arterial macrophages arise from embryonic CX3CR1+ precursors and circulating monocytes immediately after birth. Nature Immunology, 17(2), 159–168. https://doi.org/10.1038/ni.3343

Erbel, C., Tyka, M., Helmes, C. M., Akhavanpoor, M., Rupp, G., Domschke, G., … Gleissner, C. A. (2015). CXCL4-induced plaque macrophages can be specifically identified by co-expression of MMP7 + S100A8 + in vitro and in vivo. Innate Immunity, 21(3), 255–265. https://doi.org/10.1177/1753425914526461

Erbel, C., Wolf, A., Lasitschka, F., Linden, F., Domschke, G., Akhavanpoor, M., … Gleissner, C. A. (2015). Prevalence of M4 macrophages within human coronary atherosclerotic plaques is associated with features of plaque instability. International Journal of Cardiology, 186, 219–225. https://doi.org/10.1016/j.ijcard.2015.03.151

Esterbauer, H., Jürgens, G., Quehenberger, O., & Koller, E. (1987). Autoxidation of human low density lipoprotein: loss of polyunsaturated fatty acids and vitamin E and generation of aldehydes. Journal of Lipid Research, 28(5), 495–509.

Esterbauer, H., Puhl, H., Martina, R., Waeg, G., & Rabl, H. (1991). Effect of Antioxidants on Oxidative Modification of LDL. Annals of Medicine, 23(23), 573–581.

Estronca, L. M. B. B., Silva, J. C. P., Sampaio, J. L., Shevchenko, A., Verkade, P., Vaz, A. D. N., … Vieira, O. V. (2012). Molecular etiology of atherogenesis--in vitro induction of lipidosis in macrophages with a new LDL model. PloS One, 7(4), e34822. https://doi.org/10.1371/journal.pone.0034822

Fang, L., Harkewicz, R., Hartvigsen, K., Wiesner, P., Choi, S. H., Almazan, F., … Miller, Y. I. (2010). Oxidized cholesteryl esters and phospholipids in zebrafish larvae fed a high cholesterol diet: Macrophage binding and activation. Journal of Biological Chemistry, 285(42), 32343–32351. https://doi.org/10.1074/jbc.M110.137257

Fang, L., Liu, C., & Miller, Y. I. (2014). Zebrafish models of dyslipidemia: Relevance to atherosclerosis and angiogenesis. Translational Research. https://doi.org/10.1016/j.trsl.2013.09.004

Farhan, H., Kundu, M., & Ferro-Novick, S. (2017). The link between autophagy and secretion: a story of multitasking proteins. Molecular Biology of the Cell, 28(9), 1161–1164. https://doi.org/10.1091/mbc.E16-11-0762

Feil, S., Fehrenbacher, B., Lukowski, R., Essmann, F., Schulze-Osthoff, K., Schaller, M., & Feil, R. (2014). Transdifferentiation of vascular smooth muscle cells to macrophage-like cells during atherogenesis. Circulation Research, 115(7), 662–667. https://doi.org/10.1161/CIRCRESAHA.115.304634

Feingold, K. R., & Grunfeld, C. (2015). Introduction to Lipids and Lipoproteins. Endotext, 1–19. Retrieved from http://www.ncbi.nlm.nih.gov/pubmed/26247089

Ferrante, G., Nakano, M., Prati, F., Niccoli, G., Mallus, M. T., Ramazzotti, V., … Crea, F. (2010). High levels of systemic myeloperoxidase are associated with coronary plaque erosion in patients with acute coronary syndromes: A clinicopathological study. Circulation, 122(24), 2505–2513. https://doi.org/10.1161/CIRCULATIONAHA.110.955302

Finbow, M. E., & Harrison, M. A. (1997). The vacuolar H+-ATPase: a universal proton pump of eukaryotes. The Biochemical Journal, (Pt 3), 697–712. https://doi.org/10.1042/bj3240697

Foks, A. C., Engelbertsen, D., Kuperwaser, F., Alberts-Grill, N., Gonen, A., Witztum, J. L., … Lichtman, A. H. (2016). Blockade of Tim-1 and Tim-4 enhances atherosclerosis in low-density lipoprotein receptor-deficient mice. Arteriosclerosis, Thrombosis, and Vascular Biology, 36(3), 456–465. https://doi.org/10.1161/ATVBAHA.115.306860

Fowler, S., Berberian, P. a., Shio, H., Goldfischer, S., & Wolinsky, H. (1980). Characterization of cell populations isolated from aortas of rhesus monkeys with experimental atherosclerosis. Circulation Research, 46(4), 520–530. https://doi.org/10.1161/01.RES.46.4.520

Fowler, S. D., Mayer, E. P., & Greenspan, P. (1985). Foam Cells and Atherogenesis. Annals of the New York Academy of Sciences, 454(1), 79–90. https://doi.org/10.1111/j.1749-6632.1985.tb11846.x

Freemerman, A. J., Johnson, A. R., Sacks, G. N., Milner, J. J., Kirk, E. L., Troester, M. A., … Makowski, L. (2014). Metabolic reprogramming of macrophages: Glucose transporter 1 (GLUT1)-mediated glucose metabolism drives a proinflammatory phenotype. Journal of Biological Chemistry, 289(11), 7884–7896. https://doi.org/10.1074/jbc.M113.522037

Furuhashi, M., & Hotamisligil, G. S. (2008). Fatty acid-binding proteins: role in metabolic diseases and potential as drug targets. Nature Reviews Drug Discovery, 7(6), 489–503. https://doi.org/10.1038/nrd2589

Gaber, T., Strehl, C., & Buttgereit, F. (2017). Metabolic regulation of inflammation. Nature Reviews Rheumatology, 13(5), 267–279. https://doi.org/10.1038/nrrheum.2017.37

Gage, J., Hasu, M., Thabet, M., & Whitman, S. C. (2012). Caspase-1 Deficiency Decreases Atherosclerosis in Apolipoprotein E-Null Mice. Canadian Journal of Cardiology, 28(2), 222–229. https://doi.org/10.1016/j.cjca.2011.10.013

Gargiulo, S., Gramanzini, M., & Mancini, M. (2016). Molecular imaging of vulnerable plaque in animal models. Int J Mol Sci, 17(9), pii:E1511. https://doi.org/10.3390/www.mdpi.com/journal/ijms

Gaut, J. P., & Heinecke, J. W. (2001). Mechanisms for oxidizing low-density lipoprotein: Insights from patterns of oxidation products in the artery wall and from mouse models of atherosclerosis. Trends in Cardiovascular Medicine. https://doi.org/10.1016/S1050-1738(01)00101-3

Ge, W., Li, D., Gao, Y., & Cao, X. (2015). The Roles of Lysosomes in Inflammation and Autoimmune Diseases. International Reviews of Immunology, 34(5), 415–431. https://doi.org/10.3109/08830185.2014.936587

Geeraerts, X., Bolli, E., Fendt, S. M., & Van Ginderachter, J. A. (2017). Macrophage metabolism as therapeutic target for cancer, atherosclerosis, and obesity. Frontiers in Immunology. https://doi.org/10.3389/fimmu.2017.00289

Getz, G. S., & Reardon, C. A. (2017). Natural killer T cells in atherosclerosis. Nature Reviews Cardiology, 14(5), 304–314. https://doi.org/10.1038/nrcardio.2017.2

Getz, G. S., Reardon, C. A., Getz, G. S., & Reardon, C. A. (2012). Animal Models of Atherosclerosis Animal Models of Atherosclerosis. Arteriosclerosis, Thrombosis, and Vascular Biology, 32(5), 1104–1115. https://doi.org/10.1161/ATVBAHA.111.237693

Gimbrone, M. A., & García-Cardeña, G. (2013). Vascular endothelium, hemodynamics, and the pathobiology of atherosclerosis. Cardiovascular Pathology. https://doi.org/10.1016/j.carpath.2012.06.006

Gisterå, A., & Hansson, G. K. (2017a). The immunology of atherosclerosis. Nature Reviews Nephrology, 13(6), 368–380. https://doi.org/10.1038/nrneph.2017.51

Gisterå, A., & Hansson, G. K. (2017b). The immunology of atherosclerosis. Nature Reviews Nephrology, 13(6), 368–380. https://doi.org/10.1038/nrneph.2017.51

Gleissner, C. A., Shaked, I., Little, K. M., & Ley, K. (2010). CXC Chemokine Ligand 4 Induces a Unique Transcriptome in Monocyte-Derived Macrophages. The Journal of Immunology, 184(9), 4810–4818. https://doi.org/10.4049/jimmunol.0901368

Goldfischer, S., Schiller, B., & Wolinsky, H. (1975). Lipid accumulation in smooth muscle cell lysosomes im primate atherosclerosis. The American Journal of Pathology, 78(3), 497–504. Retrieved from http://www.pubmedcentral.nih.gov/articlerender.fcgi?artid=1912555&tool=pmcentrez&rendertype=abstract

Gordon, S., & Martinez, F. O. (2010). Alternative activation of macrophages: Mechanism and functions. Immunity. https://doi.org/10.1016/j.immuni.2010.05.007

Gough, P. J., Gomez, I. G., Wille, P. T., & Raines, E. W. (2006). Macrophage expression of active MMP-9 induces acute plaque disruption in apoE-deficient mice. Journal of Clinical Investigation, 116(1), 59–69. https://doi.org/10.1172/JCI25074

Grant, B. D., & Donaldson, J. G. (2009). Pathways and mechanisms of endocytic recycling. Nature Reviews Molecular Cell Biology, 10(9), 597–608. https://doi.org/10.1038/nrm2755

Graves, A. R., Curran, P. K., Smith, C. L., & Mindell, J. A. (2008). The Cl-/H+ antiporter ClC-7 is the primary chloride permeation pathway in lysosomes. Nature, 453(7196), 788–792. https://doi.org/10.1038/nature06907

Greaves, D. R., & Gordon, S. (2009). The macrophage scavenger receptor at 30 years of age: current knowledge and future challenges. Journal of Lipid Research, 50 Suppl(3), S282-6. https://doi.org/10.1194/jlr.R800066-JLR200

Griffin, E. E., Ullery, J. C., Cox, B. E., & Jerome, W. G. (2005). Aggregated LDL and lipid dispersions induce lysosomal cholesteryl ester accumulation in macrophage foam cells. Journal of Lipid Research, 46(10), 2052–2060. https://doi.org/10.1194/jlr.M500059-JLR200

Guerra, F., & Bucci, C. (2016). Multiple Roles of the Small GTPase Rab7. Cells, 5(3), 34. https://doi.org/10.3390/cells5030034

Guo, H., Callaway, J. B., & Ting, J. P.-Y. (2015). Inflammasomes: mechanism of action, role in disease, and therapeutics. Nature Medicine, 21(7), 677–687. https://doi.org/10.1038/nm.3893

Hajjar, D. P., & Hajjar, K. A. (2016). Alterations of Cholesterol Metabolism in Inflammation-Induced Atherogenesis. Journal of Enzymology and Metabolism, 1(1). Retrieved from http://www.ncbi.nlm.nih.gov/pubmed/28868527%0Ahttp://www.pubmedcentral.nih.gov/articlerender.fcgi?artid=PMC5575901

Hakala, J. K., Oksjoki, R., Laine, P., Du, H., Grabowski, G. A., Kovanen, P. T., & Pentikäinen, M. O. (2003). Lysosomal enzymes are released from cultured human macrophages, hydrolyze LDL in vitro, and are present extracellularly in human atherosclerotic lesions. Arteriosclerosis, Thrombosis, and Vascular Biology, 23(8), 1430–1436. https://doi.org/10.1161/01.ATV.0000077207.49221.06

Haley, N. J., Fowler, S., & de Duve, C. (1980). Lysosomal acid cholesteryl esterase activity in normal and lipid-laden aortic cells. Journal of Lipid Research, 21(8), 961–969.

Han, X., Kitamoto, S., Wang, H., & Boisvert, W. A. (2010). Interleukin-10 overexpression in macrophages suppresses atherosclerosis in hyperlipidemic mice. The FASEB Journal, 24(8), 2869–2880. https://doi.org/10.1096/fj.09-148155

Hansson, G. K. (2002). Innate and Adaptive Immunity in the Pathogenesis of Atherosclerosis. Circulation Research, 91(4), 281–291. https://doi.org/10.1161/01.RES.0000029784.15893.10

Hansson, G. K. (2005a). Inflammation, Atherosclerosis, and Coronary Artery Disease. New England Journal of Medicine, 352(16), 1685–1695. https://doi.org/10.1056/NEJMra043430

Hansson, G. K. (2005b). Inflammation, Atherosclerosis, and Coronary Artery Disease. New England Journal of Medicine, 352(16), 1685–1695. https://doi.org/10.1056/NEJMra043430

Haschemi, A., Kosma, P., Gille, L., Evans, C. R., Burant, C. F., Starkl, P., … Wagner, O. (2012). The sedoheptulose kinase CARKL directs macrophage polarization through control of glucose metabolism. Cell Metabolism, 15(6), 813–826. https://doi.org/10.1016/j.cmet.2012.04.023

He, L., Weber, K. J., & Schilling, J. D. (2016). Glutamine modulates macrophage lipotoxicity. Nutrients, 8(4). https://doi.org/10.3390/nu8040215

He, Y., Hara, H., & Núñez, G. (2016). Mechanism and Regulation of NLRP3 Inflammasome Activation. Trends in Biochemical Sciences. https://doi.org/10.1016/j.tibs.2016.09.002

He, Y., Xu, Y., Zhang, C., Gao, X., Dykema, K. J., Martin, K. R., … Xu, H. E. (2011). Identification of a Lysosomal Pathway That Modulates Glucocorticoid Signaling and the Inflammatory Response. Science Signaling, 4(180), ra44-ra44. https://doi.org/10.1126/scisignal.2001450

He, Y., Zeng, M. Y., Yang, D., Motro, B., & Núñez, G. (2016). NEK7 is an essential mediator of NLRP3 activation downstream of potassium efflux. Nature, 530(7590), 354–357. https://doi.org/10.1038/nature16959

Hegele, R. A. (2009). Plasma lipoproteins: genetic influences and clinical implications. Nature Reviews Genetics, 10(2), 109–121. https://doi.org/10.1038/nrg2481

Hendrikx, T., Jeurissen, M. L. J., Van Gorp, P. J., Gijbels, M. J., Walenbergh, S. M. A., Houben, T., … Shiri-Sverdlov, R. (2015). Bone marrow-specific caspase-1/11 deficiency inhibits atherosclerosis development in Ldlr-/- mice. FEBS Journal, 282(12), 2327–2338.

https://doi.org/10.1111/febs.13279

Hirsch, D., Azoury, R., & Sarig, S. (1990). Co-crystallization of cholesterol and calcium phosphate as related to atherosclerosis. Journal of Crystal Growth, 104(4), 759–765. https://doi.org/10.1016/0022-0248(90)90099-7

Hong, Y. M. (2010). Atherosclerotic cardiovascular disease beginning in childhood. Korean Circulation Journal. https://doi.org/10.4070/kcj.2010.40.1.1

Hoppe, G., Ravandi, a, Herrera, D., Kuksis, a, & Hoff, H. F. (1997). Oxidation products of cholesteryl linoleate are resistant to hydrolysis in macrophages, form complexes with proteins, and are present in human atherosclerotic lesions. Journal of Lipid Research, 38(7), 1347–1360.

Hornung, V., Bauernfeind, F., Halle, A., Samstad, E. O., Kono, H., Rock, K. L., … Latz, E. (2008). Silica crystals and aluminum salts activate the NALP3 inflammasome through phagosomal destabilization. Nature Immunology, 9(8), 847–856. https://doi.org/10.1038/ni.1631

Horton, J. D., Cohen, J. C., & Hobbs, H. H. (2007). Molecular biology of PCSK9: its role in LDL metabolism. Trends in Biochemical Sciences. https://doi.org/10.1016/j.tibs.2006.12.008

Hoseini, Z., Sepahvand, F., Rashidi, B., Sahebkar, A., Masoudifar, A., & Mirzaei, H. (2017). NLRP3 inflammasome: Its regulation and involvement in atherosclerosis. Journal of Cellular Physiology. https://doi.org/10.1002/jcp.25930

Huang, S. C. C., Smith, A. M., Everts, B., Colonna, M., Pearce, E. L., Schilling, J. D., & Pearce, E. J. (2016). Metabolic Reprogramming Mediated by the mTORC2-IRF4 Signaling Axis Is Essential for Macrophage Alternative Activation. Immunity, 45(4), 817–830. https://doi.org/10.1016/j.immuni.2016.09.016

Hughes, J. E., Srinivasan, S., Lynch, K. R., Proia, R. L., Ferdek, P., & Hedrick, C. C. (2008). Sphingosine-1-phosphate induces an antiinflammatory phenotype in macrophages. Circulation Research, 102(8), 950–958. https://doi.org/10.1161/CIRCRESAHA.107.170779

Hume, D. A. (2008). Differentiation and heterogeneity in the mononuclear phagocyte system. Mucosal Immunology, 1(6), 432–441. https://doi.org/10.1038/mi.2008.36

Huo, Y., Iadevaia, V., Yao, Z., Kelly, I., Cosulich, S., Guichard, S., … Proud, C. G. (2012). Stable isotope-labelling analysis of the impact of inhibition of the mammalian target of rapamycin on protein synthesis. Biochem. J, 444, 141–151. https://doi.org/10.1042/BJ20112107

Huotari, J., & Helenius, A. (2011). Endosome maturation. The EMBO Journal, 30(17), 3481–3500. https://doi.org/10.1038/emboj.2011.286

Hussain, M. M., Fatma, S., Pan, X., & Iqbal, J. (2005). Intestinal lipoprotein assembly. Current Opinion in Lipidology, 16(3), 281–285. https://doi.org/10.1097/01.mol.0000169347.53568.5a

Hutchins, P. M., Moore, E. E., & Murphy, R. C. (2011). Electrospray MS/MS reveals extensive and nonspecific oxidation of cholesterol esters in human peripheral vascular lesions. Journal of Lipid Research, 52(11), 2070–2083. https://doi.org/10.1194/jlr.M019174

Ibc, T., & Consortium, C. A. D. (2011). Large-scale gene-centric analysis identifies novel variants for coronary artery disease. PLoS Genetics, 7(9), e1002260. https://doi.org/10.1371/journal.pgen.1002260

Ilhan, F., & Kalkanli, S. T. (2015). Atherosclerosis and the role of immune cells. World Journal of Clinical Cases, 3(4), 345–52. https://doi.org/10.12998/wjcc.v3.i4.345

Ingersoll, M. A., Platt, A. M., Potteaux, S., & Randolph, G. J. (2011). Monocyte trafficking in acute and chronic inflammation. Trends in Immunology. https://doi.org/10.1016/j.it.2011.05.001

Itakura, E., Kishi-Itakura, C., Koyama-Honda, I., & Mizushima, N. (2012). Structures containing Atg9A and the ULK1 complex independently target depolarized mitochondria at initial stages of Parkin-mediated mitophagy. Journal of Cell Science, 125(6), 1488–1499. https://doi.org/10.1242/jcs.094110

Jaiswal, J. K., Andrews, N. W., & Simon, S. M. (2002). Membrane proximal lysosomes are the major vesicles responsible for calcium-dependent exocytosis in nonsecretory cells. Journal of Cell Biology, 159(4), 625–635. https://doi.org/10.1083/jcb.200208154

Jenkins, S. J., & Hume, D. A. (2014). Homeostasis in the mononuclear phagocyte system. Trends in Immunology. https://doi.org/10.1016/j.it.2014.06.006

Jerome, W. G. (2006). Advanced atherosclerotic foam cell formation has features of an acquired lysosomal storage disorder. Rejuvenation Research, 9(2), 245–255. https://doi.org/10.1089/rej.2006.9.245

Jerome, W. G. (2010). Lysosomes, cholesterol and atherosclerosis. Clinical Lipidology, 5(6), 853–865. https://doi.org/10.2217/clp.10.70

Jerome, W. G., Cox, B. E., Griffin, E. E., & Ullery, J. C. (2008). Lysosomal cholesterol accumulation inhibits subsequent hydrolysis of lipoprotein cholesteryl ester. Microscopy and Microanalysis : The Official Journal of Microscopy Society of America, Microbeam Analysis Society, Microscopical Society of Canada, 14(2), 138–49. https://doi.org/10.1017/S1431927608080069

Jerome, W. G., & Lewis, J. C. (1990). Early atherogenesis in white carneau pigeons: Effect of a short-term regression diet. Experimental and Molecular Pathology, 53(3), 223–238. https://doi.org/10.1016/0014-4800(90)90046-G

Jerome, W. G., & Yancey, P. G. (2003). The role of microscopy in understanding atherosclerotic lysosomal lipid metabolism. Microsc Microanal, 9(1), 54–67. https://doi.org/10.1017/S1431927603030010

Jha, A. K., Huang, S. C. C., Sergushichev, A., Lampropoulou, V., Ivanova, Y., Loginicheva, E., … Artyomov, M. N. (2015). Network integration of parallel metabolic and transcriptional data reveals metabolic modules that regulate macrophage polarization. Immunity, 42(3), 419–430. https://doi.org/10.1016/j.immuni.2015.02.005

Jia, S. J., Gao, K. Q., & Zhao, M. (2017). Epigenetic regulation in monocyte/macrophage: A key player during atherosclerosis. Cardiovascular Therapeutics. https://doi.org/10.1111/1755-5922.12262

Jiang, S., Dupont, N., Castillo, E. F., & Deretic, V. (2013). Secretory versus degradative autophagy: Unconventional secretion of inflammatory mediators. Journal of Innate Immunity. https://doi.org/10.1159/000346707

Jin, N., Lang, M. J., & Weisman, L. S. (2016). Phosphatidylinositol 3,5-bisphosphate: regulation of cellular events in space and time. Biochemical Society Transactions, 44(1), 177–184. https://doi.org/10.1042/BST20150174

Johnson, D. E., Ostrowski, P., Jaumouillé, V., & Grinstein, S. (2016). The position of lysosomes within the cell determines their luminal pH. Journal of Cell Biology, 212(6), 677–692. https://doi.org/10.1083/jcb.201507112

Johnson, J. L., Jackson, C. L., Angelini, G. D., & George, S. J. (1998). Activation of matrix-degrading metalloproteinases by mast cell proteases in atherosclerotic plaques. Arteriosclerosis, Thrombosis, and Vascular Biology, 18(11), 1707–1715. https://doi.org/10.1161/01.ATV.18.11.1707

Johnson, J. L., & Newby, A. C. (2009). Macrophage heterogeneity in atherosclerotic plaques. Current Opinion in Lipidology, 20(5), 370–378. https://doi.org/10.1097/MOL.0b013e3283309848

Kadl, A., Meher, A. K., Sharma, P. R., Lee, M. Y., Doran, A. C., Johnstone, S. R., … Leitinger, N. (2010). Identification of a novel macrophage phenotype that develops in response to atherogenic phospholipids via Nrf2. Circulation Research, 107(6), 737–746. https://doi.org/10.1161/CIRCRESAHA.109.215715

Kadl, A., Sharma, P. R., Chen, W., Agrawal, R., Meher, A. K., Rudraiah, S., … Leitinger, N. (2011). Oxidized phospholipid-induced inflammation is mediated by Toll-like receptor 2. Free Radical Biology and Medicine, 51(10), 1903–1909. https://doi.org/10.1016/j.freeradbiomed.2011.08.026

Kamari, Y., Shaish, A., Shemesh, S., Vax, E., Grosskopf, I., Dotan, S., … Harats, D. (2011). Reduced atherosclerosis and inflammatory cytokines in apolipoprotein-E-deficient mice lacking bone marrow-derived interleukin-1α. Biochemical and Biophysical Research Communications, 405(2), 197–203. https://doi.org/10.1016/j.bbrc.2011.01.008

Kamido, H., Kuksis, A., Marai, L., & Myher, J. J. (1995). Lipid ester-bound aldehydes among copper-catalyzed peroxidation products of human plasma lipoproteins. Journal of Lipid Research, 36(9), 1876–1886. Retrieved from http://www.ncbi.nlm.nih.gov/pubmed/8558076

Kanter, J. E., Kramer, F., Barnhart, S., Averill, M. M., Vivekanandan-Giri, A., Vickery, T., … Bornfeldt, K. E. (2012). Diabetes promotes an inflammatory macrophage phenotype and atherosclerosis through acyl-CoA synthetase 1. Proceedings of the National Academy of Sciences, 109(12), E715–E724. https://doi.org/10.1073/pnas.1111600109

Karakas, M., Koenig, W., Zierer, A., Herder, C., Rottbauer, W., Baumert, J., … Thorand, B. (2012). Myeloperoxidase is associated with incident coronary heart disease independently of traditional risk factors: Results from the MONICA/KORA Augsburg study. Journal of Internal Medicine, 271(1), 43–50. https://doi.org/10.1111/j.1365-2796.2011.02397.x

Karasawa, T., & Takahashi, M. (2017). The crystal-induced activation of NLRP3 inflammasomes in atherosclerosis. Inflammation and Regeneration, 37(1), 18. https://doi.org/10.1186/s41232-017-0050-9

Kaur, J., & Debnath, J. (2015). Autophagy at the crossroads of catabolism and anabolism. Nature Reviews Molecular Cell Biology, 16(8), 461–472. https://doi.org/10.1038/nrm4024

Kaushik, S., Georga, I., & Koumoundouros, G. (2011). Growth and Body Composition of Zebrafish (Danio rerio) Larvae Fed a Compound Feed from First Feeding Onward: Toward Implications on Nutrient Requirements. Zebrafish, 8(2), 87–95. https://doi.org/10.1089/zeb.2011.0696

Kelly, B., & O'Neill, L. A. (2015). Metabolic reprogramming in macrophages and dendritic cells in innate immunity. Cell Research, 25(7), 771–784. https://doi.org/10.1038/cr.2015.68

Ketelhuth, D. F. J., & Hansson, G. K. (2016). Adaptive Response of T and B Cells in Atherosclerosis. Circulation Research, 118(4), 668–678. https://doi.org/10.1161/CIRCRESAHA.115.306427

Kim, E., Goraksha-Hicks, P., Li, L., Neufeld, T. P., & Guan, K.-L. (2008). Regulation of TORC1 by Rag GTPases in nutrient response. Nature Cell Biology, 10(8), 935–945. https://doi.org/10.1038/ncb1753

Kirii, H., Niwa, T., Yamada, Y., Wada, H., Saito, K., Iwakura, Y., … Seishima, M. (2003). Lack of interleukin-1ß decreases the severity of atherosclerosis in apoE-deficient mice. Arteriosclerosis, Thrombosis, and Vascular Biology, 23(4), 656–660. https://doi.org/10.1161/01.ATV.0000064374.15232.C3

Korolchuk, V. I., & Rubinsztein, D. C. (2011). Regulation of autophagy by lysosomal positioning. Autophagy. https://doi.org/10.4161/auto.7.8.15862

Korolchuk, V. I., Saiki, S., Lichtenberg, M., Siddiqi, F. H., Roberts, E. A., Imarisio, S., … Rubinsztein, D. C. (2011). Lysosomal positioning coordinates cellular nutrient responses. Nature Cell Biology, 13(4), 453–460. https://doi.org/10.1038/ncb2204

Krawczyk, C. M., Holowka, T., Sun, J., Blagih, J., Amiel, E., DeBerardinis, R. J., … Pearce, E. J. (2010). Toll-like receptor-induced changes in glycolytic metabolism regulate dendritic cell activation. Blood, 115(23), 4742–4749. https://doi.org/10.1182/blood-2009-10-249540

Kumar, V., & Sharma, A. (2010). Mast cells: Emerging sentinel innate immune cells with diverse role in immunity. Molecular Immunology. https://doi.org/10.1016/j.molimm.2010.07.009

Kummer, J. A., Broekhuizen, R., Everett, H., Agostini, L., Kuijk, L., Martinon, F., … Tschopp, J. (2007). Inflammasome Components NALP 1 and 3 Show Distinct but Separate Expression Profiles in Human Tissues Suggesting a Site-specific Role in the Inflammatory Response. Journal of Histochemistry & Cytochemistry, 55(5), 443–452. https://doi.org/10.1369/jhc.6A7101.2006

Kyaw, T., Tay, C., Krishnamurthi, S., Kanellakis, P., Agrotis, A., Tipping, P., … Toh, B. H. (2011). B1a B lymphocytes are atheroprotective by secreting natural IgM that increases IgM deposits and reduces necrotic cores in atherosclerotic lesions. Circulation Research, 109(8), 830–840. https://doi.org/10.1161/CIRCRESAHA.111.248542

Kzhyshkowska, J., Neyen, C., & Gordon, S. (2012). Role of macrophage scavenger receptors in atherosclerosis. Immunobiology, 217(5), 492–502. https://doi.org/10.1016/j.imbio.2012.02.015

Lacy, P. (2006). Mechanisms of Degranulation in Neutrophils. Allergy, Asthma & Clinical Immunology, 2(3), 98. https://doi.org/10.1186/1710-1492-2-3-98

Langston, P. K., Shibata, M., & Horng, T. (2017). Metabolism supports macrophage activation. Frontiers in Immunology. https://doi.org/10.3389/fimmu.2017.00061

Larrayoz, I. M., Huang, J. D., Lee, J. W., Pascual, I., & Rodríguez, I. R. (2010). 7-Ketocholesterol-Induced inflammation: Involvement of multiple kinase signaling pathways via NFκB but independently of reactive oxygen species formation. Investigative Ophthalmology and Visual Science, 51(10), 4942–4955. https://doi.org/10.1167/iovs.09-4854

Leitinger, N., & Schulman, I. G. (2013). Phenotypic polarization of macrophages in atherosclerosis. Arteriosclerosis, Thrombosis, and Vascular Biology, 33(6), 1120–1126. https://doi.org/10.1161/ATVBAHA.112.300173

Levitan, I., Volkov, S., & Subbaiah, P. V. (2010). Oxidized LDL: diversity, patterns of recognition, and pathophysiology. Antioxidants & Redox Signaling. https://doi.org/10.1089/ars.2009.2733

Lewis, J. C., Taylor, R. G., & Jerome, W. G. (1985). Foam Cell Characteristics in Coronary Arteries and Aortas of White Carneau Pigeons with Moderate Hypercholesterolemia. Annals of the New York Academy of Sciences, 454(1), 91–100. https://doi.org/10.1111/j.1749-6632.1985.tb11847.x

Lewis, J. C., Taylor, R. G., & Ohta, K. (1988). Lysosomal alterations during coronary atherosclerosis in the pigeon: Correlative cytochemical and three-dimensional HVEM/IVEM observations. Experimental and Molecular Pathology, 48(1), 103–115. https://doi.org/10.1016/0014-4800(88)90049-4

Lhoták, Š., Gyulay, G., Cutz, J., Al-Hashimi, A., Trigatti, B. L., Richards, C. D., … Austin, R. C. (2016). Characterization of Proliferating Lesion-Resident Cells During All Stages of Atherosclerotic Growth. Journal of the American Heart Association, 5(8), e003945. https://doi.org/10.1161/JAHA.116.003945

Li, W., Yuan, X. M., Olsson, A. G., & Brunk, U. T. (1998). Uptake of oxidized LDL by macrophages results in partial lysosomal enzyme inactivation and relocation. Arterioscler., Thromb., Vasc. Biol., 18(2), 177–184. https://doi.org/10.1161/01.ATV.18.2.177

Libby, P. (2012). History of Discovery : Inflammation in Atherosclerosis. Arterioscler Thromb Vasc Biol., 32(9), 2045–2051. https://doi.org/10.1161/ATVBAHA.108.179705.History

Libby, P. (2013). Mechanisms of acute coronary syndromes and their implications for therapy. The New England Journal of Medicine, 368(21), 2004–13. https://doi.org/10.1056/NEJMra1216063

Libby, P., Bornfeldt, K. E., & Tall, A. R. (2016). Atherosclerosis: Successes, Surprises, and Future Challenges. Circulation Research, 118(4), 531–534. https://doi.org/10.1161/CIRCRESAHA.116.308334

Libby, P., Ridker, P. M., & Hansson, G. K. (2009). Inflammation in Atherosclerosis. From Pathophysiology to Practice. Journal of the American College of Cardiology. https://doi.org/10.1016/j.jacc.2009.09.009

Libby, P., Ridker, P. M., & Maseri, A. (2002). Inflammation and atherosclerosis. Circulation, 105(9), 1135–1143. https://doi.org/10.1161/hc0902.104353

Lichtman, A. H., Binder, C. J., Tsimikas, S., & Witztum, J. L. (2013). Adaptive immunity in atherogenesis: New insights and therapeutic approaches. Journal of Clinical Investigation. https://doi.org/10.1172/JCI63108

Lieberman, A. P., Puertollano, R., Raben, N., Slaugenhaupt, S., Walkley, S. U., & Ballabio, A. (2012). Autophagy in lysosomal storage disorders. Autophagy. https://doi.org/10.4161/auto.19469

Lievens, D., Habets, K. L., Robertson, A. K., Laouar, Y., Winkels, H., Rademakers, T., … Lutgens, E. (2013). Abrogated transforming growth factor beta receptor II (TGFβRII) signaling in dendritic cells promotes immune reactivity of T cells resulting in enhanced atherosclerosis. European Heart Journal, 34(48), 3717–3727. https://doi.org/10.1093/eurheartj/ehs106

Lillis, A. P., Muratoglu, S. C., Au, D. T., Migliorini, M., Lee, M. J., Fried, S. K., … Strickland, D. K. (2015). LDL receptor-related protein-1 (LRP1) regulates cholesterol accumulation in macrophages. PLoS ONE, 10(6). https://doi.org/10.1371/journal.pone.0128903

Lim, C. Y., & Zoncu, R. (2016). The lysosome as a command-and-control center for cellular metabolism. Journal of Cell Biology. https://doi.org/10.1083/jcb.201607005

Lim, R. S., Suhalim, J. L., Miyazaki-Anzai, S., Miyazaki, M., Levi, M., Potma, E. O., & Tromberg, B. J. (2011). Identification of cholesterol crystals in plaques of atherosclerotic mice using hyperspectral CARS imaging. Journal of Lipid Research, 52(12), 2177–2186. https://doi.org/10.1194/jlr.M018077

Linton, M. F., Yancey, P. G., Davies, S. S., Jerome, W. G. (Jay), Linton, E. F., & Vickers, K. C. (2015). The Role of Lipids and Lipoproteins in Atherosclerosis. Endotext (Vol. 111). Retrieved from http://www.ncbi.nlm.nih.gov/pubmed/15403115?dopt=Abstract%5Cnhttp://www.ncbi.nlm.nih.gov/pubmed/26844337

Liu, P. S., Wang, H., Li, X., Chao, T., Teav, T., Christen, S., … Ho, P. C. (2017). α-ketoglutarate orchestrates macrophage activation through metabolic and epigenetic reprogramming. Nature Immunology, 18(9), 985–994. https://doi.org/10.1038/ni.3796

Lopes-Virella, M. F., & Virella, G. (1996). Modified lipoproteins, cytokines and macrovascular disease in non-insulin-dependent diabetes *mellitus*. Ann Med, 28(4), 347–354. Retrieved from http://www.ncbi.nlm.nih.gov/pubmed/8862690

Luo, Y., Duan, H., Qian, Y., Feng, L., Wu, Z., Wang, F., … Yan, X. (2017). Macrophagic CD146 promotes foam cell formation and

retention during atherosclerosis. Cell Research, 27(3), 352–372. https://doi.org/10.1038/cr.2017.8

Lusis, A. J. (2000). Atherosclerosis. Nature, 407(September), 233–241. https://doi.org/10.1038/35025203

Lusis, A. J. (2012). Genetics of atherosclerosis. Trends in Genetics. https://doi.org/10.1016/j.tig.2012.03.001

Lusis, A. J., Fogelman, A. M., & Fonarow, G. C. (2004). Genetic basis of atherosclerosis: Part II - Clinical implications. Circulation. https://doi.org/10.1161/01.CIR.0000143098.98869.F8

Luzio, J. P., Pryor, P. R., & Bright, N. A. (2007). Lysosomes: fusion and function. Nature Reviews Molecular Cell Biology, 8(8), 622–632. https://doi.org/10.1038/nrm2217

Lynch, S. M., & Frei, B. (1993). Mechanisms of copper- and iron-dependent oxidative modification of human low density lipoprotein. Journal of Lipid Research, 34(10), 1745–1753.

Madamanchi, N. R., Vendrov, A., & Runge, M. S. (2005). Oxidative stress and vascular disease. Arteriosclerosis, Thrombosis, and Vascular Biology. https://doi.org/10.1161/01.ATV.0000150649.39934.13

Major, A. S., Wilson, M. T., McCaleb, J. L., Ru Su, Y., Stanic, A. K., Joyce, S., … Linton, M. F. (2004). Quantitative and Qualitative Differences in Proatherogenic NKT Cells in Apolipoprotein E–Deficient Mice. Arteriosclerosis, Thrombosis, and Vascular Biology, 24, 2351–57. https://doi.org/10.1161/01.ATV.0000147112.84168.87

Makowski, L., Boord, J. B., Maeda, K., Babaev, V. R., Uysal, K. T., Morgan, M. A., … Linton, M. F. (2001). Lack of macrophage fatty-acid-binding protein aP2 protects mice deficient in apolipoprotein E against atherosclerosis. Nature Medicine, 7(6), 699–705. https://doi.org/10.1038/89076

Malek, A. M. (1999). Hemodynamic Shear Stress and Its Role in Atherosclerosis. JAMA, 282(21), 2035. https://doi.org/10.1001/jama.282.21.2035

Manderson, A. P., Kay, J. G., Hammond, L. A., Brown, D. L., & Stow, J. L. (2007). Subcompartments of the macrophage recycling endosome direct the differential secretion of IL-6 and TNF?? Journal of Cell Biology, 178(1), 57–69. https://doi.org/10.1083/jcb.200612131

Manning-Tobin, J. J., Moore, K. J., Seimon, T. A., Bell, S. A., Sharuk, M., Alvarez-Leite, J. I., … Freeman, M. W. (2009). Loss of SR-A and CD36 activity reduces atherosclerotic lesion complexity without abrogating foam cell formation in hyperlipidemic mice. Arteriosclerosis, Thrombosis, and Vascular Biology, 29(1), 19–26. https://doi.org/10.1161/ATVBAHA.108.176644

Mantovani, A., Biswas, S. K., Galdiero, M. R., Sica, A., & Locati, M. (2013). Macrophage plasticity and polarization in tissue repair and remodelling. Journal of Pathology. https://doi.org/10.1002/path.4133

Marenberg, M. E., Risch, N., Berkman, L. F., Floderus, B., & de Faire, U. (1994). Genetic susceptibility to death from coronary heart disease in a study of twins. The New England Journal of Medicine, 330(15), 1041–6. https://doi.org/10.1056/NEJM199404143301503

Marks, M. S., Heijnen, H. F. G., & Raposo, G. (2013). Lysosome-related organelles: Unusual compartments become mainstream. Current Opinion in Cell Biology. https://doi.org/10.1016/j.ceb.2013.04.008

Marques, L., Negre-Salvayre, A., Costa, L., & Canonne-Hergaux, F. (2016). Iron gene expression profile in atherogenic Mox macrophages. Biochimica et Biophysica Acta - Molecular Basis of Disease, 1862(6), 1137–1146. https://doi.org/10.1016/j.bbadis.2016.03.004

Martin-Murphy, B. V, You, Q., Wang, H., De La Houssaye, B. a, Reilly, T. P., Friedman, J. E., & Ju, C. (2014). Mice lacking natural killer T cells are more susceptible to metabolic alterations following high fat diet feeding. PLoS ONE, 9(1), e80949. https://doi.org/10.1371/journal.pone.0080949

Martín-Sánchez, F., Diamond, C., Zeitler, M., Gomez, A. I., Baroja-Mazo, A., Bagnall, J., … Pelegrín, P. (2016). Inflammasome-dependent IL-1β release depends upon membrane permeabilisation. Cell Death and Differentiation, 23(7), 1219–1231. https://doi.org/10.1038/cdd.2015.176

Martina, J. A., Chen, Y., Gucek, M., & Puertollano, R. (2012). MTORC1 functions as a transcriptional regulator of autophagy by preventing nuclear transport of TFEB. Autophagy, 8(6), 903–914. https://doi.org/10.4161/auto.19653

Martinez, F. O. (2008). Macrophage activation and polarization. Frontiers in Bioscience, 13(13), 453. https://doi.org/10.2741/2692

Mashima, R., & Okuyama, T. (2015). The role of lipoxygenases in pathophysiology; new insights and future perspectives. Redox Biology. https://doi.org/10.1016/j.redox.2015.08.006

Mauhin, W., Lidove, O., Masat, E., Mingozzi, F., Mariampillai, K., Ziza, J.-M., & Benveniste, O. (2015). Innate and Adaptive Immune Response in Fabry Disease. JIMD Rep, 22, 1–10. https://doi.org/10.1007/8904_2014_371

Mauri, C., & Bosma, A. (2012). Immune Regulatory Function of B Cells. Annual Review of Immunology, 30(1), 221–241. https://doi.org/10.1146/annurev-immunol-020711-074934

McCarthy, C., Duffy, M. M., Mooney, D., James, W. G., Griffin, M. D., Fitzgerald, D. J., & Belton, O. (2013). IL-10 mediates the immunoregulatory response in conjugated linoleic acid-induced regression of atherosclerosis. FASEB Journal, 27(2), 499–510. https://doi.org/10.1096/fj.12-215442

McLaren, J. E., Calder, C. J., McSharry, B. P., Sexton, K., Salter, R. C., Singh, N. N., … Ramji, D. P. (2010). The TNF-like protein 1A-death receptor 3 pathway promotes macrophage foam cell formation in vitro. Journal of Immunology (Baltimore, Md. : 1950), 184(10), 5827–34. https://doi.org/10.4049/jimmunol.0903782

McLaren, J. E., Michael, D. R., Ashlin, T. G., & Ramji, D. P. (2011). Cytokines, macrophage lipid metabolism and foam cells: Implications for cardiovascular disease therapy. Progress in Lipid Research. https://doi.org/10.1016/j.plipres.2011.04.002

McLaren, J. E., Michael, D. R., Salter, R. C., Ashlin, T. G., Calder, C. J., Miller, A. M., … Ramji, D. P. (2010). IL-33 reduces macrophage

foam cell formation. Journal of Immunology (Baltimore, Md. : 1950), 185(2), 1222–9. https://doi.org/10.4049/jimmunol.1000520

Medina, D. L., Fraldi, A., Bouche, V., Annunziata, F., Mansueto, G., Spampanato, C., … Ballabio, A. (2011). Transcriptional activation of lysosomal exocytosis promotes cellular clearance. Developmental Cell, 21(3), 421–430. https://doi.org/10.1016/j.devcel.2011.07.016

Mehta, J. L., Sanada, N., Hu, C. P., Chen, J., Dandapat, A., Sugawara, F., … Sawamura, T. (2007). Deletion of LOX-1 reduces atherogenesis in LDLR knockout mice fed high cholesterol diet. Circulation Research, 100(11), 1634–1642. https://doi.org/10.1161/CIRCRESAHA.107.149724

Meiser, J., Krämer, L., Sapcariu, S. C., Battello, N., Ghelfi, J., D'Herouel, A. F., … Hiller, K. (2016). Proinflammatory macrophages sustain pyruvate oxidation through pyruvate dehydrogenase for the synthesis of itaconate and to enable cytokine expression. Journal of Biological Chemistry, 291(8), 3932–3946. https://doi.org/10.1074/jbc.M115.676817

Menu, P., Pellegrin, M., Aubert, J.-F., Bouzourene, K., Tardivel, A., Mazzolai, L., & Tschopp, J. (2011). Atherosclerosis in ApoE-deficient mice progresses independently of the NLRP3 inflammasome. Cell Death and Disease, 2(3), e137. https://doi.org/10.1038/cddis.2011.18

Merched, A. J., Ko, K., Gotlinger, K. H., Serhan, C. N., & Chan, L. (2008). Atherosclerosis: evidence for impairment of resolution of vascular inflammation governed by specific lipid mediators. The FASEB Journal, 22(10), 3595–3606. https://doi.org/10.1096/fj.08-112201

Metschnikoff, E. (1893). Leçons sur la pathologie comparée de l'inflammation. Deutsche Medizinische Wochenschrift, 19(1), 17–18. https://doi.org/10.1055/s-0029-1205315

Michael, D. R., Salter, R. C., & Ramji, D. P. (2012). TGF-β inhibits the uptake of modified low density lipoprotein by human macrophages through a Smad-dependent pathway: A dominant role for Smad-2. Biochimica et Biophysica Acta - Molecular Basis of Disease, 1822(10), 1608–1616. https://doi.org/10.1016/j.bbadis.2012.06.002

Michael W King. (2013). Introduction to Cholesterol Metabolism. Themedicalbiochemistrypage.Org. Retrieved from http://themedicalbiochemistrypage.org/cholesterol.php

Michelsen, K. S., Wong, M. H., Shah, P. K., Zhang, W., Yano, J., Doherty, T. M., … Arditi, M. (2004). Lack of Toll-like receptor 4 or myeloid differentiation factor 88 reduces atherosclerosis and alters plaque phenotype in mice deficient in apolipoprotein E. Proceedings of the National Academy of Sciences, 101(29), 10679–10684. https://doi.org/10.1073/pnas.0403249101

Miller, A. M., Xu, D., Asquith, D. L., Denby, L., Li, Y., Sattar, N., … Liew, F. Y. (2008). IL-33 reduces the development of atherosclerosis. The Journal of Experimental Medicine, 205(2), 339–346. https://doi.org/10.1084/jem.20071868

Miller, B. F., & Kothari, H. V. (1969). Increased activity of lysosomal enzymes in human atherosclerotic aortas. Experimental and Molecular Pathology, 10(3), 288–94. Retrieved from http://www.ncbi.nlm.nih.gov/pubmed/5788628

Miller, Y. I., & Shyy, J. Y. J. (2017). Context-Dependent Role of Oxidized Lipids and Lipoproteins in Inflammation. Trends in Endocrinology and Metabolism. https://doi.org/10.1016/j.tem.2016.11.002

Mills, E. L., Kelly, B., Logan, A., Costa, A. S. H., Varma, M., Bryant, C. E., … O'Neill, L. A. (2016). Succinate Dehydrogenase Supports Metabolic Repurposing of Mitochondria to Drive Inflammatory Macrophages. Cell, 167(2), 457–470.e13. https://doi.org/10.1016/j.cell.2016.08.064

Mindell, J. A. (2012). Lysosomal Acidification Mechanisms. Annual Review of Physiology, 74(1), 69–86. https://doi.org/10.1146/annurev-physiol-012110-142317

Mitchell, P. L., & McLeod, R. S. (2008). Conjugated linoleic acid and atherosclerosis: studies in animal models. Biochemistry and Cell Biology = Biochimie et Biologie Cellulaire, 86(4), 293–301. https://doi.org/10.1139/o08-070

Mizushima, N., Levine, B., Cuervo, A. M., & Klionsky, D. J. (2008). Autophagy fights disease through cellular self-digestion. Nature, 451(7182), 1069–1075. https://doi.org/10.1038/nature06639

Moore, K. J., & Freeman, M. W. (2006). Scavenger receptors in atherosclerosis: Beyond lipid uptake. Arteriosclerosis, Thrombosis, and Vascular Biology. https://doi.org/10.1161/01.ATV.0000229218.97976.43

Moore, K. J., Kunjathoor, V. V., Koehn, S. L., Manning, J. J., Tseng, A. A., Silver, J. M., … Freeman, M. W. (2005). Loss of receptor-mediated lipid uptake via scavenger receptor A or CD36 pathways does not ameliorate atherosclerosis in hyperlipidemic mice. Journal of Clinical Investigation, 115(8), 2192–2201. https://doi.org/10.1172/JCI24061

Moore, K. J., & Tabas, I. (2011). Macrophages in the pathogenesis of atherosclerosis. Cell, 145(3), 341–355. https://doi.org/10.1016/j.cell.2011.04.005

Morgan, A. J., Platt, F. M., Lloyd-Evans, E., & Galione, A. (2011). Molecular mechanisms of endolysosomal Ca2+ signaling in health and disease. The Biochemical Journal, 439(3), 349–74. https://doi.org/10.1042/BJ20110949

Moss, J. W. E., & Ramji, D. P. (2016). Cytokines: roles in atherosclerosis disease progression and potential therapeutic targets. Future Med. Chem, 8(11), 1317–1330. https://doi.org/10.4155/fmc-2016-0072

Mozaffarian, D., Benjamin, E. J., Go, A. S., Arnett, D. K., Blaha, M. J., Cushman, M., … Turner, M. B. (2015). Heart disease and stroke statistics-2015 update : A report from the American Heart Association. Circulation, 131(4), e29–e39. https://doi.org/10.1161/CIR.0000000000000152

Mukherjee, R., Kanti Barman, P., Kumar Thatoi, P., Tripathy, R., Kumar Das, B., & Ravindran, B. (2015). Non-Classical monocytes display inflammatory features: Validation in Sepsis and Systemic Lupus Erythematous. Scientific Reports, 5. https://doi.org/10.1038/srep13886

Mukherjee, S., & Maxfield, F. R. (2004). Lipid and cholesterol trafficking in NPC. Biochimica et Biophysica Acta - Molecular and

Cell Biology of Lipids. https://doi.org/10.1016/j.bbalip.2004.08.009

Mullick, A. E., Tobias, P. S., & Curtiss, L. K. (2005). Modulation of atherosclerosis in mice by Toll-like receptor 2. The Journal of Clinical Investigation, 115(11), 3149–56. https://doi.org/10.1172/JCI25482

Muñoz-Planillo, R., Kuffa, P., Martínez-Colón, G., Smith, B., Rajendiran, T., & Núñez, G. (2013). K+ Efflux Is the Common Trigger of NLRP3 Inflammasome Activation by Bacterial Toxins and Particulate Matter. Immunity, 38(6), 1142–1153. https://doi.org/10.1016/j.immuni.2013.05.016

Murphy, A. J., Akhtari, M., Tolani, S., Pagler, T., Bijl, N., Kuo, C. L., … Tall, A. R. (2011). ApoE regulates hematopoietic stem cell proliferation, monocytosis, and monocyte accumulation in atherosclerotic lesions in mice. Journal of Clinical Investigation, 121(10), 4138–4149. https://doi.org/10.1172/JCI57559

Murray, C. J. L., Vos, T., Lozano, R., Naghavi, M., Flaxman, A. D., Michaud, C., … Lopez, A. D. (2012). Disability-adjusted life years (DALYs) for 291 diseases and injuries in 21 regions, 1990-2010: A systematic analysis for the Global Burden of Disease Study 2010. The Lancet, 380(9859), 2197–2223. https://doi.org/10.1016/S0140-6736(12)61689-4

Murray, P. J., Allen, J. E., Biswas, S. K., Fisher, E. A., Gilroy, D. W., Goerdt, S., … Wynn, T. A. (2014). Macrophage Activation and Polarization: Nomenclature and Experimental Guidelines. Immunity. https://doi.org/10.1016/j.immuni.2014.06.008

Murray, R. Z. (2005). A Role for the Phagosome in Cytokine Secretion. Science, 310(5753), 1492–1495. https://doi.org/10.1126/science.1120225

Murray, R. Z., & Stow, J. L. (2014). Cytokine secretion in macrophages: SNAREs, Rabs, and membrane trafficking. Frontiers in Immunology. https://doi.org/10.3389/fimmu.2014.00538

Murthy, A., Li, Y., Peng, I., Reichelt, M., Katakam, A. K., Noubade, R., … van Lookeren Campagne, M. (2014). A Crohn's disease variant in Atg16l1 enhances its degradation by caspase 3. Nature, 506(7489), 456–462. https://doi.org/10.1038/nature13044

Nagareddy, P. R., Murphy, A. J., Stirzaker, R. A., Hu, Y., Yu, S., Miller, R. G., … Goldberg, I. J. (2013). Hyperglycemia promotes myelopoiesis and impairs the resolution of atherosclerosis. Cell Metabolism, 17(5), 695–708. https://doi.org/10.1016/j.cmet.2013.04.001

Nakamura, S., & Yoshimori, T. (2017). New insights into autophagosome–lysosome fusion. Journal of Cell Science, 130(7), 1209–1216. https://doi.org/10.1242/jcs.196352

Nakashima, Y., Wight, T. N., & Sueishi, K. (2008). Early atherosclerosis in humans: Role of diffuse intimal thickening and extracellular matrix proteoglycans. Cardiovascular Research. https://doi.org/10.1093/cvr/cvn099

Newby, a C., & Zaltsman, a B. (1999). Fibrous cap formation or destruction--the critical importance of vascular smooth muscle cell proliferation, migration and matrix formation. Cardiovascular Research, 41(2), 345–360. https://doi.org/S0008-6363(98)00286-7 [pii]

Niki, E. (2009). Lipid peroxidation: Physiological levels and dual biological effects. Free Radical Biology and Medicine. https://doi.org/10.1016/j.freeradbiomed.2009.05.032

Niki, E. (2014). Biomarkers of lipid peroxidation in clinical material. Biochimica et Biophysica Acta - General Subjects. https://doi.org/10.1016/j.bbagen.2013.03.020

Noguchi, N., Nakano, K., Aratani, Y., Koyama, H., Kodama, T., & Niki, E. (2000). Role of myeloperoxidase in the neutrophil-induced oxidation of low density lipoprotein as studied by myeloperoxidase-knockout mouse. J Biochem, 127(6), 971–976.

O'Neil, J., Hoppe, G., & Hoff, H. F. (2003). Phospholipids in oxidized low density lipoproteins perturb the ability of macrophages to degrade internalized macromolecules and reduce intracellular cathepsin B activity. Atherosclerosis, 169(2), 215–224. https://doi.org/10.1016/S0021-9150(03)00104-7

Ohkuma, S., Moriyama, Y., & Takano, T. (1982). Identification and characterization of a proton pump on lysosomes by fluorescein-isothiocyanate-dextran fluorescence. Proceedings of the National Academy of Sciences of the United States of America, 79(9), 2758–62. https://doi.org/10.1073/pnas.79.9.2758

Orekhov, A. N., Sobenin, I. A., Gavrilin, M. A., Gratchev, A., Kotyashova, S. Y., Nikiforov, N. G., & Kzhyshkowska, J. (2015). Macrophages in immunopathology of atherosclerosis: a target for diagnostics and therapy. Current Pharmaceutical Design, 21(9), 1172–9. https://doi.org/10.2174/1381612820666141013120459

Ouimet, M., Franklin, V., Mak, E., Liao, X., Tabas, I., & Marcel, Y. L. (2011). Autophagy regulates cholesterol efflux from macrophage foam cells via lysosomal acid lipase. Cell Metabolism, 13(6), 655–667. https://doi.org/10.1016/j.cmet.2011.03.023

Ouimet, M., & Marcel, Y. L. (2012). Regulation of lipid droplet cholesterol efflux from macrophage foam cells. Arteriosclerosis, Thrombosis, and Vascular Biology. https://doi.org/10.1161/ATVBAHA.111.240705

Palinski, W., & Napoli, C. (1999). Pathophysiological Events during Pregnancy Influence the Development of Atherosclerosis in Humans. Trends in Cardiovascular Medicine, 9(7), 205–214. https://doi.org/10.1016/S1050-1738(00)00022-0

Palmieri, M., Pal, R., Nelvagal, H. R., Lotfi, P., Stinnett, G. R., Seymour, M. L., … Sardiello, M. (2017). Corrigendum: mTORC1-independent TFEB activation via Akt inhibition promotes cellular clearance in neurodegenerative storage diseases. Nature Communications, 8, 15793. https://doi.org/10.1038/ncomms15793

Palsson-Mcdermott, E. M., & O'Neill, L. A. J. (2013). The Warburg effect then and now: From cancer to inflammatory diseases. BioEssays, 35(11), 965–973. https://doi.org/10.1002/bies.201300084

Pantel, A., Teixeira, A., Haddad, E., Wood, E. G., Steinman, R. M., & Longhi, M. P. (2014). Direct Type I IFN but Not MDA5/TLR3 Activation of Dendritic Cells Is Required for Maturation and Metabolic Shift to Glycolysis after Poly IC Stimulation. PLoS Biology, 12(1). https://doi.org/10.1371/journal.pbio.1001759

Paramel Varghese, G., Folkersen, L., Strawbridge, R. J., Halvorsen, B., Yndestad, A., Ranheim, T., … Sirsjö, A. (2016). NLRP3 Inflam-

masome Expression and Activation in Human Atherosclerosis. Journal of the American Heart Association, 5(5), e003031. https://doi.org/10.1161/JAHA.115.003031

Parathath, S., Mick, S. L., Feig, J. E., Joaquin, V., Grauer, L., Habiel, D. M., … Fisher, E. A. (2011). Hypoxia is present in murine atherosclerotic plaques and has multiple adverse effects on macrophage lipid metabolism. Circulation Research, 109(10), 1141–1152. https://doi.org/10.1161/CIRCRESAHA.111.246363

Parthasarathy, S., Raghavamenon, A., Garelnabi, M. O., & Santanam, N. (2010). Oxidized low-density lipoprotein. Methods in Molecular Biology (Clifton, N.J.), 610, 403–17. https://doi.org/10.1007/978-1-60327-029-8_24

Paulson, K. E., Zhu, S. N., Chen, M., Nurmohamed, S., Jongstra-Bilen, J., & Cybulsky, M. I. (2010). Resident intimal dendritic cells accumulate lipid and contribute to the initiation of atherosclerosis. Circulation Research, 106(2), 383–390. https://doi.org/10.1161/CIRCRESAHA.109.210781

Pejnovic, N., Vratimos, A., Lee, S. H., Popadic, D., Takeda, K., Akira, S., & Chan, W. L. (2009). Increased atherosclerotic lesions and Th17 in interleukin-18 deficient apolipoprotein E-knockout mice fed high-fat diet. Molecular Immunology. https://doi.org/10.1016/j.molimm.2008.12.032

Peled, M., & Fisher, E. A. (2014). Dynamic aspects of macrophage polarization during atherosclerosis progression and regression. Frontiers in Immunology. https://doi.org/10.3389/fimmu.2014.00579

Peng, K., Liu, L., Wei, D., Lv, Y., Wang, G., Xiong, W., … Qu, P. (2015). P2X7R is involved in the progression of atherosclerosis by promoting NLRP3 inflammasome activation. International Journal of Molecular Medicine, 35(5), 1179–1188. https://doi.org/10.3892/ijmm.2015.2129

Perrin-Cocon, L., Coutant, F., Agaugue, S., Deforges, S., Andre, P., & Lotteau, V. (2001). Oxidized Low-Density Lipoprotein Promotes Mature Dendritic Cell Transition from Differentiating Monocyte. The Journal of Immunology, 167(7), 3785–3791. https://doi.org/10.4049/jimmunol.167.7.3785

Peters, T. J., Müller, M., & De Duve, C. (1972). Lysosomes of the arterial wall. I. Isolation and subcellular fractionation of cells from normal rabbit aorta. The Journal of Experimental Medicine, 136(5), 1117–1139. https://doi.org/10.1084/jem.136.5.1117

Pignatelli, P., Loffredo, L., Martino, F., Catasca, E., Carnevale, R., Zanoni, C., … Violi, F. (2009). Myeloperoxidase overexpression in children with hypercholesterolemia. Atherosclerosis, 205(1), 239–243. https://doi.org/10.1016/j.atherosclerosis.2008.10.025

Pilkis, S. J., El-Maghrabi, M. R., McGrane, M., Pilkis, J., & Claus, T. H. (1982). Regulation by glucagon of hepatic pyruvate kinase, 6-phosphofructo 1-kinase, and fructose-1,6-bisphosphatase. Federation Proceedings, 41(10), 2623–8. Retrieved from http://www.ncbi.nlm.nih.gov/pubmed/6286362

Pisoni, R. L., & Thoene, J. G. (1991). The transport systems of mammalian lysosomes. BBA - Reviews on Biomembranes. https://doi.org/10.1016/0304-4157(91)90002-E

Pitsilos, S., Hunt, J., Mohler, E. R., Prabhakar, A. M., Poncz, M., Dawicki, J., … Sachais, B. S. (2003). Platelet factor 4 localization in carotid atherosclerotic plaques: Correlation with clinical parameters. Thrombosis and Haemostasis, 90(6), 1112–1120. https://doi.org/10.1160/TH03-02-0069

Poteryaev, D., Datta, S., Ackema, K., Zerial, M., & Spang, A. (2010). Identification of the switch in early-to-late endosome transition. Cell, 141(3), 497–508. https://doi.org/10.1016/j.cell.2010.03.011

Potteaux, S., Gautier, E. L., Hutchison, S. B., Van Rooijen, N., Rader, D. J., Thomas, M. J., … Randolph, G. J. (2011). Suppressed monocyte recruitment drives macrophage removal from atherosclerotic plaques of Apoe-/- mice during disease regression. Journal of Clinical Investigation, 121(5), 2025–2036. https://doi.org/10.1172/JCI43802

Pu, J., Guardia, C. M., Keren-Kaplan, T., & Bonifacino, J. S. (2016). Mechanisms and functions of lysosome positioning. Journal of Cell Science, 129(23), 4329–4339. https://doi.org/10.1242/jcs.196287

Pu, J., Schindler, C., Jia, R., Jarnik, M., Backlund, P., & Bonifacino, J. S. (2015). BORC, a Multisubunit Complex that Regulates Lysosome Positioning. Developmental Cell, 33(2), 176–188. https://doi.org/10.1016/j.devcel.2015.02.011

Puertollano, R. (2014). mTOR and lysosome regulation. F1000Prime Reports, 6. https://doi.org/10.12703/P6-52

Puntoni, M., Sbrana, F., Bigazzi, F., Minichilli, F., Ferdeghini, E., & Sampietro, T. (2011). Myeloperoxidase modulation by LDL apheresis in familial hypercholesterolemia. Lipids in Health and Disease, 10, 185. https://doi.org/10.1186/1476-511X-10-185

Qi, H., Yang, S., & Zhang, L. (2017). Neutrophil Extracellular Traps and Endothelial Dysfunction in Atherosclerosis and Thrombosis. Frontiers in Immunology, 8. https://doi.org/10.3389/fimmu.2017.00928

Quillard, T., Croce, K., Jaffer, F. a, Weissleder, R., & Libby, P. (2011). Molecular imaging of macrophage protease activity in cardiovascular inflammation in vivo. Thrombosis and Haemostasis, 105(5), 828–36. https://doi.org/10.1160/TH10-09-0589

Rahman, K., Vengrenyuk, Y., Ramsey, S. A., Vila, N. R., Girgis, N. M., Liu, J., … Fisher, E. A. (2017). Inflammatory Ly6Chimonocytes and their conversion to M2 macrophages drive atherosclerosis regression. Journal of Clinical Investigation, 127(8), 2904–2915. https://doi.org/10.1172/JCI75005

Ramji, D. P., & Davies, T. S. (2015). Cytokines in atherosclerosis: Key players in all stages of disease and promising therapeutic targets. Cytokine and Growth Factor Reviews. https://doi.org/10.1016/j.cytogfr.2015.04.003

Rao, S. K., Huynh, C., Proux-Gillardeaux, V., Galli, T., & Andrews, N. W. (2004). Identification of SNAREs Involved in Synaptotagmin VII-regulated Lysosomal Exocytosis. Journal of Biological Chemistry, 279(19), 20471–20479. https://doi.org/10.1074/jbc.M400798200

Reddy, A., Caler, E. V., & Andrews, N. W. (2001). Plasma membrane repair is mediated by Ca2+-regulated exocytosis of lysosomes. Cell, 106(2), 157–169. https://doi.org/10.1016/S0092-8674(01)00421-4

Reifenberg, K., Cheng, F., Orning, C., Crain, J., Küpper, I., Wiese, E., … Torzewski, M. (2012). Overexpression of TGF-ß1 in macrophages reduces and stabilizes atherosclerotic plaques in apoE-deficient mice. PLoS ONE, 7(7). https://doi.org/10.1371/journal.pone.0040990

Reiner, Ž., Guardamagna, O., Nair, D., Soran, H., Hovingh, K., Bertolini, S., … Ros, E. (2014). Lysosomal acid lipase deficiency - An under-recognized cause of dyslipidaemia and liver dysfunction. Atherosclerosis. https://doi.org/10.1016/j.atherosclerosis.2014.04.003

Rigotti, A., Miettinen, H. E., & Krieger, M. (2003). The role of the high-density lipoprotein receptor SR-BI in the lipid metabolism of endocrine and other tissues. Endocrine Reviews. https://doi.org/10.1210/er.2001-0037

Rink, J., Ghigo, E., Kalaidzidis, Y., & Zerial, M. (2005). Rab conversion as a mechanism of progression from early to late endosomes. Cell, 122(5), 735–749. https://doi.org/10.1016/j.cell.2005.06.043

Robbins, C. S., Chudnovskiy, A., Rauch, P. J., Figueiredo, J.-L., Iwamoto, Y., Gorbatov, R., … Swirski, F. K. (2012). Extramedullary hematopoiesis generates Ly-6C(high) monocytes that infiltrate atherosclerotic lesions. Circulation, 125(2), 364–74. https://doi.org/10.1161/CIRCULATIONAHA.111.061986

Robbins, C. S., Hilgendorf, I., Weber, G. F., Theurl, I., Iwamoto, Y., Figueiredo, J.-L., … Swirski, F. K. (2013a). Local proliferation dominates lesional macrophage accumulation in atherosclerosis. Nature Medicine, 19(9), 1166–1172. https://doi.org/10.1038/nm.3258

Robbins, C. S., Hilgendorf, I., Weber, G. F., Theurl, I., Iwamoto, Y., Figueiredo, J.-L., … Swirski, F. K. (2013b). Local proliferation dominates lesional macrophage accumulation in atherosclerosis. Nature Medicine, 19(9), 1166–1172. https://doi.org/10.1038/nm.3258

Rodriguez-Prados, J.-C., Traves, P. G., Cuenca, J., Rico, D., Aragones, J., Martin-Sanz, P., … Bosca, L. (2010). Substrate Fate in Activated Macrophages: A Comparison between Innate, Classic, and Alternative Activation. The Journal of Immunology, 185(1), 605–614. https://doi.org/10.4049/jimmunol.0901698

Rosa-Ferreira, C., & Munro, S. (2011). Arl8 and SKIP Act Together to Link Lysosomes to Kinesin-1. Developmental Cell, 21(6), 1171–1178. https://doi.org/10.1016/j.devcel.2011.10.007

Rotzius, P., Thams, S., Soehnlein, O., Kenne, E., Tseng, C.-N., Björkström, N. K., … Eriksson, E. E. (2010). Distinct infiltration of neutrophils in lesion shoulders in ApoE-/- mice. The American Journal of Pathology, 177(1), 493–500. https://doi.org/10.2353/ajpath.2010.090480

Russell, R. C., Yuan, H.-X., & Guan, K.-L. (2014). Autophagy regulation by nutrient signaling. Cell Research, 24(1), 42–57. https://doi.org/10.1038/cr.2013.166

Saftig, P., & Klumperman, J. (2009). Lysosome biogenesis and lysosomal membrane proteins: trafficking meets function. Nature Reviews Molecular Cell Biology, 10(9), 623–635. https://doi.org/10.1038/nrm2745

Sag, D., Carling, D., Stout, R. D., & Suttles, J. (2008). Adenosine 5'-monophosphate-activated protein kinase promotes macrophage polarization to an anti-inflammatory functional phenotype. Journal of Immunology (Baltimore, Md. : 1950), 181(12), 8633–41. https://doi.org/10.4049/jimmunol.181.12.8633

Samie, M. A., & Xu, H. (2014). Lysosomal exocytosis and lipid storage disorders. Journal of Lipid Research, 55(6), 995–1009. https://doi.org/10.1194/jlr.R046896

Sancak, Y., Bar-Peled, L., Zoncu, R., Markhard, A. L., Nada, S., & Sabatini, D. M. (2010). Ragulator-rag complex targets mTORC1 to the lysosomal surface and is necessary for its activation by amino acids. Cell, 141(2), 290–303. https://doi.org/10.1016/j.cell.2010.02.024

Sancak, Y., Peterson, T. R., Shaul, Y. D., Lindquist, R. A., Thoreen, C. C., Bar-Peled, L., & Sabatini, D. M. (2008). The Rag GTPases Bind Raptor and Mediate Amino Acid Signaling to mTORC1. Science, 320(5882), 1496–1501. https://doi.org/10.1126/science.1157535

Sardiello, M., Palmieri, M., di Ronza, A., Medina, D. L., Valenza, M., Gennarino, V. A., … Ballabio, A. (2009). A Gene Network Regulating Lysosomal Biogenesis and Function. Science. https://doi.org/10.1126/science.1174447

Sasmono, R. T., Oceandy, D., Pollard, J. W., Tong, W., Pavli, P., Wainwright, B. J., … Hume, D. A. (2003). A macrophage colony-stimulating factor receptor-green fluorescent protein transgene is expressed throughout the mononuclear phagocyte system of the mouse. Blood, 101(3), 1155–1163. https://doi.org/10.1182/blood-2002-02-0569

Sastre, C., Fernández-Laso, V., Madrigal-Matute, J., Muñoz-García, B., Moreno, J. A., Pastor-Vargas, C., … Blanco-Colio, L. M. (2014). Genetic deletion or TWEAK blocking antibody administration reduce atherosclerosis and enhance plaque stability in mice. Journal of Cellular and Molecular Medicine, 18(4), 721–734. https://doi.org/10.1111/jcmm.12221

Schlegel, A. (2016). Zebrafish models for dyslipidemia and atherosclerosis research. Frontiers in Endocrinology. https://doi.org/10.3389/fendo.2016.00159

Schneider, F., Sukhova, G. K., Aikawa, M., Canner, J., Gerdes, N., Tang, S.-M. T., … Libby, P. (2008). Matrix-metalloproteinase-14 deficiency in bone-marrow-derived cells promotes collagen accumulation in mouse atherosclerotic plaques. Circulation, 117(7), 931–9. https://doi.org/10.1161/CIRCULATIONAHA.107.707448

Schuett, H., Oestreich, R., Waetzig, G. H., Annema, W., Luchtefeld, M., Hillmer, A., … Grote, K. (2012). Transsignaling of interleukin-6 crucially contributes to atherosclerosis in mice. Arteriosclerosis, Thrombosis, and Vascular Biology, 32(2), 281–290. https://doi.org/10.1161/ATVBAHA.111.229435

Segrest, J. P., Jones, M. K., De Loof, H., & Dashti, N. (2001). Structure of apolipoprotein B-100 in low density lipoproteins. Journal of Lipid Research, 42, 1346–67. Retrieved from http://www.ncbi.nlm.nih.gov/pubmed/11518754

Seimon, T. A., Nadolski, M. J., Liao, X., Magallon, J., Nguyen, M., Feric, N. T., … Tabas, I. (2010). Atherogenic lipids and lipoproteins trigger CD36-TLR2-dependent apoptosis in macrophages undergoing endoplasmic reticulum stress. Cell Metabolism, 12(5), 467–482. https://doi.org/10.1016/j.cmet.2010.09.010

Serbulea, V., DeWeese, D., & Leitinger, N. (2017). The effect of oxidized phospholipids on phenotypic polarization and function of macrophages. Free Radical Biology and Medicine, 111(December 2016), 156–168. https://doi.org/10.1016/j.freeradbiomed.2017.02.035

Serhan, C. N., Chiang, N., & Van Dyke, T. E. (2008). Resolving inflammation: dual anti-inflammatory and pro-resolution lipid mediators. Nature Reviews Immunology, 8(5), 349–361. https://doi.org/10.1038/nri2294

Serhan, C. N., Yang, R., Martinod, K., Kasuga, K., Pillai, P. S., Porter, T. F., … Spite, M. (2009). Maresins: novel macrophage mediators with potent antiinflammatory and proresolving actions. The Journal of Experimental Medicine, 206(1), 15–23. https://doi.org/10.1084/jem.20081880

Settembre, C., Di Malta, C., Polito, V. A., Arencibia, M. G., Vetrini, F., Erdin, S., … Ballabio, A. (2011). TFEB Links Autophagy to Lysosomal Biogenesis. Science, 332(6036), 1429–1433. https://doi.org/10.1126/science.1204592

Settembre, C., Fraldi, A., Medina, D. L., & Ballabio, A. (2013). Signals from the lysosome: a control centre for cellular clearance and energy metabolism. Nature Reviews Molecular Cell Biology, 14(5), 283–296. https://doi.org/10.1038/nrm3565

Settembre, C., Zoncu, R., Medina, D. L., Vetrini, F., Erdin, S., Erdin, S., … Ballabio, A. (2012). A lysosome-to-nucleus signaling mechanism senses and regulates the lysosome via mTOR and TFEB. The EMBO Journal, 31(5), 1095–1108. https://doi.org/10.1038/emboj.2012.32

Shah, P. K. (2003). Mechanisms of plaque vulnerability and rupture. Journal of the American College of Cardiology, 41(4), S15–S22. https://doi.org/10.1016/S0735-1097(02)02834-6

Shemesh, S., Kamari, Y., Shaish, A., Olteanu, S., Kandel-Kfir, M., Almog, T., … Harats, D. (2012). Interleukin-1 receptor type-1 in non-hematopoietic cells is the target for the proatherogenic effects of interleukin-1 in apoE-deficient mice. Atherosclerosis, 222(2), 329–336. https://doi.org/10.1016/j.atherosclerosis.2011.12.010

Shi, C.-S., Shenderov, K., Huang, N.-N., Kabat, J., Abu-Asab, M., Fitzgerald, K. A., … Kehrl, J. H. (2012). Activation of autophagy by inflammatory signals limits IL-1β production by targeting ubiquitinated inflammasomes for destruction. Nature Immunology, 13(3), 255–263. https://doi.org/10.1038/ni.2215

Shi, C., & Pamer, E. G. (2014). Monocyte Recruitment Suring Infection and Inflammation. Nat Rev Immunol, 11(11), 762–774. https://doi.org/10.1038/nri3070.Monocyte

Shio, H., Haley, N. J., & Fowler, S. (1979). Characterization of lipid-laden aortic cells from cholesterol-fed rabbits. III. Intracellular localization of cholesterol and cholesteryl ester. Laboratory Investigation; a Journal of Technical Methods and Pathology, 41(2), 160–7. Retrieved from http://europepmc.org/abstract/MED/459432

Simonaro, C. M. (2016). Lysosomes, Lysosomal Storage Diseases, and Inflammation. Journal of Inborn Errors of Metabolism and Screening, 4, 232640981665046. https://doi.org/10.1177/2326409816650465

Singh, R. B., Mengi, S. A., Xu, Y. J., Arneja, A. S., & Dhalla, N. S. (2002). Pathogenesis of atherosclerosis: A multifactorial process. Experimental and Clinical Cardiology. https://doi.org/10.1007/978-94-007-7920-4_9

Small, D. M. (1988). George Lyman Duff memorial lecture. Progression and regression of atherosclerotic lesions. Insights from lipid physical biochemistry. Arteriosclerosis, Thrombosis, and Vascular Biology, 8(2), 103–129. https://doi.org/10.1161/01.ATV.8.2.103

Smedby, O. (1996). Geometric risk factors for atherosclerosis in the aortic bifurcation: a digitized angiography study. Annals of Biomedical Engineering, 24(4), 481–8. https://doi.org/10.1007/BF02648110

Smedby, O., Johansson, J., Mölgaard, J., Olsson, A. G., Walldius, G., & Erikson, U. (1995). Predilection of atherosclerosis for the inner curvature in the femoral artery. A digitized angiography study. Arteriosclerosis, Thrombosis, and Vascular Biology, 15(7), 912–7. https://doi.org/10.1161/01.ATV.15.7.912

Soehnlein, O. (2012). Multiple roles for neutrophils in atherosclerosis. Circulation Research. https://doi.org/10.1161/CIRCRESAHA.111.257535

Soehnlein, O., Drechsler, M., Doring, Y., Lievens, D., Hartwig, H., Kemmerich, K., … Weber, C. (2013). Distinct functions of chemokine receptor axes in the atherogenic mobilization and recruitment of classical monocytes. EMBO Molecular Medicine, 5(3), 471–481. https://doi.org/10.1002/emmm.201201717

Soehnlein, O., & Swirski, F. K. (2013). Hypercholesterolemia links hematopoiesis with atherosclerosis. Trends in Endocrinology and Metabolism. https://doi.org/10.1016/j.tem.2012.10.008

Sottero, B., Gamba, P., Longhi, M., Robbesyn, F., Abuja, P. M., Schaur, R. J., … Leonarduzzi, G. (2005). Expression and synthesis of TGFbeta1 is induced in macrophages by 9-oxononanoyl cholesterol, a major cholesteryl ester oxidation product. BioFactors, 24(1–4), 209–216. https://doi.org/10.1002/biof.5520240125

Spalinger, M. R., Rogler, G., & Scharl, M. (2014). Crohn's disease: Loss of tolerance or a disorder of autophagy? Digestive Diseases, 32(4), 370–377. https://doi.org/10.1159/000358140

Stadler, N., Lindner, R. A., & Davies, M. J. (2004). Direct Detection and Quantification of Transition Metal Ions in Human Atherosclerotic Plaques: Evidence for the Presence of Elevated Levels of Iron and Copper. Arteriosclerosis, Thrombosis, and Vascular Biology, 24(5), 949–954. https://doi.org/10.1161/01.ATV.0000124892.90999.cb

Steinberg, D., Parthasarathy, S., Carew, T. E., Khoo, J. C., & Witztum, J. L. (1989). Beyond cholesterol: Modifications of low-density lipoprotein that increase its atherogenicity. New England Journal of Medicine, 320(14), 915–924. https://doi.org/10.1016/S0065-2776(06)94007-3

Stewart, C. R., Stuart, L. M., Wilkinson, K., van Gils, J. M., Deng, J., Halle, A., … Moore, K. J. (2010). CD36 ligands promote sterile inflammation through assembly of a Toll-like receptor 4 and 6 heterodimer. Nature Immunology, 11(2), 155–161. https://doi.org/10.1038/ni.1836

Stöger, J. L., Gijbels, M. J. J., van der Velden, S., Manca, M., van der Loos, C. M., Biessen, E. A. L., … de Winther, M. P. J. (2012). Distribution of macrophage polarization markers in human atherosclerosis. Atherosclerosis, 225(2), 461–468. https://doi.org/10.1016/j.atherosclerosis.2012.09.013

Stoletov, K., Fang, L., Choi, S. H., Hartvigsen, K., Hansen, L. F., Hall, C., … Miller, Y. I. (2009). Vascular lipid accumulation, lipoprotein oxidation, and macrophage lipid uptake in hypercholesterolemic zebrafish. Circulation Research, 104(8), 952–960. https://doi.org/10.1161/CIRCRESAHA.108.189803

Stratman, A. N., & Davis, G. E. (2012). Endothelial cell-pericyte interactions stimulate basement membrane matrix assembly: influence on vascular tube remodeling, maturation, and stabilization. Microscopy and Microanalysis : The Official Journal of Microscopy Society of America, Microbeam Analysis Society, Microscopical Society of Canada, 18(1), 68–80. https://doi.org/10.1017/S1431927611012402

Subramanian, M., Thorp, E., & Tabas, I. (2015). Identification of a non-growth factor role for GM-CSF in advanced atherosclerosis: Promotion of macrophage apoptosis and plaque necrosis through IL-23 signaling. Circulation Research, 116(2), e13–e24. https://doi.org/10.1161/CIRCRESAHA.116.304794

Sullivan, J. L. (2009). Iron in arterial plaque: A modifiable risk factor for atherosclerosis. Biochimica et Biophysica Acta - General Subjects. https://doi.org/10.1016/j.bbagen.2008.06.005

Sun, J., Sukhova, G. K., Wolters, P. J., Yang, M., Kitamoto, S., Libby, P., … Shi, G.-P. (2007). Mast cells promote atherosclerosis by releasing proinflammatory cytokines. Nature Medicine, 13(6), 719–724. https://doi.org/10.1038/nm1601

Swanson, J., Bushnell, A., & Silverstein, S. C. (1987). Tubular lysosome morphology and distribution within macrophages depend on the integrity of cytoplasmic microtubules. Proceedings of the National Academy of Sciences, 84(7), 1921–1925. https://doi.org/10.1073/pnas.84.7.1921

Swirski, F. K., Libby, P., Aikawa, E., Alcaide, P., Luscinskas, F. W., Weissleder, R., & Pittet, M. J. (2007). Ly-6Chi monocytes dominate hypercholesterolemia-associated monocytosis and give rise to macrophages in atheromata. Journal of Clinical Investigation, 117(1), 195–205. https://doi.org/10.1172/JCI29950

Tabas, I. (1999). Nonoxidative modifications of lipoproteins in atherogenesis. Annual Review of Nutrition, 19, 123–139. https://doi.org/10.1146/annurev.nutr.19.1.123

Tabas, I. (2010a). Macrophage death and defective inflammation resolution in atherosclerosis. Nature Reviews. Immunology, 10(1), 36–46. https://doi.org/10.1038/nri2675

Tabas, I. (2010b). The role of endoplasmic reticulum stress in the progression of atherosclerosis. Circulation Research. https://doi.org/10.1161/CIRCRESAHA.110.224766

Tabas, I., & Bornfeldt, K. E. (2016). Macrophage Phenotype and Function in Different Stages of Atherosclerosis. Circulation Research, 118(4), 653–667. https://doi.org/10.1161/CIRCRESAHA.115.306256

Tabas, I., García-Cardeña, G., & Owens, G. K. (2015). Recent insights into the cellular biology of atherosclerosis. Journal of Cell Biology, 209(1), 13–22. https://doi.org/10.1083/jcb.201412052

Tabas, I., & Lichtman, A. H. (2017). Monocyte-Macrophages and T Cells in Atherosclerosis. Immunity, 47(4), 621–634. https://doi.org/10.1016/j.immuni.2017.09.008

Tacke, F., Alvarez, D., Kaplan, T. J., Jakubzick, C., Spanbroek, R., Llodra, J., … Randolph, G. J. (2007). Monocyte subsets differentially employ CCR2, CCR5, and CX3CR1 to accumulate within atherosclerotic plaques. Journal of Clinical Investigation, 117(1), 185–194. https://doi.org/10.1172/JCI28549

Tannahill, G. M., Curtis, A. M., Adamik, J., Palsson-McDermott, E. M., McGettrick, A. F., Goel, G., … O'Neill, L. A. J. (2013). Succinate is an inflammatory signal that induces IL-1β through HIF-1α. Nature, 496(7444), 238–242. https://doi.org/10.1038/nature11986

Tapper, H., & Sundler, R. (1992). Cytosolic pH regulation in mouse macrophages. Proton extrusion by plasma-membrane-localized H+-ATPase. Biochem J, 281, 245–250.

Tawakol, A., Singh, P., Mojena, M., Pimentel-Santillana, M., Emami, H., Macnabb, M., … Boscá, L. (2015). HIF-1α and PFKFB3 mediate a tight relationship between proinflammatory activation and anerobic metabolism in atherosclerotic macrophages. Arteriosclerosis, Thrombosis, and Vascular Biology, 35(6), 1463–1471. https://doi.org/10.1161/ATVBAHA.115.305551

Thorp, E., Cui, D., Schrijvers, D. M., Kuriakose, G., & Tabas, I. (2008). Mertk receptor mutation reduces efferocytosis efficiency and promotes apoptotic cell accumulation and plaque necrosis in atherosclerotic lesions of Apoe-/- mice. Arteriosclerosis, Thrombosis, and Vascular Biology, 28(8), 1421–1428. https://doi.org/10.1161/ATVBAHA.108.167197

Thorp, E., & Tabas, I. (2009). Mechanisms and consequences of efferocytosis in advanced atherosclerosis. Journal of Leukocyte Biology, 86(5), 1089–1095. https://doi.org/10.1189/jlb.0209115

Titos, E., Rius, B., González-Périz, A., López-Vicario, C., Morán-Salvador, E., Martínez-Clemente, M., … Clària, J. (2011). Resolvin D1 and Its Precursor Docosahexaenoic Acid Promote Resolution of Adipose Tissue Inflammation by Eliciting Macrophage Polarization toward an M2-Like Phenotype. The Journal of Immunology, 187(10), 5408–5418. https://doi.org/10.4049/jimmunol.1100225

Tontonoz, P., Nagy, L., Alvarez, J. G. A., Thomazy, V. A., & Evans, R. M. (1998). PPARγ promotes monocyte/macrophage differentiation and uptake of oxidized LDL. Cell, 93(2), 241–252. https://doi.org/10.1016/S0092-8674(00)81575-5

Tsimikas, S., Miyanohara, A., Hartvigsen, K., Merki, E., Shaw, P. X., Chou, M. Y., … Witztum, J. L. (2011). Human oxidation-specific antibodies reduce foam cell formation and atherosclerosis progression. Journal of the American College of Cardiology, 58(16), 1715–1727. https://doi.org/10.1016/j.jacc.2011.07.017

Tupin, E., Nicoletti, A., Elhage, R., Rudling, M., Ljunggren, H.-G., Hansson, G. K., & Berne, G. P. (2004). CD1d-dependent Activation of NKT Cells Aggravates Atherosclerosis. The Journal of Experimental Medicine, 199(3), 417–422. https://doi.org/10.1084/

jem.20030997

Upston, J. M., Neuzil, J., & Stocker, R. (1996). Oxidation of LDL by recombinant human 15-lipoxygenase: evidence for alpha-tocopherol-dependent oxidation of esterified core and surface lipids. Journal of Lipid Research, 37(12), 2650–61. Retrieved from http://www.ncbi.nlm.nih.gov/pubmed/9017516

Usui, F., Shirasuna, K., Kimura, H., Tatsumi, K., Kawashima, A., Karasawa, T., … Takahashi, M. (2012). Critical role of caspase-1 in vascular inflammation and development of atherosclerosis in Western diet-fed apolipoprotein E-deficient mice. Biochemical and Biophysical Research Communications, 425(2), 162–168. https://doi.org/10.1016/j.bbrc.2012.07.058

Van De Veerdonk, F. L., & Dinarello, C. A. (2014). Deficient autophagy unravels the ROS paradox in chronic granulomatous disease. Autophagy, 10(6), 1141–1142. https://doi.org/10.4161/auto.28638

Van den Bossche, J., Baardman, J., Otto, N. A., van der Velden, S., Neele, A. E., van den Berg, S. M., … de Winther, M. P. J. (2016). Mitochondrial Dysfunction Prevents Repolarization of Inflammatory Macrophages. Cell Reports, 17(3), 684–696. https://doi.org/10.1016/j.celrep.2016.09.008

Van den Bossche, J., O'Neill, L. A., & Menon, D. (2017). Macrophage Immunometabolism: Where Are We (Going)? Trends in Immunology. https://doi.org/10.1016/j.it.2017.03.001

van Es, T., van Puijvelde, G. H. M., Michon, I. N., van Wanrooij, E. J. A., de Vos, P., Peterse, N., … Kuiper, J. (2011). IL-15 aggravates atherosclerotic lesion development in LDL receptor deficient mice. Vaccine, 29(5), 976–983. https://doi.org/10.1016/j.vaccine.2010.11.037

van Kampen, E., Jaminon, A., van Berkel, T. J. C., & Van Eck, M. (2014). Diet-induced (epigenetic) changes in bone marrow augment atherosclerosis. Journal of Leukocyte Biology, 96(5), 833–841. https://doi.org/10.1189/jlb.1A0114-017R

van Meer, G., Voelker, D. R., & Feigenson, G. W. (2008). Membrane lipids: where they are and how they behave. Nature Reviews Molecular Cell Biology, 9(2), 112–124. https://doi.org/10.1038/nrm2330

Van Tits, L. J. H., Stienstra, R., van Lent, P. L., Netea, M. G., Joosten, L. A. B., & Stalenhoef, A. F. H. (2011). Oxidized LDL enhances proinflammatory responses of alternatively activated M2 macrophages: A crucial role for Krüppel-like factor 2. Atherosclerosis, 214(2), 345–349. https://doi.org/10.1016/j.atherosclerosis.2010.11.018

Van Vré, E. A., Ait-Oufella, H., Tedgui, A., & Mallat, Z. (2012). Apoptotic cell death and efferocytosis in atherosclerosis. Arteriosclerosis, Thrombosis, and Vascular Biology, 32(4), 887–893. https://doi.org/10.1161/ATVBAHA.111.224873

Vance, J. E., & Vance, D. E. (2008). Biochemistry Of Lipids, Lipoproteins And Membranes. Biochemistry of Lipids, Lipoproteins and Membranes. https://doi.org/10.1016/B978-0-444-53219-0.X5001-6

VanderLaan, P. A., Reardon, C. A., Sagiv, Y., Blachowicz, L., Lukens, J., Nissenbaum, M., … Getz, G. S. (2007). Characterization of the Natural Killer T-Cell Response in an Adoptive Transfer Model of Atherosclerosis. The American Journal of Pathology, 170(3), 1100–1107. https://doi.org/10.2353/ajpath.2007.060188

Vats, D., Mukundan, L., Odegaard, J. I., Zhang, L., Smith, K. L., Morel, C. R., … Chawla, A. (2006). Oxidative metabolism and PGC-1beta attenuate macrophage-mediated inflammation. Cell Metabolism, 4(1), 13–24. https://doi.org/10.1016/j.cmet.2006.05.011

Vazquez, A., Liu, J., Zhou, Y., & Oltvai, Z. N. (2010). Catabolic efficiency of aerobic glycolysis: The Warburg effect revisited. BMC Systems Biology, 4(1), 58. https://doi.org/10.1186/1752-0509-4-58

Vellodi, A. (2005). Lysosomal storage disorders. British Journal of Haematology. https://doi.org/10.1111/j.1365-2141.2004.05293.x

Vink, A., Schoneveld, A. H., Lamers, D., Houben, A. J. S., van der Groep, P., van Diest, P. J., & Pasterkamp, G. (2007). HIF-1alpha expression is associated with an atheromatous inflammatory plaque phenotype and upregulated in activated macrophages. Atherosclerosis, 195(2). https://doi.org/10.1016/j.atherosclerosis.2007.05.026

Viola, J. R., Lemnitzer, P., Jansen, Y., Csaba, G., Winter, C., Neideck, C., … Soehnlein, O. (2016). Resolving Lipid Mediators Maresin 1 and Resolvin D2 Prevent Atheroprogression in Mice. Circulation Research, 119(9), 1030–1038. https://doi.org/10.1161/CIRCRESAHA.116.309492

Vonderheit, A., & Helenius, A. (2005). Rab7 associates with early endosomes to mediate sorting and transport of Semliki forest virus to late endosomes. PLoS Biology, 3(7), 1225–1238. https://doi.org/10.1371/journal.pbio.0030233

Walter, M. F., Jacob, R. F., Jeffers, B., Ghadanfar, M. M., Preston, G. M., Buch, J., & Mason, R. P. (2004). Serum levels of thiobarbituric acid reactive substances predict cardiovascular events in patients with stable coronary artery disease: A longitudinal analysis of the PREVENT study. Journal of the American College of Cardiology, 44(10), 1996–2002. https://doi.org/10.1016/j.jacc.2004.08.029

Wang, J. C., & Bennett, M. (2012). Aging and atherosclerosis: Mechanisms, functional consequences, and potential therapeutics for cellular senescence. Circulation Research. https://doi.org/10.1161/CIRCRESAHA.111.261388

Wang, J., Tan, G.-J., Han, L.-N., Bai, Y.-Y., He, M., & Liu, H.-B. (2017). Novel biomarkers for cardiovascular risk prediction. Journal of Geriatric Cardiology : JGC, 14(2), 135–150. https://doi.org/10.11909/j.issn.1671-5411.2017.02.008

Wang, Y., Chen, T., Han, C., He, D., Liu, H., An, H., … Cao, X. (2007). Lysosome-associated small Rab GTPase Rab7b negatively regulates TLR4 signaling in macrophages by promoting lysosomal degradation of TLR4. Blood, 110(3), 962–971. https://doi.org/10.1182/blood-2007-01-066027

Wang, Y., Wang, G. Z., Rabinovitch, P. S., & Tabas, I. (2014). Macrophage mitochondrial oxidative stress promotes atherosclerosis and nuclear factor-κB-mediated inflammation in macrophages. Circulation Research, 114(3), 421–433. https://doi.org/10.1161/CIRCRESAHA.114.302153

Warburg, O. (1927). THE METABOLISM OF TUMORS IN THE BODY. The Journal of General Physiology, 8(6), 519–530. https://doi.org/10.1085/jgp.8.6.519

Warnatsch, A., Ioannou, M., Wang, Q., & Papayannopoulos, V. (2015). Neutrophil extracellular traps license macrophages for cytokine production in atherosclerosis. Science, 349(6245), 316–320. https://doi.org/10.1126/science.aaa8064

Wartosch, L., Bright, N. A., & Luzio, J. P. (2015). Lysosomes. Current Biology, 25(8), R315–R316. https://doi.org/10.1016/j.cub.2015.02.027

Wight, T. N. (1989). Cell biology of arterial proteoglycans. Arteriosclerosis (Dallas, Tex.), 9, 1–20. https://doi.org/10.1161/01.ATV.9.1.1

Wigren, M., Nilsson, J., & Kolbus, D. (2012). Lymphocytes in atherosclerosis. Clinica Chimica Acta. https://doi.org/10.1016/j.cca.2012.04.031

Wild, P. S., Zeller, T., Schillert, A., Szymczak, S., Sinning, C. R., Deiseroth, A., … Blankenberg, S. (2011). A genome-wide association study identifies LIPA as a susceptibility gene for coronary artery disease. Circulation: Cardiovascular Genetics, 4(4), 403–412. https://doi.org/10.1161/CIRCGENETICS.110.958728

Wildgruber, M., Aschenbrenner, T., Wendorff, H., Czubba, M., Glinzer, A., Haller, B., … Zernecke, A. (2016). The "intermediate" CD14++ CD16+ monocyte subset increases in severe peripheral artery disease in humans. Scientific Reports, 6. https://doi.org/10.1038/srep39483

Winder, W. W., Holmes, B. F., Rubink, D. S., Jensen, E. B., Chen, M., & Holloszy, J. O. (2000). Activation of AMP-activated protein kinase increases mitochondrial enzymes in skeletal muscle. Journal of Applied Physiology (Bethesda, Md. : 1985), 88(6), 2219–2226.

Witztum, J. L., & Lichtman, A. H. (2014). The influence of innate and adaptive immune responses on atherosclerosis. Annual Review of Pathology, 9(July 2013), 73–102. https://doi.org/10.1146/annurev-pathol-020712-163936

Wolfs, I. M. J., Donners, M. M. P. C., & de Winther, M. P. J. (2011). Differentiation factors and cytokines in the atherosclerotic plaque micro-environment as a trigger for macrophage polarisation. Thrombosis and Haemostasis, 106(5), 763–771. https://doi.org/10.1160/TH11-05-0320

Woollard, K. J., & Geissmann, F. (2010). Monocytes in atherosclerosis: subsets and functions. Nature Reviews Cardiology, 7(2), 77–86. https://doi.org/10.1038/nrcardio.2009.228

Xiao, N., Yin, M., Zhang, L., Qu, X., Du, H., Sun, X., … Pan, J. (2009). Tumor necrosis factor-alpha deficiency retards early fatty-streak lesion by influencing the expression of inflammatory factors in apoE-null mice. Molecular Genetics and Metabolism, 96(4), 239–244. https://doi.org/10.1016/j.ymgme.2008.11.166

Xu, H., & Ren, D. (2015). Lysosomal Physiology. Annual Review of Physiology, 77(1), 57–80. https://doi.org/10.1146/annurev-physiol-021014-071649

Yancey, P. G., & Jerome, W. G. (2001). Lysosomal cholesterol derived from mildly oxidized low density lipoprotein is resistant to efflux. Journal of Lipid Research, 42(3), 317–327.

Yao, M., Liu, X., Li, D., Chen, T., Cai, Z., & Cao, X. (2009). Late endosome/lysosome-localized Rab7b suppresses TLR9-initiated proinflammatory cytokine and type I IFN production in macrophages. Journal of Immunology, 183(3), 1751–1758. https://doi.org/10.4049/jimmunol.0900249

Yasuda, Y., Li, Z., Greenbaum, D., Bogyo, M., Weber, E., & Brömme, D. (2004). Cathepsin V, a novel and potent elastolytic activity expressed in activated macrophages. Journal of Biological Chemistry, 279(35), 36761–36770. https://doi.org/10.1074/jbc.M403986200

Yin, H., Xu, L., & Porter, N. A. (2011). Free radical lipid peroxidation: Mechanisms and analysis. Chemical Reviews. https://doi.org/10.1021/cr200084z

Yoshida, H., & Kisugi, R. (2010). Mechanisms of LDL oxidation. Clinica Chimica Acta. https://doi.org/10.1016/j.cca.2010.08.038

Yu, L., McPhee, C. K., Zheng, L., Mardones, G. A., Rong, Y., Peng, J., … Lenardo, M. J. (2010). Termination of autophagy and reformation of lysosomes regulated by mTOR. Nature, 465(7300), 942–946. https://doi.org/10.1038/nature09076

Yuan, X. M., Li, W., Brunk, U. T., Dalen, H., Chang, Y. H., & Sevanian, A. (2000). Lysosomal destabilization during macrophage damage induced by cholesterol oxidation products. Free Radical Biology and Medicine, 28(2), 208–218. https://doi.org/10.1016/S0891-5849(99)00220-8

Yurdagul, A., Finney, A. C., Woolard, M. D., & Orr, A. W. (2016). The arterial microenvironment: the where and why of atherosclerosis. Biochemical Journal, 473(10), 1281–1295. https://doi.org/10.1042/BJ20150844

Yvan-Charvet, L., Welch, C., Pagler, T. A., Ranalletta, M., Lamkanfi, M., Han, S., … Tall, A. R. (2008). Increased inflammatory gene expression in ABC transporter-deficient macrophages: Free cholesterol accumulation, increased signaling via toll-like receptors, and neutrophil infiltration of atherosclerotic lesions. Circulation, 118(18), 1837–1847. https://doi.org/10.1161/CIRCULATIONAHA.108.793869

Zerial, M., & McBride, H. (2001). Rab proteins as membrane organizers. Nature Reviews. Molecular Cell Biology, 2(2), 107–117. https://doi.org/10.1038/35052055

Zernecke, A. (2015). Dendritic cells in atherosclerosis: evidence in mice and humans. Arterioscler Thromb Vasc Biol, 35(4), 763–770. https://doi.org/10.1161/ATVBAHA.114.303566

Zernecke, A., & Weber, C. (2010). Chemokines in the vascular inflammatory response of atherosclerosis. Cardiovascular Research. https://doi.org/10.1093/cvr/cvp391

Zheng, F., Xing, S., Gong, Z., & Xing, Q. (2013). NLRP3 inflammasomes show high expression in Aorta of patients with atherosclerosis. Heart Lung and Circulation, 22(9), 746–750. https://doi.org/10.1016/j.hlc.2013.01.012

Zhu, X., Lee, J. Y., Timmins, J. M., Brown, J. M., Boudyguina, E., Mulya, A., … Parks, J. S. (2008). Increased cellular free cholesterol in

macrophage-specific Abca1 knock-out mice enhances proinflammatory response of macrophages. Journal of Biological Chemistry, 283(34), 22930–22941. https://doi.org/10.1074/jbc.M801408200

Zoncu, R., Bar-Peled, L., Efeyan, A., Wang, S., Sancak, Y., & Sabatini, D. M. (2011). mTORC1 Senses Lysosomal Amino Acids Through an Inside-Out Mechanism That Requires the Vacuolar H+-ATPase. Science, 334(6056), 678–683. https://doi.org/10.1126/science.1207056

02 MATERIAL AND METHODS

2.1 REAGENTS

All chemical reagents were of analytical grade or higher and purchased from Sigma-Aldrich unless otherwise specified.

2.2 CHOLESTERYL HEMIESTERS (CHE) PREPARATION

2.2.1 Liposomes preparation

Lipid aqueous solution was prepared by mixing POPC (1-palmitoyl-2-oleoyl-sn-glycero-3-phosphocholine, Avanti Polar Lipids) and Cholesteryl hemisuccinate (ChS), ChA (synthesized by our collaborators in Coimbra University) or free cholesterol (FC) at a 35:65 molar ratio in an azeotropic mixture of chloroform and methanol and then incubated for 30 min. The solvent was evaporated using a rotary evaporator and dried for 30 min in a 65°C water bath. The lipid film was hydrated with a buffer solution of 20 mM Hepes, 0.11 M NaCl, 1 mM EDTA, pH 7.4 in a water bath at 65°C for at least 1 h. The samples were submitted to mild sonication for 5 min and extruded through a polycarbonate filters (Nucleopore) with a pore diameter of 0.4 µm, this process was repeated at least 6 times. During the extrusion the water-jacketed extruder (Lipex Biomembranes, Vancouver, British Columbia, Canada) was maintained at 65°C. To determine ChE and FC concentration we used the Libermann-Burchard protocol (Huang, Chen, Wefler, & Raftery, 1961).

2.2.2 LDL isolation and ChS incorporation

Human blood was collected from healthy volunteers at CNC, University of Coimbra and CEDOC, NOVA Medical School. Written informed consent was obtained from all volunteers and approved by the Ethical Review Board of Faculty of Medicine of University of Coimbra and NOVA Medical School. LDL were isolated as described previously (O V Vieira, Laranjinha, Madeira, & Almeida, 1996). ChS-LDL were prepared by incubating Native (Nat)-LDL with ChS-POPC (35:65) unilamellar liposomes as was described in (Estronca et al., 2012).

2.3 ASSESSMENT OF *IN VITRO* EFFECTS OF CHE ON CELL FUNCTION

2.3.1 RAW 264.7

RAW 264.7 (ATCC) macrophages were grown at 37°C under 5% of CO_2 control environment in DMEM supplemented with 10% (vol/vol, from Gibco Inc) fetal bovine serum (FBS), 100 U/ml of penicillin (Gibco Inc) and streptomycin (Gibco Inc), 1 mM of Pyruvate (Gibco Inc), as previously described in (Estronca et al., 2012).

2.3.2 Cell toxicity and cell counting

The toxicity in RAW cells was measured by the MTT assay as previously described (Otilia V. Vieira et al., 2008). For bone-marrow derived macrophages (BMDM, isolation protocol at section 2.4.2), ChS toxicity was evaluated by MTS assay used as previously reported (Flore et al., 2014) and by MTT to measure ChA toxicity. BMDM treated with ChA were also counted using DAPI staining under a fluorescence microscope. Additionally, apoptosis induction after lipid treatment was evaluated using FITC Annexin V Apoptosis Detection Kit I (BD Pharmingen), with some adaption from the original protocol. To avoid an increase in membrane permeability induced by cells detachment procedures, the cells were stained as indicated by the manufacture in the plates and imaged using a fluorescence microscope.

2.3.3 Cells staining and image acquisition

2.3.3.1 Staining and confocal microscopy

Cells were seeded on glass coverslips. After each assay, cells were fixed in 4% PFA, quenched with 0.05 M NH_4Cl, permeabilized in PBS with 0.05% saponin and blocked with 2.5% fish-gelatin according to standard procedures. Primary antibodies used were: mouse anti-LAMP-2 (1:100; Hybridoma Bank, ABL-93), anti-EEA-1 (1:25; Santa Cruz) and mouse anti-Ki67 (1:500; Millipore, AB9260). Secondary antibodies used were conjugated to Cy3 and Cy5 (1:500; Jackson ImmunoResearch Laboratories, Inc.). DAPI was used to visualize nuclei (1:800; Fluka). Neutral lipids were stained with BODIPY 493/503 (diluted 1:700 in PBS from a saturated ethanolic solution of BODIPY, from Thermo Fisher Scientific) for 1 h. For mitochondrial imaging, before fixation, macrophages were loaded with MitoTracker Red CMXRos (Life Technologies).

Coverslips were mounted with mowiol/DABCO and imaged using a LSM 710 laser scanning confocal microscope (ZEISS). Quantification of the number and size of the lipid-rich structures and lysosomes were performed using ImageJ software.

For live imaging, cells were seeded in Lab-Teck Chambered plate (Nunc) plate and lysosomes were labeled using 50 µg/mL of dextran conjugated with Alexa 647 (Thermo Fisher Scientific). To ensure that dextran was labelled lysosomes the overnight pulse was followed by a 3 h chase.

2.3.3.2 Transmission Electron microscopy

Cells were seeded on glass coverslips and after ChA-treatment cells were fixed in 0.1 M phosphate buffer containing 2% PFA/2% glutaraldehyde (Electron Microscopy Sciences) and processed for standard epon resin embedding. 70 nm sections were analyzed in a Jeol 1010 TEM and imaged using a Gatan Orius SC1000B charge-coupled device camera. These experiences were performed by our collaborators at University College London.

2.3.4 ChS uptake

After incubating RAW cells with ^{3}H-ChS-LDL or Nat-LDL at 37°C, cell-associated radioactivity and total cell protein were measured as a function of time in the macrophages. ^{3}H-ChS was synthesized from [^{3}H]-Cholesterol (GE Healthcare) by our collaborator from University of Coimbra – Chemistry department.

2.3.5 BSA and dextran internalization and trafficking

For the endocytosis assays, cells were incubated with 400 µg/mL BSA-Texas Red (Thermo Fisher Scientific) or FITC-dextran for 30 or 180 min in medium without serum. In order to avoid BSA degradation, NH_4Cl was added to neutralize the lysosomal pH 20 min after initiation of the incubation with cargo. After incubation, RAW cells were washed with PBS and detached using FACS buffer. Cargo internalization was evaluated by flow cytometry.

For BSA-Texas red uptake measurements, the controls and the fluorescent-labelled samples were run on a BD FACScantoTMII flow cytometer (Becton Dickinson) cell sorter equipped with a 50 mW solid state 561 nm laser used for Texas Red excitation. Texas Red was measured using a 610/20 nm bandpass emission filter.

For dextran uptake quantification, the controls and fluorescent-labelled samples were run on a BD FACScantoTMII flow cytometer (Becton Dickinson) equipped with a 488nm laser (20 mW solid state) for scatter measurements and FITC excitation. FITC was detected using a 530/30 nm bandpass emission filter. These cells were fixed with PFA. This fixation procedure eliminates the quenching effect of pH on the FITC fluorescence.

To follow the intracellular transport of BSA-Texas Red and dextran to the lysosomes, cells were incubated with 400 µg/mL BSA-Texas Red and and 100 µg/mL rhodamine-dextran for 30 min at 37°C (pulse), after which the cells were washed 3 times to remove the non-internalized cargo, and then incubated again at 37°C for different time points (chase). In BSA uptake

experiments, cells were then fixed for 30 min with 4% PFA, followed by immunostaining for LAMP-2. To follow the transport of rodhamine-dextran into lysosomes, these organelles were previously labelled with Alexa Fluor 647-dextran with an overnight pulse and chased for 3h. Samples were then observed under a confocal microscope. The co-localization values were calculated using confocal single slices and the plugin Coloc2 of ImageJ software.

To quantify the positioning of dextran labelled lysosomes, a homemade software was developed. Cell membrane and nucleus contours were extracted manually using ImageJ selection tools. Lysosome location and coordinates were detected automatically using ICY Spot Detector plugin. Cell and nuclei contours and lysosomes XY coordinates were exported for posterior analysis on a custom Matlab Script. Distances were measured using the Euclidian distance between the lysosome, cell membrane, cell nuclei and nuclei centroid. The measurement axis was defined as a straight line that crossed the nuclei centroid and the lysosome. All calculations and the appropriate ratios were calculated using Matlab.

2.3.6 Phagocytic assays

Aged Red blood cells (RBC), labelled with CellTrace CFSE (from molecular probes) and IgG-opsonized latex beads were prepared as described before, as well as the phagocytosis assay (Viegas, Estronca, & Vieira, 2012). For the phagocytosis assay a pulse-chase experiment was performed: the pulse time was 15 min, followed by the 30 min of chase time.

RBCs were obtained from human blood collected from healthy volunteers at CEDOC in accordance with protocols approved by the ethics committee (Ethical Review Board of the NOVA Medical School) and following the Declaration of Helsinki. Written informed consent was obtained from all volunteers.

2.3.7 Transferrin recycling

After lipid treatment, cells were pulsed with 0.2 mg/mL tetramethylrhodamine-transferrin for 10 min, washed with PBS and chased. Then, cells were fixed after 0, 5, 10, 20 and 40 min of chase time. For the representative images the coverslips were mounted and imaged using confocal microscopy. To quantify the fluorescence of transferrin, cells were detached using FACS buffer and analyzed using FACAriaTMIII (Becton Dickinson) cell sorter equipped with a 50 mW solid state 561 nm laser. Tetramethylrhodamine-transferrin was measured using a 610/20 nm bandpass emission filter. Data was analysed by FlowJo software.

2.3.8 Cargo exit from the lysosomes towards the Golgi

After macrophages treatment with ChE, cells were incubated with BODIPY-LacCer (2.5 μM) in DMEM with 1% FBS for 45 min. To label lysosomes, cells were stained with Lysotracker-red (200 nM) for 15 min at 37°C, in Chapter 3, or loaded with Alexa-647 dextran, in Chapter 5. Cell surface

fluorescence of LacCer was removed by washing the cells 3 times with 10% serum. Cells were followed under a confocal microscope for 3 h at 37°C in RPMI with 10 mM Hepes and 10% FBS. Co-localization analysis was performed using ImageJ with JACoP (Chapter 3) or Coloc2 (Chapter 5) plugin. Bafilomycin (100 nM) was added 30 min before imaging acquisition (Chapter 5).

2.3.9 Evaluation of the lysosomal degradation capacity

The lysosomal degradative capacity was measured by pulsing ChA-treated macrophages with DQ-BSA (20 µg/mL) for 3 h in medium without serum. After the pulse, the fluorescence emission was followed for 4 h using a fluorimeter SpectraMax Gemini EM (Molecular Devices) with excitation at 590 nm and emission at 620 nm. The fluorescence was normalized to the total cellular protein content, measured using a BCA kit (Thermo Fisher Scientific) and the results were expressed as Relative Fluorescence Intensity/mg of cell protein. The representative images were obtained in the same conditions; however, cells were seeded in coverslips and imaged after 4 h of chase.

The cathepsin L activity was evaluated by normalizing Magic Red (Immunochemistry Technologies) fluorescence to Alexa Fluor 647–dextran Fluorescence labeled lysosomes. Lysosomes were labeled by incubating macrophages overnight with 50 µg/mL Alexa Fluor 647–dextran followed by a chase of 3 h. Next, the cells were incubated with Magic Red cathepsin L substrate for 15 min, washed and imaged under a confocal microscope. As positive control, lysosomes were alkalinized with 100 nM of bafilomycin (InvivoGen) added 1 h before Magic Red.

2.3.10 Lysosome pH measurement

Lysosome pH was measured by simultaneously incubating RAW cells with 50 µg/mL of dextran conjugated with Alexa 647 and 50 µg/mL pHrodo (in Chapter 3, Thermo Fisher Scientific) or 250 µg/mL fluorescein (FITC)-conjugated dextran (in Chapter 5) at 37°C, 5% CO_2, during an overnight pulse. Then, cells were washed and chased during 3 h with fresh culture medium and imaged using confocal microscopy. The acquisition settings were not changed between different samples. To measure the fluorescence intensity ratio between pHrodo/FITC- and Alexa Fluor 647-dextran within the lysosomes, the organelles were delimited and the fluorescence intensity was quantified through the ImageJ software.

In Chapter 3: it was confirmed that fluorescence intensity of Alexa Fluor 647 is not affected by pH (Chapter 3, Supplementary Figure 3.2A) whereas that of pHrodo does. The fluorescence of Alexa Fluor 647 was measured in 0.2 M sodium acetate buffer between pH 3.5 and pH 7.5 using a Zenyth 3100 microplate reader from Anthos.

2.3.11 Filipin staining and binding experiments

After cells treatment with ChE, cells were fixed with PFA and then incubated with Filipin

(25 µg/ml in PBS) during 30 min at room temperature. The coverslips were mounted and imaged using confocal microscopy.

The binding capacity of Filipin to free cholesterol and to ChS or ChA was performed using a spectral assay. Several dilutions of POPC-FC (1:1) and POPC-ChS (1:1), in Chapter 3, or POPC-FC (3.5:6.5 molar ratio) and POPC-ChA (3.5:6.5 molar ratio) liposomes, in Chapter 5, were prepared and were incubated overnight with a 50 µM aqueous solution of Filipin at RT. Absorption spectra were obtained using the plate reader Spectramax i3x from Molecular Devices by measuring the absorbance ratio (Abs_{320}/Abs_{356}) and the corresponding Filipin-free lipid suspensions were used as blanks. Filipin-sterol association curves used the Abs_{320}/Abs_{356} as a function of sterol concentration (FC, ChS or ChA) and were fitted with theoretical curves using the Hill Equation.

2.3.12 LAMP-2 staining at the plasma membrane and flow cytometry analysis

RAW 264.7 cells were treated for 72 h with or without lipids and then washed with HBSS (from Gibco Inc). The cells were incubated at 37°C with 4 mM $CaCl_2$, in the presence or absence of 5 µM ionomycin, for 5 min. After incubation, cells were cooled to 4°C, washed with flow cytometer buffer (PBS supplemented with 1% FBS and 2 mM EDTA), stained with rat anti-LAMP-2 antibody (1:50 in flow cytometer buffer, hybridoma bank: ABL-93), which recognizes the LAMP2-luminal domain, for 30 min and with a secondary Cy5-anti rat antibody (1:250, Jackson ImmunoResearch Laboratories) for another 30 min. Before analysis, cells were also stained with 50 µg/mL propidium iodide (PI). Data were acquired in a BD FACS-cantoTMII flow cytometer (Becton Dickinson): PI fluorescence and LAMP-2 were measured in the PI channel (585/42 BP) and Cy5 channel (665/20 BP), respectively. The software for acquisition was BD FACSDIVA, and data from at least 5000 cells were analyzed with FlowJo. All PI-positive cells were excluded for the quantification.

2.3.13 β-hexosaminidase release assay

Macrophages were washed with Ca^{2+}- and Mg^{2+}-free ice-cold HBSS. The β-hexosaminidase (β-hex) release assay was performed as described by Rodríguez *et al.*, 1997 and Kima *et al.*, 2000. Briefly, after 72 h of incubation with and without lipids cells were washed with ice-cold HBSS and stimulated with 4 mM $CaCl_2$, in the presence or absence of 5 µM ionomycin, for 10 min at 37°C. Cells were placed on ice, and cell supernatants containing the released β-hex were collected. In parallel, cells were lysed with 1% IGEPAL/dH_2O and diluted 1:5 in dH_2O, as previously described in Encarnação *et al*. 2016. β-Hex activity was determined by incubating cell supernatants and lysates in a 96-well plate with 6 mM of the substrate 4-methyl-umbelliferyl-N-acetyl-β-D-glucosaminide (4-MU-β-D-GlcNAc; Glycosynth) resuspended in HBSS with 40 mM sodium citrate and 88 mM Na_2PO_4, pH 4.5, for 15 min at 37°C. Fluorescence was measured in a plate-spectrofluorimeter at excitation 365 nm/emission 450 nm. Protein content from cell supernatants and lysates were determined using the BCA protein assay kit (Thermo Fisher Scientific), as described by the manufacturer.

β-Hex activity is expressed as fluorescence (365 nm/450 nm) per milligram of cell protein. The total β-hex activity is the sum of the β-hex activity in the supernatant and β-hex activity in the cell lysate. β-Hex released is expressed as the percentage of β-hex activity in the supernatant relative to the total β-hex activity.

2.3.14 Plasma membrane staining with FM4-64 and its internalization

Cells were incubated with 30 µg/mL FM4-64 (Thermo Fisher Scientific) in DMEM, during 15 min on ice and then washed with PBS. Cells were then incubated with DMEM without phenol red, supplemented with 10% of FBS and 10 mM Hepes. Live cells were imaged at 37°C under a confocal microscope. Images were acquired time 0, 15 and 45 min after chase.

2.3.15 Immunoblotting

After incubation with ChE, RAW cells were lysed with ice-cold lysis buffer (50 mM Tris-HCl, pH 7.4, 150 mM NaCl, 0.5 mM EDTA, and 1% IGEPAL) in the presence of protease inhibitors for 30 min on ice, followed by centrifugation at 20,000 g for 30 min at 4°C. For quantification of total protein concentration, it was used the DC protein assay kit (Bio-Rad). The samples were loaded on a 12% SDS polyacrylamide gels and transferred onto activated PVDF membranes in transfer buffer (25 mM Tris, 192 mM glycine, and 20% ethanol) for 2 h at 300 mA at 4°C. Membranes were blocked by incubation for 1h at room temperature with blocking buffer (5% nonfat dry milk and 0.1% Tween-20 in PBS). Then, membranes were incubated at 4°C for 16 h in blocking buffer containing mouse anti-LAMP-2 (1:1000) and anti-calnexin (1:10000, from Sicgen). Then the blots were incubated for 1 h with donkey anti–rat, donkey anti–mouse and donkey anti–rabbit IgG conjugated to horseradish peroxidase (1:5000). Blots were visualized using ECL Prime Western Blot Detection reagent (GE Healthcare) and a Chemidoc Touch Imaging System (Bio-Rad Laboratories). Bands were quantified using Image Lab software from Bio-Rad.

2.3.16 Protein assay

The protein content of cell extracts was measured by the bicinchoninic acid (BCA, Pierce) or by a modified Lowry method (BioRad) assay using bovine serum albumin as a standard.

2.4 INFLAMMATORY EFFECTS ON PRIMARY HUMAN AND BMDM

2.4.1 Blood-derived monocyte isolation and *in vitro* differentiation into macrophages

Experiments were performed as previously described (Cunha et al., 2017), using buffy coats isolated from healthy donors (n = 4) supplied by the Hospital of Braga, after approval of the Competent Ethics Committee (CEC). The human samples received were handled in accord-

ance with the guidelines approved by the CEC. All the donors agreed and signed an authorized consent (ethical approval reference SECVF014/ 2015). After buffy coat preparation, monocytes were isolated by centrifugation using Histopaque-1077 followed by immunomagnetic separation using a human anti-CD14 purification kit (Miltenyi Biotec). The cell purity was confirmed by flow cytometry and was always superior to 95%. Purified monocytes were then directly used or differentiated *in vitro* into monocyte-derived macrophages (MDM). Cells were cultured in RPMI 1640 medium containing heat-inactivated fetal bovine serum (10%, FBS, Gibco Inc), L-glutamine (2 mM, Gibco Inc), penicillin (50 U/mL, Gibco Inc), streptomycin (50 µg/mL, Gibco Inc) and Hepes (10 mM, Gibco Inc), and supplemented with 20 ng/mL human macrophage colony stimulating factor (M-CSF, Peprotech) for 7 days at 37 °C, 5 % CO_2. On day 3, new medium was added to the culture to replenish essential nutrients. In monocyte to macrophage differentiation experiments, M-CSF-containing culture media was supplemented with 10 or 25 µM of ChA (sub-toxic concetrations). After differentiation, cell culture media was harvested for cytokine quantification. This set of experiments was performed by our collaborators from Life and Health Sciences Research Institute (ICVS), at University of Braga.

2.4.2 Bone marrow isolation and differentiation into macrophages

Bone marrow cell suspensions were obtained by flushing the femurs and tibias of 8- to 12-week-old mice with complete RPMI 1640 (+10% FCS, +1% Pen/Strep, Gibco Inc). Monocytes were differentiated into bone marrow-derived macrophages (BMDM) by culturing plated cells for 7 days in medium supplemented with 30% L929-cell conditioned medium (LCCM), in a humidified incubator at 37°C, 5 % CO_2. The assays were performed with BMDM cultures on day seven.

L929-cell line (Kindly provided by Prof. Ira Tobas, Columbia University, USA) was cultured to produced LCCM enriched in M-CSF, as previously described (Warren, 1985).

Mice were bred and maintained according to protocols approved by the Portuguese Directorate for Veterinary Medicine Department (Direcção Geral de Veterinária) ethics committees according to Portuguese law (Decreto-Lei 113/2013). C57BL/6 mice were provided by Charles River; *Nrf2*$^{-/-}$ mice were provided by the RIKEN BioResource Center (Koyadai, Tsukuba, Ibaraki, Japan); *tlr4*$^{-/-}$ knockout mice were bred and housed at ICVS, University of Braga. Mice were bred and maintained for experiments in accordance with the European Union Directive 2010/63/EU and the Animal Scientific Procedures Act, 1986.

2.4.3 Cell culture and treatment with ChA

Isolated human monocytes were seeded and incubated with 10 or 25 µM of ChA at 37°C, 5% CO_2. POPC liposomes (vehicle) were used as control in all the experiments. After 24 h of incubation, cell were analysed by flow cytometry and the supernatants were harvested for ELISA analysis.

After differentiation, BMDM were detached with a cell scraper (Sarstedt) and seeded. After adhesion, different concentrations of ChE were added to cells in supplemented RPMI with 30% of LCCM and incubated at 37 °C under a humidified 5% CO_2 air atmosphere.

2.4.4 Measurement of cytokines

Supernatants from monocyte, MDM or BMDM cultures were analyzed for IL-1α, IL-1β or IL-10 using the DuoSet ELISA development system (R&D systems). TNFα, IL-6 and IL-4 were measured using a Q-Plex chemiluminescent antibody array (Quansys Biosciences). To determine the cytokine concentration in the samples assessed by ELISA, optical density (O.D.) values were corrected for background in a blank buffer sample and a 7-point standard concentration curve (non-linear power function curve) was used to calculate the values. Q-plex array microplates were imaged using a ChemiDoc touch (Bio-Rad) with the following exposure settings: optimal auto exposure, 2x2 binning. To calculate the concentrations of TNF-α, IL-6, and IL-4; the bespoke Q-view software package (Quansys Biosciences) was used according to manufacturer's instructions.

2.4.5 Measurement of nitrites and reactive oxygen species (ROS)

Supernatants from BMDM cultures were assessed for the presence of nitrites using Griess reagent according to the manufacturer's instructions. To determine the nitrite concentration in the samples assessed, O.D. values were corrected for background in a blank buffer sample and an 8-point standard concentration curve (non-linear power function curve), constructed using a 100 µM $NaNO_3$ solution, was used.

Intracellular ROS levels were evaluated through MitoSOX staining (Thermo Fisher Scientific) prepared in PBS and incubated for 20 min. After incubation, cells were washed twice, and fluorescence was measured (λ_{ex} 485 nm/λ_{em} 530 nm and λ_{ex} 510 nm/λ_{em} 580 nm, respectively) using a TECAN infinite F200 PRO spectrofluorimeter. ROS generation was calculated as an increase over baseline levels, determined for untreated cells (100%), and normalized by total cell count for each condition.

2.4.6 Flow cytometry of monocytes

MDM were detached by incubation with TrypLE Express solution (Thermo Fisher Scientific) at 37°C for 10 min. For the analysis of surface markers, monocytes and MDM were incubated for 20 min with saturating concentrations of monoclonal antibodies against HLA-DR (Biolegend), CD86 (Biolegend), CD206 (Biolegend) and CD163 (Biolegend). Cells were also stained with dihydrorhodamine 123 (DHR) and 4-Amino-5-Methylamino-2',7' Difluorofluorescein Diacetate (DAF-FM). Positive controls for surface marker analysis were obtained by polarizing macrophages with 10 ng/mL of LPS plus 100 U/mL of IFN-ϒ (Peprotech) for M1 and with 20 ng/mL of IL-4 (Peprotech) for M2. This set of experiments was performed by our collaborators from ICVS, at University of Braga.

2.4.7 Migration Assay

Murine aorta smooth muscle cells (MOVAS, CRL-2797, ATCC) were grown in DMEM supplemented with 10 % FBS (Gibco Inc) and 0.2 mg/ml G-418. MOVAS were seeded in 12-well plates until confluent. Before the scratch, MOVAS were treated with mitomycin C (10 µg/mL), which is a cell proliferation inhibitor, to exclude the proliferation factor on cell migration. The monolayer wound was performed using a sterile 200 µl pipette tip and washed with PBS to remove cell debris. Next, conditioned media from BMDM treated for 20 h with or without ChA was added and the wound was monitored for 8 h. The wounds were imaged with a phase contrast microscope. For quantification, boundaries were marked using ImageJ software (3 different fields per well) and the recovery area was calculated and compared between the different conditions.

Conditioned media was obtained from BMDM exposed for 24 h to different concentrations of ChA. After BMDM treatment, the supernatants were collected and centrifuged for 5 min at 1200 rpm.

2.5 CHE DETECTION IN CARDIOVASCULAR PATIENTS

2.5.1 Plasma samples

Blood samples were obtained from 3 groups of donors: the first group (86 subjects, 64 women and 22 men, ages 36-82 years), labeled “Control”, were randomly taken from the population of the Coimbra and Lisbon, Portugal, regions who satisfied the criterion that they had never had any CVD-related health complaints. The second group (72 subjects, ages 36-92 years), labelled acute coronary syndrome, “ACS”, was composed of patients admitted to Hospital Santa Cruz, Carnaxide, Portugal, who suffered ST-segment elevation myocardial infarction (20 subjects, 4 women and 16 men), Non-ST-segment elevation myocardial infarction (34 subjects, 7 women and 27 men) or unstable angina (18 subjects, 5 women and 14 men). The third group, labeled angina pectoris, “SAP” (82 subjects, 28 women and 54 men, ages 36-89 years) was composed of patients admitted to Hospital Santa Cruz, Carnaxide, Portugal, suffering from stable angina pectoris. For the purpose of this report, we will consider the groups ACS and SAP to be suffering from cardiovascular disease (CVD).

Blood was obtained from all donors after explaining the purpose and obtaining written informed consent from them or their legal representatives. The entire process was approved by the Ethical Review Board of the Faculty of Medicine of the New University of Lisbon and the Ethical Committee for Health of Centro Hospitalar de Lisboa Ocidental, which includes Hospital Santa Cruz and Hospital Egas Moniz. The sample collection and data analysis was carried out according to universal bioethical principles (Universal Declaration on Bioethics and Human Rights of UNESCO; The Charter of Fundamental Rights of the EU, 2000; Helsinki

Declaration of June 1964; Directive 95/46/EC) and complied with national legislation for the scientific use of human biological samples (Law nº 12/2005; and Decree Law nº 131/2014). Blood samples were drawn into tubes containing an anti-coagulant immediately after admission to the hospital and obtaining written informed consent. Samples were processed within 24 h of the time of collection. Plasma was obtained by centrifugation of the blood at 500 g for 10 min at 4 °C and stored at −80°C until required for lipidomic analysis.

2.5.2 Lipid extraction for mass spectrometry lipidomics

Mass spectrometry-based lipid analysis was performed at Lipotype GmbH (Dresden, Germany) as described (Surma et al., 2015). For lipid extraction an equivalent of 1 µL of undiluted plasma was used. Internal standards were pre-mixed with the organic solvents mixture and included: ChA and ChS. All liquid handling steps were performed using Hamilton Robotics STARlet robotic platform with the Anti Droplet Control feature for organic solvents pipetting. This set of experiments (from 2.5.2 to 2.5.4 section) was performed by our collaborators from Lypotipe, Desdren - Germany.

2.5.3 Mass spectromety data acquisition

Samples were analyzed by direct infusion in a QExactive mass spectrometer (Thermo Scientific) equipped with a TriVersa NanoMate ion source (Advion Biosciences). Samples were analyzed in both positive and negative ion modes with a resolution of $R_{m/z=200}$=280000 for MS and $R_{m/z=200}$=17500 for tandem mass spectrometry (MS/MS) experiments, in a single acquisition. MS/MS was triggered by an inclusion list encompassing corresponding MS mass ranges scanned in 1 Da increments.

2.5.4 Lipidomic data analysis and post-processing

Data were analyzed with in-house developed lipid identification software based on LipidXplorer (Herzog et al., 2011, 2012). Data post-processing and normalization were performed using an in-house developed data management system. Only lipid identifications with a signal-to-noise ratio >5, and a signal intensity 5-fold higher than in corresponding blank samples were considered for further data analysis. Using 8 reference samples per 96-well plate batch, lipid amounts were corrected for batch variations. Amounts were also corrected for analytical drift, if the p-value of the slope was below 0.05 with an R2 greater than 0.6 and the relative drift was above 5%. Median coefficient of (sub-)species variation as accessed by reference samples was 8.7%. An occupational threshold of 80% was applied to the data, keeping lipid species, which were present in at least 80% of the subjects in at least one cohort. Data were analysed with R version 3.3.3 (R Development Core Team, 2016) using tidyverse packages version 1.1.1 (Wickham, 2016) and plots were created with ggplot2 version 2.2.1 (Wickham, 2009). Networks were produced with Cytoscape version 3.5.0 (Shannon et al., 2003).

2.6 METABOLIC EFFECT OF CHE IN PRIMARY MACROPHAGES

2.6.1 Metabolite quantification

Total glucose and lactate concentrations in the culture supernatant were determined with automated enzymatic assays (YSI 7100 Multiparameter Bioanalytical System; Dayton, OH, USA). The rate between lactate and glutamate production and glucose and glutamine consumption was obtained by linear regression of the metabolite concentrations and normalized to the total protein. The ratio between lactate/glucose and glutamine/glutamate was determined for each time point.

2.6.2 Seahorse experiment

Metabolic analyses were performed using the Seahorse XF96 Extracellular Flux Analyzer, which enables the real time, simultaneous rate measurements of oxygen consumption (OCR) and extracellular acidification rate (ECAR) by creating a transient microchamber within each well of specialized cell culture microplates. For the Agilent Cell Mito Stress Test, after ChA incubation, cell culture medium was exchanged to DMEM (without phenol red from sigma D5030) supplemented with 2 mM of glutamine and 11.1 mM of glucose. Following instrument calibration, basal OCR was measured followed by sequential injections of 2 µM of oligomycin, 2 µM FCCP, and a combination of 1 µM rotenone and 1 µM antimycin A. The same conditions were used for endogenous fatty acid oxidation (FAO) assay with some differences. Cells were incubated with DMEM supplemented only with 2.34 mM glutamine and 0.5 mM of carnitine. Before plate reading, cells were incubated 15 min before the experiment with 40 µM of etomoxir. For the Agilent Seahorse XF Glycolytic Rate Assay, culture medium was also exchanged with DMEM supplemented with 2 mM glutamine, 10 mM glucose, 1 mM pyruvate and 5 mM Hepes. Following basal ECAR measurement, cells were sequentially injected with rotenone/antimycin A and 50 mM 2-deoxy-D-glucose (2-DG). Each experiment had at least three biological replicates, and both OCR and ECAR values were normalized to protein in each well, by sulforhodamine B (SRB) assay (as describe in (Vichai & Kirtikara, 2006)). For Seahorse data analysis, Wave Desktop software (Agilent) was used.

2.7 CHE EFFECTS ON ZEBRAFISH LARVAE

2.7.1 Zebrafish maintenance and feeding

Zebrafish lines were maintained in accordance with Institutional and National animal care protocols, in a re-circulating system at 28°C on a 14-hour-light and 10-hour-dark cycle.

Wild-type (AB), *Pu.1:EGFP (pU1::Gal4, UAS::GFP), fli1:EGFP* and SH378, the later kindly donating by Sheffield University- Tg(*mpeg.mCherryCAAX SH378, mpx:EGFP i114*), zebrafish were crossed and collected and kept in E3 zebrafish embryo medium at 28°C until reaching the desired developmental stage. Zebrafish larvae were fed twice a day for 10 days, starting at the 5 days post-fertilization (dpf), with normal diet (from Mucedola, control), FC-enriched (normal food supplemented with 2 or 4% FC, w/w, corresponding to 26 or 52 µmol per gram of food, respectively), ChS-enriched diet (normal food supplemented with 5% ChS w/w, or 52 µmol per gram of food) or (3 or 6% ChA w/w, the same molarity than FC 2% or 4% respectively). Food was prepared as described in (Stoletov et al., 2009). To visualize lipid accumulation in the vessels, food was also supplemented with 10 µg/g of red fluorescent cholesteryl ester (CholEsteryl BODIPY 542/563 C11, from Thermo Fisher Scientific).

2.7.2 ChE toxicity to zebrafish larvae

Zebrafish survival was assessed on the 5dpf larvae, that received different diets for 10 days. Larvae were fed twice a day with different concentrations of FC, ChS or ChA. Thirty five larvae were placed in each test chamber for each food condition. Dead larvae were removed daily. Larval death was expressed as a fraction of the total number of individuals subjected to a given condition and compared to a control population receiving a normal diet.

The toxicity observed for zebrafish larvae fed with 6% ChA was very high. Therefore, the majority of the experiments were performed in zebrafish fed with a diet enriched with 3% of ChA.

2.7.3 Preparation of zebrafish cell suspension and FACS

After 10 days of feeding with the different diets, larvae were sacrificed on ice to maintain cell viability, and transferred to PBS containing 0.1 mg/mL liberase. Tissues were digested at 28°C for 20-30 min and mechanically dissociated by resuspending the tissue every 5 min. Cell suspension was passed thought a CellTrics 30 µm filter directly to a new Eppendorf and heat inactivated-FBS was added (10% final concentration). The cell suspension was then sorted in a FACSAriaIII high speed cell sorter (Becton Dickinson) equipped with a 561 nm laser (50 mW solid state) and a 630/75 nm BP for mCherry excitation. PBS was used as sheath fluid, and run at a constant pressure of 207 kPa with a 100 µm nozzle and a frequency of drop formation of approximately 30 kHz. Cells were directly collected into individual wells of a Lab-Tek Chambered plate (Nunc) and allowed to adhere at room temperature for 2 h.

2.7.4 Oil Red-O staining of zebrafish larvae

Larvae were fixed with 4% PFA and rinsed three times with PBS containing 0.5% Tween-20 (PBS-T) as previous described (Kim et al., 2013). Briefly, larvae were stained with Oil Red in 60% isopropanol, prepared from a stock solution at 0.5% w/v in 100% isopropanol for 15 min. They were then rinsed twice with 60% isopropanol, for 5 min and finally with PBS-T.

2.7.5 Acid organelles ("Lysosomes") and neutral lipid staining

After cell sorting, macrophages were incubated for 20 min with BODIPY 493/503 (1:500) and LysoTracker (1:1000), and imaged using confocal microscopy. Alternatively, 15 dpf zebrafish larvae were incubated in a 1:100 dilution of LysoTracker Green in E3 medium at 28.5 °C for 45 min to 1 h, washed twice then imaged (live).

2.7.6 Confocal imaging and analysis

Prior to imaging, zebrafish larvae were fixed in 4 % PFA and mounted with a coverslip using mounting media (1 g of DABCO in 10 mL PBS and 40 mL glycerol) prior to imaging. For live imaging, larvae were anesthetized with tricaine methanesulfonate and mounted in 1 % low melting point agarose in E3 medium. A Zeiss LSM710 confocal microscope was used and optical sections in the tail area were acquired with a 40x objective.

Image analysis was performed using the imageJ software. Lipid structures were delineated and the area measured. The lipid intensity was normalized to the total area of the vasculature analyzed. For quantification of myeloid cells in the caudal vein, fluorescent cells were counted and normalized to the length of the analyzed segment of the vasculature.

For single cell live imaging, cells were imaged in Lab-Tek Chambered plate (Nunc) using the water 40x objective. The area and intensity of structures was measure using ImageJ software.

2.8 ASSESSEMENT OF CHE EFFECT ON GENE EXPRESSION

2.8.1 Quantitative RT-PCR

Total RNA was extracted with Trizol reagent according to manufacturer's instructions. Reverse transcription was performed using the NZY first-strand cDNA synthesis kit (NZYtech). Quantitative PCR was performed in a 96-well optical plate using SYBR green master mix (NZYtech). PCR and data acquisition was performed using the AB7300 Real-Time PCR thermal cycler with Step One software (v2.2.2; Applied Biosystems). GAPDH and PGK1 were used as housekeeping gene to normalize the expression in mouse cells. In zebrafish, eef1al1 - eukaryotic elongation factor 1 alpha like 1 and rpl13a - ribosomal protein L13a were used as housekeeping genes to normalize the mRNA expression levels. Target gene expression was determined by relative quantification (ΔΔCt method) to the housekeeping reference genes and the control sample.

The following mouse and zebrafish forward and reverse primers were used:

Table 2.1 | Primers sequences for qRT-PCR.

Gene	Primer sequences
ki67 m	(GGGAAGCCCATCACCATCTTC; AGAGGGGCCATCCACAGTCT)
hmox-1 m	(CTAAGACCGCCTTCCTGCTC; GGGCAGTATCTTGCACCAGG)
il-1β m	(TGCCACCTTTTGACAGTGATGA; GCGAGATTTGAAGCTGGATGC)
il-6 m	(TCCAGTTGCCTTCTTGGGAC; GTACTCCAGAAGACCAGAGG)
il-10 m	(TGGCCCAGAAATCAAGGAGC; CAGCAGACTCAATACACACT)
il-1α m	(GGGAAGATTCTGAAGAAGAG; GAGTAACAGGATATTTAGAGTCG)
prx m	(CAAGGAGGATTGGGACCCATGAAC; GCCCCTGAAAGAGATACCTTCATCAGC)
tfeb m	(AGGAGCGGCAGAAGAAAGAC; CAGGTCCTTCTGCATCCTCC)
lamp1 m	(ACATCAGCCCAAATGACACA; GGCTAGAGCTGGCATTCATC)
p62 m	(GTCTTCTGTGCCTGTGCTGGAA; TCTGCTCCACCAGAAGATCCCA)
Lipa m	(CTAGAATCTGCCAGCAAGCC; AGTATTCACCGAATCCCTCG)
lamp-1 m	(ACATCAGCCCAAATGACACA; GGCTAGAGCTGGCATTCATC)
arl8 m	CCGCCATGCTGGCGCTCATCTC; AGGTCTCAGCTTCTCCGGGATT)
rab3a m	(GCATGAATTCATGATGGCTTCCGCCACAGACTCTCGCTAT; ACTCGTCGACCAGCAAGGTCCATTCGCTTTATTG)
rab10 m	(AAGAGAATTCGAGCCGCTCCTCCCAATGGCG; CAATGTCGACGACAAACGCTACTAAGACCCACTC)
rab7am	(CCCCAACACTTTCAAAACCC;TGGCCCGGTCATTCTTGTCC)
pgk1m	(ATGGATGAGGTGGTGAAAGC; CAGTGCTCACATGGCTGACT)
gapdh m	(GGGTCCCAGCTTAGGTTCATC; AGGAGACAACCTGGTCCTCA)
v-cam1 dr	(TTGCAGTTGTTTCCCACACG; CCTAACGCGGTCCAGACAAA)
il-1β dr	(GTAACCTGTACCTGGCCTGC; AACAGCAGCTGGTCGTATCC)
il-6 dr	(ACGTGAAGACACTCAGAGACG; CGTTAGACATCTTTCCGTGCTG)
tnf-α dr	(CAGGGCAATCAACAAGATGG; TGGTCCTGGTCATCTCTCCA)
eef1al1 dr	(CCTTCAAGTACGCCTGGGTGTT; CACAGCACAGTCAGCCTGAGAA)
rpl13a dr	(TGACAAGAGAAAGCGCATGGTT; GCCTGGTACTTCCAGCCAACTT)

m- *mus musculus*
dr- *danio rerio*

2.9 STATISTICAL ANALYSIS

Results are expressed as the mean ± standard error of the mean (SEM). Statistical significance was assessed by one two-way ANOVA with a Turkey post-test or t-test. A p value of 0.05 was considered to be statistically significant.

2.10 REFERENCES

Cunha, C., Gonçalves, S. M., Duarte-Oliveira, C., Leite, L., Lagrou, K., Marques, A., … Carvalho, A. (2017). IL-10 overexpression predisposes to invasive aspergillosis by suppressing antifungal immunity. Journal of Allergy and Clinical Immunology, 140(3), 867–870.e9. https://doi.org/10.1016/j.jaci.2017.02.034

Estronca, L. M. B. B., Silva, J. C. P., Sampaio, J. L., Shevchenko, A., Verkade, P., Vaz, A. D. N., … Vieira, O. V. (2012). Molecular etiology of atherogenesis - in vitro induction of lipidosis in macrophages with a new LDL model. PLoS ONE, 7(4). https://doi.org/10.1371/journal.pone.0034822

Flore, V., Donfack, D., Roque, S., Trigo, G., Valere, P., Fokou, T., … Boyom, F. F. (2014). Antimycobacterial activity of selected medicinal plants extracts from Cameroon. International Journal of Biological and Chemical Sciences, 8(February), 273–288.

Herzog, R., Schuhmann, K., Schwudke, D., Sampaio, J. L., Bornstein, S. R., Schroeder, M., & Shevchenko, A. (2012). Lipidxplorer: A software for consensual cross-platform lipidomics. PLoS ONE, 7(1). https://doi.org/10.1371/journal.pone.0029851

Herzog, R., Schwudke, D., Schuhmann, K., Sampaio, J. L., Bornstein, S. R., Schroeder, M., & Shevchenko, A. (2011). A novel informatics concept for high-throughput shotgun lipidomics based on the molecular fragmentation query language. Genome Biology, 12(1), R8. https://doi.org/10.1186/gb-2011-12-1-r8

Huang, T. C., Chen, C. P., Wefler, V., & Raftery, A. (1961). A Stable Reagent for the Liebermann-Burchard Reaction: Application to Rapid Serum Cholesterol Determination. Analytical Chemistry, 33(10), 1405–1407. https://doi.org/10.1021/ac60178a040

Kim, S. H., Scott, S. A., Bennett, M. J., Carson, R. P., Fessel, J., Brown, H. A., & Ess, K. C. (2013). Multi-organ Abnormalities and mTORC1 Activation in Zebrafish Model of Multiple Acyl-CoA Dehydrogenase Deficiency. PLoS Genetics, 9(6). https://doi.org/10.1371/journal.pgen.1003563

R Development Core Team. (2016). R: A Language and Environment for Statistical Computing. R Foundation for Statistical Computing Vienna Austria, 0, {ISBN} 3-900051-07-0. https://doi.org/10.1038/sj.hdy.6800737

Shannon, P., Markiel, A., Ozier, O., Baliga, N. S., Wang, J. T., Ramage, D., … Ideker, T. (2003). Cytoscape: A software Environment for integrated models of biomolecular interaction networks. Genome Research, 13(11), 2498–2504. https://doi.org/10.1101/gr.1239303

Stoletov, K., Fang, L., Choi, S. H., Hartvigsen, K., Hansen, L. F., Hall, C., … Miller, Y. I. (2009). Vascular lipid accumulation, lipoprotein oxidation, and macrophage lipid uptake in hypercholesterolemic zebrafish. Circulation Research, 104(8), 952–960. https://doi.org/10.1161/CIRCRESAHA.108.189803

Surma, M. A., Herzog, R., Vasilj, A., Klose, C., Christinat, N., Morin-Rivron, D., … Sampaio, J. L. (2015). An automated shotgun lipidomics platform for high throughput, comprehensive, and quantitative analysis of blood plasma intact lipids. European Journal of Lipid Science and Technology, 117(10), 1540–1549. https://doi.org/10.1002/ejlt.201500145

Vichai, V., & Kirtikara, K. (2006). Sulforhodamine B colorimetric assay for cytotoxicity screening. Nature Protocols, 1(3), 1112–1116. https://doi.org/10.1038/nprot.2006.179

Viegas, M. S., Estronca, L. M. B. B., & Vieira, O. V. (2012). Comparison of the Kinetics of Maturation of Phagosomes Containing Apoptotic Cells and IgG-Opsonized Particles. PLoS ONE, 7(10). https://doi.org/10.1371/journal.pone.0048391

Vieira, O. V., Hartmann, D. O., Cardoso, C. M. P., Oberdoerfer, D., Baptista, M., Santos, M. A. S., Vaz, W. L. C. (2008). Surfactants as microbicides and contraceptive agents: A systematic In Vitro study. PLoS ONE, 3(8). https://doi.org/10.1371/journal.pone.0002913

Vieira, O. V, Laranjinha, J. a, Madeira, V. M., & Almeida, L. M. (1996). Rapid isolation of low density lipoproteins in a concentrated fraction free from water-soluble plasma antioxidants. Journal of Lipid Research, 37(12), 2715–2721. Retrieved from http://www.ncbi.nlm.nih.gov/pubmed/9017522

Warren, M. K. & Vogel, S. N. (1985). Bone marrow - derived macrophages: development and regulation of differentiation markers by colony-stimulating factor and interferons a jornal Immunol. 134, 982-9

Wickham, H. (2009). ggplot2 Elegant Graphics for Data Analysis. Media (Vol. 35). https://doi.org/10.1007/978-0-387-98141-3

Wickham, H. (2016). tidyverse: Easily Install and Load “Tidyverse” Packages. R package version 1.0.0. Retrieved from https://cran.r-project.org/package=tidyverse

03 CHOLESTERYL HEMIESTERS ALTER LYSOSOME STRUCTURE AND FUNCTION AND INDUCE PROINFLAMMATORY CYTOKINE PRODUCTION IN MACROPHAGES

The work presented in this chapter was published in: Domingues, Neuza*; Estronca, Luís MBB*; Silva, João; Encarnação, Marisa R; Mateus, Rita; Silva, Diogo; Santarino, Inês B; Saraiva, Margarida; Soares, Maria IL; Melo, Teresa MVD Pinho; Jacinto, António; Vaz, Winchil LC; Vieira, Otília V. (2017); Cholesteryl hemiesters alter lysosome structure and function and induce proinflammatory cytokine production in macrophages; Biochimica et Biophysica Acta (BBA)-Molecular and Cell Biology of Lipids 1862(2):210-220; doi: 10.1016/j.bbalip.2016.10.009

*Equally contributed

3.1 ABSTRACT

RATIONALE: Cholesteryl hemiesters are oxidation products of polyunsaturated fatty acid esters of cholesterol. Their oxo-ester precursors have been identified as important components of the "core aldehydes" of human atheromata and in oxidized lipoproteins (ox-LDL). We had previously shown, for the first time, that a single compound of this family, cholesteryl hemisuccinate (ChS), is sufficient to cause irreversible lysosomal lipid accumulation (lipidosis), and is toxic to macrophages. These features, coupled to others such as inflammation, are typically seen in atherosclerosis.

OBJECTIVE: To obtain insights into the mechanism of cholesteryl hemiester-induced pathological changes in lysosome function and induction of inflammation *in vitro* and assess their impact *in vivo*.

METHODS AND RESULTS: We have examined the effects of ChS on macrophages (murine cell lines and primary cultures) in detail. Specifically, lysosomal morphology, pH, and proteolytic capacity were examined. Exposure of macrophages to sub-toxic ChS concentrations caused enlargement of the lysosomes, changes in their luminal pH, and accumulation of cargo in them. In primary mouse bone marrow-derived macrophages (BMDM), ChS-exposure increased the secretion of IL-1β, TNF-α and IL-6. In zebrafish larvae (wild-type AB and *PU.1:EGFP*), fed with a ChS-enriched diet, we observed lipid accumulation, myeloid cell-infiltration in their vasculature and decrease in larval survival. Under the same conditions the effects of ChS were more profound than the effects of free cholesterol (FC).

CONCLUSIONS: Our data strongly suggest that cholesteryl hemiesters are proatherogenic lipids able to mimic features of ox-LDL both *in vitro* and *in vivo*.

3.2 INTRODUCTION

The factors that initiate atherosclerotic lesions and influence their progression are extremely complex and still relatively poorly understood (Aluganti Narasimhulu et al., 2016). One of the early distinguishing characteristics of the process, already described by de Duve and colleagues in the 1970s (Peters, Müller, & De Duve, 1972), is the presence of macrophage-derived foam cells in the arterial wall. They result from ingestion of lipid accumulated in the vascular wall by the macrophages and storage of these lipids in lipid droplets, which leads to the formation of intravascular "fatty streaks". This process is, initially, reversible. However, with time, the internalized lipid cannot be metabolically processed by macrophages,

and accumulates in their lysosomal compartment resulting in an irreversible phenotype that has the characteristics of lipidosis manifested in several lipid storage diseases (Jerome, 2010a; Schmitz & Grandl, 2009). Importantly, the exact molecular mechanisms involved in lysosomal lipid accumulation have not been identified. There is a consensus that foam cell formation requires entrapment of low density lipoproteins (LDL) within the arterial intima followed by some modification of the entrapped LDL particles (Brown & Goldstein, 1983). One modification that LDL particles undergo in the arterial intima is oxidation (Berliner, Leitinger, & Tsimikas, 2009; Jiang, Yang, Chandrakala, Pressley, & Parthasarathy, 2011; JW, 1997; Steinberg, 2009; Stocker, 2004). This modification is important because it allows macrophages to take up these particles through unregulated scavenger receptor pathways (Brown & Goldstein, 1983) or through micropinocytosis (Choi et al., 2009).

Cholesteryl hemiesters are oxidation products of the core aldehydes present in human atheromata (Hutchins, Moore, & Murphy, 2011a) and also in oxidized LDL (ox-LDL) (Kamido, Kuksis, Marai, & Myher, 1995). So far, although considerable attention has been paid in the literature to the atherogenicity of oxidized phospholipids (Podrez et al., 2002; Salomon, 2012) and oxysterols (Luu, Sharpe, Capell-Hattam, Gelissen, & Brown, 2016) the possible effects of oxidation end products of cholesteryl esters have been largely ignored in the literature. Oxidation of lipids containing polyunsaturated fatty acids is quite complex and results in a plethora of products (Salomon, 2012). One of the end products of oxidation of cholesteryl-esters of polyunsaturated fatty acids is the family of cholesteryl hemiesters (Estronca et al., 2012). We decided to examine this group of compounds as possible etiological agents of atherogenesis and recently showed (Estronca et al., 2012) that a single compound of this chemical family, cholesteryl hemisuccinate (ChS), when incorporated into native LDL (Nat-LDL) particles and presented to macrophages *in vitro* was sufficient to mimic two important features of the fate of macrophages exposed to ox-LDL: 1) cells exposed to ChS-LDL irreversibly accumulate undigested lipid in enlarged lysosomes; and 2) ChS is cytotoxic and provokes apoptotic cell death.

While the toxicity of ox-LDL and some of its oxidized lipids to macrophages has been well documented, the expansion and malfunction of the lysosomal compartment in macrophages in the initial stages of atherogenesis has been largely unexplored (de Duve, 1974; Jerome, 2010). In this work we examine the effects of long-term sub-toxic exposure of macrophages to ChS-LDL (Nat-LDL loaded with ChS), on lysosome morphology and function. Similar to our earlier work on this subject (Estronca et al., 2012), ChS was used as a model of the cholesteryl-hemiester family of compounds that are expected to be produced from polyunsaturated fatty acid esters of cholesterol. The work has been extended to an *in vivo* model by studying the effects of ChS, presented as part of the diet, on zebrafish larvae.

We show that ChS-LDL, at sub-lethal concentrations, induce formation of enlarged lysosomes in macrophages *in vitro*. The degradative and exit capacity of endocytic cargo by the lysosomes is inhibited. These outcomes seem to be correlated with accumulation of ChS in

the lysosomal membranes and an increase in lysosomal luminal pH. ChS-LDL also trigger a proinflammatory response in mouse primary bone marrow-derived macrophages (BMDM). Finally, by enriching the diet of zebrafish larvae with ChS it is possible to mimic the *in vitro* phenotypes observed, namely, the intravascular lipid accumulation, the inflammation-induced infiltration of myeloid cells in the caudal vein, and also larval death.

3.3 RESULTS

3.3.1 Long-term exposure to sub-toxic ChS-LDL concentrations caused lysosome enlargement in macrophages

Atheroma formation *in vivo* is a very slow pathological process, developing over many years and often decades, initiated by formation of irreversible foam cells from macrophages that invade the vasculature. The acute toxic effects of ChS on macrophages, examined in our previous work (Estronca et al., 2012) include irreversible lipidosis, some enlargement of the lysosomes and apoptotic cell death. However, acute toxicity cannot be the only determinant in the development of atheromata. We, therefore, assessed the effect of long-term exposure of macrophages *in vitro* to sub-toxic concentrations of ChS upon lysosomes of the cells. To determine suitable ChS concentrations for our experimental purposes, RAW 264.7 macrophages (hereafter referred to as RAW cells) were exposed to different ChS-LDL concentrations for twenty days as shown in Figure 3.1A. Henceforward, any reference to the concentration of "ChS-LDL" implies the ChS concentration in the cell culture medium, the ChS having been loaded into Nat-LDL particles at a ratio of 1000 molecules of ChS per LDL particle as previously described in detail (Estronca et al., 2012). LDL was used as a carrier of the ChS and the ChS/LDL ratio was not supposed to reflect any physiological relevance. Our previous work (Estronca et al., 2012) had shown that acetylated-LDL or phosphatidylcholine liposomes are equally effective carriers for the ChS. The cell cultures were split every two days and, to avoid LDL oxidation due to reactive oxygen species pro-

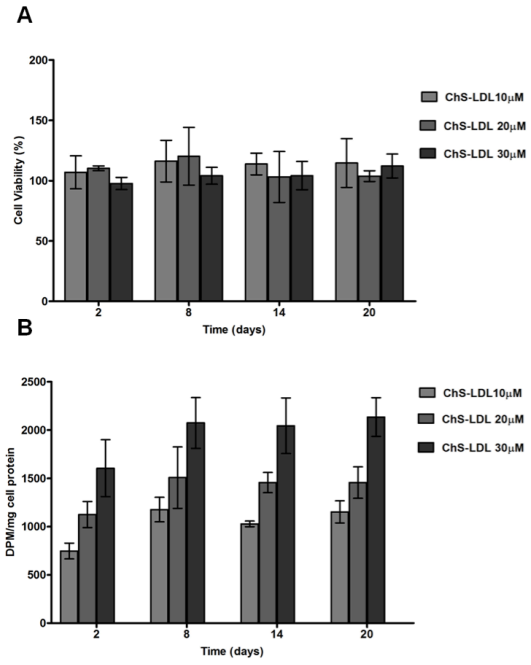

Figure 3.1 | Viability of RAW macrophages exposed for twenty days to ChS-LDL is not affected.

RAW cells were exposed to different concentrations of ChS-LDL and were followed during 20 days. Nat-LDL were used as control. **A.** Shows cell viability assessed by the MTT assay and expressed relative to the viability of control cells exposed to Nat-LDL. **B.** Shows the incorporation of intracellular radioactivity as a function of time when RAW cells were exposed to different concentrations of ^{3}H-ChS-LDL as indicated in the graph. After incubation the cells were acid washed and scraped. The radioactivity and protein were quantified as described in the Methods section. Values are Mean±SEM of three separate experiments.

duced by RAW cells, fresh ChS-LDL were added at each splitting. Cell viability, assessed by the MTT assay, was expressed as percentage of the viability of control cells exposed to Nat-LDL that were used in all *in vitro* experiments described below. Cell proliferation rates were evaluated by counting the cells at each splitting and examining for 5-ethynyl-2'-deoxyuridine incorporation (Inácio et al., 2016) (data not shown). No differences were observed between untreated cells and those treated with Nat-LDL. The three different ChS-LDL concentrations tested were not toxic during the experimental time (Figure 3.1A). To ensure that ChS-LDL were being internalized, RAW cells were treated under the same conditions with ^{3}H-ChS-LDL and the intracellular radioactivity was examined as a function of incubation time (Figure 3.1B). For all concentrations tested, radioactivity accumulated within the cells in a ChS-LDL concentration-dependent manner and was saturable within the first eight days of incubation (Figure 3.1B). We concluded that, at the concentrations tested, ChS-LDL were being internalized by the cells without loss of cell viability.

Taking into account the results described, further experiments used ChS-LDL at a ChS concentration of 30 µM. RAW cells were exposed to ChS-LDL for 20 days and lysosomal area and morphology was assessed as a first evaluation of lysosomal function. The first observation was the appearance of large lysosomal structures. The size of the lysosomes was quantified by measuring the area of LAMP-2-positive structures in control and ChS-LDL-treated cells (Figure 3.2A). Single 0.419 µm thick slices at the maximal cell perimeter were quantified for each case.

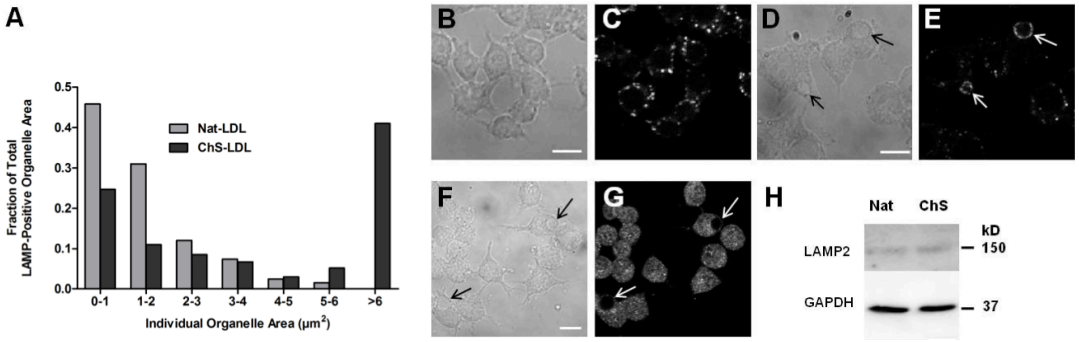

Figure 3.2 | RAW macrophages exposed to sub-toxic concentrations of ChS-LDL exhibit lysosomal enlargement

RAW cells were treated for 20 days with 30 µM ChS-LDL (corresponding to 16 µg ApoB/mL), or Nat-LDL (16 µg ApoB/mL). **A.** Shows the fraction of total LAMP-positive organelles as a function of individual Lamp-positive organelle area. 55 cells exposed to Nat-LDL and 50 cells exposed to ChS-LDL were used to obtain these results. **B.** is a DIC image and **C.** is the corresponding LAMP-2-stained image of RAW cells incubated with Nat-LDL. **D.** and **F.** are DIC images of RAW cells incubated with ChS-LDL and **E.** and **G.** are the corresponding LAMP-2 and EEA-1-stained images, respectively. All panels show confocal single slice images. Arrows point to the vacuoles. Bars, 10 µm. **H.** Shows LAMP-2 protein levels in lysates of cells treated with Nat-LDL or ChS-LDL. GAPDH was used as loading control.

Lysosome area in ChS-LDL treated cells (n = 50 cells) was strikingly higher than in control cells (n = 55 cells) and ~40% of the LAMP-positive organelle area was due to organelles with an area bigger than 6 µm^2 (Figure 3.2A, D and E). This feature was not observed in macrophages incubated with Nat-LDL (Figure 3.2A-C). Importantly, the number of lysosomes per cell was similar in control and ChS-LDL-treated cells. All LAMP-2-positive structures observed in ChS-LDL were not decorated with EEA-1, a marker for early endosomes (Figure 3.2F-G). Thus,

the large vacuolar LAMP-2-positive organelles, whose formation was induced by exposure to sub-toxic concentrations of ChS-LDL, were not hybrid organelles of the endocytic compartment. To conclude this set of experiments and to ensure that lysosomal biogenesis was not affected by ChS-LDL treatment we performed a Western blot to assess LAMP-2 protein levels. As shown in Figure 3.2H, LAMP-2 levels were similar in cells incubated with Nat-LDL and ChS-LDL. These results suggest that sub-toxic concentrations of ChS-LDL induced the formation of enlarged lysosomes in RAW macrophages without changes in their biogenesis.

3.3.2 Lysosomes in macrophages exposed to ChS-LDL could not degrade endocytic cargo

Since lysosomes play a central role in receiving and degrading macromolecules from the endocytic membrane-trafficking pathways we examined the effect of ChS in lysosomal degradation of endocytic cargo. Supplementary Figure 3.1 shows that neither uptake nor transport of endocytic cargo (BSA conjugated with Texas red) to the lysosomes were affected by exposure to ChS-LDL when compared to the control (Nat-LDL). Our next step was to verify whether there was efficient degradation of endocytic cargo in the ChS-treated-cells as compared with the control cells. As endocytic cargo we used DQ-BSA, a fluorogenic substrate for lysosomal proteases. Because this cargo is heavily labeled with BODIPY, a strong fluorescence quenching effect is observed. However, upon enzymatic cleavage of the DQ-BSA to dye-labeled peptides in the acidic lysosomal compartments this quenching is relieved, producing brightly fluorescent products. As shown in Figure 3.3 A-E, the rate of degradation of DQ-BSA by the lysosomal proteases was significantly slower in RAW cells exposed to ChS-LDL as compared to controls, suggesting that the catalytic activity of this organelle was affected.

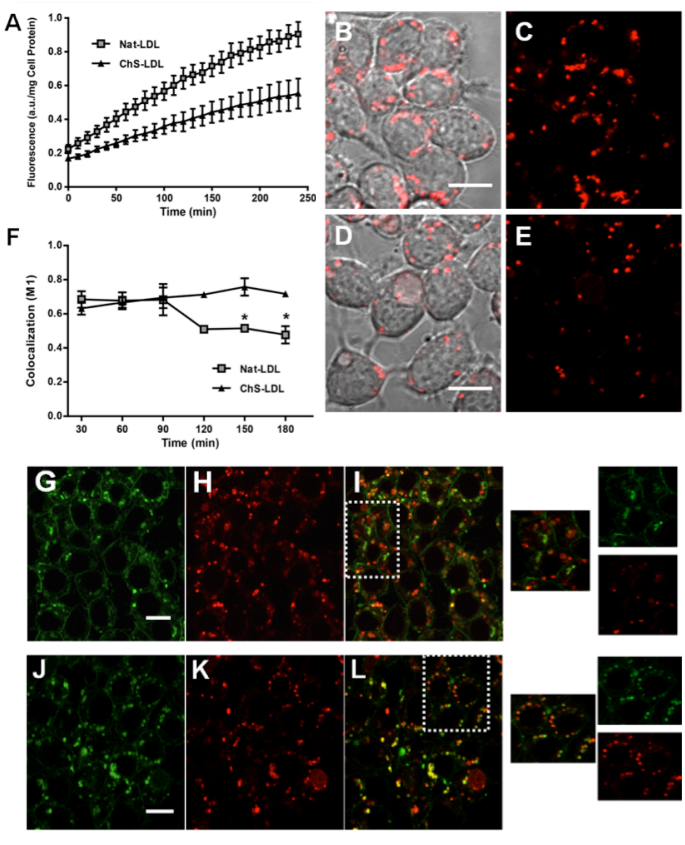

Figure 3.3 | Lysosomal cargo degradation and exit are inhibited in RAW macrophages treated with ChS-LDL.

Macrophages were treated for 20 days with 30 µM ChS-LDL or with the corresponding amount of Nat-LDL. **A.** Time-course of DQ-BSA degradation in RAW cells exposed to Nat-LDL and ChS-LDL. **B – E.** Representative fluorescence images of the results obtained in **A.** at 250 min. **B.** and **C.**, control cells; **D.** and **E.**, cells treated with ChS-LDL. **B.** and **D.** are fluorescent images showing the degraded DQ-BSA merged with the corresponding DIC images.**C.** and **E.** are fluorescence images showing the degraded DQ-BSA. Bars, 10 µm. In **F – L.,** cells were treated as before and then incubated with BODIPY-LacCer and Lysotracker red (to visualize the acidic organelles). **F.**, Overlap quantitation of BODIPY-LacCer and Lysotracker. Colocalization was calculated in a pulse chase experiments for >100 cells using the Manders (M1) coefficient from JACoP plugin (ImageJ). Data represent the Mean±SEM of three independent experiments. Statistical significance was assessed by a one-way ANOVA with a Bonferroni post-test: *, $p < 0.05$. **G – L.** Show representative fluorescence images at 180 min chase. **G – I.**, Cells treated with Nat-LDL; **J – L.** Cells treated with ChS-LDL. **G.** and **J.**, BODIPY-LacCer; **H.** and **K.**, Lysotracker; **I.** and **L.** are the corresponding merged images. Bars, 10 µm. Zoomed regions of the regions outlined in **I.** and **L.** are also shown.

To assess whether lysosomal exit capacity contributed to lysosomal enlargement in cells treated with ChS-LDL we measured the egress of Lactosylceramide (LacCer) conjugated with BODIPY towards the Golgi. Glycosphingolipids are known to be internalized by endocytosis in a clathrin-independent, caveolae-related mechanism. LacCer, which is not recycled to the plasma membrane, is transported to lysosomes and from there to the Golgi apparatus (Choudhury et al., 2002; Sharma et al., 2003). RAW cells that had been previously exposed to ChS-LDL were incubated with LacCer and their lysosomes stained with LysoTracker. The kinetics of exit of the LacCer from lysosomes towards the TGN were followed by confocal microscopy in a pulse-chase experiment (Figure 3.3F). Similarly to BSA, LacCer delivery to lysosomes did not appear to be impaired in ChS-LDL treated cells since the degree of co-localization of LacCer and Lysotracker was very similar in control and treated cells at 30 min chase (Figure 3.3F). However, with increasing time, co-localization of LacCer and lysosomes decreased in control cells but not in ChS-LDL-treated macrophages. This is clearly seen in the micrographs at 180 min chase (Figure 3.3 G-L and in the zooms of the regions outlined in panels I and L), suggesting that the LacCer exit from lysosomes was inhibited in ChS-LDL treated cells.

We, therefore, conclude that while endocytic cargo was taken up and delivered to the lysosomes at comparable rates in the control and ChS-LDL-treated cells, lysosomal degradation and cargo exit were strongly inhibited in ChS-LDL-treated cells. But why were the lysosomal proteases and cargo exit in ChS-LDL-treated cells affected? To answer this question we measured the lysosomal luminal pH and assessed whether ChS, a non-hydrolysable cholesteryl hemiester (Estronca et al., 2012), was accumulated in lysosomal membranes.

3.3.3 ChS-LDL exposure caused alteration of lysosomal pH

Lysosomal enzymes require an acidic pH to function properly. Failure to maintain a low pH within the lysosomes would inhibit the lysosomal cargo hydrolysis. We, therefore, measured the lysosomal luminal pH. Cells (Nat-LDL treated controls and ChS-LDL-treated) were incubated simultaneously with dextrans conjugated with Alexa Fluor 647 (whose fluorescence is not affected by pH in the range between 4 and 8) and with the pH-sensitive pHrodo dye (which has a pKa ≈ 6.8) (Supplementary Figure 3.2A). Like the other endocytic probes used above, the uptake of dextran, a fluid phase marker, was not affected by ChS (Supplementary Figure 3.2B). Changes in pH were measured by quantifying the ratio of emission at two different wavelengths 584 and 645 nm for pHrodo and Alexa Fluor 647, respectively. Figure 3.4A shows that the fluorescence intensity of pHrodo relative to the fluorescence intensity of Alexa fluor 647 is decreased in cells treated with ChS-LDL compared with control cells. Considering the expected ratio (for equal internalization of the two fluorescent dextrans) and the pH-titration curves for pHrodo and Alexa fluor 647 (Supplementary Figure 3.2A), a rough estimate of the lyosomal pH in ChS-treated macrophages is ≥6, a significant rise in lysosomal pH with ChS-LDL treatment. Since optimal lysosome function requires the ability to maintain an acidic pH, typically between 4.5 and 5.0 (Mindell, 2012), the inhibition of cargo degradation can be explained, at least in part, by changes in lysosome pH and subsequent impairment of lysosomal enzyme activity.

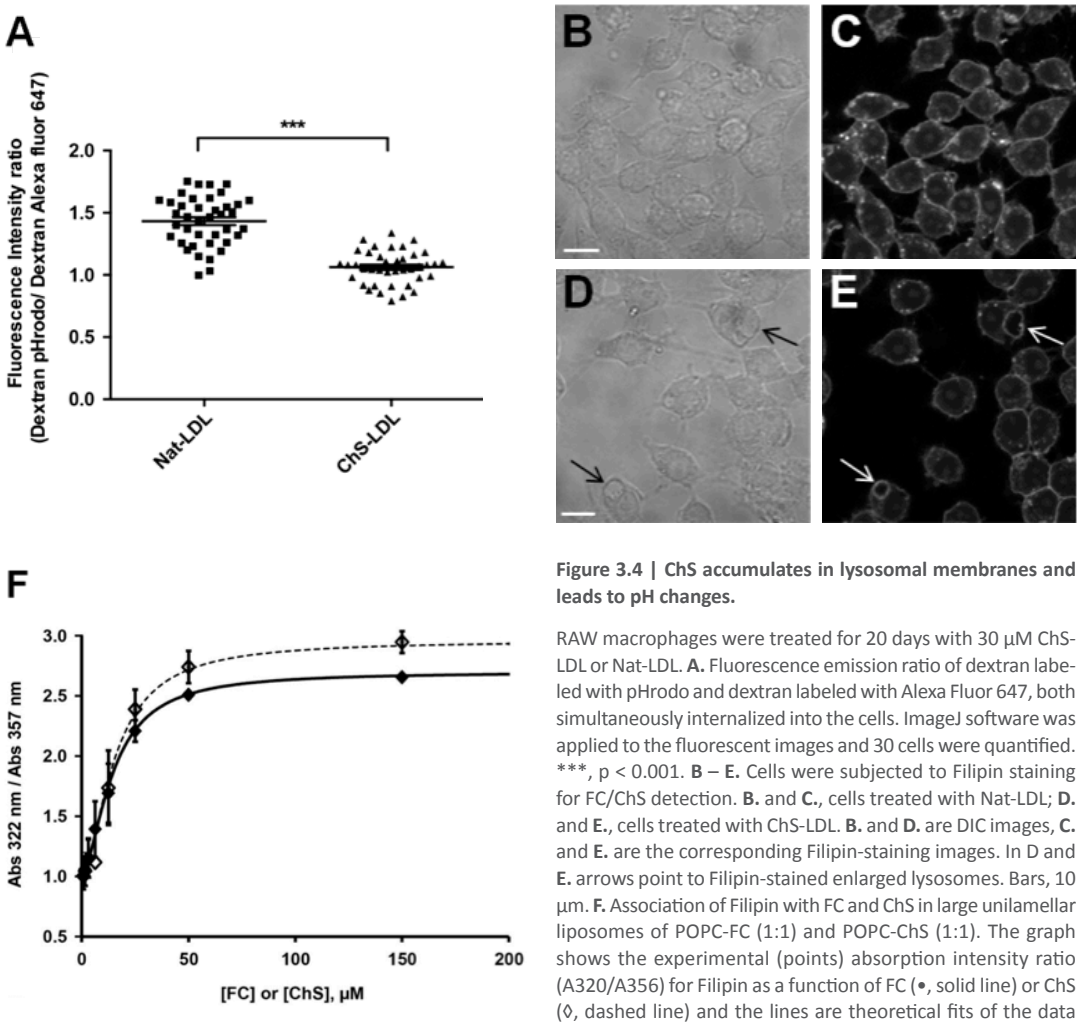

Figure 3.4 | ChS accumulates in lysosomal membranes and leads to pH changes.

RAW macrophages were treated for 20 days with 30 µM ChS-LDL or Nat-LDL. **A.** Fluorescence emission ratio of dextran labeled with pHrodo and dextran labeled with Alexa Fluor 647, both simultaneously internalized into the cells. ImageJ software was applied to the fluorescent images and 30 cells were quantified. ***, $p < 0.001$. **B – E.** Cells were subjected to Filipin staining for FC/ChS detection. **B.** and **C.**, cells treated with Nat-LDL; **D.** and **E.**, cells treated with ChS-LDL. **B.** and **D.** are DIC images, **C.** and **E.** are the corresponding Filipin-staining images. In D and **E.** arrows point to Filipin-stained enlarged lysosomes. Bars, 10 µm. **F.** Association of Filipin with FC and ChS in large unilamellar liposomes of POPC-FC (1:1) and POPC-ChS (1:1). The graph shows the experimental (points) absorption intensity ratio (A320/A356) for Filipin as a function of FC (•, solid line) or ChS (◊, dashed line) and the lines are theoretical fits of the data to the Hill equation. The apparent dissociation constant is 93 µM for the Filipin-FC complex and 97 µM for the Filipin-ChS complex, with a Hill coefficient of 1.7 in both cases.

We enquired why ChS-LDL exposure could change the lysosomal luminal pH. When RAW cells were exposed to ChS-LDL and stained with Filipin, a dye used to stain FC, the membrane of the enlarged lysosomes were stained brightly (Figure 3.4D and E), similar to the plasma membranes of the control and ChS-treated cells (Figure 3.4B-E) which are known to contain FC.

Filipin is used as a histochemical stain for FC (Norman et al., 1972) but there is no report demonstrating that this probe is also able to stain ChS. We showed in Figure 3.4F that filipin associates with FC and ChS in liposomes containing these sterols in a similar manner. The experimental data in Figure 3.4F was fitted with the Hill equation with dissociation constants for the filipin-FC and filipin-ChS complexes of 93 and 97 µM, respectively, and Hill coefficients of 1.7 for both curves. This suggests that both, the association free energy and association stoichiometry, of filipin with FC and with ChS are identical when these sterols are embedded in phosphatidylcholine bilayers. This result may appear to contradict earlier reports that filipin associates with FC but not with its esters in bilayer membranes (Norman et al., 1972; Schroeder, Holland, & Bieber, 1972). However, it is also possible that the cholesteryl esters used in the earlier work (cholesteryl palmitate and cholesteryl acetate, both neutral cholesteryl esters) were in an isotropic solution state in the bilayer midplane and not in the

anisotropic state expected for both FC and ChS when incorporated into membranes. A more detailed study of the molecular interaction and photophysics of filipin-sterol complexes in membranes may be justified in the future. Thus, the filipin staining of the membranes of enlarged lysosomes, combined with the knowledge that ChS is poorly hydrolyzed in cells (Estronca et al., 2012), suggests the presence of ChS in them. ChS-induced changes in the biophysical properties of these membranes could be responsible for the luminal pH changes which in turn inhibit cargo degradation and possibly its exit.

In light of our data demonstrating the development of lysosomal dysfunction in ChS-LDL-treated macrophages and taking into account that lysosome dysfunction has recently been proposed to result in an increased proinflammatory response (Emanuel et al., 2014) we assessed whether the ChS-LDL were also able to trigger inflammation, an important feature in atherogenesis.

3.3.4 ChS is proinflammatory

We assessed the ability of Chs-LDL exposure to induce inflammatory cytokine secretion by BMDM. Specifically, we determined the levels of IL-1β, TNFα and IL-6 produced by these cells under conditions where cell death did not occur (Figure 3.5A). Pre-incubation of BMDM with ChS-LDL for 24 h and further stimulation with LPS for another 24 h induced a 2.5-fold increase of IL-1β release compared to Nat-LDL or to untreated control cells (Figure 3.5A). A similar pattern was also observed for TNF-α and IL-6 (Figure 3.5B and 5C, respectively). Statistically different release of the three proinflammatory cytokines was always observed between the cells treated with ChS-LDL and Nat-LDL. In contrast, the effect of ChS-LDL on the secretion of the anti-inflammatory molecule IL-10 was not statistically different (Figure 3.5D). These results suggest that exposure of the BMDM to ChS-LDL was sufficient to induce an imbalance between pro- and anti-inflammatory cytokines phenocopying what happens in atheroma formation (Hansson, Libby, & Tabas, 2015; Libby & Hansson, 2015; Libby, Ridker, & Maseri, 2002).

3.3.5 *In vitro* and *in vivo* ChS effects were positively correlated

In previous work (Estronca et al., 2012) we showed that exposure of macrophages to high concentrations of ChS-LDL for short periods of time (up to 48 h) induced irreversible lipid accumulation in the lysosomal compartment (lipidosis) followed by cell death. Furthermore, these macrophages, that normally hydrolyze cholesteryl esters very efficiently, were neither able to hydrolyze cholesteryl esters nor ChS (Estronca et al., 2012). In this work we show, for the first time, that ChS at subtoxic concentrations induces lysosomal malfunction and is highly proinflammatory. To further characterize the effects of ChS-LDL *in vivo*, we decided to pursue our experiments in zebrafish larvae. This *in vivo* model has recently been shown to be suitable for studying the high-cholesterol diet-induced accumulation of lipids and myeloid cells in the circulatory vasculature walls (Fang et al., 2011; Stoletov et al., 2009).

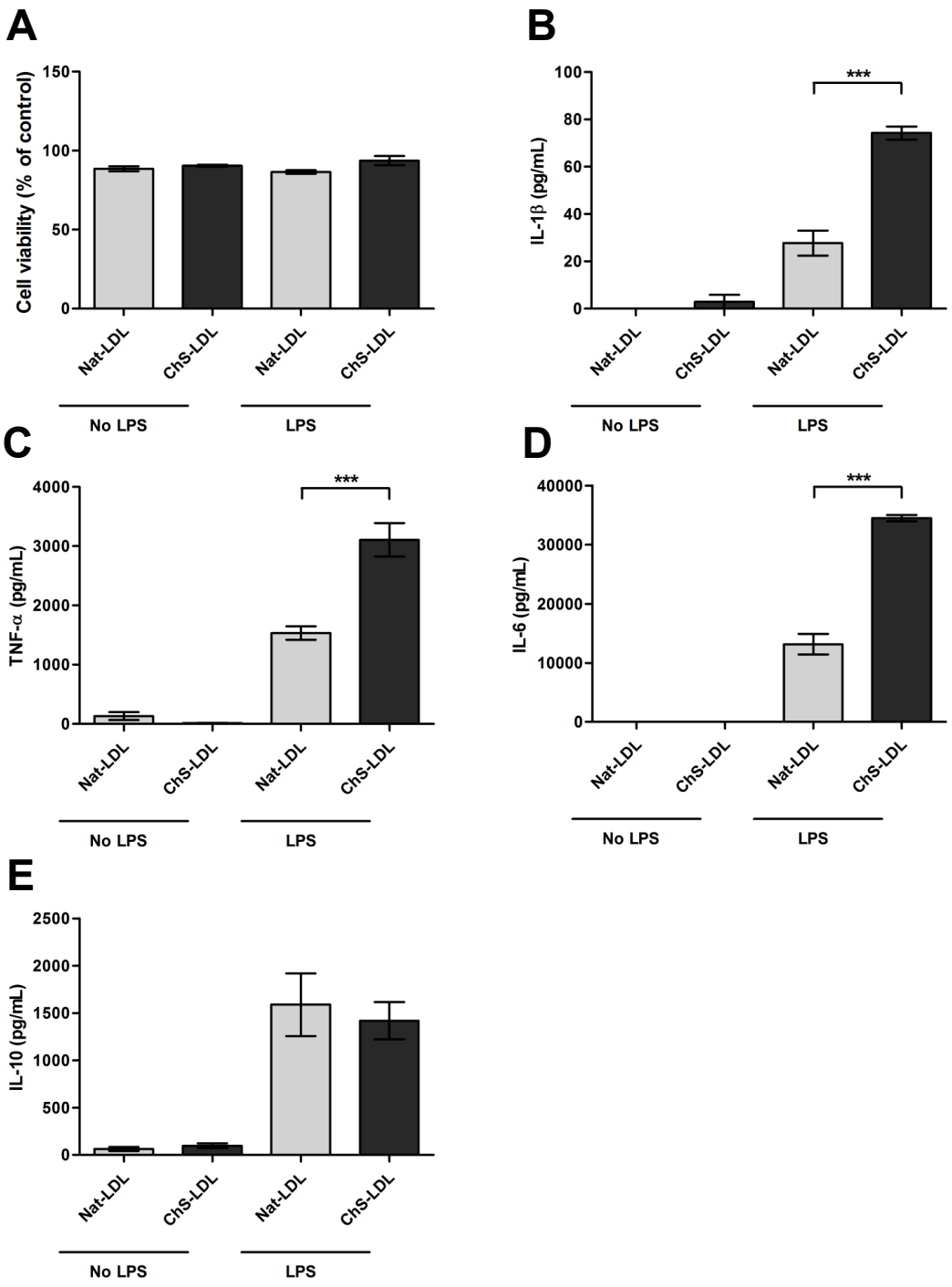

Figure 3.5 | ChS-LDL triggers release of proinflammatory cytokines.

BMDM were incubated with 200 µg/ml of ChS-LDL or with 200 µg/mL of Nat-LDL for 24 h. After supernatant collection, cells were stimulated for 3 h with 20 ng/mL of LPS or incubated with cell culture medium. In the end the supernatants were collected. Cytokine secretion was analyzed by Elisa as described in Materials and Methods. The results compare treatment with Nat-LDL and ChS-LDL for: **A.** Cell viability; **B.** IL-1β secretion; **C.** TNF-α secretion; **D.** IL-6 secretion; and **E.** IL-10 secretion by BMDM. ***, $p < 0.001$.

We started by assessing the percentage of survival of zebrafish larvae fed with a diet enriched in ChS. As controls, we used fish larvae fed with a normal diet (negative control) and a diet enriched in FC (positive control). In all cases larvae were fed for 10 days, starting at 5 days post-fertilization with the same molar concentration of ChS and FC. As shown in Figure 3.6A, both FC- and Chs-enriched diets decreased larvae survival in a dose-dependent manner; the ChS-enriched diet being significantly more lethal.

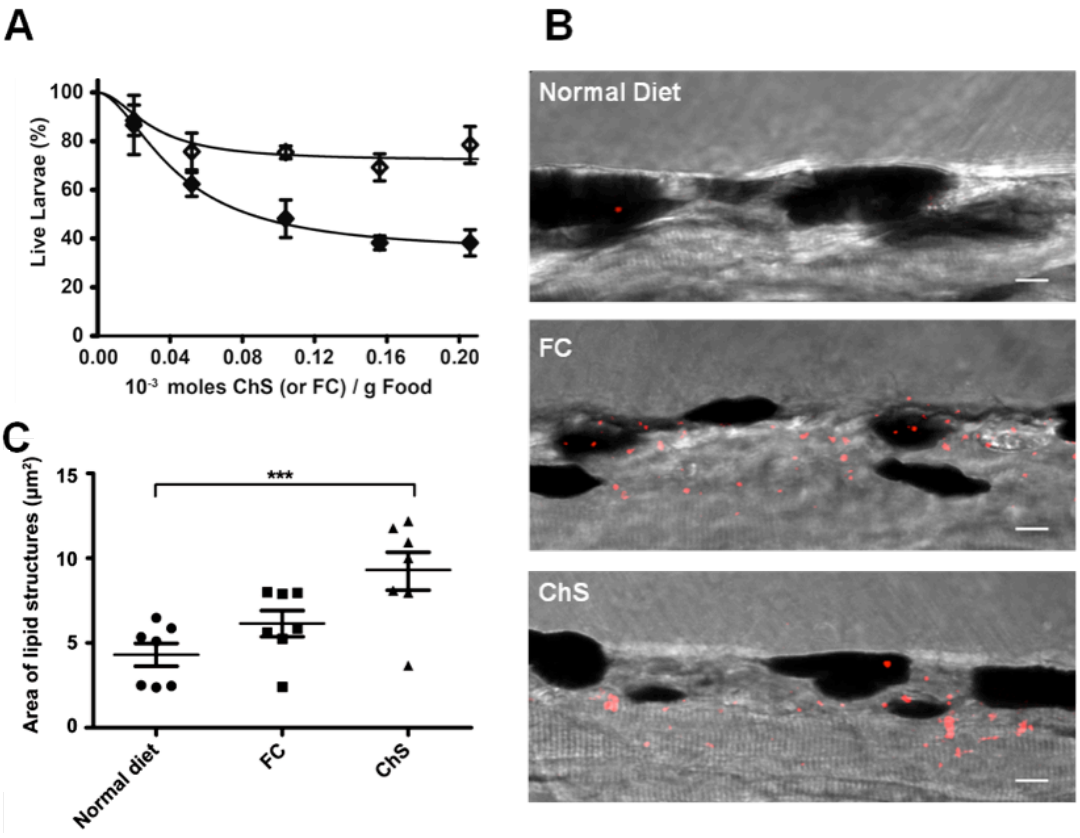

Figure 3.6 | ChS induces lipid accumulation in zebrafish larvae.

Five-day old zebrafish larvae (AB) were fed for 10 days with normal-, FC-, or ChS-enriched diets. To visualize lipid accumulation the diet was also supplemented with 10 µg/g of a red fluorescent cholesteryl ester. **A.** Larvae survival as a function of FC (◊) or ChS (◆) concentration in the diet of three independent experiments (each experiment with 35 larvae). The error bars indicate the SEM. **B.** Merge of fluorescence (lipid in red) and the corresponding DIC images of caudal vein in AB larvae fed as described above with 50 µmoles of FC or ChS/g of food. Fluorescent lipid deposits were observed only in the blood vessel wall of larvae fed with a diet enriched in FC or ChS. Scale bars, 20 µm. **C.** Graph showing the area of the lipid structures in the zebrafish caudal vein. Fluorescent images of 5-10 larvae were quantified. The horizontal lines indicate the mean values and the error bars indicate the SEM; ***, $p < 0.001$.

To assess whether ChS was able to induce lipid accumulation in the caudal vein, we used the zebrafish larvae that survived feeding with a 4% (w/w) FC-supplemented diet (described in the literature as the amount of dietary FC that is sufficient to induce lipid accumulation in the caudal vasculature (Choudhury et al., 2002)), or a 5% (w/w) ChS-supplemented diet (Note that 4% w/w FC and 5% w/w ChS correspond to the same number of moles of these compounds in the supplemented diet). The larval diet was supplemented in all cases with a trace amount of a red fluorescent cholesteryl ester. As shown in Figure 3.6B, ChS- and FC-fed larvae showed many focal areas of bright red fluorescence, which we interpreted as lipid accumulation in the vessel wall of the caudal vein. Larvae fed with a normal diet did not exhibit this behavior. The area of the bright red fluorescent structures in the vessel walls, obtained by confocal z-stacks of the AB zebrafish larvae, was quantified. The area of the lipid deposits in the caudal vein was higher in ChS- than in FC-fed larvae (Figure 3.6C). These results are well correlated with the accumulation of lipids induced by ChS-LDL in macrophages (Estronca et al., 2012).

As shown above, ChS-LDL was able to induce secretion of proinflammatory cytokines in primary macrophages. Since one of the hallmarks of inflammation in atherogenesis is the

infiltration of myeloid cells into the blood vessels, we assessed leukocyte accumulation in FC- and ChS-fed zebrafish vasculature using transgenic PU.1-EGFP zebrafish in which macrophages and granulocytes express GFP. As before, larvae were fed with normal, ChS- or FC-enriched diets for 10 days, starting at 5 days post-fertilization. Feeding with ChS and FC resulted in the recruitment of green fluorescent myeloid cells to the caudal vein (Figure 3.7), suggesting accumulation of macrophages and/or granulocytes in the vascular wall. Comparison of Figure 3.7A and 7B shows that ChS induced a higher accumulation of myeloid cells than FC in the vasculature of the transgenic zebrafish larvae. We conclude that ChS induces inflammation *in vivo*, a result that is well correlated with the *in vitro* results (Figure 3.5). Additionally, the cells that invade the vasculature are full of neutral lipids, as visualized by confocal microscopy after Oil-Red staining (Figure 3.7C).

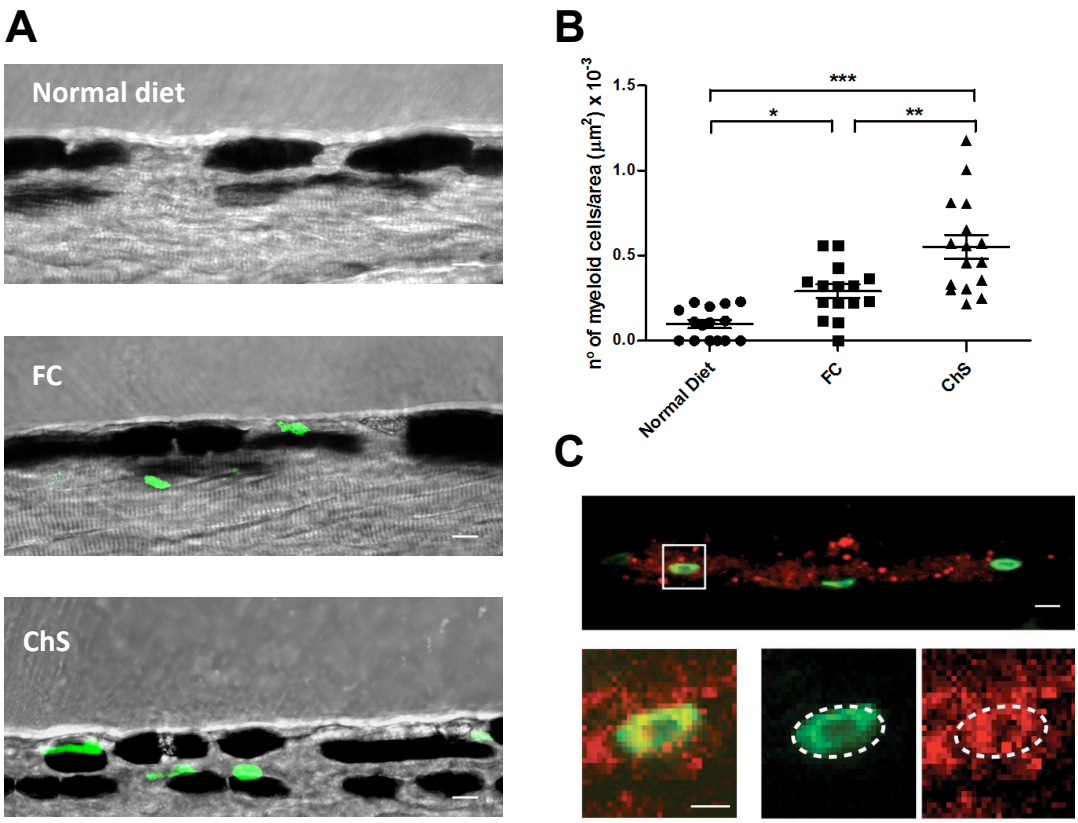

Figure 3.7 | ChS induces myeloid cell recruitment to the vasculature in zebrafish larvae.

Five-day-old *PU.1:EGFP* zebrafish larvae were fed for 10 days with normal-, FC- or ChS-enriched diet for 10 days. **A.** Merge of fluorescent and DIC images of the caudal vein of *PU.1:EGFP* zebrafish larvae. Green fluorescent myeloid cells accumulated in the blood vessel wall of larvae fed with FC or ChS and were almost absent in the blood vessel wall of larvae fed a normal diet. Scale bars, 20 µm. **B.** Quantification of the number of myeloid cells per unit area. The horizontal lines indicate the mean values and the error bars the SEM; *, $p < 0.05$. **, $p < 0.01$. ***, $p < 0.001$. **C.** *PU.1:EGFP* larvae after 10 days feeding were fixed and stained for neutral lipids with Oil-red (red fluorescence). The square in the merged image was zoomed and the green and red channels separated to show a representative myeloid cell full of neutral lipids. Scale bars, 10 µm.

3.4 DISCUSSION

Physical trapping of LDL particles in the arterial intima followed by their modification is generally understood to be the first step in atherogenesis. Inspite of much debate over the past three to four decades as to the exact nature of the modification of the trapped LDL, oxidative modification appears to command a majority consensus. Polyunsaturated fatty acids (PUFA) are among the chemical components of LDL that are most vulnerable to oxidation. In LDL particles these PUFA appear as components of phospholipids and esters of cholesterol. Oxidative scission of PUFA-cholesteryl esters leads to the formation of oxo-esters of cholesterol which have been identified in the "core aldehyde" fraction of *ex vivo* samples of human atheromata (Hutchins, Moore, & Murphy, 2011) and have long been known to be components of oxidized LDL (Kamido et al., 1995). As we have argued earlier (Estronca et al., 2012), oxo-esters of cholesterol can be expected to be further oxidized to the corresponding hemiesters of cholesterol. Indeed, these hemiesters of cholesterol are detectable in the plasma of human blood (W. Vaz, et al., unpublished results). Work from other laboratories has identified them as the components of ox-LDL that bind to the plasma protein, β2-glycoprotein-1, resulting in complexes that may be related to increased acute coronary syndrome risk (Greco et al., 2010; K Kobayashi et al., 2001; Kazuko Kobayashi et al., 2003).

In previous work (Estronca et al., 2012) we had shown that ChS loaded into native, non-oxidized LDL and presented to macrophages *in vitro* induced lipidosis in these cells, forming irreversible "foam cells", and leading to dose-dependent cell death. In the present work we have shown that long-term exposure to sub-toxic concentrations of ChS leads to lysosomal malfunction and an inflammatory response in macrophages *in vitro*. The lysosomal malfunction is characterized by an expansion of the lysosomal compartment, unaffected endocytic cargo uptake and delivery to lysosomes, and a reduction in hydrolytic capacity and exit of cargo from the lysosomes. The demonstrated accumulation of ChS in lysosomal membranes of macrophages exposed to ChS-LDL probably alters their biophysical properties and, consequently, the activity of V-H^+ATPase, the proton transporter responsible for lysosomal acidification (Cox, Lee, Dale, Calafat, & Greenberg, 2000). The resulting increase in lysosomal luminal pH leads to impairment of cargo degradation and transport across the lysosomal membrane that together culminate in the formation of large lysosomes.

Lysosomal dysfunction is also a critical step in local inflammation in the vessel wall in atherosclerosis (Moore & Tabas, 2011). The observation that ChS also triggers the production of several proinflammatory cytokines including IL-1β, TNF-α and IL-6, previously described to contribute to formation of atherosclerotic lesions (Moore & Tabas, 2011; Tedgui, 2006), correlates well with this information.

Recently, zebrafish have been proposed as an *in vivo* model for studies on atherogenesis (Fang et al., 2011; Stoletov et al., 2009). The proteins involved in the transport of dietary fat and lipids and inflammatory pathways in zebrafish are conserved relative to mammals (Progatzky et al., 2014; Stein, Caccamo, Laird, & Leptin, 2007; Van Der Vaart, Spaink, & Meijer, 2012). Many of the proatherogenic properties of ChS observed *in vitro* were also observed *in vivo* in the zebrafish model in which ChS was delivered through the diet. Dietary ChS was more toxic to the zebrafish than FC at the same molar fraction in the food. Vascular lipid deposition and myeloid cell accumulation in the caudal vein of zebrafish larvae was observed for both FC- and ChS-enriched diets but the results were significantly more pronounced for ChS- than for FC-fed larvae. Hence the *in vivo* animal model results strongly confirm the *in vitro* observations using macrophage cell cultures.

Our achievements provide an important conceptual advance vis-à-vis the existing knowledge on two of the salient features of atherosclerosis – lipidosis and inflammation. We have shown, for the first time, that a single product of the oxidation of the low density lipoproteins, ChS, is sufficient to induce both the initiation of atheroma formation (lipidosis) and exacerbate the pathology (inflammation). Simultaneously, we are providing significant new mechanistic insights, showing very clearly that lysosomal malfunction is an important step in the ChS-induced pathogenic process.

Furthermore, one of the guiding motives of our work is the conviction that identification of the chemical etiology of atherogenesis will permit induction of well-defined pathological states in appropriate *in vitro* or *in vivo* models in a controlled manner and lead to the subsequent identification of appropriate pharmacological approaches that may identify therapeutic agents.

3.5 ACKNOWLEDGMENTS/GRANTS SUPPORT

This work was supported by iNOVA4Health - UID/Multi/04462/2013, a program financially supported by Fundação para a Ciência e Tecnologia (FCT) / Ministério da Educação e Ciência, through national funds and co-funded by FEDER under the PT2020 Partnership Agreement is acknowledged.

FCT fellowship references: SFRH/BPD/26843/2006, SFRH/BD/62126/2009, SFRH/BD/90258/2012, SFRH/BD/84685/2012, SFRH/BPD/102229/2014, SFRH/BD/52293/2013

3.6 REFERENCES

Aluganti Narasimhulu, C., Fernandez-Ruiz, I., Selvarajan, K., Jiang, X., Sengupta, B., Riad, A., & Parthasarathy, S. (2016). Atherosclerosis - Do we know enough already to prevent it? Current Opinion in Pharmacology, 27, 92–102. https://doi.org/10.1016/j.coph.2016.02.006

Berliner, J. A., Leitinger, N., & Tsimikas, S. (2009). The role of oxidized phospholipids in atherosclerosis: Fig. 1. Journal of Lipid Research, 50(Supplement), S207–S212. https://doi.org/10.1194/jlr.R800074-JLR200

Brown, M. S., & Goldstein, J. L. (1983). Lipoprotein Metabolism in the Macrophage: Implications for Cholesterol Deposition in Atherosclerosis. Annual Review of Biochemistry, 52(1), 223–261. https://doi.org/10.1146/annurev.bi.52.070183.001255

Cardoso, C. M. P., Jordao, L., & Vieira, O. V. (2010). Rab10 regulates phagosome maturation and its overexpression rescues Mycobacterium-containing phagosomes maturation. Traffic, 11(2), 221–235. https://doi.org/10.1111/j.1600-0854.2009.01013.x

Choi, S. H., Harkewicz, R., Lee, J. H., Boullier, A., Almazan, F., Li, A. C., … Miller, Y. I. (2009). Lipoprotein accumulation in macrophages via toll-like receptor-4-dependent fluid phase uptake. Circulation Research, 104(12), 1355–1363. https://doi.org/10.1161/CIRCRESAHA.108.192880

Choudhury, A., Dominguez, M., Puri, V., Sharma, D. K., Narita, K., Wheatley, C. L., … Pagano, R. E. (2002). Rab proteins mediate Golgi transport of caveola-internalized glycosphingolipids and correct lipid trafficking in Niemann-Pick C cells. Journal of Clinical Investigation, 109(12), 1541–1550. https://doi.org/10.1172/JCI200215420

Cox, D., Lee, D. J., Dale, B. M., Calafat, J., & Greenberg, S. (2000). A Rab11-containing rapidly recycling compartment in macrophages that promotes phagocytosis. Proceedings of the National Academy of Sciences of the United States of America, 97(2), 680–5. https://doi.org/10.1073/pnas.97.2.680

de Duve, C. (1974). The participation of lysosomes in the transformation of smooth muscle cells to foamy cells in the aorta of cholesterol-fed rabbits. Acta Cardiologica, Suppl 20, 9–25.

Emanuel, R., Sergin, I., Bhattacharya, S., Turner, J. N., Epelman, S., Settembre, C., … Razani, B. (2014). Induction of lysosomal biogenesis in atherosclerotic macrophages can rescue lipid-induced lysosomal dysfunction and downstream sequelae. Arteriosclerosis, Thrombosis, and Vascular Biology, 34(9), 1942–1952. https://doi.org/10.1161/ATVBAHA.114.303342

Estronca, L. M. B. B., Silva, J. C. P., Sampaio, J. L., Shevchenko, A., Verkade, P., Vaz, A. D. N., … Vieira, O. V. (2012). Molecular etiology of atherogenesis - *in vitro* induction of lipidosis in macrophages with a new LDL model. PLoS ONE, 7(4). https://doi.org/10.1371/journal.pone.0034822

Fang, L., Green, S. R., Baek, J. S., Lee, S. H., Ellett, F., Deer, E., … Miller, Y. I. (2011). *In vivo* visualization and attenuation of oxidized lipid accumulation in hypercholesterolemic zebrafish. Journal of Clinical Investigation, 121(12), 4861–4869. https://doi.org/10.1172/JCI57755

Flore, V., Donfack, D., Roque, S., Trigo, G., Valere, P., Fokou, T., … Boyom, F. F. (2014). Antimycobacterial activity of selected medicinal plants extracts from Cameroon. International Journal of Biological and Chemical Sciences, 8(February), 273–288.

Greco, T. P., Conti-Kelly, A. M., Anthony, J. R., Greco, T., Doyle, R., Boisen, M., … Lopez, L. R. (2010). Oxidized-LDL/beta(2)-glycoprotein I complexes are associated with disease severity and increased risk for adverse outcomes in patients with acute coronary syndromes. Am J Clin Pathol, 133(5), 737–43. https://doi.org/10.1309/AJCP88WVRDRDFBAS

Hansson, G. K., Libby, P., & Tabas, I. (2015). Inflammation and plaque vulnerability. Journal of Internal Medicine. https://doi.org/10.1111/joim.12406

Hutchins, P. M., Moore, E. E., & Murphy, R. C. (2011a). Electrospray MS/MS reveals extensive and nonspecific oxidation of cholesterol esters in human peripheral vascular lesions. Journal of Lipid Research, 52(11), 2070–2083. https://doi.org/10.1194/jlr.M019174

Inácio, Â. S., Domingues, N. S., Nunes, A., Martins, P. T., Moreno, M. J., Estronca, L. M., … Vieira, O. V. (2016). Quaternary ammonium surfactant structure determines selective toxicity towards bacteria: Mechanisms of action and clinical implications in antibacterial prophylaxis. Journal of Antimicrobial Chemotherapy, 71(3), 641–654. https://doi.org/10.1093/jac/dkv405

Inácio, Â. S., Mesquita, K. A., Baptista, M., Ramalho-Santos, J., Vaz, W. L. C., & Vieira, O. V. (2011). *In vitro* surfactant structure-toxicity relationships: Implications for surfactant use in sexually transmitted infection prophylaxis and contraception. PLoS ONE, 6(5). https://doi.org/10.1371/journal.pone.0019850

Jerome, W. G. (2010a). Lysosomes, cholesterol and atherosclerosis. Clinical Lipidology, 5(6), 853–865. https://doi.org/10.2217/clp.10.70

Jiang, X., Yang, Z., Chandrakala, A. N., Pressley, D., & Parthasarathy, S. (2011). Oxidized low density lipoproteins-do we know enough about them? Cardiovascular Drugs and Therapy, 25(5), 367–377. https://doi.org/10.1007/s10557-011-6326-4

JW, H. (1997). Mechanisms of oxidative damage of low density lipoprotein in human atherosclerosis. Current Opinion in Lipidology, 8(5), 268–74.

Kamido, H., Kuksis, A., Marai, L., & Myher, J. J. (1995). Lipid ester-bound aldehydes among copper-catalyzed peroxidation products of human plasma lipoproteins. Journal of Lipid Research, 36(9), 1876–1886. Retrieved from http://www.ncbi.nlm.nih.gov/pubmed/8558076

Kim, S. H., Scott, S. A., Bennett, M. J., Carson, R. P., Fessel, J., Brown, H. A., & Ess, K. C. (2013). Multi-organ Abnormalities and mTORC1 Activation in Zebrafish Model of Multiple Acyl-CoA Dehydrogenase Deficiency. PLoS Genetics, 9(6). https://doi.org/10.1371/journal.pgen.1003563

Kobayashi, K., Kishi, M., Atsumi, T., Bertolaccini, M. L., Makino, H., Sakairi, N., … Matsuura, E. (2003). Circulating oxidized LDL forms complexes with beta2-glycoprotein I: implication as an atherogenic autoantigen. Journal of Lipid Research, 44, 716–26. https://doi.org/10.1194/jlr.M200329-JLR200

Kobayashi, K., Matsuura, E., Liu, Q., Furukawa, J., Kaihara, K., Inagaki, J., … Koike, T. (2001). A specific ligand for beta(2)-glycoprotein I mediates autoantibody-dependent uptake of oxidized low density lipoprotein by macrophages. Journal of Lipid Research, 42(5), 697–709. Retrieved from http://www.ncbi.nlm.nih.gov/pubmed/11352976

Libby, P., & Hansson, G. K. (2015). Inflammation and immunity in diseases of the arterial tree: Players and layers. Circulation Research. https://doi.org/10.1161/CIRCRESAHA.116.301313

Libby, P., Ridker, P. M., & Maseri, A. (2002). Inflammation and atherosclerosis. Circulation, 105(9), 1135–1143. https://doi.org/10.1161/hc0902.104353

Luu, W., Sharpe, L. J., Capell-Hattam, I., Gelissen, I. C., & Brown, A. J. (2016). Oxysterols: Old Tale, New Twists. Annual Review of Pharmacology and Toxicology, 56(1), 447–467. https://doi.org/10.1146/annurev-pharmtox-010715-103233

Mindell, J. A. (2012). Lysosomal Acidification Mechanisms. Annual Review of Physiology, 74(1), 69–86. https://doi.org/10.1146/annurev-physiol-012110-142317

Moore, K. J., & Tabas, I. (2011). Macrophages in the pathogenesis of atherosclerosis. Cell, 145(3), 341–355. https://doi.org/10.1016/j.cell.2011.04.005

Norman, A. W., Demel, R. A., de Kruyff, B., & van Deenen, L. L. (1972). Studies on the biological properties of polyene antibiotics. Evidence for the direct interaction of filipin with cholesterol. Journal of Biological Chemistry, 247(6), 1918–1929.

Peters, T. J., Müller, M., & De Duve, C. (1972). Lysosomes of the arterial wall. I. Isolation and subcellular fractionation of cells from normal rabbit aorta. The Journal of Experimental Medicine, 136(5), 1117–1139. https://doi.org/10.1084/jem.136.5.1117

Podrez, E. A., Poliakov, E., Shen, Z., Zhang, R., Deng, Y., Sun, M., … Hazen, S. L. (2002). A novel family of atherogenic oxidized phospholipids promotes macrophage foam cell formation via the scavenger receptor CD36 and is enriched in atherosclerotic lesions. Journal of Biological Chemistry, 277(41), 38517–38523. https://doi.org/10.1074/jbc.M205924200

Progatzky, F., Sangha, N. J., Yoshida, N., McBrien, M., Cheung, J., Shia, A., … Dallman, M. J. (2014). Dietary cholesterol directly induces acute inflammasome-dependent intestinal inflammation. Nature Communications, 5, 5864. https://doi.org/10.1038/ncomms6864

Salomon, R. G. (2012). Structural identification and cardiovascular activities of oxidized phospholipids. Circulation Research. https://doi.org/10.1161/CIRCRESAHA.112.275388

Schmitz, G., & Grandl, M. (2009). Endolysosomal phospholipidosis and cytosolic lipid droplet storage and release in macrophages. Biochimica et Biophysica Acta - Molecular and Cell Biology of Lipids. https://doi.org/10.1016/j.bbalip.2008.12.007

Schroeder, F., Holland, J. F., & Bieber, L. L. (1972). Fluorometric Investigations of the Interaction of Polyene Antibiotics with Sterols. Biochemistry, 11(16), 3105–3111. https://doi.org/10.1021/bi00766a026

Sharma, D. K., Choudhury, A., Singh, R. D., Wheatley, C. L., Marks, D. L., & Pagano, R. E. (2003). Glycosphingolipids internalized via caveolar-related endocytosis rapidly merge with the clathrin pathway in early endosomes and form microdomains for recycling. Journal of Biological Chemistry, 278(9), 7564–7572. https://doi.org/10.1074/jbc.M210457200

Stein, C., Caccamo, M., Laird, G., & Leptin, M. (2007). Conservation and divergence of gene families encoding components of innate immune response systems in zebrafish. Genome Biology, 8(11), R251. https://doi.org/10.1186/gb-2007-8-11-r251

Steinberg, D. (2009). The LDL modification hypothesis of atherogenesis: an update. Journal of Lipid Research, 50(Supplement),

S376–S381. https://doi.org/10.1194/jlr.R800087-JLR200

Stocker, R. (2004). Role of Oxidative Modifications in Atherosclerosis. Physiological Reviews, 84(4), 1381–1478. https://doi.org/10.1152/physrev.00047.2003

Stoletov, K., Fang, L., Choi, S. H., Hartvigsen, K., Hansen, L. F., Hall, C., … Miller, Y. I. (2009). Vascular lipid accumulation, lipoprotein oxidation, and macrophage lipid uptake in hypercholesterolemic zebrafish. Circulation Research, 104(8), 952–960. https://doi.org/10.1161/CIRCRESAHA.108.189803

Tedgui, A. (2006). Cytokines in Atherosclerosis: Pathogenic and Regulatory Pathways. Physiological Reviews, 86(2), 515–581. https://doi.org/10.1152/physrev.00024.2005

Van Der Vaart, M., Spaink, H. P., & Meijer, A. H. (2012). Pathogen recognition and activation of the innate immune response in zebrafish. Advances in Hematology. https://doi.org/10.1155/2012/159807

Vieira, O. V, Laranjinha, J. a, Madeira, V. M., & Almeida, L. M. (1996). Rapid isolation of low density lipoproteins in a concentrated fraction free from water-soluble plasma antioxidants. Journal of Lipid Research, 37(12), 2715–2721. Retrieved from http://www.ncbi.nlm.nih.gov/pubmed/9017522

3.7 SUPPLEMENTAL INFORMATION

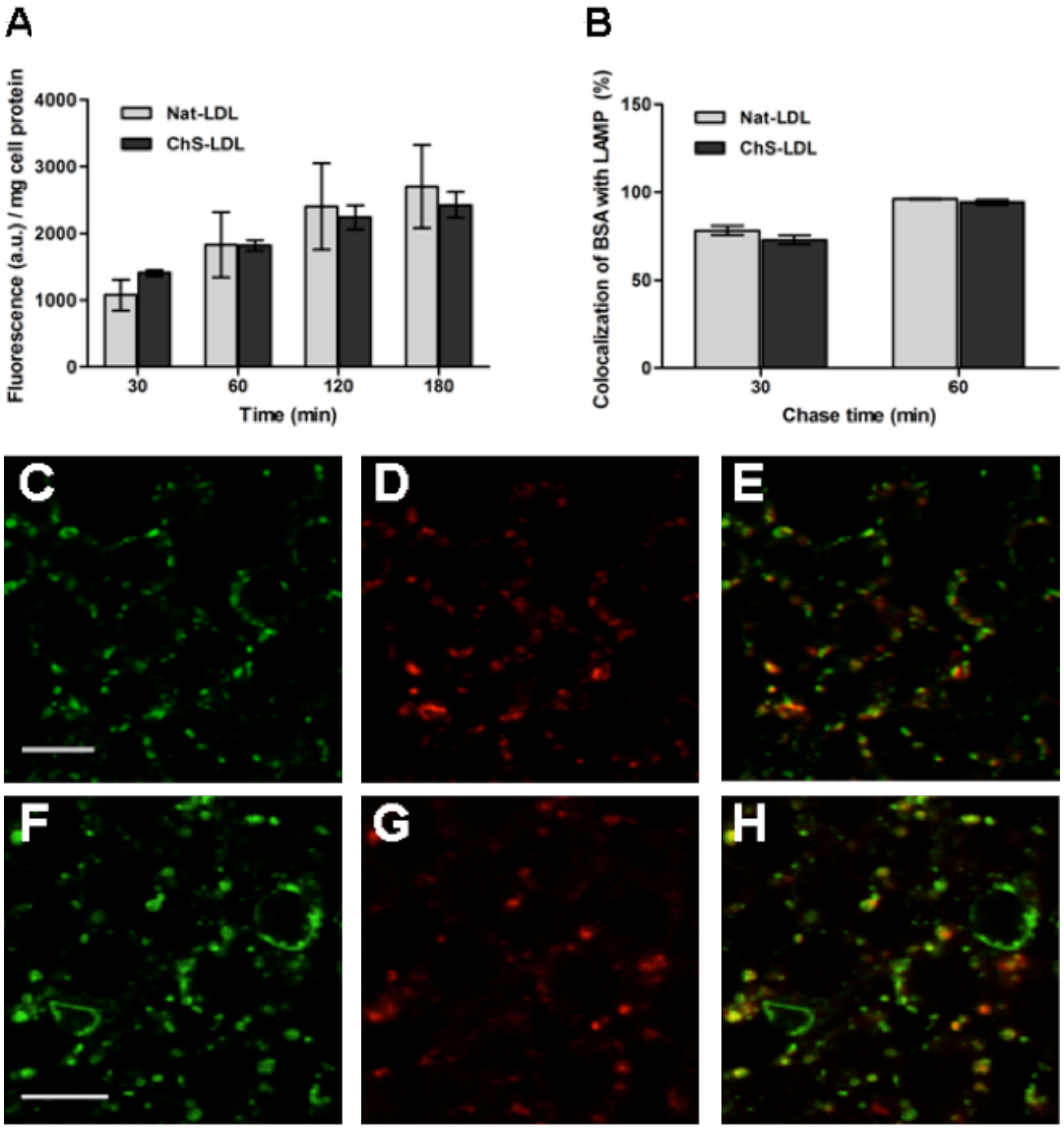

Supplementary Figure 3.1 | BSA internalization and transport to the lysosomes is not affected by ChS-LDL.

Macrophages were treated for 10 days with 30 µM ChS-LDL or Nat-LDL. **A.** BSA-Texas Red internalization for different incubation times as indicated in graph abscissa. To avoid lysosomal degradation of the internalized cargo the lysosomal pH was neutralized. **B.** Transport of BSA positive vesicles towards the lysosomes. Macrophages were incubated with BSA-Texas red for 30 min (pulse) and then chased for 30 min or 60 min. At the end of each experiment, the cells were fixed, immunostained for LAMP-2, analyzed under a confocal microscope and the degree of colocalization between BSA-containing vesicles and LAMP was quantified to obtain the cargo that had reached the lysosomes. This was done by analyzing confocal single-slice images and counting the BSA-containing vesicles that were positive and negative for LAMP. The degree of BSA-Texas Red and LAMP-2 co-localization, indicates the cargo that had reached the lysosomes. Results are means ± SEM of at least three different experiments. **C – H.**, representative fluorescence images of the results obtained in **B.** at 30 min chase time. **C – E.** Control cells. **F – H.** Cells incubated with ChS-LDL. **C.** and **F.** show LAMP-2 staining. **D.** and **G.** show BSA-Texas Red. **E.** and **H.** are the merged images.

The results depicted in this figure were obtained by treating the cells for 10 days with 16.5 µg/mL of ChS-LDL or Nat-LDL. For the endocytosis assays, cells were incubated with 400 µg/mL BSA-Texas Red for 30, 60, 120 and 180 min in medium without serum. In all cases, in order to avoid BSA degradation, NH_4Cl was added to neutralize the lysosomal pH 20 min after ini-

tiation of the incubation with cargo. After incubation, RAW cells were washed with PBS and scraped in 1 mL water. The fluorescence was analyzed in a Varian Cary Eclipse Fluorescence Spectrophotometer, with excitation at 580 nm and emission at 610 nm. The total cellular protein content was measured by BCA as described below.

To follow the intracellular transport of BSA-Texas Red to the lysosomes, cells were incubated with 400 µg/mL BSA-Texas Red for 30 min at 37°C (pulse), after which the cells were washed 3 times, to remove the non-internalized BSA, and then incubated again at 37°C for different time points (chase). Cells were then fixed for 30 min with 4% PFA, followed by immunostaining for LAMP-2. The samples were then observed under a confocal microscope for BSA-Texas Red and LAMP. The co-localization values were calculated using confocal single slices.

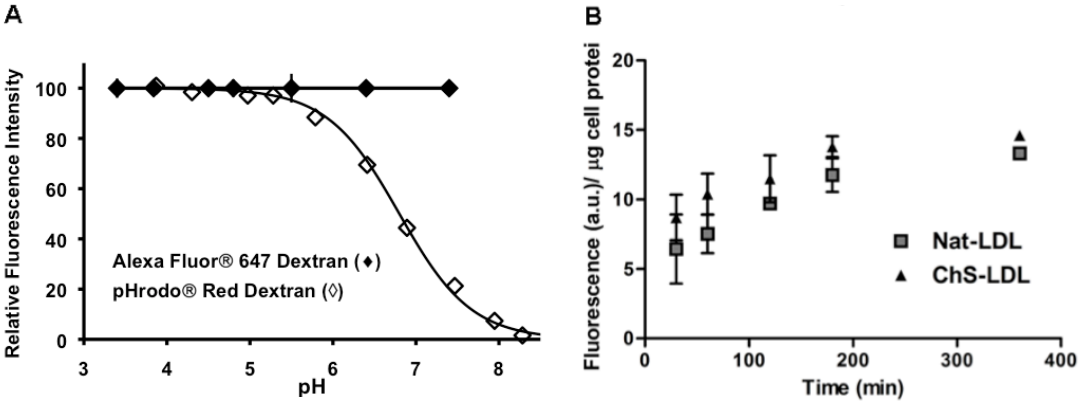

Supplementary Figure 3.2 | Effect of ChS on lysosomal pH and dextran endocytosis.

A. Fluorescence of dextran-Alexa 647 (in 0.2 M sodium acetate buffer) and dextran-pHrodo (supplier's specifications) as a function of pH. **B.** Dextran uptake in Nat-LDL and ChS-LDL-treated cells as a function of time. Results are mean±SEM of 3 independent experiments.

To assess endocytosis of dextran conjugated with tetramethylrhodamine, a fluid phase endocytic marker, this was added to RAW cells treated with Nat-LDL (control) or ChS-LDL and its uptake was measured in function of time. The protocol followed was similar to the above described with excitation at 535 nm and emission at 595 nm. The fluorescence was measured using a Zenyth 3100 microplate reader from Anthos. Protein was quantified using the BCA assay.

04 A NOVEL IMMUNOMETABOLIC PHENOTYPE IN MACROPHAGES LOADED WITH CHOLESTERYL HEMIESTERS FOUND INCREASED IN PLASMA OF ATHEROSCLEROTIC CARDIOVASCULAR PATIENTS

4.1 ABSTRACT

Atherosclerosis is a chronic inflammatory disease that progresses silently for years before becoming clinically evident. An early detection of advanced and unstable atherosclerotic plaques can diminish the human burden of atherosclerosis cardiovascular disease (ASCVD). Using a high-resolution shotgun lipidomics approach, we detected an oxidized lipid (Ox-Lp) family, cholesteryl hemiesters (ChE), which was significantly increased in the plasma of ASCVD patients. Through *in vitro* experiments with human monocytes, we showed the proatherogenic properties of the most abundant ChE detected in human plasma, ChA. Monocytes treated with ChA developed a novel activated phenotype with elevated CD206 expression, IL-1β release and reactive oxygen species (ROS) production. Differentiation of monocytes into macrophages in the presence of ChA resulted in increased HLA-DR and CD206 expression, and IL-1β, IL-6 and IL-10 production by the mature macrophage population. To further investigate the cellular effects of ChA, we used bone marrow-derived macrophages (BMDM) and describe a novel foamy macrophage phenotype. ChA-loaded BMDM revealed an unusual cytokine profile with expression and release of pro- and anti-inflammatory cytokines: IL-1β, IL-6, TNF-α and IL-10, an increase in antioxidant gene expression and the ability to proliferate. Additionally, we observed that ChA-induced IL-1β release is mediated by toll-like receptor4 (TLR4) stimulation and through induced lysosome destabilization. Finally, ChA-loaded macrophages became metabolically reprogrammed through activating the TLR4 signal transduction pathway. ChA increased lactate production in BMDM, without an increase in the glycolytic flux, enhanced glutamate secretion and mitochondrial respiration. Our data demonstrate the detection of ChA levels in human plasma can be used as an early diagnostic tool for advanced atheroma plaques in ASCVD. Furthermore, we present evidence that a novel immunometabolic activation state is induced in response to this Ox-Lp.

4.2 INTRODUCTION

Atherosclerosis is a chronic inflammatory disease of the medium and large size arteries. Fatty streaks in arterial walls gradually develop into plaque atheroma and the acute rupture of these atheromatous plaques causes local thrombosis, leading to partial or total occlusion of the affected artery (Bentzon, Otsuka, Virmani, & Falk, 2014). Despite the advances in diagnosis and treatment of atherosclerosis, cardiovascular diseases (CVDs) are the leading cause of vascular disease worldwide (Herrington, Lacey, Sherliker, Armitage, & Lewington, 2016). Atherogenesis occurs when low-density lipoprotein (LDL) infiltrates the subendothelial space of arteries becoming oxidized-LDL (ox-LDL) (Tabas, García-Cardeña, & Owens, 2015). Ox-Lp activate endothelial and vascular smooth muscle cells (SMCs) which release chemotactic

signals to attract circulating monocytes (Weber & Noels, 2011). Monocyte-to-macrophage differentiation, which can be initiated by physiological or atherogenic factors, is a pivotal process in atherogenesis (Woollard & Geissmann, 2010). However, the monocyte-differentiation signaling pathways that are activated by atherogenic factors, such as Ox-Lp, are still poorly defined. Moreover, monocyte-derived macrophages (MDM) develop into lipid-loaded foamy macrophages, due to uncontrolled ox-LDL internalization and defective hydrolysis, and adopt a proinflammatory phenotype through a mechanism that is not fully understood (Chinetti-Gbaguidi, Colin, & Staels, 2014; Cochain & Zernecke, 2017). The rise in proinflammatory mediators leads in turn to additional rounds of monocyte recruitment and accumulation of other inflammatory cells, allowing fatty streaks to increase in size and develop into plaques (Weber & Noels, 2011). In established atherosclerotic lesions, it has been reported that the macrophage population is maintained by proliferation rather than monocyte recruitment (Lhoták et al., 2016; Murphy & Tall, 2014; Robbins et al., 2013a). By suppressing this proliferative capacity of macrophages, plaque inflammation is inhibited, alleviating atherosclerosis (Tang et al., 2015). Furthermore, plaque stability determines whether atherosclerosis is clinically silent or pathogenic, since unstable plaques can rupture. Stable plaques have a protective thick fibrous cap, consisting mainly of SMCs and extracellular matrix components (Sakakura et al., 2013). However, in advanced disease, local matrix metalloprotease production augments the degradation of the fibrous cap, increasing the risk of lesion rupture and subsequent thrombosis (Moore & Tabas, 2011). In order to limit the CVD burden, novel biomarkers of plaque instability need to be identified to facilitate early detection and treatment of the disease.

Macrophages demonstrate considerable plasticity and are able to adapt their phenotype in response to their microenvironment and in agreement with their functional requirements (Mantovani, et al., 2013; Mosser, Zhang, & David M. Mosser and Xia Zhang, 2008). Historically, macrophages were defined according to their activation state for which two main groups existed: “classically activated” (M1) or “alternatively activated” (M2 macrophages) (Gordon, 2003; Gordon & Taylor, 2005; C. D. Mills, Kincaid, Alt, Heilman, & Hill, 2000). In addition to these canonical phenotypes, emerging evidence suggests that other distinct macrophage phenotypes are driven by the complex atherosclerotic microenvironment (Chinetti-Gbaguidi, Colin, & Staels, 2014; Feig et al., 2011), including the Mox phenotype, derived from macrophages exposed to 1-palmitoyl-2-arachidonoyl-sn-glycero-3-phosphorylcholine (OxPAPC) (Kadl et al., 2010). The Mox phenotype is triggered by the activation of the nuclear factor erythroid 2-related factor 2 (Nrf2), increasing the expression of antioxidant genes, such as, as hemoxygenase-1 (Hmox-1) and exhibiting reduced phagocytic and chemotactic capacities. This macrophage phenotype also presents an increase in some proinflammatory markers, including IL-1β (Kadl et al., 2011). In advanced atherosclerotic lesions of mice, Mox macrophages comprise approximately 30% of the total number of macrophages (Kadl et al., 2011).

In response to proinflammatory stimuli, macrophages undergo profound metabolic remodeling to support the biosynthetic and bioenergetic requirements of the cell (Kelly & O'Neill, 2015). Briefly, the metabolism of M1 macrophages is characterized by enhanced glycolysis, flux through the pentose phosphate pathway (PPP), fatty acid synthesis, and a truncated tricarboxylic acid (TCA) cycle, leading to accumulation of succinate and citrate. The metabolic profile of M2 macrophages is defined by oxidative phosphorylation (OXPHOS), fatty acid oxidation (FAO), decreased glycolysis and PPP flux (E. L. Mills & O'Neill, 2016). However, this is a simplistic view and recently evidence has shown that macrophage metabolism upon stimulation is more complex (Van den Bossche, O'Neill, & Menon, 2017), and, to date, is poorly characterized in atherosclerotic macrophages.

Our group has been interested in studying the atherogenic properties of ChE, which are stable end products of cholesteryl ester (CE) oxidation, and one of the major components of LDL. Using *in vitro* approaches, we showed that a single member of the ChE family was able to induce irreversible lipid accumulation, lysosomal dysfunction and increase the proinflammatory capacity of primary macrophages (Domingues et al., 2017; Estronca et al., 2012). We also reported that administration of this Ox-Lp to zebrafish increased vascular lipid accumulation, as well as, myeloid cell infiltration into the caudal vein (Domingues et al., 2017). Thus, in this work we sought to identify this class of Ox-Lp family in human plasma from patients who had suffered a cardiovascular event, comparing levels with those found in healthy subjects. After the identification of the main ChE detected in human plasma, we also aimed to clarify its effects on early stages of atherogenic events, by measuring their effects on inflammatory reprogramming of immune cells and consequent cellular function and metabolism.

Here, we demonstrated that the most abundant ChE detected in human plasma, ChA, induced activation of human monocytes following acute exposure and during the differentiation into macrophages. We also observed that ChA promotes an unusual inflammatory cytokine profile in murine BMDM, through TLR4 activation, inducing a lipid-loaded macrophage with a functional phenotype similar to previously described Mox-like phenotype. In addition, the ChA-induced macrophage phenotype showed an increase in proliferative capacity. Finally, we reveal new insights into the metabolic shift in macrophages upon Ox-Lp stimulation. ChA induced an increase in lactate and glutamate production, presenting non-activated glycolysis and activated OXPHOS. This work contributes towards the development of new strategies to diagnose advanced atherosclerotic plaques in ASCVD through the detection of ChE levels in human plasma; and to the cellular knowledge of the immunometabolic macrophages phenotype induced by ChA.

4.3 RESULTS

4.3.1 ChE are present in human blood and are raised in cardiovascular disease patients

ChE, end product of CE oxidation, were detected and quantified by shotgun lipidomics in plasma of ASCVD patients. As can be observed ChE were increased in all ASCVD pathology cohorts when compared with the control (healthy cohort) (Figure 4.1). To the best of our knowledge, this is the first time that these lipids have been detected and quantified in CVD patients and this outcome led us to explore the proatherogenic potential of this family of lipids *in vitro* and *in vivo*. Here we have decided to focus on the most abundant ChE identified in human plasma, ChA.

This results section was in collaboration with Lipotype GmbH, at Max Planck - Institute Spin-off Company, and Hospital of Santa Cruz. Thus, for now, we are not allowed to publish more detail in the results description.

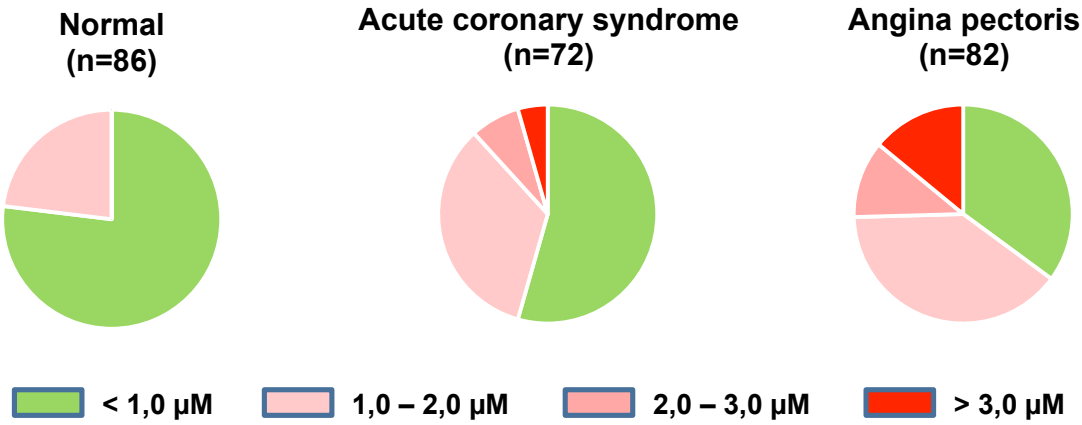

Figure 4.1 | Comparison of the blood plasma concentrations of cholesteryl hemiesters in the Normal and in Cardiovascular disease (CVD) cohorts. The results were obtained by shotgun lipidomics.

4.3.2 The surface and secretory profile of human monocytes is dynamically altered after exposure to ChA

Monocytes are heterogeneous with crucial roles in inflammation, immune defence, and homeostasis by sensing their local environment (Boyette et al., 2017; Yang, Zhang, Yu, Yang, & Wang, 2014). The role of monocytes in atherogenesis through their differentiation into macrophages which are transformed into foam cells upon lipid loading, is well established (Leitinger & Schulman, 2013; Lusis, 2000; Moore & Tabas, 2011). Despite increasing interest in monocyte subsets in recent years, adequate characterization of their role and inflammatory response in the context of atherosclerosis is lacking. Thus, we aimed to study the

effect of ChA on monocyte differentiation and polarisation. Human monocytes ($CD14^+$ cells) were incubated for 24 h with ChA, at sub-toxic doses, and specific cell surface markers were analysed by flow cytometry. After ChA pre-incubation, monocytes presented a decrease in HLA-DR expression and no major difference was observed in CD86 surface levels, both markers of classically activated monocytes (Figure 4.2A and B). Moreover, the quantification of alternatively activated surface markers CD206 and CD163 in monocytes treated with ChA revealed an increase in CD206 and a no different decrease in CD163 surface levels as compared with control cells (Figure 4.2C and D).

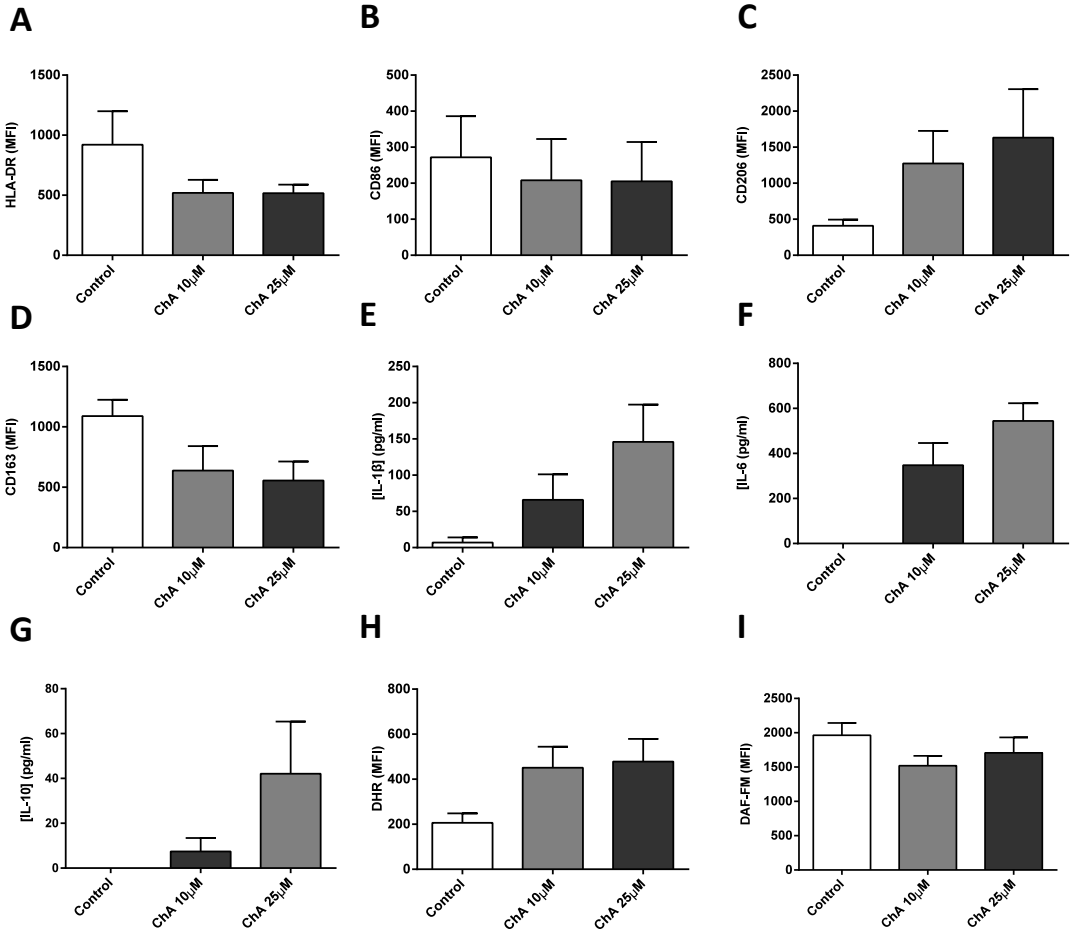

Figure 4.2 | In presence of ChA, human primary monocytes acquire a pro-inflammatory profile.

Peripheral blood was harvested from human volunteers. Mononuclear leukocytes (PBMCs) were isolated from whole blood. $CD14^+$ cells were purified from total PBMCs by FACS. $CD14^+$ monocytes were cultured in the presence of ChA (10 μM or 25 μM) or POPC (control) for 24 h. After this time period, a representative sample of monocytes from all 4 donors were stained with monoclonal antibodies to determine surface expression of HLA-DR **(A)**, CD86 **(B)**, CD206 **(C)**, CD163 **(D)**; data represent the mean fluorescence intensity (MFI) ±SEM for 4 subjects. Cell culture supernatants were analysed by ELISA for IL-1β **(E)**, IL-6 **(F)** and IL-10 release **(G)** in two of the four donors. Values represent the mean±SEM amount of cytokine released (in pg/ml) from both subjects. Further samples of monocytes were stained with DHR (**H**, n=2) and DAF-FM (**I**, n=4) probes to assess reactive oxygen species production and nitric oxide, respectively.

To further characterize the activation stage of monocytes exposed to ChA, the cytokine profile after lipid incubation was measured. Isolated monocytes were incubated for 24 h with ChA or POPC vehicle and then cytokines production was quantified. The results in Figure 4.2E-G demonstrate that ChA pre-treated monocytes showed elevated levels of IL-1β, IL-6 and IL-10 release, relative to control. ChA stimulation had no effect on TNF-α release (data not shown). Finally, the oxidative burst induced by ChA-loaded monocytes was quantified

through the measurement of dihydrorhodamine 123 (DHR) fluorescence, a ROS indicator, and 4-Amino-5-Methylamino-2',7' Difluorofluorescein Diacetate (DAF-FM), which reacts quantitatively with nitric oxide (NO). The results in Figure 4.2H and I demonstrated an increase in ROS production in ChA-treated monocytes and no difference in NO levels, compared with control cells. Together, the results showed that ChA induces alterations in the monocyte phenotype, presenting an increase in CD206 levels. These monocytes have elevated IL-1β release and ROS levels than control cells, both normally associated with a proinflammatory profile, as well as an increase in IL-6 and IL-10 production.

4.3.3 Monocyte differentiation in the presence of ChA induces an activated macrophage phenotype

Monocytes recruited to arterial intima are susceptible to several different stimuli, such as lipids, cytokines, iron and calcium, which can influence the phenotypic polarization of macrophages and their subsequent activation (Colin, Chinetti-Gbaguidi, & Staels, 2014). Therefore, we investigated whether the presence of ChA would have an impact upon the differentiation process of human monocyte-derived macrophages (MDM). For this, monocyte differentiation was induced by M-CSF in the absence (control) or presence of ChA at sub-toxic concentrations. After the differentiation period, the expression of several cell surface markers was assessed by flow cytometry. Firstly, the percentage of $CD14^{+}CD16^{+}$ double positive cells and $CD16^{+}$ surface expression after differentiation was evaluated (Figure 4.3A and B). ChA did not affect the monocyte differentiation yield, with the percentage of $CD14^{int/+}CD16^{+}$ cells similar to that in control cells (Figure 4.3A). We observed that the presence of ChA led to an increase in $CD16^{+}$ macrophages compared with control cells (Figure 4.3B). Moreover, MDM in the presence of ChA revealed an increase in median fluorescence intensity (MFI) levels of HLA-DR and no differences in the CD86 levels when compared with control cells (Figure 4.3C and D). These proteins are both surface markers of activated (M1) macrophages. In addition, alternatively activated (M2) markers analysis revealed an increase in CD206 expression in MDM differentiated with ChA and no striking differences in CD163 (Figure 4.3E and F). To detemine potential ChA-driven alterations in the inflammatory response of these macrophages, we quantified the same cytokines examined in monocytes after MDM differentiation. MDM in the presence of ChA demonstrate an increase in IL-1β, IL-6 and IL-10 release (Figure 4.3G-I). TNF-α was also measured, but was not detected (data not shown). Moreover, no differences between the different differentiation conditions were observed when comparing the MFI of DHR dye used for ROS detection in MDM (Figure 4.3J and K). These results indicate that the differentiation of monocytes in the presence of ChA programmed a distinct transcriptional phenotype in the resulting macrophages, which included release of both pro- and anti-inflammatory cytokines.

4.3.4 ChA-stimulated BMDM secrete pro- and anti-inflammatory cytokines

Macrophage polarization produces a diverse spectrum of phenotypes in response to a broad range of stimuli (Chinetti-Gbaguidi et al., 2014; Murray et al., 2014; Xue et al., 2014). To further

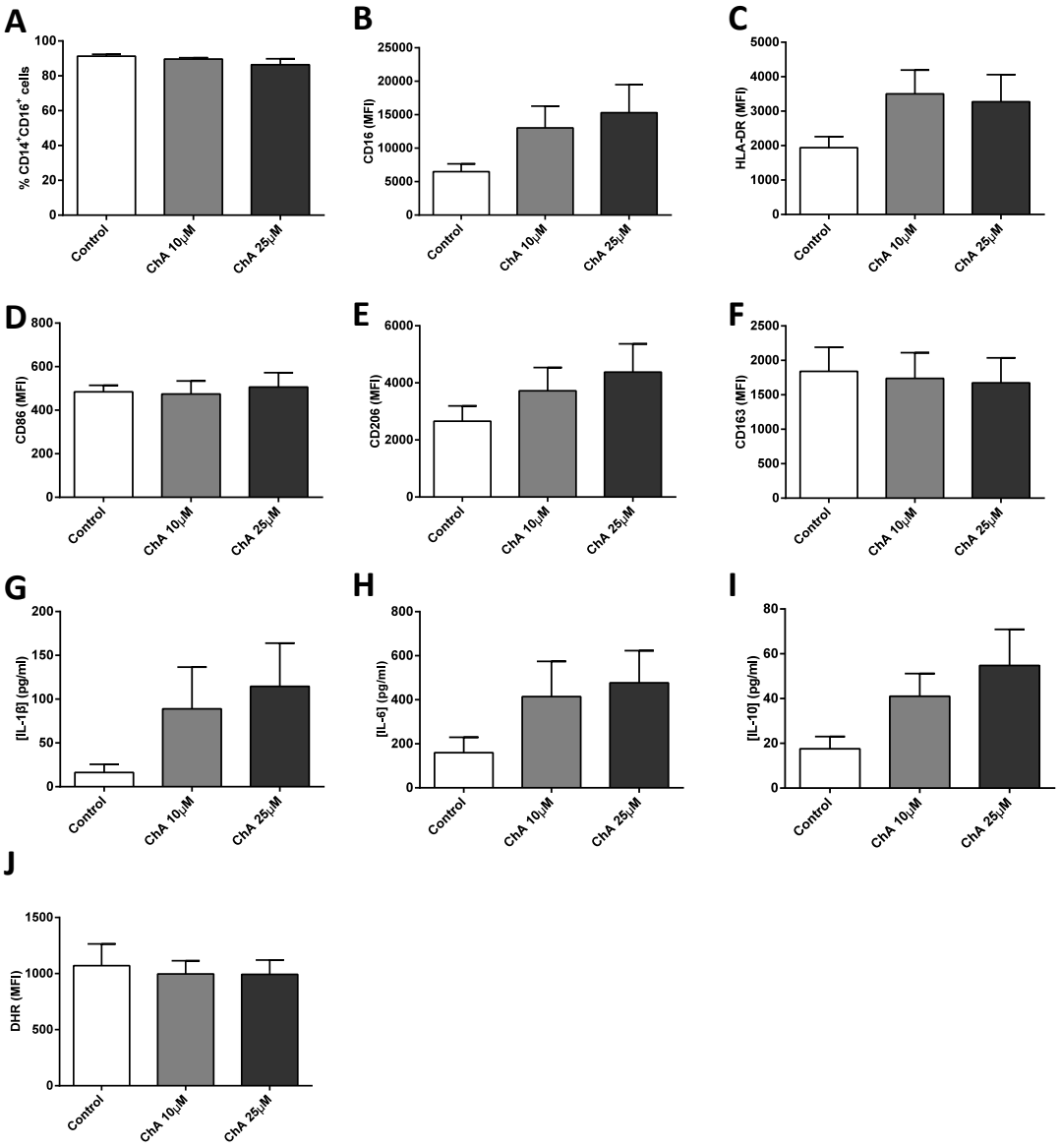

Figure 4.3 | In human primary macrophages ChA triggers pro-inflammatory cytokines secretion.

PBMCs were isolated from whole blood from human volunteers (n=4). $CD14^+$ monocytes were purified from total PBMCs by FACS, and differentiated using rM-CSF alone or in the presence of ChA (10 μM or 25 μM) or POPC for 7 days. On day 3 of 7, fresh media containing rM-CSF was added to all cultures. After 7 days, representative samples of differentiated macrophages were stained with monoclonal antibodies to determine purity (CD14+ CD16+ , A) and surface expression of CD16 **(B)**, HLA-DR **(C)**, CD86 **(D)**, CD206 **(E)**, CD163 **(F)**. Data represent the mean fluorescence intensity (MFI) ±SEM for 4 subjects. Cell culture supernatants were analyzed by ELISA for IL-1β, IL-6 and IL-10 release **(C)**. Data represent the mean amount of cytokine released (in pg/ml) for 4 subjects. Further samples of macrophages were stained with DHR probe, to assess reactive oxygen species production **(J)**. Data represent MFI for 4 subjects.

assess the effects of ChA on *in vitro* macrophages, we used primary mouse BMDM that had been fully differentiated in the presence of L929-cell conditioned medium (LCCM) for 7 days. Macrophage treatment with concentrations up to 500 μM ChA did not induce apoptotic nor necrotic cell death (Supplementary Figure 4.1). To characterize the imprinted ChA-induced phenotype, primary mouse BMDMs were cultured in the presence of ChA for 4h or 24h to quantify mRNA expression and cytokine release, respectively. ChA treatment led to a concentration-dependent increase in the gene transcription of IL-1β, TNF-α, IL-6, IL-1α and IL-10 cytokines (Figure 4.4A-C and G-H). Cytokine release was determined by ELISA and confirmed the distinct inflammatory nature of these ChA-loaded cells, being observed an increasing in the IL-1β, TNF-α, IL-6, IL-1α and IL-10 release (Figure 4.4D-F and K). Moreover, ChA also induced a small increase in NO production in macrophages (Figure 4.4I).

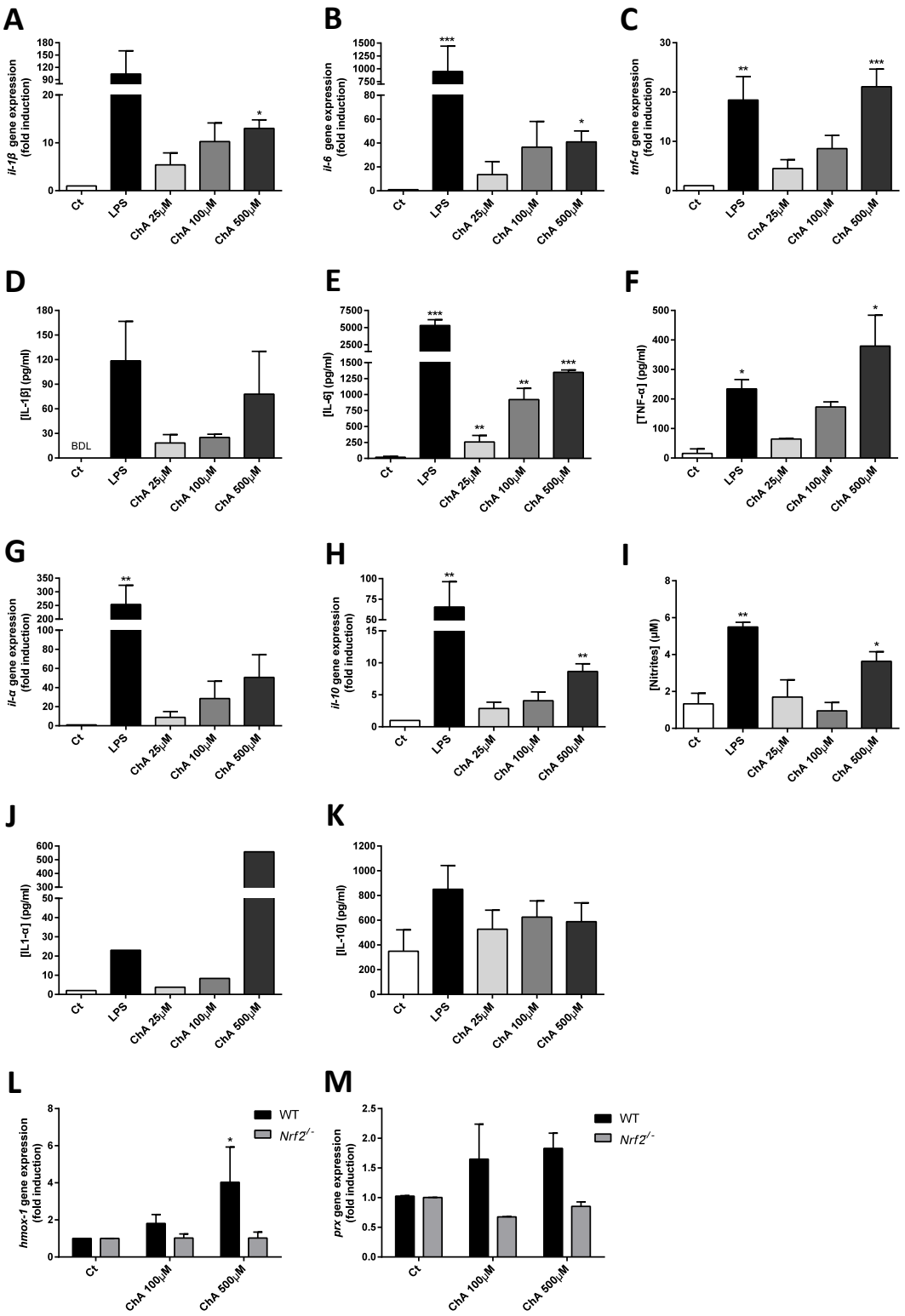

Figure 4.4 | ChA induces a novel cytokine phenotype in BMDM, increasing the expression of redox-regulating genes via the Nrf-2 pathway (preliminary results)

A-K. In BMDM stimulated with ChA, a novel expression profile of both pro- and anti-inflammatory cytokines was observed. Cells were either unstimulated or stimulated with LPS (250 ng/mL or 50ng/mL) or ChA (25, 100, 500 μM) for 4 h or 24 h for mRNA quantification or cytokine secretion, respectively. After 4 h, RNA was isolated and analyzed by qPCR for IL-1β **(A)**, IL-6 **(B)**, TNF-α **(C)**, IL-1α **(G)** and IL-10 **(H)** expression. Data represents the mean±SEM of three independent experiments. In addition, cell culture supernatants were analyzed by ELISA for IL-1β **(D)**, IL-1α **(E)** and IL-10 **(F)** release and using an antibody cytokine array for TNF-α **(B)** and IL-6 **(C)** release. Data represent the mean±SEM of two (TNF-α, IL-1α, IL-6, IL-10, IL-4) or three (IL-1β) independent experiments. **I.** Macrophages loaded with ChA present a increase in nitrites oxide (NO) production. After 24h of cell treatment, the supernatants were assessed for the production of nitrites using the Griess assay. Data represent the mean±SEM of three independent experiments. **L** and **M.** ChA induces the expression of two redox-regulating genes, hemoxigenase-1 (Hmox-1) and peroxiredoxin-1 (Prx), in BMDM via Nrf2 signaling. Concurrent cultures of wild-type C57/BL6 and Nrf2$^{-/-}$ BMDMs were plated. Both groups were either unstimulated or stimulated with ChA (250 μM or 500 μM) for 72 h. RNA was subsequently isolated and analyzed by qPCR for Hmox-1 and Prx expression. Data represent the mean±SEM of two independent experiments.

Macrophage treatment with OxPAPC induces a specific macrophage phenotype – Mox phenotype, which it is characterized by the increase in anti-oxidant related genes via Nrf2 (Kadl et al., 2010). Thus, to further investigate the ChA-induced macrophage phenotype, the mRNA expression of Hmox-1 was quantified over time. Hmox-1 gene expression was increased after a short exposure to ChA (a 4 h incubation increased expression (data not shown)), which was sustained up to 72 h post-stimulation (Figure 4.4L). The mRNA expression of an additional redox-regulating gene, peroxiredoxin-1 (Prx) (Figure 4.4M) was also quantified after 72 h of ChA incubation. As both of these redox-regulating genes are controlled by the Nrf2 pathway (Gorrini et al., 2013), we investigated whether their expression was under its control. In *Nrf2*$^{-/-}$ macrophages, a reduction in Hmox-1 and Prx mRNA expression was observed in ChA-stimulated macrophages (Figure 4.4L and M). Thus, in ChA-activated BMDM a distinctive transcriptional phenotype is apparent.

4.3.5 ChA-induced IL-1β release is via TLR4 stimulation and dependent on signals conferred by destabilized lysosomes

IL-1β has been extensively studied in atherosclerosis pathology because of its early identification of its proinflammatory properties, being targeted in a large clinical trial on coronary artery diseases (Ridker et al., 2017). Ox-LDL and Ox-Lp can activate TLR4, stimulating an inflammatory response (Choi et al., 2009; Choi, Sviridov, & Miller, 2017). We therefore sought to evaluate whether TLR4 has a role in ChA-induced IL-1β release. BMDM from *tlr4*$^{-/-}$ mice were loaded with ChA and IL-1β gene expression and release were quantified. In Figure 4.5A and B, in *tlr4*$^{-/-}$ macrophages IL-1β mRNA expression and release were abrogated, compared with wild-type (WT) cells. These results showed that ChA-induced IL-1β release is mediated by TLR4 ligation at the cell surface.

In atherosclerosis, cholesterol crystals form in foam cells and can activate the PYD domain-containing protein 3 (NLRP3) inflammasome, leading to IL 1β release (Duewell et al., 2010; Emanuel et al., 2014; Rajaṁaki et al., 2010). We therefore explored the effect of ChA on NLRP3 activation and subsequent IL-1β release by using AcYVAD-AOM, an inhibitor of caspase-1, an inflammasome component, and by specific NLRP3 inhibition using MCC950. Results demonstrated that IL-1β release in ChA-loaded macrophages was diminished by caspase-1 inhibition, as well as when NLRP3 is inhibited (Figure 4.5C). Thus, the results demonstrated that IL-1β is released via NLRP3 activation. Moreover, IL-1β release is a tightly regulated process, requiring two signals to produce and release bioactive mature cytokines. The first signal primes cells to express cytokine and inflammasome component, with the second signal, such as mitochondrial ROS, cathepsin B release from dysfunctional lysosomes and endoplasmic reticulum (ER) stress, required to activate inflammasome assembly, leading to maturation and release of IL-1β. Since ChA is sufficient to induce IL-1β release, we investigated the origin of ChA-induced signal 2. We verified that macrophages incubated with ChA have an increase in mitochondrial ROS production (Figure 4.5D) with an increased mitochondrial potential (Figure 4.5E). In addition, through immunofluorescence, enlarged

lysosomes was observed (Figure 4.5F). Thus, to identify the origin of the ChA-induced signal 2 required for IL-1β release, we used a specific cathepsin B inhibitor (ZRLR), an ER stress inhibitor (4-PBA) and the ROS scavenger N-acetyl-L-cysteine (NAC), which was efficient in the reduction of ROS production induced by ChA (Figure 4.5D). In Figure 4.5G, the results revealed that the higher suppression of ChA-induced IL-1β secretion was obtained when cathepsin B was inhibited. This finding suggested that the main contributor for the signal 2 necessary for IL-1β secretion was the enlarged lysosomes. Together, these results suggested that ChA provided both signals required for NLRP3 activation by priming the cells via TLR4 (signal 1), and through lysosomal destabilization (signal 2), which activated caspase-1 and consequently induced IL-1β maturation and release.

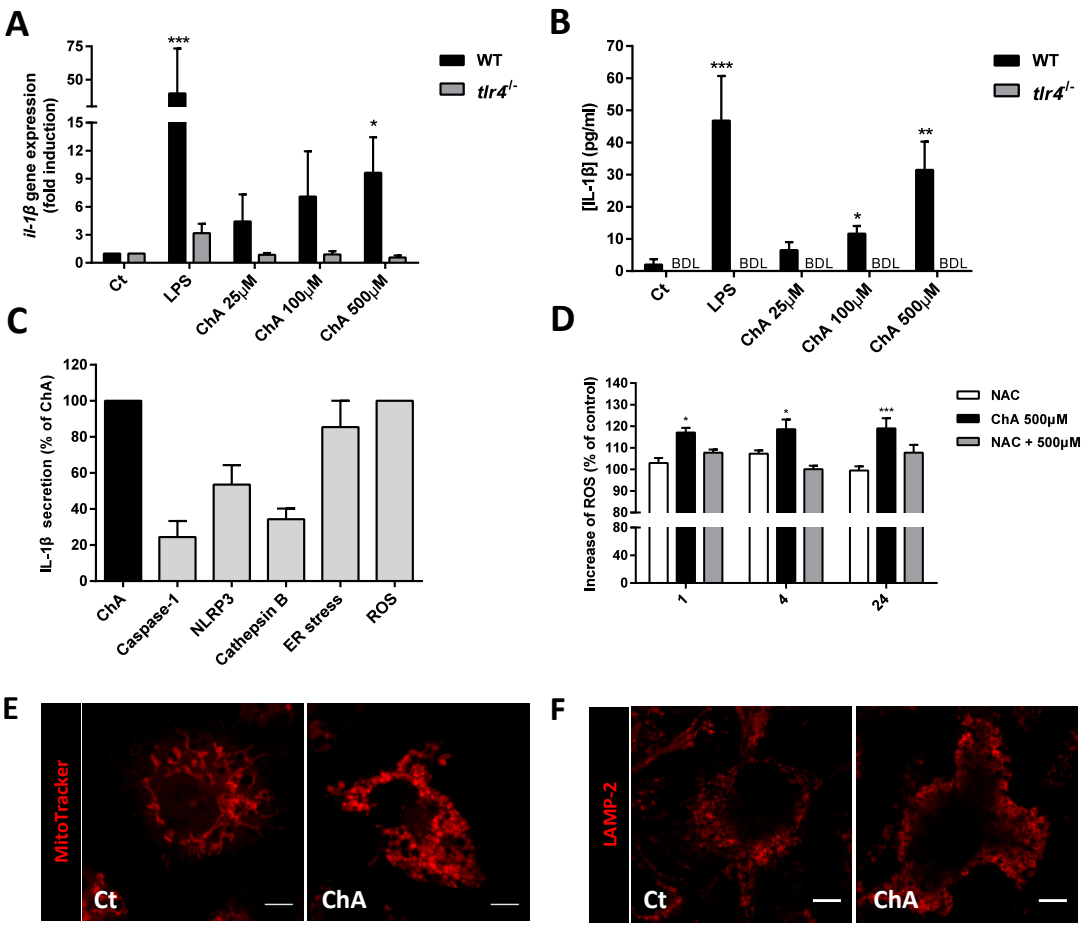

Figure 4.5 | ChA is recognized by TLR4 and induces IL-1β secretion via caspase-1 inflammasome and lysosomal destabilization (preliminary results).

A. Measurement of IL-1β mRNA expression in Wild-type C57/BL6 (WT) and *tlr4*$^{-/-}$ mouse BMDM by qPCR. Both cultures were stimulated with LPS (250 ng/mL) or ChA (25, 100, 500 µM) for 4 h. **B.** Quantification of IL-1β secretion by ELISA in the supernatants of WT and *tlr4*$^{-/-}$ BMDM incubated for 24 h with LPS or ChA (25, 100, 500 µM). Data represent the mean±SEM of three independent experiments. **C.** Lysosome dysfunction promote NLRP3-dependent IL-1β release in ChA-stimulated BMDM. WT BMDM cultures were pre-incubated for at least 1 h in the presence of specific inhibitors of: caspase-1 (Ac-YVAD-AOM), NLRP3 (CRID-3), Cathepsin B (ZRLR), ER stress (4-PBA) and ROS (N-acetyl-L cystein (NAC)) or a media only control. Cells pre-incubated with an inhibitor were stimulated with 500 µM ChA for 24 h. Cell culture supernatants were analyzed by ELISA for IL-1β release. Raw values for cytokine release (in pg/mL) were converted into a % inhibition of release compared with the value for ChA alone. Data represent the mean±SEM of two independent experiments. **D.** ChA induces an increase in ROS production, inhibited by N-acetyl-L-cysteine (NAC). BMDM were exposured to ChA for different incubation times with or without NAC, a ROS scavanger. ROS production was assessed by MitoSOX staining. Data represent the mean±SEM of six independent experiments. **E.** Confocal mitochondrial imaging of BMDM incubated with or without ChA. ChA induces a increased in mitochondrial potential evaluated by MitoTracker Red CMXRos, which the accumulation is dependent upon membrane potential. Scale bar 5µm. **F.** ChA induces lysosomal enlargement. Lysosomal were imaged by confocal microscopy through LAMP-2 immunostaining. Scale bar 5 µm.

4.3.6 In ChA-derived foam cells phagocytosis is impaired

The presence of lipid-laden foam cells in atheroma is one of the first well characterized and pivotal features in the pathogenesis of atherosclerosis (de Duve, 1974; Libby, 2012; Moore & Tabas, 2011). One of the fundamental steps in foam cell formation is the rate of CE hydrolysis and cholesterol re-esterification for lipid droplet storage. Therefore, we aimed to evaluate the ChA ability in foam cells induction. To test the effect of ChA on macrophage foam cell formation, BMDM were incubated for 72 h with and without ChA, using cells treated with the POPC vehicle as control. Neutral lipid accumulation was firstly evaluated by BODIPY 493/503 staining. We found that primary macrophages loaded with ChA presented an overall increase in lipidic structures (Figure 4.6A) and no lipid deposits were observed in control macrophages. Therefore, using transmission electron microscopy (TEM), we further examined the profiles of lipid accumulation in macrophages in culture treated with ChA or vehicle (Figure 4.6B). The electron micrographs confirmed the foamy appearance of ChA-laden macrophages, a morphology that was derived from cytoplasmic lipid droplets, round non-dense structures. However, single membrane-bound not dense structures were also observed, which featured the morphology of lipid accumulation in lysosomes. This results still need to be confirmed by immune Immuno-gold EM data.

To further characterize the potential atherogenic effect of ChA, the biological function of these foam cells was evaluated. Since macrophages are professional phagocytes, we started by assessing the phagocytotic capacity of the macrophage after ChA treatment through engulfment assays conducted using either labeled IgG-opsonized latex beads or aged RBCs, an apoptotic cell model. The results in Figure 4.6C and D showed a decrease in bead internalization capacity and a complete abrogation of apoptotic cell engulfment when macrophages were treated with ChA, compared with control cells (Figure 4.6E and F). We then questioned if this decrease in phagocytic capacity was associated with actin cytoskeletal effects induced by ChA. Indeed, macrophages treated with ChA present actin disorganization compared with control macrophages (Figure 4.6G). In control cells, actin filaments are elongated, whereas in ChA-treated macrophages there is actin disorganization, with a puncta appearance. This effect on the actin cytoskeleton can be responsible for the defective engulfment observed in ChA-loaded macrophages.

Stimulated macrophages can secrete multiple cytokines and chemokines that generate a cascade of events in adjacent cells including, for instance, smooth muscle cells (SMCs). To evaluate the chemoattractant properties of ChA-loaded macrophages on SMCs, conditioned media from macrophages was used to examine the effect on SMC migration, using a wound-healing assay (Figure 4.6H). The results revealed a dose-dependent decrease in SMC migration when exposed to conditioned media from ChA-treated macrophages. Thus, we demonstrated that ChA-laden macrophages present features of atherogenic foam cells, followed by a loss of macrophage function.

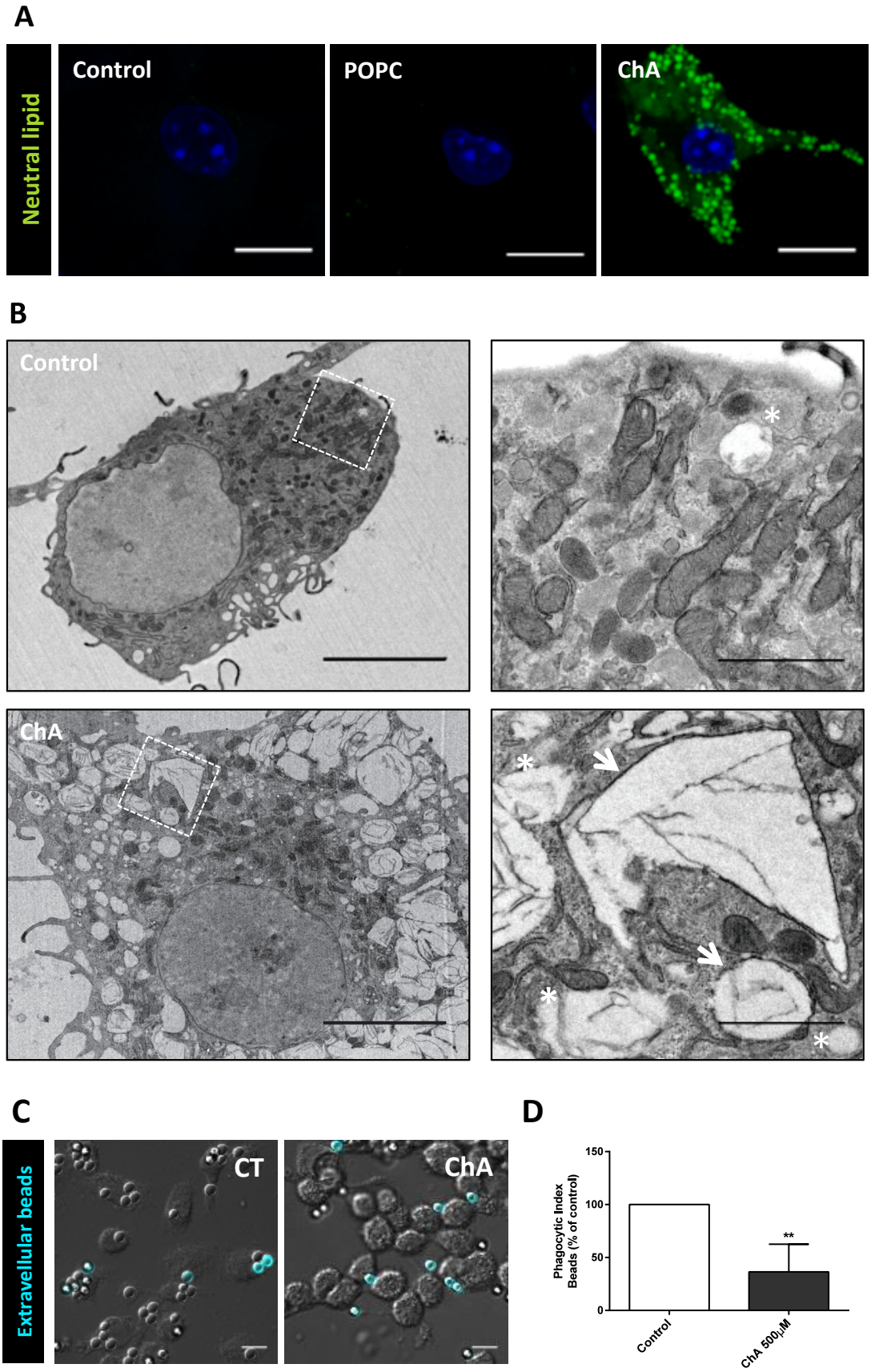

Figure 6 (continued)

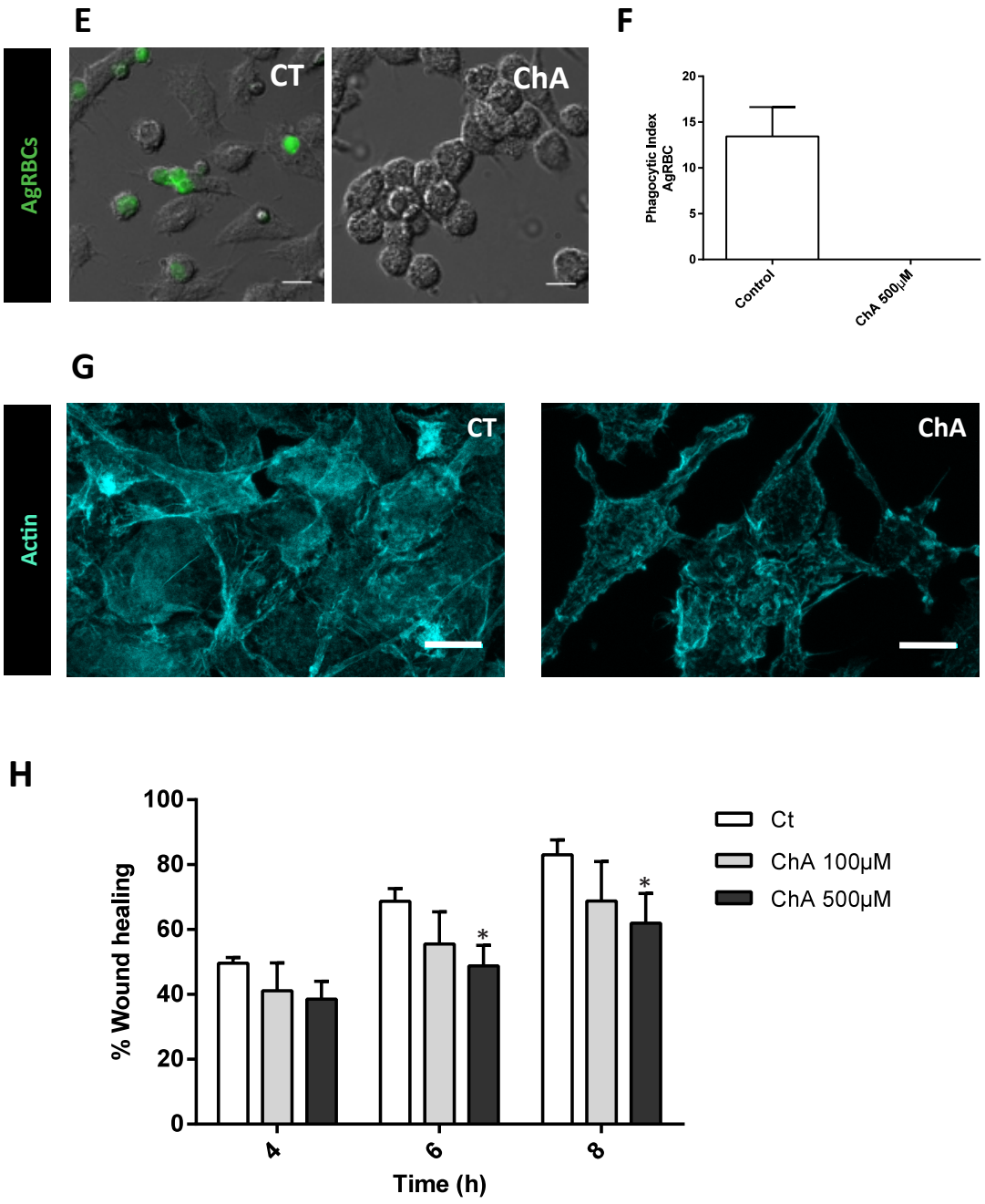

Figure 4.6 | ChA dynamically alters macrophage morphology and function.

A-B. ChA induced a foamy feature in macrophages. BMDMs were incubated during 72 h with vehicle (control) and ChA and then stained with BODIPY 493/503 to visualized neutral lipids **(A).** Cells were imaged using confocal microscopy. Bars, 10 µm; Representative transmission electron micrographs of BMDM incubated with vehicle and ChA for 72 h **(B)**. Bars, 5 µm and 1 µm in the zoomed images. **C-F.** Diminishment of macrophages phagocytic capacity after ChA treatment. **C.** After 72 h of incubation with or without ChA, primary macrophages were loaded with IgG opsonized latex beads during 15 min and the non-phagocytosed beads were stained using antibodies and excluded from the calculations (cyan labeled beads). **D.** Quantification of phagocytic index after cells ingest IgG-opsonized latex bead. Data shows the phagocytic index as percentage to control cells and are means±SEM of three independent experiments (at least 200 cells for each condition); Treated macrophages were pulsed with aged red blood cells (AgRBCs, green) during 15 min **(E)**. Non-internalized cells were lysed; **F.** Quantification of phagocytic index. Data shows the phagocytic index as means±SEM of three independent experiments (at least 200 cells for each condition); **G.** Cells were ChA treated and stained with phalloidin (cyan) for actin label. Cells were imaged using confocal microscopy; **H.** Quantification of smooth muscle cell migration after incubation with supernatants from primary macrophages treated 24 h with ChA; Bars, 10 µm. ***, p<0.001; **, p<0.01; *, p<0.05.

4.3.7 Macrophages proliferate in response to ChA

It has already been reported that atherosclerotic plaque macrophages have the capacity to proliferate, being responsible for the maintenance of macrophage population in advanced

lesions (Lhoták et al., 2016; Robbins et al., 2013b; Tang et al., 2015). However, the specific molecular component of ox-LDL behind the proliferative capacity of macrophages has not yet been identified. Incubation of primary macrophages with ChA for 72 h induced a dose-dependent increase in the MTT signal (Figure 4.7A), suggesting an increase in cell viability. To confirm this result, after treatment, total cell number was measured and we also found an increased in cell numbers in ChA-treated macrophages (Figure 4.7B). To verify if the increase in cell number was a result of proliferation rather than an inhibition of macrophage apoptosis, Ki67 levels were assessed. Ki67 protein is strictly associated with cell proliferation (Scholzen & Gerdes, 2000). The results showed that macrophages incubated with ChA present elevated Ki67 mRNA levels from 24-72 h post-stimulation (Figure 4.7C). To validate this result, the percentage of Ki67 positive cells was also assessed. The results showed that ChA induced an increase in the levels of Ki67 positive cells (Figure 4.7D and E).

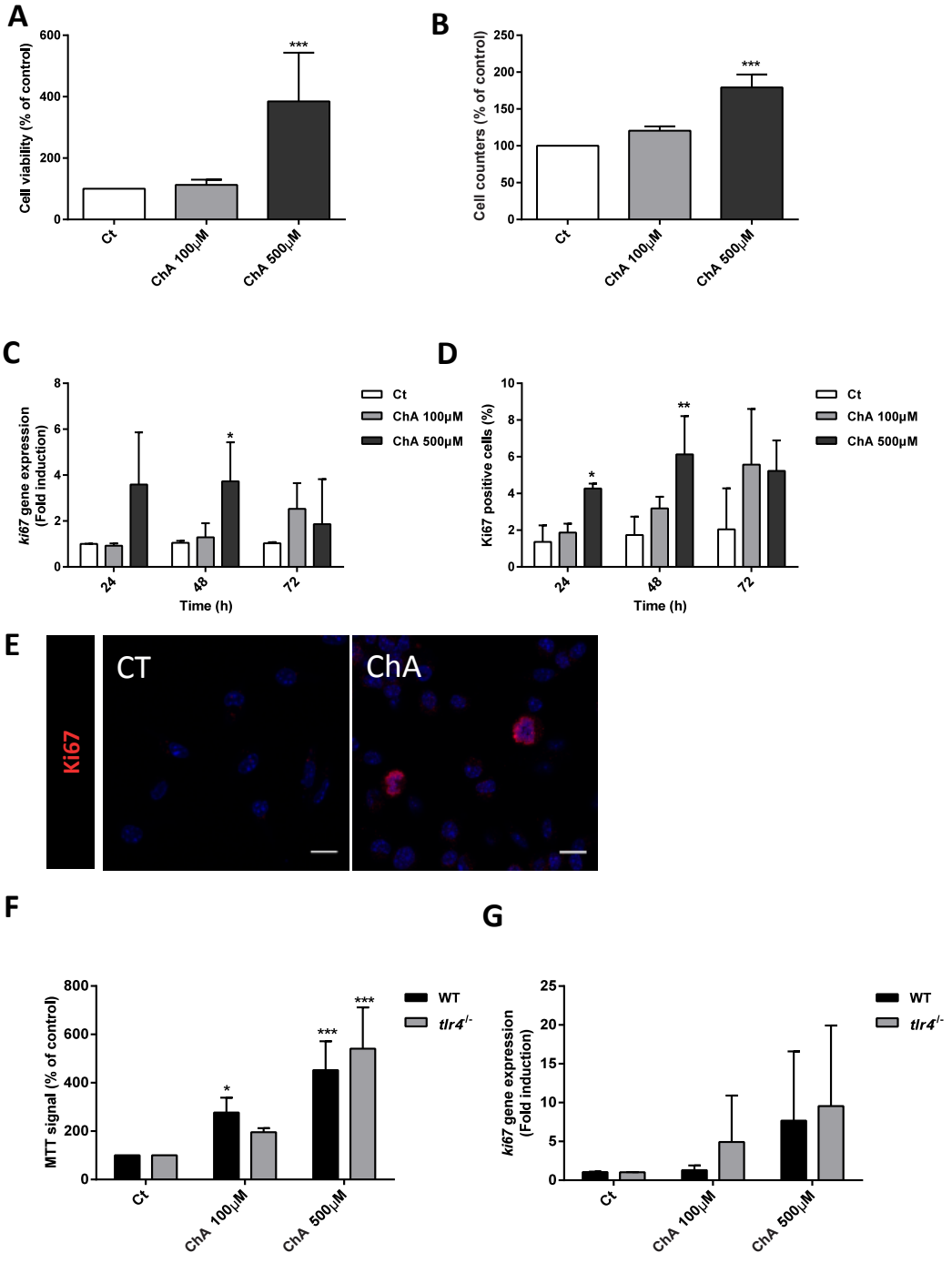

Figure 4.7 | ChA induce bone-marrow derived macrophages proliferation.

A. ChA induces an increase in cell viability. Primary macrophages were incubated during 72 h with vehicle (control) or ChA and cell viability was assessed by the MTT assay and is expressed relative to the viability of control cells. **B.** Effect of ChA on the cell number. The number of cells was quantified under a fluorescence microscope after staining the cells with DAPI. **C.** ChA induced a increase in Ki67 gene expression, a marker of proliferating cells. mRNA levels of ki67 was accessed by qPCR after different incubation time. **D.** Percentage of Ki67-proliferative cells measured by immunofluorescence using an anti-Ki67. Cells were imaged using a fluorescence microscope. **E.** Representative images of BMDM immunostained to Ki67 after 72 h of ChA incubation. **F.** Effect of ChA on cell viability, measured by MTT assay, on wild-type (WT)-BMDM and *tlr4*$^{-/-}$ BMDM exposed to ChA for 72 h. Cell viability is expressed as percentage of the viability of control cells. **G.** Quantification of Ki67 mRNA levels in WT-BMDM and *tlr4*$^{-/-}$ BMDM exposed to ChA for 48h. Results are mean±SEM of at least three independent experiments. Bars, 10 μm. ***, p<0.001; **, p<0.01; *, p<0.05.

When TLRs are activated, they initiate a series of downstream signaling events that drive inflammatory responses, as shown above, as well as cell proliferation and survival (Hasan et al., 2007; Li, Jiang, & Tapping, 2010). Since, ChA can trigger TLR4 signaling, and this receptor had been shown to be involved in macrophage proliferation (Fang et al., 2017), we questioned if it could also have a role in ChA-induced cell proliferation. To evaluate the effect of TLR4 on cell proliferation, *tlr4*$^{-/-}$ BMDM were used. Figure 4.7F and G show that no difference between WT and TLR4-depleted BMDM was apparent, either in the MTT signal or Ki67 mRNA expression, suggesting that TLR4 signaling is not involved in ChA-induced macrophage proliferation.

4.3.8 ChA increases lactate and glutamate production via TLR4

Studies focussed on metabolic reprogramming in macrophage activation and plasticity has highlighted the crucial role of metabolic pathways on the immune response. Furthermore, metabolic reprogramming in proliferating cells is characterized by an increase in aerobic glycolysis (Hsu & Sabatini, 2008; Vander Heiden, Cantley, & Thompson, 2009). Since we observed ChA-induced alterations in the inflammatory and proliferative capacity of BMDM, we aimed to measure the metabolic alterations associated with this phenotype. Firstly, glucose and glutamine consumption, and lactate and glutamate production in the supernatant after ChA incubation were measured. An increase in glucose (Supplementary Figure 4.2A) and glutamine consumption (Supplementary Figure 4.2C) were found, as well as an increase in lactate (Supplementary Figure 4.2B) and glutamate production (Supplementary Figure 4.2D), reflecting an increase lactate/glucose and glutamate/glutamine ratio (Figure 4.8 A and B).

TLR4 signaling has been implicated in aerobic glycolysis in activated macrophages (M1) (Kelly & O'Neill, 2015; Langston, Shibata, & Horng, 2017). In this way, in order to dissect the signaling behind ChA-stimulated, glucose and glutamine consumption and lactate and glutamate production macrophages were analysed in *tlr4*$^{-/-}$ macrophages (Supplementary Figure 4.2E-H). TLR4 deletion reduced glucose consumption and lactate production, reflecting a decrease in ratio lactate/glucose (Figure 4.8C), with the same inhibitory effect on glutamine and glutamate metabolism (Supplementary Figure 4.2G-H). These results demonstrate that increased glucose and glutamine oxidation, as well as the production of lactate and glutamate by macrophages in response to ChA are dependent on the TLR4 signaling pathway.

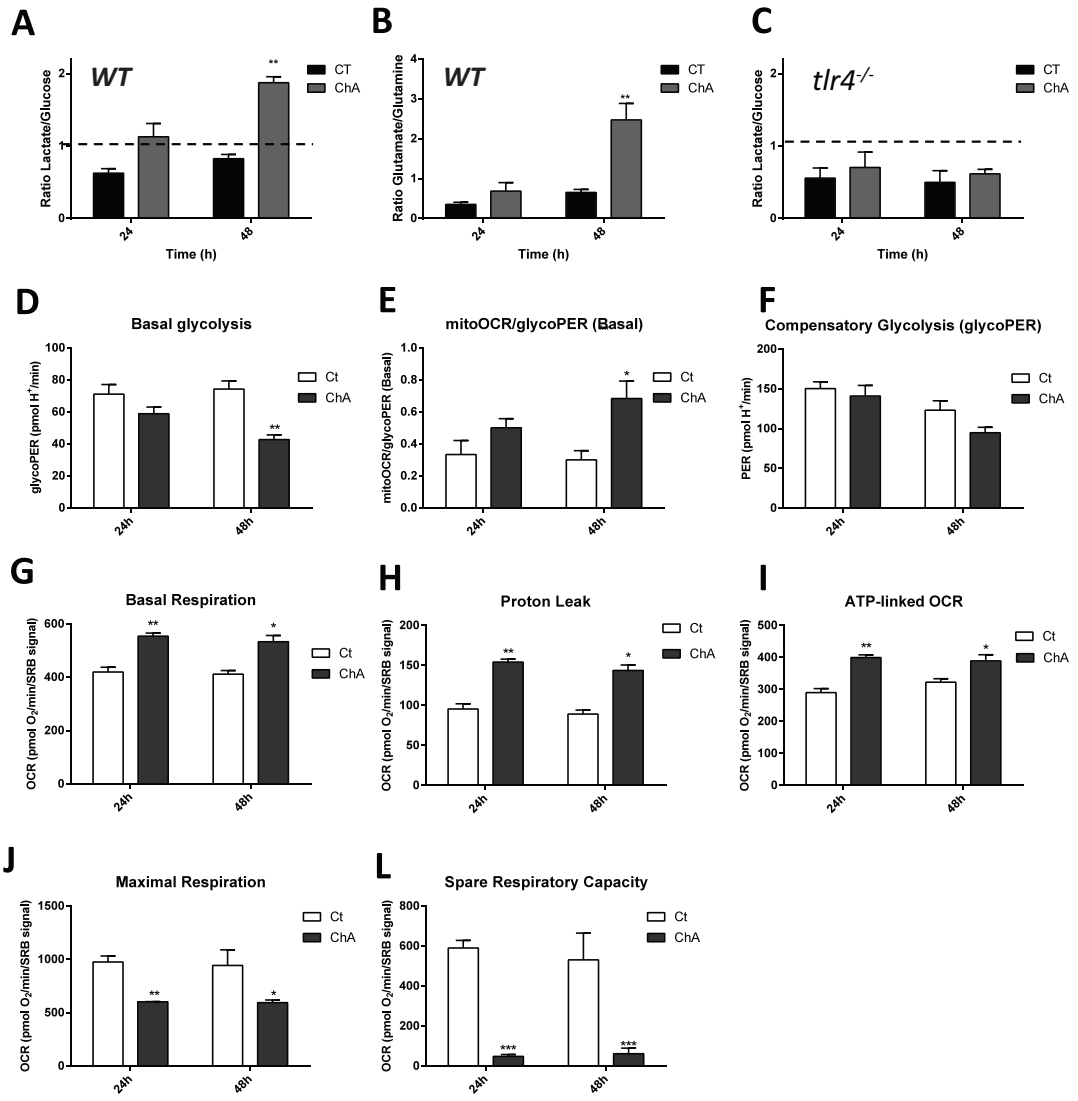

Figure 4.8 | ChA stimulates the lactate production in a TLR4-dependent manner and increases mitochondrial respiration.

A and **B.** ChA induces a metabolic shift of macrophages increasing lactate and glutamate production; ratio between lactate and glucose **(A)**, glutamate and glutamine **(B)** in WT-BMDM. **C.** Lactate and glucose ratio in *tlr4*$^{-/-}$ macrophages. Concentration of these metabolites were measured in the culture supernatant. **D-F.** Measurement of glycolytic rate in primary macrophages BMDM treated with ChA or vehicle for 24 and 48 h. Proton efflux rate (PER) and oxygen consumption rate (OCR) was measured and the followed parameters were obtained: basal glycolysis **(D)**, ratio between OCR associated with mitochondrial respiration (mitoOCR) and the PER resulting from glycolysis (PERglyco) **(E)** and compensory glycolysis **(F)** upon rotenone/antimycin A injection (1 µM each). PER was determined taken into account the culture medium acidification after the different treatments. **G-L.** OCR measurement of macrophages after ChA and vehicle treatment for 24 or 48 h. After baseline OCR evaluation **(G)**, the mitochondrial stressor effect was followed by sequential injection of oligomycin (2 µM), FCCP (2 µM), and rotenone/antimycin A (1 µM each). With this approach, the direct effect of the stressor on OCR can be determined by the measurement of individual paramaters: OCR associated to proton leak **(H)**, ATP-linked OCR **(I)**, maximal respiration capacity **(J)** and spare respiratory capacity **(L)**. Data shown the mean±SEM of three independent experiences. ***, p<0.001; **, p<0.01; *, p<0.05.

4.3.9 Glycolytic flux is decreased and mitochondrial respiration is stimulated in ChA-loaded macrophages

Although LPS-stimulated macrophages have been associated with an enhanced glycolytic metabolism and impaired mitochondrial OXPHOS, several reports have demonstrated that this is not strictly true (Kelly & O'Neill, 2015; Tur, Vico, Lloberas, Zorzano, & Celada, 2017; Van den Bossche et al., 2017). Therefore, in order to better characterize the ChA-induced metabolic shift in macrophages, we evaluated the glycolytic rate and the mitochondrial respiratory ca-

pacity upon ChA treatment. The results from Figure 4.8D, showed a significant decrease in the glycolytic proton efflux rate (glycoPER) in cells treated with ChA, with a decreased percentage of PER associated to glycolysis (Supplementary Figure 4.3A). A raised mitochondrial oxygen consumption rate (MitoOCR)/glycoPER ratio was also observed, suggesting an increase in oxygen consumption associated with glucose oxidation in ChA-loaded macrophages (Figure 4.8E). When mitochondrial ATP production was blocked, ChA-treated macrophages experienced a decrease in compensatory glycolysis (Figure 4.8F). This indicates that ChA-incubated cells were not able to increase aerobic glycolysis to meet energy demands. Additionally, the decrease in glycolytic rate was accompanied by an increase in mitochondrial respiration. In Figure 4.8G, by measuring the basal oxygen consumption rate (OCR) in the presence of glucose and glutamine, the results revealed an increase in oxygen consumption in ChA-treated cells compared with controls cells, as well as an increase in mitochondrial proton leak (Figure 4.8H). The portion of basal respiration in ChA-treated macrophages used for ATP production was higher in these cells than in control cells (Figure 4.8I). Moreover, when OCR was stimulated by the mitochondrial uncoupler carbonyl cyanide-4-(trifluoromethoxy) phenylhydrazone (FCCP), which mimics a physiological "energy demand" by stimulating the respiratory chain to operate at maximum capacity, ChA-treated cells presented a lower maximal response than control cells (Figure 4.8J). This result was accompanied by a substantial decrease in spare respiratory capacity in ChA-loaded cells (Figure 4.8L). Finally, to measure the portion of oxygen consumption that was not related with mitochondrial respiration, inhibitors of the mitochondrial respiratory chain, rotenone and antimycin A, were added. The results showed that ChA-loaded cells had not others activated pathways that could be affecting the oxygen consumption (Supplementary Figure 4.3B).

Since TLR4 had a role in glucose and glutamine consumption induced by ChA, we also evaluated the effect of this receptor in mitochondrial respiration. The results revealed that TLR4 has a prominent role in the mitochondrial metabolic alteration induced by ChA. In ChA-treated *tlr4*$^{-/-}$ macrophages; the basal respiration, proton leak, ATP-linked OCR, maximal respiration and spare respiratory capacity were no different to WT cells (Supplementary Figure 4.3C-G). These results indicate that the metabolic shift induced by ChA in macrophages is regulated via TLR4 signaling.

4.3.10 Glutamine and endogenous lipids are not the main fuel for mitochondrial respiration

It is now well established that glutamine uptake and glutaminolysis are increased in activated macrophages (He, Weber, & Schilling, 2016; Langston et al., 2017; Liu et al., 2017; O'Neill, Kishton, & Rathmell, 2016), as well as in ChA-loaded macrophages (Figure 4.8B). We therefore explored the role of glutaminolysis in mitochondrial respiration. Results in Figure 4.9A and B show a small increase in the OCR associated with basal glutamine consumption and proton leak in ChA-treated cells, compared with controls. We examined OCR linked to ATP production, maximal mitochondrial respiration and spare respiratory capacity and found all of these parameters were decreased in cells treated with ChA (Figure 4.9C-E). This suggests only a modest contribution of glutamine oxidation via α-ketoglutarate, an intermediary me-

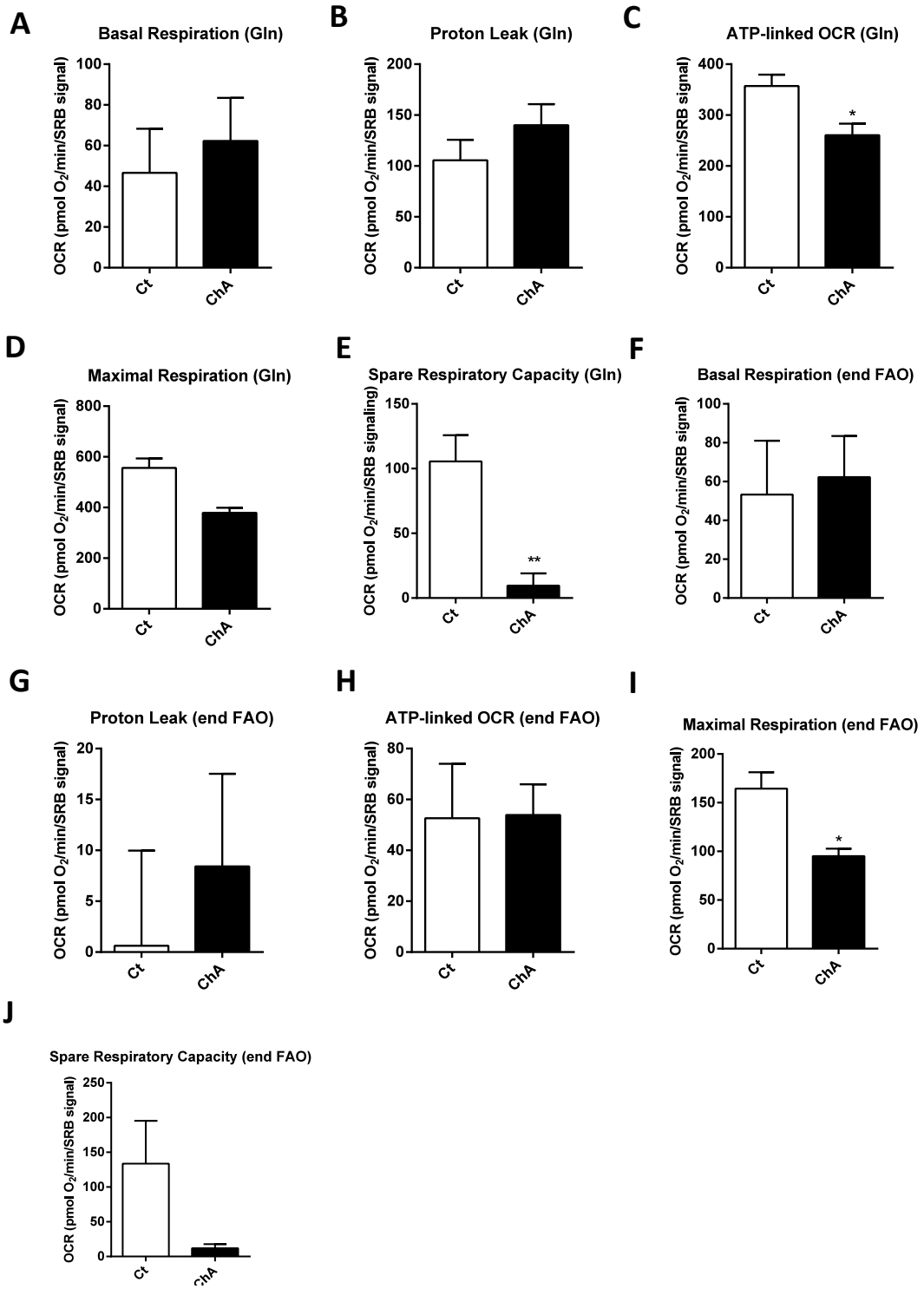

Figure 4.9 | Despite the ChA-loaded macrophages present an increased glutamine (Gln) consumption and an increase in lipid accumulation, there is no stimulation of glutaminolysis or endogenous fatty acid oxidation (FAO) to fuel mitochondrial respiration.

A-J. Measurement of oxygen consumption rate (OCR) associated with basal respiration **(A,F)**, pronton leak **(B,G)**, ATP production **(C,H)**, maximal response (D,I) and spare respiratory capacity **(E,J)** after incubation of macrophages with ChA for 24 h or 48 h. The mitochondrial respiration induced by glutamine **(A-E)** and by endogenous fatty acid **(F-J)** was performed in culture medium with glutamine with or without etomoxir. The values are the mean±SEM of three independent experiments; **, p<0.01; *, p<0.05.

tabolite of TCA cycle, indicating that increased glutamine consumption in ChA-loaded cells (Supplementary Figure 4.2C) was not associated with mitochondrial respiration. Furthermore, since macrophages incubated with ChA presented an increase in lipid accumulation, we considered the possibility of endogenous lipid affecting mitochondrial respiration. Through endogenous lipid oxidation, NADH, $FADH_2$ and acetyl-CoA are generated, which enters the

TCA cycle, activating the respiratory pathway for the production of ATP. OCR was measured in the presence or absence of etomoxir, a carnitine palmitoyl transferase inhibitor and by evaluating the difference in OCR response during the MitoStress protocol, we were able to measure the portion of mitochondrial respiration associated with endogenous FAO. We found that ChA did not elicit an increase in endogenous FAO, presenting a basal respiration rate similar to the control level, nor did it affect ATP production resulting from OCR (Figure 4.9F and H). Proton leak was markedly increased and the maximal response and mitochondrial spare respiratory capacity was diminished in response to ChA loading. Thus, our data suggests that proton leak and mitochondrial capacity in response to an "energy demand" is a ChA-induced effect independent of fuel driven respiratory activation.

4.4 DISCUSSION

Among the several risk factors already identified, blood cholesterol level is one of the main indicators of CVD risk. The correlation between CVD incidence and total cholesterol in LDL is well established (Ference et al., 2017; Herrington et al., 2016; Lin et al., 2017; Ridker, 2014; Silverman et al., 2016). However, cholesterol-LDL or any of the existing risk factors of ASCVD, are good predictors for unstable atherosclerotic plaques. In this work, we identified a novel putative biomarker for advanced atherosclerotic plaques.

CE are one of the main components of LDL particles and, due to their unsaturated bounds, are susceptible to oxidation. Several oxo-esters have been proposed as the oxidative end products of CE (Kamido, Kuksis, Marai, & Myher, 1995), but in a highly oxidative environment, such as a necrotic plaque core, these compounds will be completely oxidized to ChE, the stable end products of CE oxidation. Consequently, due to the amphiphilic properties of ChE, these compounds may partition into serum components. Our results showed that ChE detected in the plasma are increased in ASCVD patients. The increased concentration of ChE in human plasma from ASCVD patients compared with healthy controls revealed the diagnostic/prognostic potential of these ChE in CVD. However, to draw further conclusions we need to increase the size of our cohort and perform longitudinal studies. In this work we demonstrated the atherogenic properties of the most abundant ChE in human plasma – ChA.

Monocytes in the blood stream are one of the first innate cells to contact with Ox-Lp from the LDL particles. In hypercholesterolemia, circulating monocytes become foamy (Wu & Ballantyne, 2017; Xu et al., 2015), increasing IL-1β and TNF-α gene expression in mouse monocytes (Xu et al., 2015). Our results showed that ChA also induces a phenotypically change in *in vitro* human monocytes, with an increase in CD206 expression and in the release of proinflammatory cytokines IL-1β, IL-6, and anti-inflammatory IL-10 cytokine (Figure 4.2), with no TNF-α increase. CD206, a marker of alternatively activated monocytes (Saha, Bruneau, Kodys, & Szabo, 2015; Tiemessen et al., 2007), is important in endocytosis and

phagocytosis, being associated with an increase in phagocytic activity in atherosclerosis macrophages (Chistiakov, Bobryshev, & Orekhov, 2015). However, despite the increased CD206 levels ChA-loaded monocytes are also producers of IL-1β and ROS. These findings suggest a distinct monocyte phenotype from the ones already described in literature: activated (M1) and alternatively activated (M2) monocytes (Mukhopadhyay et al., 2015). Moreover, IL-1β is a crucial cytokine implicated in the initiation and development of atherosclerosis (Baldrighi, Mallat, Li, & al., 2017; Chi, Messas, Levine, Graves, & Amar, 2004; Libby, 2017) and was detected upon ChA-monocyte stimulation. Monocytes secrete IL-1β mature cytokine following a single stimulus (Netea et al., 2009). For example, TLR4 was already demonstrate to induce an increase in IL-1β secretion (Hadadi et al., 2016; Ward et al., 2010). The exact mechanism behind the ChA induction of IL-1β in monocytes was not yet discovered. However once ChA-induced IL-1β release via TLR4 on BMDM (Figure 4.5A), we can speculate that TLR4 can also play a role in ChA-induced IL-1β secretion in human monocytes. Furthermore, additional information will be needed for an accurate monocyte phenotype characterization.

Human monocytes treated with ChA during differentiation into macrophages released higher levels of inflammatory cytokines than control cells, had increased surface HLA-DR, a marker of proinflammatory macrophages, and CD206. This phenotypical shift was accompanied by an increase in IL-1β, IL-6 and IL-10 secretion. In THP-1 cells, monocyte differentiation into macrophages was shown be regulated by the oxidation levels of LDL particles: low-ox-LDL induced an proinflammatory M1 phenotype, with increased CD86 and TNF-α production, whereas highly-ox-LDL induced CD206 expression and production of IL-6, reflecting the M2 macrophage phenotype (Seo, Yang, Yoo, & Choi, 2015). Thus, the differentiation of monocytes into macrophages in the presence of ChA may engineer a novel macrophage phenotype: increasing HLA-DR and CD206, inflammatory cell surface markers of activated (M1) and alternatively activated macrophages (M2), respectively, and IL-1β secretion. These results will be further investigated using ChA during BMDM differentiation process. Interestingly, ChA also induced dual inflammatory features in murine macrophages, with increased expression and release of proinflammatory cytokines IL-1β, IL-6, TNF-α and IL-1α and anti-inflammatory cytokine, IL-10. It is unusual for both pro- and anti-inflammatory cytokines to be immediately expressed in the same subtype of macrophages and we observed this phenotype in both human and murine macrophages. Only M2b macrophages express IL-1β, IL-6, TNF-α and IL-10; however, their surface markers are $CD86^{+}$ and $MHCII^{+}$ (Anderson, Gerber, & Mosser, 2002; Ohlsson et al., 2014), but in our human macrophages, only HLA-DR, an MHC class II, are upregulated. On another hand, in M2a the profile of surface markers has some similarities with ChA-induced macrophages, presenting an increase in CD206 and HLA-DR, but both phenotypes have a distinct cytokine profile (Ohlsson et al., 2014; Roszer, 2015). Furthermore, in BMDM ChA induced a functional and some transcriptional similarities with the Mox phenotype. Both macrophage phenotypes present an increase in expression of the antioxidant gene Hmox-1, which is triggered by the activation of transcription factor Nrf2 and an increase in IL-1β release. At the functional level, Mox and ChA-loaded macrophages also present analogous phenotypic characteristics with a decrease in phagocytic capacity, related to actin cytoskeletal changes, and reduced chemoattractant

properties (Figure 4.5C-H) (Kadl et al., 2010). However, we detected TNF-α release, which was not observed in Mox macrophages, therefore our ChA-induced macrophage phenotype encompasses aspects of the M1, M2 and Mox phenotypes.

We found that IL-1β release in ChA-treated cells is mediated via TLR4. Several Ox-Lp, as oxidized CE and oxPAPC, have been reported to stimulate this receptor, inducing an inflammatory response (Bochkov et al., 2002; Choi et al., 2009, 2017; Imai et al., 2008; Walton et al., 2003). Here, we also verified that IL-1β secretion mediated by ChA stimulation is via NLRP3 activation and ChA is able to induce both signals required for IL-1β release. Activation of the NLRP3 inflammasome is regulated at both transcriptional and post-translational levels. The first signal in inflammasome activation involves the cell priming, induced by the TLR/nuclear factor (NF)-κB pathway, to upregulate the expression of NLRP3 inflammasome components. Signal 2 is transduced by several extra- or intracellular stimuli to activate the NLRP3 inflammasome - a multi-protein complex consisting of NLRP3, the adaptor protein ASC, and pro-caspase-1 (Guo, Callaway, & Ting, 2015; Lamkanfi & Dixit, 2014). The second signal transmitted by ChA is via its effect on lysosome destabilization (Figure 4.5G). BMDM loaded cells presented an increase in lipid accumulation in cytosolic lipid droplets, as well as in lysosomes with a modified morphology (Figure 4.6B) which can originate an increase in lysosomal proteases leak, as cathepsin B. Cytosolic cathepsin B activate caspase-1 with consequent IL-1β release. To confirm this hypothesis lysosomal membrane integrity of ChA-loaded macrophages still need to be addressed. In atherosclerosis, cholesterol crystals induce lysosomal destabilization, increasing IL-1β release through NLRP3 activation (Duewell et al., 2010; Emanuel et al., 2014; Rajaḿaki et al., 2010).

It has been demonstrated that local macrophage proliferation can maintain macrophage numbers in inflammatory (Jenkins et al., 2011) and normal tissues (Hashimoto et al., 2013; Yona et al., 2013). In the context of atherosclerosis, macrophage proliferation dominates in advanced atherosclerotic plaques (Robbins et al., 2013b). We found that this new ChA-induced macrophage phenotype presented an increase in proliferative capacity when compared with the control cells (Figure 4.7A-E). Our results are in agreement with several reports indicating the ox-LDL efffect on increased macrophage numbers through growth factor induction (Hundal et al., 2001; Ishii et al., 2009; Orekhov, R. Andreeva, Mikhailova, & Gordon, 1998; Rekhter & Gordon, 1995; Winder et al., 2000). TLR4 activation and its downstream pathways PI3K/Akt and MAPK/ERK are believed to be involved in downstream signaling (Andrés, Pello, & Silvestre-Roig, 2012; Wang, Zhu, Huang, Li, & Zhu, 2013). However, the proliferative capacity of ChA-loaded macrophages was not TLR4-dependent. Thus, it seems that the proliferative capacity of these macrophages is independent of the inflammatory effects induced by ChA, at least the ones that are TLR4-dependent. Further experiments are needed to decipher the mechanism underlying ChA-induced proliferation.

In ChA-loaded macrophages, we also observed an increase in glucose consumption and an increase in lactate secretion (Figure 4.8A). However, when the glycolytic rate in these cells

was evaluated we found a reduction in basal glycolysis (Figure 4.8C). In addition, elevated glutamine consumption in cells treated with ChA was apparent (Figure 4.8B), without a striking increase in the OCR associated with glutamine oxidation (Figure 4.9A). Through α-ketoglutarate production via glutaminolysis, glutamine can fuel the TCA cycle and induces mitochondrial respiration. Previous studies indicate that: i) activated macrophages present a truncated TCA cycle (Jha et al., 2015), ii) glutaminolysis is crucial for macrophage activation (Liu et al., 2017), iii) activated macrophages present an increase in lactate and glutamate secretion (O'Neill et al., 2016; O'Neill & Pearce, 2016); we hypothesized the existence of a new metabolic shift in atherogenic macrophages (Figure 4.10). Upon ChA stimulation, macrophages increase glucose and glutamine uptake in a mechanism dependent on TLR4 (Figure 4.8C and D). Then, glucose is mainly oxidized to ribose-5-phosphate in the PPP for biosynthesis and converted to pyruvate for carbon supply to the TCA cycle. Since at equilibrium, ChA is partitioned in all cellular membranes, including the mitochondrial membranes, ChA increases the proton leak of these organelles by interfering with the biophysical membrane properties (Figure 4.8H). In response, ChA-loaded cells increased OXPHOS respiration to compensate proton dissipation, presenting an increase in basal respiration (Figure 4.8G). Due to the already increased respiration rate or due to the effect of ChA on mitochondrial membranes (or both); upon stimulation of mitochondrial respiration with FCCP, ChA treated cells were unable to increase oxygen consumption to compensate the induced energy demand (Figure 4.8J and L). In addition, as in the LPS-induced truncated TCA cycle, we hypothesized that in ChA-loaded cells the same or similar TCA cycle fragmentation occurred. In M1 macrophages, a metabolic break was identified at isocitrate dehydrogenase (IDH), the enzyme that converts isocitrate to α-ketoglutarate (Jha et al., 2015). Several mechanisms have been proposed to explain carbon flow within a dysfunctional TCA cycle, such as glutamine-dependent anaplerosis through α-ketoglutarate or glutamine-derived succinate replenishment via the GABA shunt pathway (Geeraerts, Bolli, Fendt, & Van Ginderachter, 2017). Therefore, we expect that glutaminolysis is upregulated in ChA-loaded cells, supplying carbons for the truncated TCA cycle and also increase the cellular levels of glutamate (Figure 4.8B). However, the accumulation in TCA metabolites, such as citrate, already reported in LPS-stimulated cells (Jha et al., 2015; O'Neill et al., 2016), can shift glutaminolysis to produce lactate, which has been described in proliferating cells (Feron, 2009; Wise et al., 2008). Thus, glutaminolysis could be the main pathway responsible for lactate secretion in ChA-loaded macrophages. Glutaminolysis in lipid-loaded cells has been correlated with an increase in lysosome dysfunction, inflammasome activation and cell death (He et al., 2016). Thus, inhibition of glutaminolysis in ChA-loaded cells is a crucial next step in the dissection of the mechanism involved in ChA induced inflammation and the metabolic shift. These two cellular effects are likely to be correlated through TLR4 signaling, since the absence of TLR4 led to a reduction in metabolic reprogramming in ChA-laden macrophages.

In conclusion, we detected for the first time in human plasma an Ox-Lp family, ChE, which was significantly increased in ASCVD patients. Through different techniques and experimental approaches we showed the proatherogenic potential of the most abundant ChE detected

in our study. Circulating or recruited monocytes to the atheroma lesion suffer phenotypical changes when contact with ChA, inducing the secretion of IL-1β and ROS production. When these immune cells were differentiated in the presence of ChA, inflammatory activation of the resulting macrophages was also observed. We described a new foamy macrophage phenotype with a unique cytokine profile and the capacity to proliferate. A more detailed mechanistic investigation of the inflammatory response induced by ChA revealed that IL-1β release is mediated by induced lysosomal destabilization. Finally, the observed unique inflammatory phenotype was accompanied by atypical metabolic reprogramming, both effects depending on TLR4 signaling. Together, our results contribute towards an improved early diagnosis of ASCVD and increase our knowledge of foam cell phenotypic diversity.

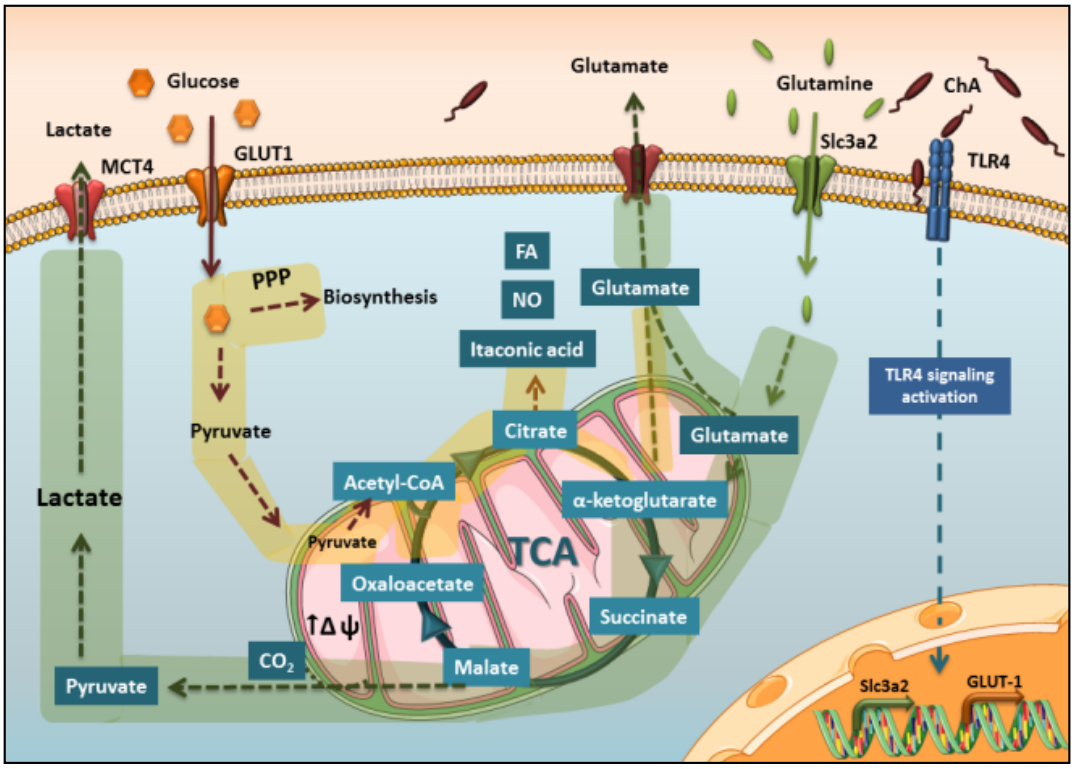

Figure 4.10 | Schematic representation of metabolic shif induced by ChA-laden macrophages.

Upon ChA stimulation, macrophages increase the glucose and glutamine internalization, through a possible increase in the expression of glucose transporters (GLUT-1) and glutamine (Slc3a2) , and consumption trough toll-like receptor4 (TLR4) signaling. Glucose is oxidized mainly through pentose phosphate pathway (PPP) and into pyruvate, which can enter in tricarboxylic acid (TCA) cycle. Due to a truncated TCA cycle, there is a citrate accumulation, which can be a subtract for lipid biosynthesis, nitrites production or itaconic acid, an antimicrobial metabolite. For TCA metabolites replacement, cells increased glutaminolysis: glutamine is oxidized into glutamate that can be secreted or converted to α-ketoglutarate, a intermidiated of TCA cycle; α-ketoglutarate is oxidized into succinate and consequently to malate, which can then be oxidized into pyruvate. Cytosolic pyruvate can then be converted into lactate. Macrophages loaded with ChA also present an increasing in mitochondrial potencial (Δψ) and in proton leak, which can induce an oxidative phosphorylation augment to compensate this mitochondrial impairement.

4.5 REFERENCES

Allain, C. C., Poon, L. S., Chan, C. S. G., Richmond, W., & Fu, P. C. (1974). Enzymatic Determination of Total Serum Cholesterol. Clin. Chem., 20(4), 470–475. Retrieved from http://www.clinchem.org/content/20/4/470.short

Anderson, C. F., Gerber, J. S., & Mosser, D. M. (2002). Modulating macrophage function with IgG immune complexes. Journal of Endotoxin Research, 8(6), 477–481. https://doi.org/10.1179/096805102125001118

Andrés, V., Pello, O. M., & Silvestre-Roig, C. (2012). Macrophage proliferation and apoptosis in atherosclerosis. Current Opinion in Lipidology, 23(5), 429–438. https://doi.org/10.1097/MOL.0b013e328357a379

Baldrighi, M., Mallat, Z., Li, X., & al., et. (2017). NLRP3 inflammasome pathways in atherosclerosis. Atherosclerosis, 32(0), 291. https://doi.org/10.1016/j.atherosclerosis.2017.10.027

Bentzon, J. F., Otsuka, F., Virmani, R., & Falk, E. (2014). Mechanisms of plaque formation and rupture. Circulation Research, 114(12), 1852–1866. https://doi.org/10.1161/CIRCRESAHA.114.302721

Bochkov, V. N., Kadl, A., Huber, J., Gruber, F., Binder, B. R., & Leitinger, N. (2002). Protective role of phospholipid oxidation products in endotoxin-induced tissue damage. Nature, 419(6902), 77–81. https://doi.org/10.1038/nature01023

Boyette, L. B., MacEdo, C., Hadi, K., Elinoff, B. D., Walters, J. T., Ramaswami, B., … Metes, Di. M. (2017). Phenotype, function, and differentiation potential of human monocyte subsets. PLoS ONE, 12(4). https://doi.org/10.1371/journal.pone.0176460

Chi, H., Messas, E., Levine, R. A., Graves, D. T., & Amar, S. (2004). Interleukin-1 receptor signaling mediates atherosclerosis associated with bacterial exposure and/or a high-fat diet in a murine apolipoprotein E heterozygote model: Pharmacotherapeutic implications. Circulation, 110(12), 1678–1685. https://doi.org/10.1161/01.CIR.0000142085.39015.31

Chinetti-Gbaguidi, G., Colin, S., & Staels, B. (2014). Macrophage subsets in atherosclerosis. Nature Reviews Cardiology, 12(1), 10–17. https://doi.org/10.1038/nrcardio.2014.173

Chistiakov, D. A., Bobryshev, Y. V., & Orekhov, A. N. (2015). Changes in transcriptome of macrophages in atherosclerosis. Journal of Cellular and Molecular Medicine, 19(6), 1163–1173. https://doi.org/10.1111/jcmm.12591

Choi, S. H., Harkewicz, R., Lee, J. H., Boullier, A., Almazan, F., Li, A. C., … Miller, Y. I. (2009). Lipoprotein accumulation in macrophages via toll-like receptor-4-dependent fluid phase uptake. Circulation Research, 104(12), 1355–1363. https://doi.org/10.1161/CIRCRESAHA.108.192880

Choi, S. H., Sviridov, D., & Miller, Y. I. (2017). Oxidized cholesteryl esters and inflammation. Biochimica et Biophysica Acta - Molecular and Cell Biology of Lipids, 1862(4), 393–397. https://doi.org/10.1016/j.bbalip.2016.06.020

Cochain, C., & Zernecke, A. (2017). Macrophages in vascular inflammation and atherosclerosis. Pflugers Archiv European Journal of Physiology, 469(3–4), 485–499. https://doi.org/10.1007/s00424-017-1941-y

Colin, S., Chinetti-Gbaguidi, G., & Staels, B. (2014). Macrophage phenotypes in atherosclerosis. Immunological Reviews, 262(1), 153–166. https://doi.org/10.1111/imr.12218

Cunha, C., Gonçalves, S. M., Duarte-Oliveira, C., Leite, L., Lagrou, K., Marques, A., … Carvalho, A. (2017). IL-10 overexpression predisposes to invasive aspergillosis by suppressing antifungal immunity. Journal of Allergy and Clinical Immunology, 140(3), 867–870.e9. https://doi.org/10.1016/j.jaci.2017.02.034

de Duve, C. (1974). The participation of lysosomes in the transformation of smooth muscle cells to foamy cells in the aorta of cholesterol-fed rabbits. Acta Cardiologica, Suppl 20, 9–25.

Domingues, N., Estronca, L. M. B. B., Silva, J., Encarnação, M. R., Mateus, R., Silva, D., … Vieira, O. V. (2017). Cholesteryl hemiesters alter lysosome structure and function and induce proinflammatory cytokine production in macrophages. Biochimica et Biophysica Acta - Molecular and Cell Biology of Lipids, 1862(2), 210–220. https://doi.org/10.1016/j.bbalip.2016.10.009

Duewell, P., Kono, H., Rayner, K. J., Sirois, C. M., Vladimer, G., Bauernfeind, F. G., … Latz, E. (2010). NLRP3 inflammasomes are required for atherogenesis and activated by cholesterol crystals. Nature, 466(7306), 652–652. https://doi.org/10.1038/nature09316

Emanuel, R., Sergin, I., Bhattacharya, S., Turner, J. N., Epelman, S., Settembre, C., … Razani, B. (2014). Induction of lysosomal biogenesis in atherosclerotic macrophages can rescue lipid-induced lysosomal dysfunction and downstream sequelae. Arteriosclerosis, Thrombosis, and Vascular Biology, 34(9), 1942–1952. https://doi.org/10.1161/ATVBAHA.114.303342

Estronca, L. M. B. B., Silva, J. C. P., Sampaio, J. L., Shevchenko, A., Verkade, P., Vaz, A. D. N., … Vieira, O. V. (2012). Molecular etiology of atherogenesis--in vitro induction of lipidosis in macrophages with a new LDL model. PloS One, 7(4), e34822. https://doi.org/10.1371/journal.pone.0034822

Fang, W., Bi, D., Zheng, R., Cai, N., Xu, H., Zhou, R., … Xu, X. (2017). Identification and activation of TLR4-mediated signaling pathways by alginate-derived guluronate oligosaccharide in RAW264.7 macrophages. Scientific Reports, 7(1), 1–13. https://doi.org/10.1038/s41598-017-01868-0

Feig, J. E., Rong, J. X., Shamir, R., Sanson, M., Vengrenyuk, Y., Liu, J., … Fisher, E. A. (2011). HDL promotes rapid atherosclerosis regression in mice and alters inflammatory properties of plaque monocyte-derived cells. Proceedings of the National Academy

of Sciences, 108(17), 7166–7171. https://doi.org/10.1073/pnas.1016086108

Ference, B. A., Ginsberg, H. N., Graham, I., Ray, K. K., Packard, C. J., Bruckert, E., … Catapano, A. L. (2017). Low-density lipoproteins cause atherosclerotic cardiovascular disease. 1. Evidence from genetic, epidemiologic, and clinical studies. A consensus statement from the European Atherosclerosis Society Consensus Panel. Eur Heart J. https://doi.org/10.1093/eurheartj/ehx144

Feron, O. (2009). Pyruvate into lactate and back: From the Warburg effect to symbiotic energy fuel exchange in cancer cells. Radiotherapy and Oncology. https://doi.org/10.1016/j.radonc.2009.06.025

Geeraerts, X., Bolli, E., Fendt, S. M., & Van Ginderachter, J. A. (2017). Macrophage metabolism as therapeutic target for cancer, atherosclerosis, and obesity. Frontiers in Immunology. https://doi.org/10.3389/fimmu.2017.00289

Gordon, S. (2003). Alternative activation of macrophages. Nature Reviews Immunology, 3(1), 23–35. https://doi.org/10.1038/nri978

Gordon, S., & Taylor, P. R. (2005). Monocyte and macrophage heterogeneity. Nature Reviews Immunology, 5(12), 953–964. https://doi.org/10.1038/nri1733

Gorrini, C., Baniasadi, P. S., Harris, I. S., Silvester, J., Inoue, S., Snow, B., … Gauthier, M. L. (2013). BRCA1 interacts with Nrf2 to regulate antioxidant signaling and cell survival. The Journal of Experimental Medicine, 210(8), 1529–1544. https://doi.org/10.1084/jem.20121337

Guo, H., Callaway, J. B., & Ting, J. P.-Y. (2015). Inflammasomes: mechanism of action, role in disease, and therapeutics. Nature Medicine, 21(7), 677–687. https://doi.org/10.1038/nm.3893

Hadadi, E., Zhang, B., Baidzajevas, K., Yusof, N., Puan, K. J., Ong, S. M., … Wong, S. C. (2016). Differential IL-1β secretion by monocyte subsets is regulated by Hsp27 through modulating mRNA stability. Scientific Reports, 6. https://doi.org/10.1038/srep39035

Hasan, U. A., Caux, C., Perrot, I., Doffin, A.-C., Menetrier-Caux, C., Trinchieri, G., … Vlach, J. (2007). Cell proliferation and survival induced by Toll-like receptors is antagonized by type I IFNs. Proceedings of the National Academy of Sciences, 104(19), 8047–8052. https://doi.org/10.1073/pnas.0700664104

Hashimoto, D., Chow, A., Noizat, C., Teo, P., Beasley, M. B., Leboeuf, M., … Merad, M. (2013). Tissue-resident macrophages self-maintain locally throughout adult life with minimal contribution from circulating monocytes. Immunity, 38(4), 792–804. https://doi.org/10.1016/j.immuni.2013.04.004

He, L., Weber, K. J., & Schilling, J. D. (2016). Glutamine modulates macrophage lipotoxicity. Nutrients, 8(4). https://doi.org/10.3390/nu8040215

Herrington, W., Lacey, B., Sherliker, P., Armitage, J., & Lewington, S. (2016). Epidemiology of Atherosclerosis and the Potential to Reduce the Global Burden of Atherothrombotic Disease. Circulation Research, 118(4), 535–546. https://doi.org/10.1161/CIRCRESAHA.115.307611

Herzog, R., Schuhmann, K., Schwudke, D., Sampaio, J. L., Bornstein, S. R., Schroeder, M., & Shevchenko, A. (2012). Lipidxplorer: A software for consensual cross-platform lipidomics. PLoS ONE, 7(1). https://doi.org/10.1371/journal.pone.0029851

Herzog, R., Schwudke, D., Schuhmann, K., Sampaio, J. L., Bornstein, S. R., Schroeder, M., & Shevchenko, A. (2011). A novel informatics concept for high-throughput shotgun lipidomics based on the molecular fragmentation query language. Genome Biology, 12(1), R8. https://doi.org/10.1186/gb-2011-12-1-r8

Hsu, P. P., & Sabatini, D. M. (2008). Cancer cell metabolism: Warburg and beyond. Cell, 134(5), 703–707. https://doi.org/10.1016/j.cell.2008.08.021

Hundal, R. S., Salh, B. S., Schrader, J. W., Gómez-Muñoz, a, Duronio, V., & Steinbrecher, U. P. (2001). Oxidized low density lipoprotein inhibits macrophage apoptosis through activation of the PI 3-kinase/PKB pathway. Journal of Lipid Research, 42(9), 1483–1491.

Imai, Y., Kuba, K., Neely, G. G., Yaghubian-Malhami, R., Perkmann, T., van Loo, G., … Penninger, J. M. (2008). Identification of Oxidative Stress and Toll-like Receptor 4 Signaling as a Key Pathway of Acute Lung Injury. Cell, 133(2), 235–249. https://doi.org/10.1016/j.cell.2008.02.043

Inácio, Â. S., Mesquita, K. A., Baptista, M., Ramalho-Santos, J., Vaz, W. L. C., & Vieira, O. V. (2011). In vitro surfactant structure-toxicity relationships: Implications for surfactant use in sexually transmitted infection prophylaxis and contraception. PLoS ONE, 6(5). https://doi.org/10.1371/journal.pone.0019850

Ishii, N., Matsumura, T., Kinoshita, H., Motoshima, H., Kojima, K., Tsutsumi, A., … Araki, E. (2009). Activation of AMP-activated protein kinase suppresses oxidized low-density lipoprotein-induced macrophage proliferation. Journal of Biological Chemistry, 284(50), 34561–34569. https://doi.org/10.1074/jbc.M109.028043

Jenkins, S. J., Ruckerl, D., Cook, P. C., Jones, L. H., Finkelman, F. D., van Rooijen, N., … Allen, J. E. (2011). Local Macrophage Proliferation, Rather than Recruitment from the Blood, Is a Signature of TH2 Inflammation. Science, 332(6035), 1284–1288. https://doi.org/10.1126/science.1204351

Jha, A. K., Huang, S. C. C., Sergushichev, A., Lampropoulou, V., Ivanova, Y., Loginicheva, E., … Artyomov, M. N. (2015). Network integration of parallel metabolic and transcriptional data reveals metabolic modules that regulate macrophage polarization. Immunity, 42(3), 419–430. https://doi.org/10.1016/j.immuni.2015.02.005

Kadl, A., Meher, A. K., Sharma, P. R., Lee, M. Y., Doran, A. C., Johnstone, S. R., … Leitinger, N. (2010). Identification of a novel macrophage phenotype that develops in response to atherogenic phospholipids via Nrf2. Circulation Research, 107(6), 737–746. https://doi.org/10.1161/CIRCRESAHA.109.215715

Kadl, A., Sharma, P. R., Chen, W., Agrawal, R., Meher, A. K., Rudraiah, S., … Leitinger, N. (2011). Oxidized phospholipid-induced inflammation is mediated by Toll-like receptor 2. Free Radical Biology and Medicine, 51(10), 1903–1909. https://doi.org/10.1016/j.

freeradbiomed.2011.08.026

Kamido, H., Kuksis, A., Marai, L., & Myher, J. J. (1995). Lipid ester-bound aldehydes among copper-catalyzed peroxidation products of human plasma lipoproteins. Journal of Lipid Research, 36(9), 1876–1886. Retrieved from http://www.ncbi.nlm.nih.gov/pubmed/8558076

Kelly, B., & O'Neill, L. A. (2015). Metabolic reprogramming in macrophages and dendritic cells in innate immunity. Cell Research, 25(7), 771–784. https://doi.org/10.1038/cr.2015.68

Lamkanfi, M., & Dixit, V. M. (2014). Mechanisms and functions of inflammasomes. Cell. https://doi.org/10.1016/j.cell.2014.04.007

Langston, P. K., Shibata, M., & Horng, T. (2017). Metabolism supports macrophage activation. Frontiers in Immunology. https://doi.org/10.3389/fimmu.2017.00061

Leitinger, N., & Schulman, I. G. (2013). Phenotypic polarization of macrophages in atherosclerosis. Arteriosclerosis, Thrombosis, and Vascular Biology, 33(6), 1120–1126. https://doi.org/10.1161/ATVBAHA.112.300173

Lhoták, Š., Gyulay, G., Cutz, J., Al-Hashimi, A., Trigatti, B. L., Richards, C. D., … Austin, R. C. (2016). Characterization of Proliferating Lesion-Resident Cells During All Stages of Atherosclerotic Growth. Journal of the American Heart Association, 5(8), e003945. https://doi.org/10.1161/JAHA.116.003945

Li, X., Jiang, S., & Tapping, R. I. (2010). Toll-like receptor signaling in cell proliferation and survival. Cytokine. https://doi.org/10.1016/j.cyto.2009.08.010

Libby, P. (2012). History of Discovery : Inflammation in Atherosclerosis. Arterioscler Thromb Vasc Biol., 32(9), 2045–2051. https://doi.org/10.1161/ATVBAHA.108.179705.History

Libby, P. (2017). Interleukin-1 Beta as a Target for Atherosclerosis Therapy. Journal of the American College of Cardiology, 70(18), 2278–2289. https://doi.org/10.1016/j.jacc.2017.09.028

Lin, F.-J., Tseng, W.-K., Yin, W.-H., Yeh, H.-I., Chen, J.-W., & Wu, C.-C. (2017). Residual risk factors to predict major adverse cardiovascular events in atherosclerotic cardiovascular disease patients with and without diabetes *mellitus*. Scientific Reports, 7(1). https://doi.org/10.1038/s41598-017-08741-0

Liu, P. S., Wang, H., Li, X., Chao, T., Teav, T., Christen, S., … Ho, P. C. (2017). α-ketoglutarate orchestrates macrophage activation through metabolic and epigenetic reprogramming. Nature Immunology, 18(9), 985–994. https://doi.org/10.1038/ni.3796

Lusis, A. J. (2000). Atherosclerosis. Nature, 407(September), 233–241. https://doi.org/10.1038/35025203

Mantovani, A., Biswas, S. K., Galdiero, M. R., Sica, A., & Locati, M. (2013). Macrophage plasticity and polarization in tissue repair and remodelling. Journal of Pathology. https://doi.org/10.1002/path.4133

Mills, C. D., Kincaid, K., Alt, J. M., Heilman, M. J., & Hill, A. M. (2000). M-1/M-2 Macrophages and the Th1/Th2 Paradigm. The Journal of Immunology, 164(12), 6166–6173. https://doi.org/10.4049/jimmunol.164.12.6166

Mills, E. L., & O'Neill, L. A. (2016). Reprogramming mitochondrial metabolism in macrophages as an anti-inflammatory signal. European Journal of Immunology, 46(1), 13–21. https://doi.org/10.1002/eji.201445427

Moore, K. J., & Tabas, I. (2011). Macrophages in the pathogenesis of atherosclerosis. Cell, 145(3), 341–355. https://doi.org/10.1016/j.cell.2011.04.005

Mosser, D. M., Zhang, X., & David M. Mosser and Xia Zhang. (2008). Activation of Murine Macrophages. Current Protocols in Immunology, Chapter 14, Unit 14.2. https://doi.org/10.1002/0471142735.im1402s83.Activation

Mukhopadhyay, D., Mukherjee, S., Roy, S., Dalton, J. E., Kundu, S., Sarkar, A., … Chatterjee, M. (2015). M2 Polarization of Monocytes-Macrophages Is a Hallmark of Indian Post Kala-Azar Dermal Leishmaniasis. PLoS Neglected Tropical Diseases, 9(10). https://doi.org/10.1371/journal.pntd.0004145

Murphy, A. J., & Tall, A. R. (2014). Proliferating macrophages populate established atherosclerotic lesions. Circulation Research, 114(2), 236–238. https://doi.org/10.1161/CIRCRESAHA.113.302813

Murray, P. J., Allen, J. E., Biswas, S. K., Fisher, E. A., Gilroy, D. W., Goerdt, S., … Wynn, T. A. (2014). Macrophage Activation and Polarization: Nomenclature and Experimental Guidelines. Immunity. https://doi.org/10.1016/j.immuni.2014.06.008

Netea, M. G., Nold-Petry, C. A., Nold, M. F., Joosten, L. A. B., Opitz, B., Van Der Meer, J. H. M., … Dinarello, C. A. (2009). Differential requirement for the activation of the inflammasome for processing and release of IL-1β in monocytes and macrophages. Blood, 113(10), 2324–2335. https://doi.org/10.1182/blood-2008-03-146720

O'Neill, L. A. J., Kishton, R. J., & Rathmell, J. (2016). A guide to immunometabolism for immunologists. Nature Reviews Immunology. https://doi.org/10.1038/nri.2016.70

O'Neill, L. A. J., & Pearce, E. J. (2016). Immunometabolism governs dendritic cell and macrophage function. The Journal of Experimental Medicine, 213(1), 15–23. https://doi.org/10.1084/jem.20151570

Ohlsson, S. M., Linge, C. P., Gullstrand, B., Lood, C., Johansson, Å., Ohlsson, S., … Hellmark, T. (2014). Serum from patients with systemic vasculitis induces alternatively activated macrophage M2c polarization. Clinical Immunology, 152(1–2), 10–19. https://doi.org/10.1016/j.clim.2014.02.016

Orekhov, A. N., R. Andreeva, E., Mikhailova, I. A., & Gordon, D. (1998). Cell proliferation in normal and atherosclerotic human aorta: Proliferative splash in lipid-rich lesions. Atherosclerosis, 139(1), 41–48. https://doi.org/10.1016/S0021-9150(98)00044-6

R Development Core Team. (2016). R: A Language and Environment for Statistical Computing. R Foundation for Statistical Computing Vienna Austria, 0, {ISBN} 3-900051-07-0. https://doi.org/10.1038/sj.hdy.6800737

Rajaḿaki, K., Lappalainen, J., Öörni, K., Välimäki, E., Matikainen, S., Kovanen, P. T., & Kari, E. K. (2010). Cholesterol crystals activate the NLRP3 inflammasome in human macrophages: A novel link between cholesterol metabolism and inflammation. PLoS ONE, 5(7). https://doi.org/10.1371/journal.pone.0011765

Rekhter, M. D., & Gordon, D. (1995). Active proliferation of different cell types, including lymphocytes, in human atherosclerotic plaques. American Journal of Pathology, 147(3), 668–677.

Ridker, P. M. (2014). LDL cholesterol: Controversies and future therapeutic directions. The Lancet, 384(9943), 607–617. https://doi.org/10.1016/S0140-6736(14)61009-6

Ridker, P. M., Everett, B. M., Thuren, T., MacFadyen, J. G., Chang, W. H., Ballantyne, C., … Glynn, R. J. (2017). Antiinflammatory Therapy with Canakinumab for Atherosclerotic Disease. New England Journal of Medicine, NEJMoa1707914. https://doi.org/10.1056/NEJMoa1707914

Robbins, C. S., Hilgendorf, I., Weber, G. F., Theurl, I., Iwamoto, Y., Figueiredo, J.-L., … Swirski, F. K. (2013a). Local proliferation dominates lesional macrophage accumulation in atherosclerosis. Nature Medicine, 19(9), 1166–1172. https://doi.org/10.1038/nm.3258

Robbins, C. S., Hilgendorf, I., Weber, G. F., Theurl, I., Iwamoto, Y., Figueiredo, J.-L., … Swirski, F. K. (2013b). Local proliferation dominates lesional macrophage accumulation in atherosclerosis. Nature Medicine, 19(9), 1166–1172. https://doi.org/10.1038/nm.3258

Roszer, T. (2015). Understanding the mysterious M2 macrophage through activation markers and effector mechanisms. Mediators of Inflammation. https://doi.org/10.1155/2015/816460

Saha, B., Bruneau, J. C., Kodys, K., & Szabo, G. (2015). Alcohol-induced miR-27a regulates differentiation and M2 macrophage polarization of normal human monocytes. Journal of Immunology (Baltimore, Md. : 1950), 194(7), 3079–3087. https://doi.org/10.4049/jimmunol.1402190

Sakakura, K., Nakano, M., Otsuka, F., Ladich, E., Kolodgie, F. D., & Virmani, R. (2013). Pathophysiology of atherosclerosis plaque progression. Heart Lung and Circulation. https://doi.org/10.1016/j.hlc.2013.03.001

Scholzen, T., & Gerdes, J. (2000). The Ki-67 protein: From the known and the unknown. Journal of Cellular Physiology. https://doi.org/10.1002/(SICI)1097-4652(200003)182:3<311::AID-JCP1>3.0.CO;2-9

Seo, J. W., Yang, E. J., Yoo, K. H., & Choi, I. H. (2015). Macrophage differentiation from monocytes is influenced by the lipid oxidation degree of low density lipoprotein. Mediators of Inflammation, 2015. https://doi.org/10.1155/2015/235797

Shannon, P., Markiel, A., Ozier, O., Baliga, N. S., Wang, J. T., Ramage, D., … Ideker, T. (2003). Cytoscape: A software Environment for integrated models of biomolecular interaction networks. Genome Research, 13(11), 2498–2504. https://doi.org/10.1101/gr.1239303

Silverman, M. G., Ference, B. A., Im, K., Wiviott, S. D., Giugliano, R. P., Grundy, S. M., … Sabatine, M. S. (2016). Association Between Lowering LDL-C and Cardiovascular Risk Reduction Among Different Therapeutic Interventions. JAMA, 316(12), 1289. https://doi.org/10.1001/jama.2016.13985

Surma, M. A., Herzog, R., Vasilj, A., Klose, C., Christinat, N., Morin-Rivron, D., … Sampaio, J. L. (2015). An automated shotgun lipidomics platform for high throughput, comprehensive, and quantitative analysis of blood plasma intact lipids. European Journal of Lipid Science and Technology, 117(10), 1540–1549. https://doi.org/10.1002/ejlt.201500145

Tabas, I., García-Cardeña, G., & Owens, G. K. (2015). Recent insights into the cellular biology of atherosclerosis. Journal of Cell Biology, 209(1), 13–22. https://doi.org/10.1083/jcb.201412052

Tang, J., Lobatto, M. E., Hassing, L., van der Staay, S., van Rijs, S. M., Calcagno, C., … Mulder, W. J. M. (2015). Inhibiting macrophage proliferation suppresses atherosclerotic plaque inflammation. Science Advances, 1(3), e1400223–e1400223. https://doi.org/10.1126/sciadv.1400223

Tiemessen, M. M., Jagger, A. L., Evans, H. G., Van Herwijnen, M. J. C., John, S., & Taams, L. S. (2007). CD4+CD25+Foxp3+ regulatory T cells induce alternative activation of human monocytes/macrophages. PNAS, 104, 19446 –19451. https://doi.org/10.1073/pnas.0706832104

Tur, J., Vico, T., Lloberas, J., Zorzano, A., & Celada, A. (2017). Macrophages and Mitochondria: A Critical Interplay Between Metabolism, Signaling, and the Functional Activity. In Advances in Immunology (Vol. 133, pp. 1–36). https://doi.org/10.1016/bs.ai.2016.12.001

Van den Bossche, J., O'Neill, L. A., & Menon, D. (2017). Macrophage Immunometabolism: Where Are We (Going)? Trends in Immunology. https://doi.org/10.1016/j.it.2017.03.001

Vander Heiden, M. G., Cantley, L. C., & Thompson, C. B. (2009). Understanding the Warburg Effect: The Metabolic Requirements of Cell Proliferation. Science, 324(5930), 1029–1033. https://doi.org/10.1126/science.1160809

Vichai, V., & Kirtikara, K. (2006). Sulforhodamine B colorimetric assay for cytotoxicity screening. Nature Protocols, 1(3), 1112–1116. https://doi.org/10.1038/nprot.2006.179

Viegas, M. S., Estronca, L. M. B. B., & Vieira, O. V. (2012). Comparison of the Kinetics of Maturation of Phagosomes Containing Apoptotic Cells and IgG-Opsonized Particles. PLoS ONE, 7(10). https://doi.org/10.1371/journal.pone.0048391

Walton, K. A., Hsieh, X., Gharavi, N., Wang, S., Wang, G., Yeh, M., … Berliner, J. A. (2003). Receptors involved in the oxidized 1-palmitoyl-2-arachidonoyl-sn-glycero-3-phosphorylcholine-mediated synthesis of interleukin-8: A role for toll-like receptor 4 and a glycosylphosphatidylinositol-anchored protein. Journal of Biological Chemistry, 278(32), 29661–29666. https://doi.org/10.1074/jbc.M300738200

Wang, L., Zhu, R., Huang, Z., Li, H., & Zhu, H. (2013). Lipopolysaccharide-induced toll-like receptor 4 signaling in cancer cells promotes cell survival and proliferation in hepatocellular carcinoma. Digestive Diseases and Sciences, 58(8), 2223–2236. https://doi.org/10.1007/s10620-013-2745-3

Ward, J. R., West, P. W., Ariaans, M. P., Parker, L. C., Francis, S. E., Crossman, D. C., … Wilson, H. L. (2010). Temporal interleukin-1beta secretion from primary human peripheral blood monocytes by P2X7-independent and P2X7-dependent mechanisms. Journal of Biological Chemistry, 285(30), 23147–23158. https://doi.org/10.1074/jbc.M109.072793

Weber, C., & Noels, H. (2011). Atherosclerosis: Current pathogenesis and therapeutic options. Nature Medicine. https://doi.org/10.1038/nm.2538

Wickham, H. (2009). ggplot2 Elegant Graphics for Data Analysis. Media (Vol. 35). https://doi.org/10.1007/978-0-387-98141-3

Wickham, H. (2016). tidyverse: Easily Install and Load "Tidyverse" Packages. R package version 1.0.0. Retrieved from https://cran.r-project.org/package=tidyverse

Winder, W. W., Holmes, B. F., Rubink, D. S., Jensen, E. B., Chen, M., & Holloszy, J. O. (2000). Activation of AMP-activated protein kinase increases mitochondrial enzymes in skeletal muscle. Journal of Applied Physiology (Bethesda, Md. : 1985), 88(6), 2219–2226.

Wise, D. R., DeBerardinis, R. J., Mancuso, A., Sayed, N., Zhang, X.-Y., Pfeiffer, H. K., … Thompson, C. B. (2008). Myc regulates a transcriptional program that stimulates mitochondrial glutaminolysis and leads to glutamine addiction. Proceedings of the National Academy of Sciences, 105(48), 18782–18787. https://doi.org/10.1073/pnas.0810199105

Woollard, K. J., & Geissmann, F. (2010). Monocytes in atherosclerosis: subsets and functions. Nature Reviews Cardiology, 7(2), 77–86. https://doi.org/10.1038/nrcardio.2009.228

Wu, H., & Ballantyne, C. M. (2017). Dyslipidaemia: PCSK9 inhibitors and foamy monocytes in familial hypercholesterolaemia. Nature Reviews Cardiology. https://doi.org/10.1038/nrcardio.2017.75

Xu, L., Dai Perrard, X., Perrard, J. L., Yang, D., Xiao, X., Teng, B. B., … Wu, H. (2015). Foamy monocytes form early and contribute to nascent atherosclerosis in mice with hypercholesterolemia. Arteriosclerosis, Thrombosis, and Vascular Biology, 35(8), 1787–1797. https://doi.org/10.1161/ATVBAHA.115.305609

Xue, J., Schmidt, S. V., Sander, J., Draffehn, A., Krebs, W., Quester, I., … Schultze, J. L. (2014). Transcriptome-Based Network Analysis Reveals a Spectrum Model of Human Macrophage Activation. Immunity, 40(2), 274–288. https://doi.org/10.1016/j.immuni.2014.01.006

Yang, J., Zhang, L., Yu, C., Yang, X.-F., & Wang, H. (2014). Monocyte and macrophage differentiation: circulation inflammatory monocyte as biomarker for inflammatory diseases. Biomarker Research, 2(1), 1. https://doi.org/10.1186/2050-7771-2-1

Yona, S., Kim, K. W., Wolf, Y., Mildner, A., Varol, D., Breker, M., … Jung, S. (2013). Fate Mapping Reveals Origins and Dynamics of Monocytes and Tissue Macrophages under Homeostasis. Immunity, 38(1), 79–91. https://doi.org/10.1016/j.immuni.2012.12.001

4.6 SUPPLEMENTAL INFORMATION

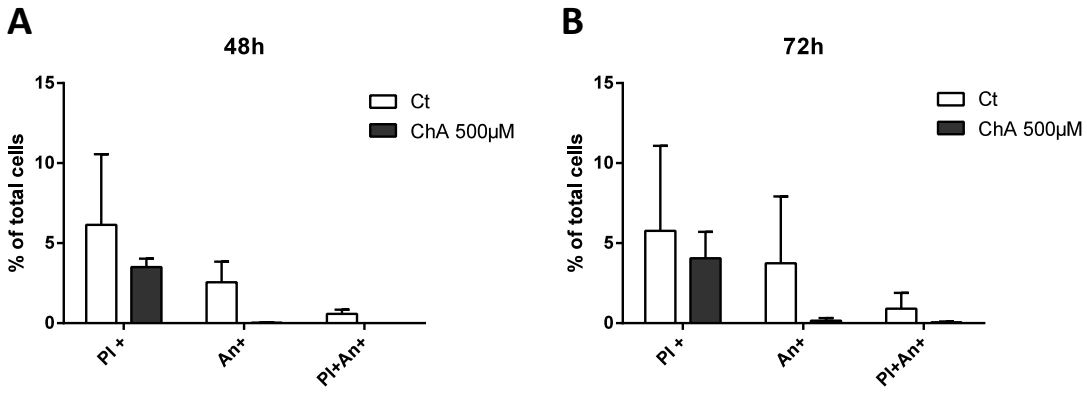

Supplementary Figure 4.1 | ChA do not induces macrophages cell death.

BMDM were incubated for 48 h (A) or 72 h (B) with ChA or vehicle (control) and the percentage of annexin (An^+) propidium iodide (PI^+) and An and PI positive cells (An^+PI^+) were evaluated without cell detachment. Data are mean±SEM of two independent experiments.

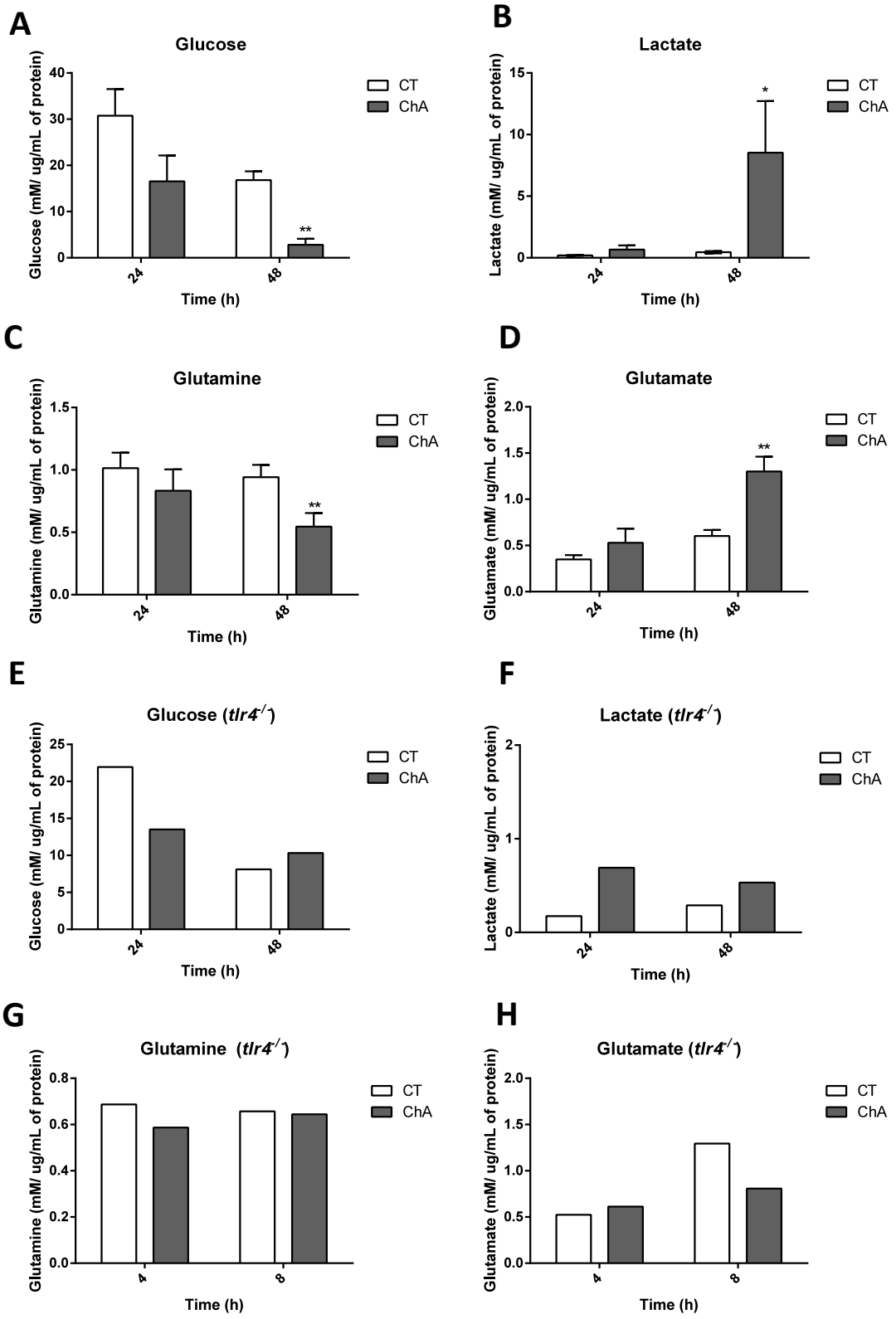

Supplementary Figures 4.2 | ChA induces glucose and glutamine consumption in an TLR4 dependent pathway.

A-H. Quantification of metabolites concentration in the supernatants after 24 h or 48 h of WT (n=3) and *tlr4*$^{-/-}$ (n=1) macrophages lipid treatment. Glucose, lactate, glutamine and glutamate concentrations in the culture supernatant were determined with automated enzymatic assays and normalized to the total cell protein. The values are the mean±SEM; **, p<0.01; *, p<0.05.

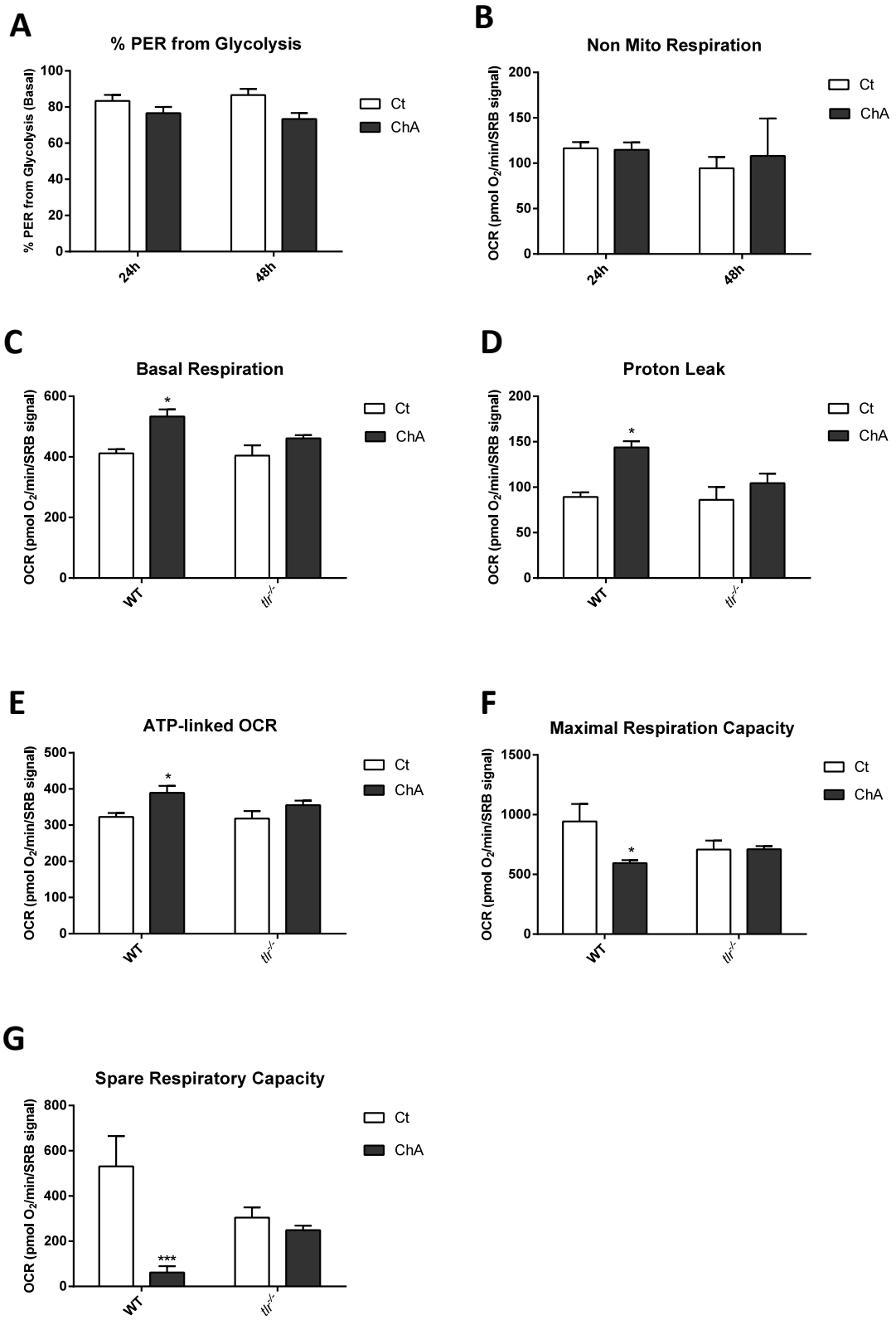

Supplementary Figures 4.3 | Metabolic shift induced by ChA-treated macrophages. Mitochondrial effect induced by ChA is TLR4 dependent.

A. Effect of ChA on the percentage of proton efflux rate (PER) associated to glycolysis; **B.** Quantification of OCR resulting from non-mitochondrial oxygen consumption after BMDM treatment with ChA or vehicle (control) for 24 h or 48 h; **C-H.** Measurement of OCR associated with basal respiration **(D)**, pronton leak **(E)**, ATP production **(F)**, maximal response **(G)** and spare respiratory capacity **(H)** after incubation of WT and *tlr4*$^{-/-}$ macrophages with ChA for 24 h or 48 h. The values are the mean±SEM of three independent experiments; ***, p<0.001; *, p<0.05.

05 EXOCYTOSIS OF DYSFUNCTIONAL LYSOSOMES AS A NEW PARADIGM SHIFT IN THE PATHOGENESIS OF ATHEROSCLEROSIS

5.1 ABSTRACT

Atherosclerosis is a chronic inflammatory disease, characterized by retention of low-density lipoproteins (LDL) in the arterial intima that undergo modifications such as oxidation. A key event in the atherogenic process is the formation of lipid-loaded macrophages, also known as lipidotic cells, which exhibit an irreversible accumulation of undigested lipids in the late endocytic compartments. However, some of the etiological factors involved in this outcome are not known. We have identified, in the plasma of cardiovascular disease (CVD) patients using a shotgun lipidomics approach, a new family of oxidized lipids named cholesteryl hemiesters (ChE), which form as end products of cholesteryl ester (CE) oxidation. Here, we report that the most abundant ChE (ChA) in blood causes lysosomal enlargement, peripheral lysosomal positioning, reduced lysosomal cargo degradation and lipidosis in macrophages. As a result of lysosomal-induced stress, ChA stimulated an increase in lysosomal biogenesis. It was also revealed that ChA induced a delay in the cellular trafficking interfering with macrophage function. Importantly, dysfunctional enlarged peripheral lysosomes are mostly exocytic, secreting their undigested luminal contents into the extracellular milieu, which can contribute to the pathology. In conclusion, we identified ChA as a proatherogenic lipid being responsible for the exocytosis of dysfunctional lysosomes and this is a new paradigm shift in pathogenesis of atherosclerosis.

5.2 INTRODUCTION

According to the World Health Organization, cardiovascular diseases are the principal cause of death worldwide and atherosclerosis is the leading cause of vascular disease. Macrophages are one of the central players in atherosclerotic initiation and progression (Still and Marriott 1964). After subendothelial retention of LDL and its oxidative modification in the arterial intima, macrophages phagocytose this deposited lipid. Progressively, macrophage dysfunction leads to inefficient digestion of these particles, the formation of foam cells, subsequent cell apoptosis, and defective cellular debris clearance (reviewed in (Libby, Ridker, and Maseri 2002; Moore and Tabas 2011)). Thus, understanding the cellular processes behind macrophage dysfunction is a fundamental step in the atherosclerosis field.

Initially, oxidized-LDL (ox-LDL) is internalized by macrophages and processed inside lysosomes. However, with increasing ox-LDL concentration, lysosomes lose their capacity to degrade these particles, culminating in their accumulation. Interestingly, this accumulation exhibits the same characteristics as those observed in the lipidosis manifested in several

lipid storage diseases (Schulze and Sandhoff 2011; Yancey and Jerome 1998; Jerome et al. 2008; Griffin et al. 2005; Jerome 2010). There is already some experimental evidence raising the possibility that lysosome dysfunction is a crucial step in lipidosis and atherosclerotic plaque development (Jerome 2006; Emanuel et al. 2014; Sergin et al. 2017). Jerome and colleagues observed one of the first signs of lysosome dysfunction in macrophages from atherosclerotic plaques. In contrast to the early stages of atherosclerosis, where ox-LDL lipids were effectively hydrolyzed in the lysosome and then stored as lipid droplets in the cytosol, disease progression renders this process inefficient, leading to ox-LDL accumulation within lysosomes (Yancey and Jerome 1998). More recently, it was observed that macrophages isolated from the atherosclerotic plaques of *ApoE*$^{-/-}$ mice fed for 2 months with a Western diet also displayed features of lysosome dysfunction (Emanuel et al. 2014). Interestingly, the same group showed that induction of lysosomal biogenesis in macrophages has anti-atherogenic effects (Emanuel et al. 2014).

Ox-LDL contains an enormous variety of oxidized lipid products with biological activity (Miller and Shyy 2017). ChE, stable oxidized end-products of CE, one of the main components of LDL, are present in ox-LDL (Kamido et al. 1995) and their precursors have been detected in human atheromata (Hutchins, Moore, and Murphy 2011). Through shotgun lipidomics, our group together with Prof. Kai Simons (Lipotype, Dresden, Germany) has detected and identified the most abundant ChE in human plasma - ChA (Chapter 4). It was also observed that patients with cardiovascular pathologies of atherosclerotic origin have higher levels of ChE in the plasma, compared with healthy donors. Our group started by showing the atherogenic capacity of ChE using cholesteryl hemisuccinate (ChS), the only commercial available ChE, incorporated into native LDL particles (ChS-LDL). Through short- (Estronca et al. 2012) and long-term treatment (Domingues et al. 2017) of macrophages with these particles, it was found that ChS-LDL was sufficient to mimic important features of atherogenesis: 1) ChS is cytotoxic and provokes apoptotic cell death; 2) Cells exposed to ChS-LDL irreversibly accumulate undigested lipid (lipidosis) in enlarged lysosomes; 3) Macrophages exhibited lysosomal dysfunction: inhibition of lysosomal cargo degradation and a delay in cargo exit from lysosomes. Thus, the present work aims to identify and understand the mechanism of the molecular etiology of lipidosis and lysosome dysfunction induced by ChA, in macrophages.

Here we show that lysosomes are affected by ChA; changing their intracellular redistribution and morphology, restricting their degradative capacity, and inducing lipid accumulation. One important finding was that enlarged and dysfunctional lysosomes are more exocytic, acting as a probable emergency mechanism, which can initiate and perpetuate inflammation, contributing to atherogenesis.

5.3 RESULTS

5.3.1 ChA induces lysosome enlargement and lipid accumulation in murine macrophages

Macrophages play a critical role in the initiation and development of atherosclerosis. Uncontrolled internalization of ox-LDL through scavenger receptors leads to the accumulation of lipids in cytosolic lipid droplets, forming foam cells, or inside lysosomes – lipidosis (Griffin et al. 2005; Estronca et al. 2012; Yancey and Jerome 2001) at the later stages of atherogenesis. To assess if ChA was affecting lysosomes, RAW 264.7 and BMDM were incubated with ChA-POPC liposomes at a ratio of 65:35. We used POPC liposomes as a ChA vehicle instead of LDL because the lipid was causing aggregation of the latter particles. The toxicity induced by ChA:POPC liposomes towards RAW macrophages is shown in Supplementary Figure 5.1A.

Changes in lysosome morphology are an important first step in the evaluation of lysosomal function. Lysosomes were visualized with antibodies against the lysosomal associated membrane protein-2 (LAMP-2), a transmembrane protein, by immunofluorescence (IF) under a confocal microscope. After 72 h of incubation with 1500 μM ChA, macrophages exhibited a significant increase in lysosomal size in comparison with control cells (cells incubated with POPC liposomes) in a dose dependent manner (Figure 5.1A and D). Furthermore, in ChA-loaded cells, LAMP-2-positive structures were not positive for Early Endosome Antigen 1 (EEA-1), a marker for early endosomes (Supplementary Figure 5.1B). Thus, these large LAMP-positive organelles were not hybrid organelles of the endocytic compartment, as previously demonstrated for ChS (Domingues et al. 2017). Additionally, an increase of neutral lipid accumulation was observed, visualized by BODIPY staining, both in cytosolic lipid droplets and inside lysosomes (Figure 5.1A and C) in ChA-treated cells compared with control cells.

Previous work in our laboratory with ChS showed that the endolysosomal lipid accumulation induced by this oxidized lipid was irreversible (Estronca et al. 2012). Therefore, we sought to determine if ChA was having the same effect. Lysosome morphology and lipid accumulation reversibility in RAW cells was performed through a pulse-chase experiment. Cells were treated for 72 h with ChA and then chased for another 72 h (Figure 5.1B, E and F). Lysosome morphology and neutral lipid fluorescence were analyzed as described above. The results showed that for the lower lipid concentration (25 μM), lipid accumulation and lysosome area were completely reversible (Figure 5.1E and F). However, for the higher concentrations of ChA a delay in cell recovery for both measured parameters was observed. After the chase, ChA-laden cells still presented significant lipid accumulation and an increase in lysosomal area compared with control cells. Moreover, to gain more insights at the ultrastructural level, we subjected ChA-treated RAW cells to transmission electron microscopy (TEM). As can be observed in Figure 5.2, in ChA-treated BMDM there was an increase in the number

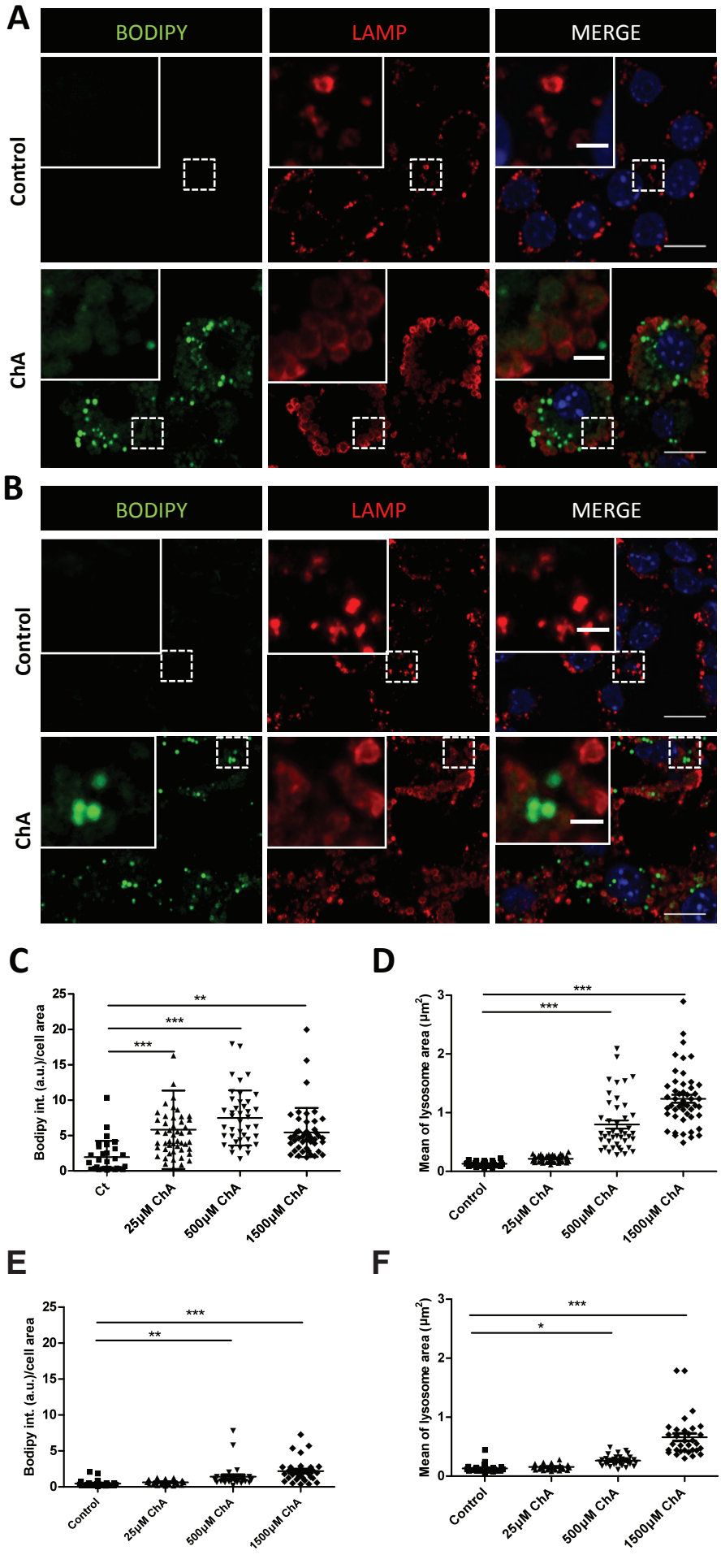
A
BODIPY
LAMP
MERGE
Control
ChA
B
BODIPY
LAMP
MERGE
Control
ChA
C
Bodipy int. (a.u.)/cell area
Ct
25µM ChA
500µM ChA
1500µM ChA
D
Mean of lysosome area (µm²)
Control
25µM ChA
500µM ChA
1500µM ChA
E
Bodipy int. (a.u.)/cell area
Control
25µM ChA
500µM ChA
1500µM ChA
F
Mean of lysosome area (µm²)
Control
25µM ChA
500µM ChA
1500µM ChA

Figure 5.1 | ChA induces lysosomal enlargement and neutral lipid accumulation in RAW 264.7 macrophages.

A and **B.** Representative images of control RAW cells or cells incubated with 1500 µM of ChA. **A.** RAW macrophages were incubated with POPC (control) or ChA liposomes for 72 h and then stained with DAPI, BODIPY and anti-Lysosomal Associated membrane Protein-2 (LAMP-2, a marker of late endocytic compartments) antibodies to visualize nucleus, neutral lipids and late endocytic compartments, respectively. The merged image shows neutral lipids in green, late endocytic compartments in red and nucleus in blue. The insets are enlargements of the areas outlined with the white dashed boxes. **B.** Macrophages were incubated with POPC (control) or ChA for 72 h (pulse) after this incubation time the lipids were removed and macrophages were incubated again for 72 h (chase). As in **A.**, Macrophages were stained with DAPI, BODIPY and LAMP-2 antibodies. The merged image shows neutral lipids in green, late endocytic compartments in red and nucleus in blue. The insets are enlargements of the areas outlined with the white dashed boxes. Bars, 10 µm and 2 µm in the insets. **C**-**F**. Quantification of total neutral lipid accumulation and lysosomal area in macrophages pulsed during 72 h with ChA (**C** and **D**) and chased 72 h (**E** and **F**). The results are the mean±SEM of three independent experiments. In every experiment at least 20 individual cells were analyzed. ***, p<0.001; **, p<0.01; *, p<0.05.

of large vesicles present at the periphery of the cells, compared with control cells. We await Immuno-gold TEM data to confirm if these peripheral vesicles are LAMP-positive and correspond to the enlarged late endosomes/lysosomes observed under the confocal microscope.

To confirm if these results were also observed in an *in vitro* model of post-mitotic macrophages with higher physiological relevance, we decided to repeat the same experiments in primary macrophages. BMDM were exposed to 500 µM ChA for 72 h (Figure 5.3A) and then chased for an additional 72 h period of time (Figure 5.3B). The results depicted in Figure 5.3A and quantified in Figures 5.3C and D showed that in BMDM, ChA also induced lysosome enlargement and neutral lipid accumulation within these organelles and in cytosolic lipid droplets (as already observed in chapter 4). However, and in contrast with what was observed in RAW cells, these outcomes were irreversible (Figure 5.3E and F). The lower concentration of ChA necessary to observe lysosome morphological changes and lipid accumulation, as well as the irreversibility of these phenotypes were probably due to the fact that BMDM are post-mitotic cells in contrast with the RAW cells that divide every 12 h.

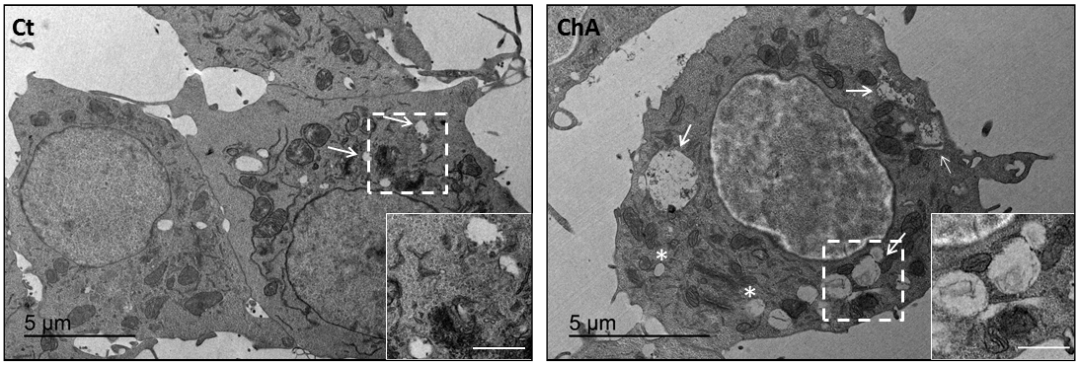

Figure 5.2 | ChA induces lysosomal enlargement and neutral lipid accumulation in RAW 264.7 macrophages.

Transmission electron microscopy of cells treated for 72 h with POPC liposomes (Ct) and ChA liposomes. In macrophages treated with ChA, cytoplasmic lipid droplets (organelles with a single monolayer, *) and vesicular enlarged structures with a bilayer and with electron dense material are visible in cells treated with ChA. In Ct and ChA macrophages the arrows point to bilayer vesicles with electron dense material inside. Bars, 5µm and the inserts 2 µm.

Since enlargement of lysosomes and lipidosis was observed in both type of macrophages and it was easier to manipulate and image RAW cells, we decided to pursue the experiments in these cells.

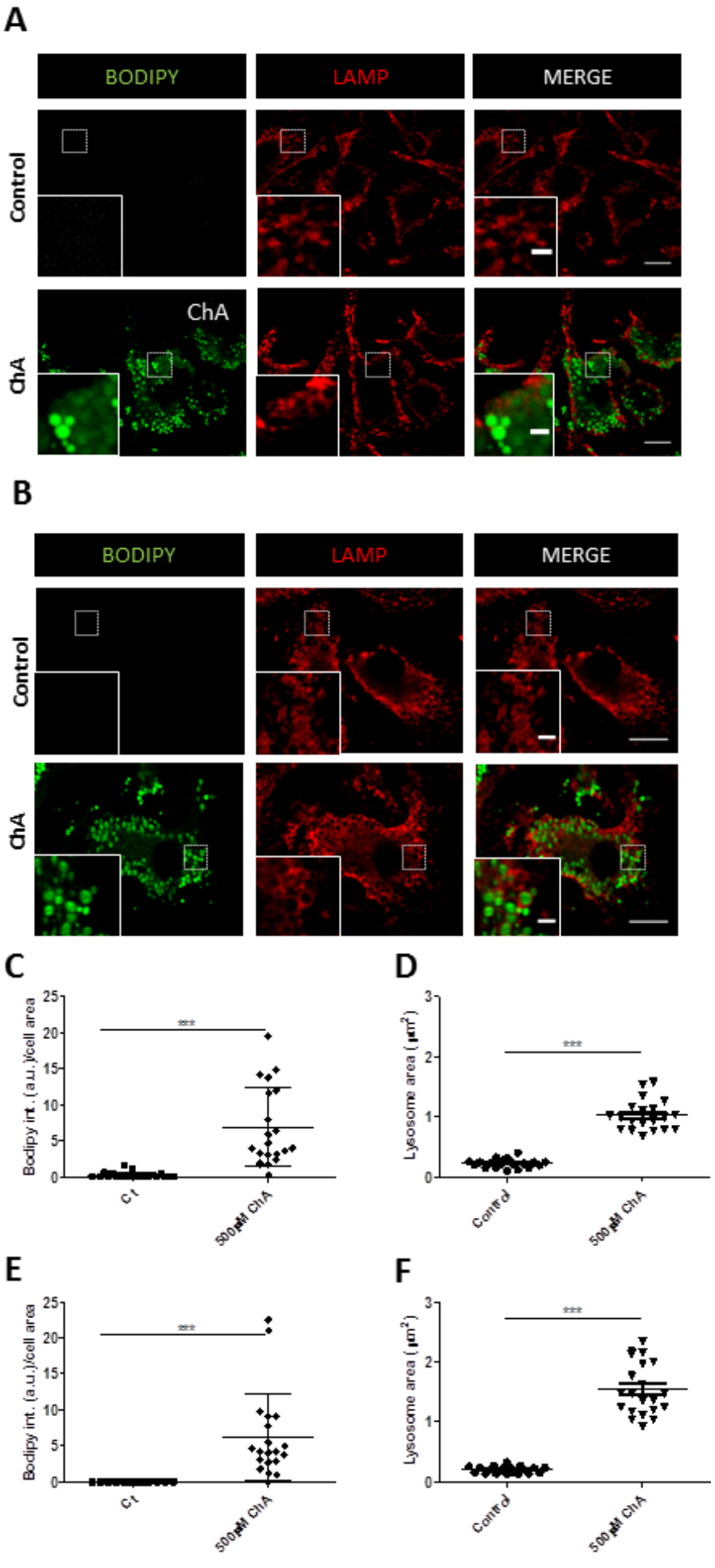
A
BODIPY
LAMP
MERGE
Control
ChA
ChA
B
BODIPY
LAMP
MERGE
Control
ChA
C
Bodipy int. (a.u.)/cell area
***
Ctrl
500µM ChA
D
Lysosome area (µm²)
***
Control
500 µM ChA
E
Bodipy int. (a.u.)/cell area
***
Ctrl
500µM ChA
F
Lysosome area (µm²)
***
Control
500 µM ChA

Figure 5.3 | ChA induces irreversible lysosomal lipid accummulation in primary Bone Marrow Derived Macrophages (BMDM).

BMDM were exposed to POPC (control) or to ChA for 72 h **(A)** and chased for another 72 h **(B)**. Then cells were fixed and double labeled with BODIPY and anti-LAMP-2 antibodies to visualize neutral lipids and late endocytic compartments, respectively. The merged image shows neutral lipids in green and late endocytic compartments in red. The insets are enlargements of the areas outlined with the white dashed boxes. Bars, 10 µm and 2 µm in insets. **C-F**, Quantification of neutral lipid accumulation and lysosomal area in BMDM pulsed during 72 h with POPC or ChA (**C** and **D**, respectively) and chased for 72 h (**E** and **F**, respectively). The results are the mean±SEM of 20 individual cells analyzed. ***, p<0.001.

5.3.2 ChA interferes with lysosome positioning

The cellular lysosomal population is very heterogeneous not only in subcellular distribution, but also in composition and luminal pH (Johnson et al. 2016; Luzio, Pryor, and Bright 2007). To better characterize and quantify the effect of ChA on lysosome positioning, we used bespoke analysis software, produced in house. The distance from the nucleus (centroide) to lysosomes was assessed in control and ChA-treated cells. As schematically illustrated in Figure 5.4A, lysosome-nucleus membrane distance was normalized to the distance between the nuclear membrane and the cell membrane in same direction. Thus, if the value of the measured distance was lower than 0.5, it means that lysosomes were in the perinuclear region. On the other hand, values close to 1 indicated a closer proximity to the plasma membrane (PM). This normalization was required, because of the different cell sizes observed after ChA-treatment. In Figure 5.4B, the plotted normalized lysosomal distances showed a normal distribution in cells treated with ChA, with an average value of 0.687 from the nuclear membrane. This distribution means that 50% of total analyzed lysosomes were at a distance between 0.687 and 1, indicating a more peripheral lysosomal distribution in ChA-treated cells, while in control cells lysosomes are randomly distributed.

To confirm this result, ChA-treated cells were fixed, stained with LAMP antibodies and an inward region of 2 µm from the boundary of the cells was defined to create two different cell areas. Peripheral cell area was defined as area 1 and the perinuclear region as area 2 (Figure 5.4C). The definition of these areas was not possible in control cells due to the reduced cytoplasmatic volume, which in several cells was lower than 2 µm between the cell membrane and nucleus. Through the total lysosomal fraction analysis, it was observed that macrophages exposed to ChA presented an increase in the lysosomal population in the peripheral region (Figure 5.4D). Additionally, measuring the lysosome area of lysosomal population from area 1 and 2, it was also demonstrated that peripheral lysosomes were enlarged compared with those in the perinuclear area (Figure 5.4E).

5.3.3 ChA affects transport of endocytic cargo to the lysosomes

Macrophages are specialized phagocytic cells, capable of internalizing a wide variety of cargo by receptor mediated or through a non-specific pathway. Alterations in lysosome morphology and positioning are expected to affect intracellular trafficking. Thus, we investigated whether this was indeed the case in ChA-treated macrophages. We started by challenging the cells with different types of endocytic cargo and then followed their intracellular transport.

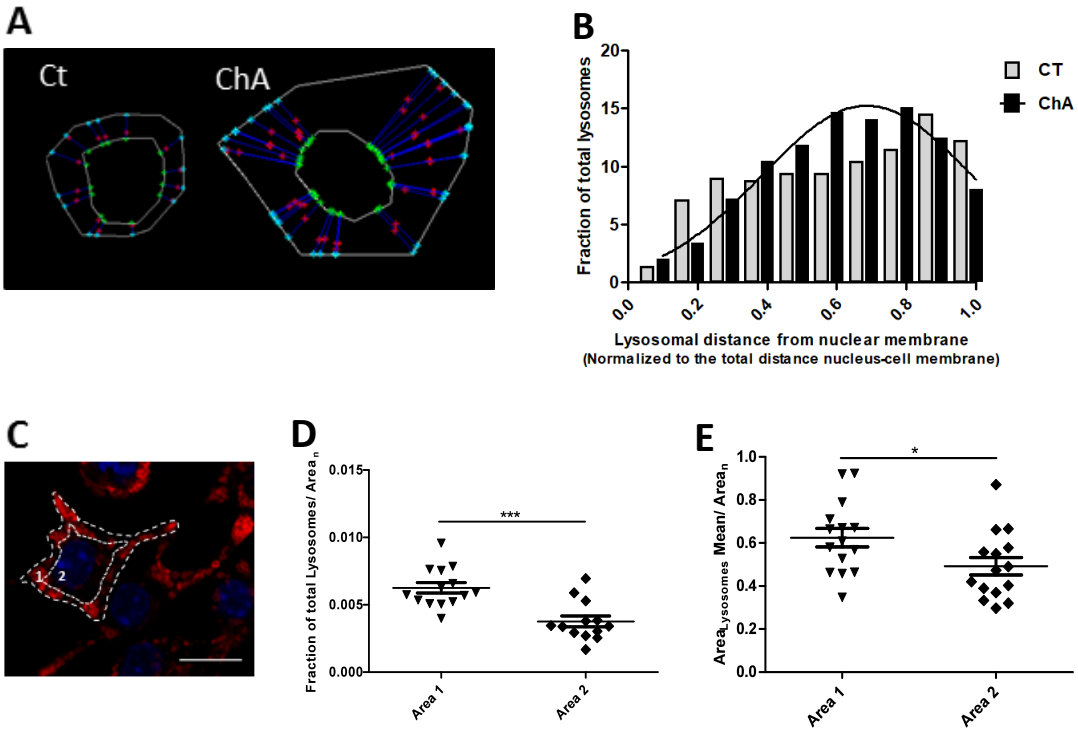

Figure 5.4 | In ChA treated macrophages lysosomes are in the cell periphery.

Macrophages incubated with 1500 µM ChA for 72 h were pulsed with FITC-dextran and then chased to stain lysosomes. After fixation, cells were imaged using confocal microscopy. The distance between each lysosome and the nucleus membrane was performed using a in-house developed software and normalized to the total distance between nucleus and cell membrane. **A.** Schematic presentation of the methodology used to measure lysosome positioning in cells treated with POPC or ChA. **B.** The distribution of lysosome in ChA-treated cells was fitted with a gaussian curve. In ChA incubated RAW macrophages, lysosome positioning is markedly altered with most residing in the peripheral region adjacent to the cell membrane. 20 cells were analyzed from two independent experiments. **C.** Lysosomal distribution in two defined areas: area (1) was defined as cell peripheral and area (2) as perinuclear area. Macrophages incubated with ChA for 72 h were stained with LAMP-2 antibodies to visualize lysosomes. **D-E.** Quantification of lysosomes number **(D)** and area **(E)** per area 1 and 2. Bars, 10 µm. Data represent the mean±SEM of two independent experiments. Number of cells 15. Statistical significance was assessed by a t-test: *, p<0.05 and **, p<0.01.

ChA-treated macrophages (for 72 h) were loaded with BSA conjugated with Texas Red, transferrin conjugated with rhodamine or with fluorescent-labeled dextran, a fluid phase marker. As shown in Figure 5.5A and quantified in B, BSA uptake was not reduced by ChA treatment. Similar results were observed for transferrin (Figure 5.5E, 0 mim and Supplementary Figure 5.3E) and for dextran (Supplementary Figure 5.2A and B). These results suggested that independently of internalization pathway, receptor-mediated or not, the uptake of endocytic cargo was not affected by ChA.

Regardless of the internalization mode, endocytosed cargo is delivered to the early endosomes, where cargo sorting occurs. Cargo-specific sorting leads to distinct subsequent cargo itineraries. Cargo can be routed from the early endosomes to late endosomes and lysosomes for degradation or can be recycled back to the PM, fast recycling or to the Trans Golgi Network (TGN). BSA and dextran are both targeted to lysosomes while transferrin follows the fast recycling pathway. Next, we sought to investigate whether the transport of endocytic cargo (BSA conjugated with Texas Red or dextran) to the lysosomes and recycling (transferrin) were affected in macrophages exposed to ChA. As shown in Figure 5.5C and D and Supplementary Figure 5.2C and D, transport of BSA and dextran to the lysosomes was delayed in ChA-treated cells. Cargo delivery to lysosomes was quantified in fixed cells immunostained for LAMP after

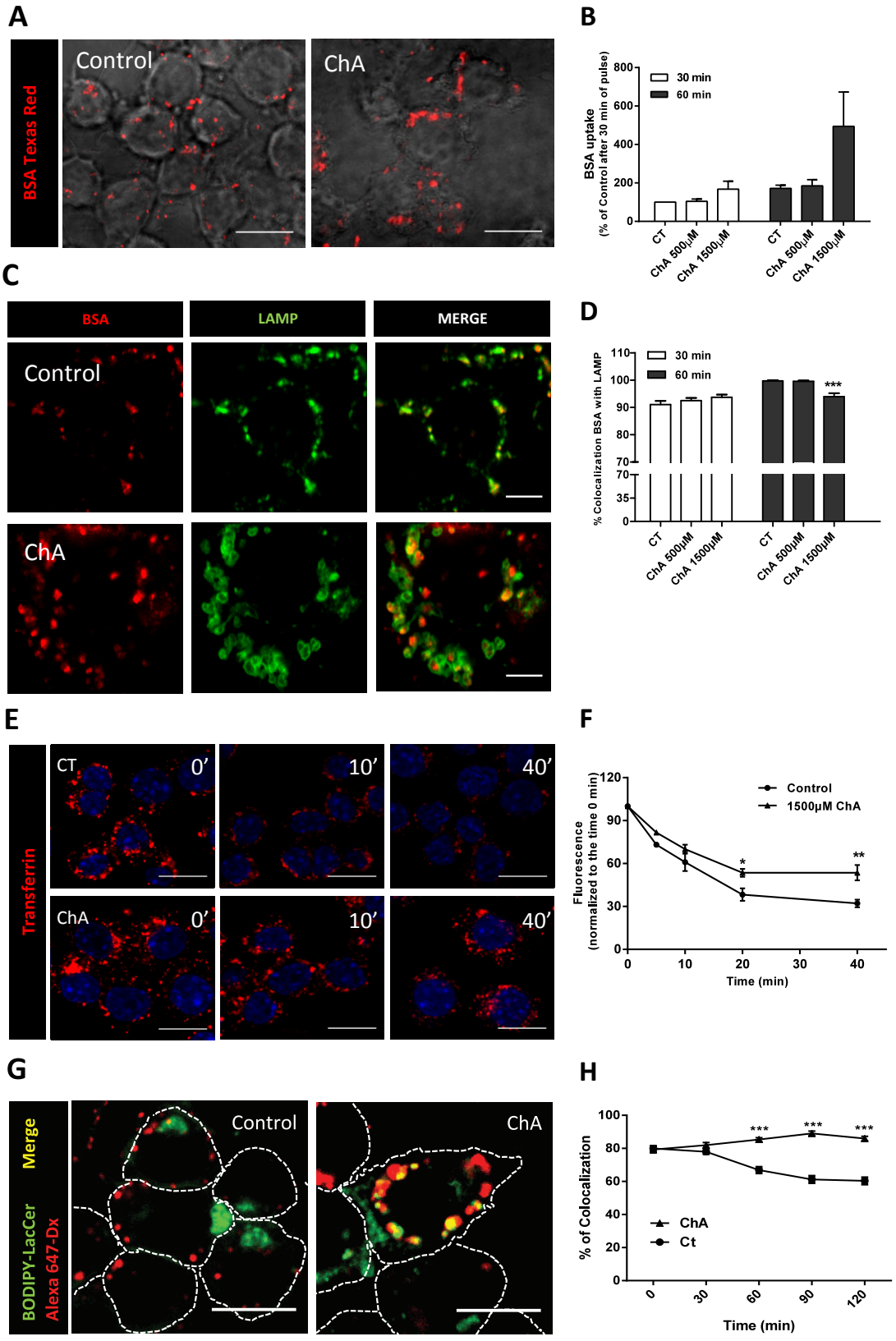

Figure 5.5 | ChA has an effect on the transport of internalized cargo to the lysosomes.

A. Effect of ChA on BSA-Texas Red internalization. Representative confocal images of fixed cells incubated with BSA for 60 min. To avoid BSA degradation the lysosomal pH was neutralized with ammonium chloride. This chemical was added 20 min after BSA addition. The fluorescence images are merged with the corresponding DIC images. **B.** BSA-Texas Red-uptake quantified by Flow Cytometry; **C.** Representative confocal images of BSA-Texas Red pulsed macrophages, chased for 60 min and stained with LAMP-2. The first and the second columns show BSA (red), and LAMP-2 (green) staining, respectively. The third column are composites of the BSA and LAMP-2. **D.** Overlap quantitation of BSA positive and LAMP-2 positive vesicles. POPC- and ChA-treated macrophages were pulsed with BSA-Texas Red during 30 min and then chased for 30 min or 60 min. The colocalization between BSA-containing vesicles and LAMP was quantified in confocal images by ImageJ. **E.** Recycling of Rhodamine-transferrin in control and ChA treated cells. Cells were incubated with fluorescent transferrin for 15 min (0 min chase) and then pulsed for

the indicated different times. **F.** Fluorescence measurement of Rhodamine-transferrin in control and ChA-treated cells by Flow Citometry. **G.** BODIPY-lactosylceramide (LacCer) sorting to trans-Golgi network of control and ChA-loaded cells. Lysosomes were labeled with Alexa Fluor-647 dextran. Cells were chased for 180 min and imaged **H.** Quantitation of BODIPY-LacCer and lysosomes colocalization. Colocalization was calculated in a pulse chase experiments for at least 100 cells. Data represent the mean±SEM of two independent experiment. In **B**, **D** and **F**, the results are mean±SEM of at least three different experiments. Statistical significance was assessed by a one-way ANOVA with a Bonferroni post-test: *, $p < 0.05$; ***, $p<0.001$; **, $p<0.01$. Bars, 10 µm.

challenging the cells for 30 min with endocytic cargo followed by 30 or 60 min of chase. A decrease in the colocalization between internalized cargo and LAMP-positive organelles was an indication of a delay in cargo delivery to lysosomes. In the case of dextran the experiment was performed in a different manner. Cells were initially pulsed with Alexa 647-dextran and then chased to label the lysosomes. Next, the cells were pulsed again with Rhodamine-dextran for 15 min and the degree of colocalization between the two dextrans was assessed, reflecting the percentage of cargo delivery to lysosomes (Supplementary Figure 5.2C and D).

In an attempt to determine if the effect of ChA on cargo transport to the lysosomes was occurring at the early stages of endosome maturation, we decided to measure the rate of transferrin recycling in ChA-loaded macrophages. As shown in Figure 5.5E and F, transferrin recycling was slower in ChA-treated cells than in control cells, reflecting a delay in transferrin-receptor recycling back to the PM. We further confirmed the ChA-laden cell defect in the early stages of endosome maturation by measuring the capacity of macrophages to recycle BODIPY-LacCer from late endosomes/lysosomes to TGN. In Figure 5.5G and H, the results showed that after the pulse with fluorescent lipid, cells presented higher values of colocalization between lipid and lysosomes (label with Alexa 647-dextran). In control cells, the percentage of colocalization was reduced after 60 min of chase due to lipid sorting to TGN. However, in ChA-loaded macrophages the levels of BODIPY-LacCer in lysosomes increased over the chase time, indicating no lipid recycling to the TGN. Identical results were observed when macrophages were treated with bafilomycin A (Supplementary Figure 5.3F and G), a vacuolar-type proton-ATPase (V-H^+ATPase) inhibitor that increases lysosomal pH. This result suggested a pH-dependent effect of late-endocytic vesicles on BODIPY-LacCer recycling. Altogether, our data showed that in ChA-loaded macrophages, vesicular transport is affected since the early stages of the process: recycling of early/sorting- endosome components, which in turn will affect the endosome maturation process, i.e., fusion with LAMP-positive or dextran-loaded structures.

5.3.4 The lysosomes in ChA-treated macrophages are dysfunctional

The lysosome receives extracellular and cytosolic macromolecules for degradation, being a crucial organelle in intra- and extra-cellular clearance. Then, it was investigated whether there was efficient lysosomal degradation of endocytic cargo in the ChA-treated cells. For this purpose, we used DQ-BSA, a heavily labeled BODIPY substrate for lysosomal proteases which the fluorescence is strongly quenched. However, upon DQ-BSA enzymatic cleavage to dye-labeled peptides in the acidic lysosomal compartments, this quenching is relieved, producing brightly fluorescent products.

The results depicted in Figure 5.6A showed a higher enzymatic cleavage of DQ-BSA in control cells than in ChA-loaded cells. Furthermore, the rate of DQ-BSA degradation by the lysosomal proteases was significantly slower in cells exposed to ChA compared to controls, suggesting that the catalytic activity of this organelle was affected (Figure 5.6B). However, possible defects in the endocytic pathway can also lead to inhibition of DQ-BSA degradation. To circumvent this problem we measured the activity of lysosomal cathepsin L with a fluorogenic assay using the "Magic Red" cathepsin substrate. The activity of cathepsin L is pH dependent and the maximal proteolytic activity is reached in a pH specific range: between 4.5 and 5.5 (Mason, Green, and Barrett 1985). Bafilomycin A was used as a control. For this set of experiments, the lysosomes were previously labeled with Alexa 647-dextran, in which fluorescence is not pH-dependent, and then the magic red substrate was added. The cathepsin L proteolytic activity was quantified by dividing the fluorescence intensities of the cathepsin L substrate with the Alexa 647-dextran labeled lysosomes. Cells illustrated in Figure 5.6C show a pseudocolor scale that indicates the proteolytic activity of lysosomes. It is clear that enlarged lysosomes from cells incubated with ChA showed a lower ratiometric value than control cells (Figure 5.6D). Thus, despite the delay in lysosomal cargo delivery, enlarged lysosomes also present a defect in cargo degradation.

The proteolytic activity of lysosomal enzymes is strictly dependent on pH values. A slight variation in lysosomal pH can compromise the degrative capacity of these organelles. Thus, we quantified the lysosome luminal pH in ChA-treated cells. Lysosomal pH was measured by using dextran conjugated with fluorescein isothiocyanate (FITC) and dextran conjugated with Alexa Fluor 647. FITC-dextran is known to be pH sensitive, exhibiting a 95% decrease in fluorescence intensity as the pH decreased from 10 to 3 (Canton and Grinstein 2015; Johnson et al. 2016). As described above and as a positive control, macrophages were treated with bafilomycin A. As visualized in Figure 5.6E and quantified in Figure 5.6F, ChA increased the lysosome pH, reflecting an increase in the FITC/Alexa 647-dextran ratio, which in turn can explain the reduction of degradative capacity of these organelles.

Finally, it was verified if changes in lysosome function could be explained by ChA accumulation in lysosomes. Filipin, a dye used to stain free cholesterol (FC), exhibited a similar binding affinity to FC and to ChA and showed dissociation constants of 95 and 100μM for filipin-FC and filipin-ChA, respectively (Supplementary Figure 5.3). This result indicates that filipin staining was a well-suited methodology to evaluate ChA deposits in macrophages. Representative images in Figure 5.6G showed that in ChA-treated cells, filipin staining was very bright in the membrane and also in the lumen of the enlarged lysosomes being the signal stronger than in the PM. In control cells filipin stained the PM and also other intracellular vesicles (probably endoplasmic reticulum (ER)) with similar fluorescence intensities. These results suggested an accumulation of ChA in lysosomes due to the lower hydrolyzation capacity of cells to convert ChE into cholesterol for ER processing and storage or reverse cholesterol transport.

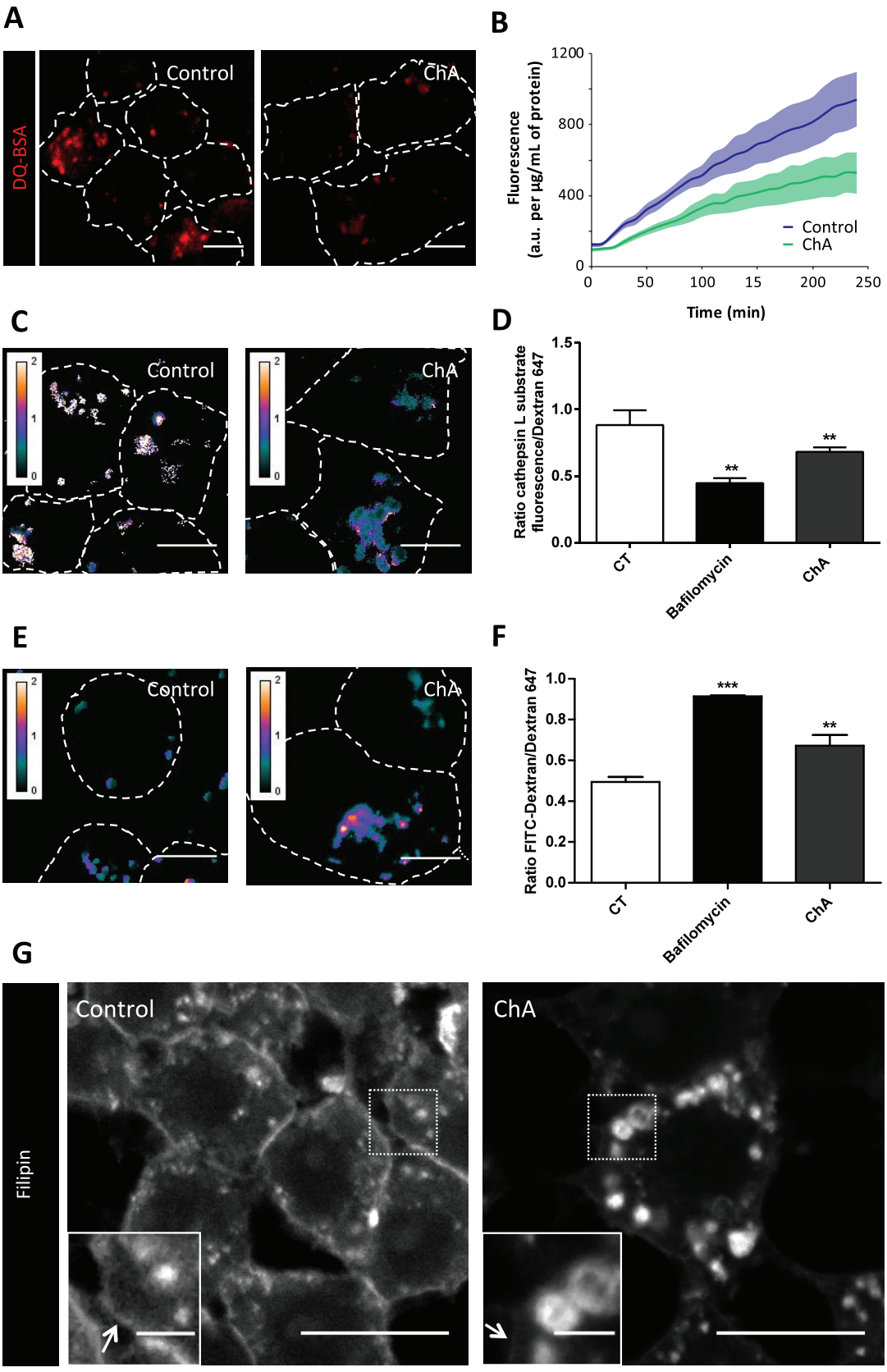

Figure 5.6 | ChA induces lysosome dysfunction.

RAW macrophages were treated for 72 h with POPC or ChA. **A.** Representative images of lysosomal degradative capacity of DQ-BSA. Cells were loaded for 3 h with DQ-BSA, chased 4h to allow degradation and imaged using confocal microscopy. Bars, 5µm. **B.** Time-course of DQ-BSA degradation in RAW cells. Fluorescence was measured using a microplate fluorescence reader. Error area represent SEM (n = 3). **C.** After cells treatment, lysosomes were loaded with Alexa Fluor 647–dextran and incubated for 15 min with Magic Red cathepsin L substrate. Cells were imaged by confocal microscopy and the representative image is

a ratio between Magic Red and Alexa Fluor 647–dextran fluorescences. Bars, 5 µm. **D.** Cathepsin L activity was quantified in control and ChA-treated cells by normalizing Magic Red fluorescence to Alexa Fluor 647–dextran fluorescence. As positive control, lysosomes were alkalinized with bafilomycin before Magic Red addition. n = 15 cells for each condition from two independent experiments; **E.** The lysosomes of treated RAW cells were loaded with FITC-dextran, a pH-sensitive dye and Alexa Fluor 647-dextran, a pH-insensitive dye. Ratiometric images were obtained through confocal microscopy. **F.** Quantification of the changes in lysosomal pH of live cells measured in confocal images by normalizing FITC-fluorescence to Alexa Fluor 647–dextran fluorescence. Bafilomycin was used as positive control. n = 15 cells for each condition from two independent experiments. Error bars represent SEM. ***, p<0.001; **, p<0.01. **G.** Filipin staining , a free cholesterol probe, of control and ChA-treated cells. The insets are enlargements of the areas outlined with the white dashed boxes. Arrows point to the plasma membrane of the cells. Bars, 10 µm in main images and 2 µm in the insets.

5.3.5 ChA induces lysosome stress leading to the transcriptional upregulation of autophagy-lysosomal biogenesis genes

Lysosomes are able to sense their content in stress conditions and regulate their own biogenesis by a lysosome-nucleus signaling pathway. This mechanism involves the transcription factor EB (TFEB), a master lysosomal biogenesis factor, which is responsible for the increase in transcription of several lysosomal and autophagy genes (Settembre et al. 2011). The induction of lysosomal stress with potent lysosomal inhibitors, such as chloroquine or atherogenic lipids, such as cholesterol crystals, was demonstrated in macrophages. Stressed lysosomes upregulate the genes involved in autophago-lysosome formation, including acid hydrolases, important in macromolecule degradation (Emanuel et al. 2014). Thus, we tested if some of these genes were also upregulated in cells treated with ChA. Macrophages treated for 72 h with ChA showed an increase in *tfeb* gene transcription (Figure 5.7A) as well as some of its lysosomal and autophagy target genes: *lamp-1, lysosomal acid lipase (lipa)* and *p62* (Figure 5.7B-D). To confirm these findings, lysosomal biogenesis was assessed by quantifying the LAMP-2 protein levels through Western blot. As observed in Figure 5.6E and F, LAMP-2 levels were increased in ChA-treated cells in a dose-dependent manner. Altogether, these results suggested that ChA induces lysosome stress and the upregulation of autophagy-lysosomal biogenesis genes that could be a compensatory mechanism to balance lysosome dysfunction.

5.3.6 The peripheral lysosomes are exocytic

In non-professional secretory cells, it was demonstrated that membrane proximal lysosomes are the lysosomes responsible for Ca^{2+}-mediated exocytosis (Jaiswal, Andrews, and Simon 2002). Due to the peripheral lysosomal positioning in ChA-treated cells, we hypothesized that these lysosomes were more exocytic than in control cells. To assess lysosome exocytosis, flow cytometry-based was performed to detect a luminal domain in LAMP-2 at the PM. In basal conditions, without any exocytic stimulus, macrophages incubated with ChA showed higher levels of LAMP-2 at the cell surface (Figure 5.8A, B and C) than the control cells. To test the contribution of membrane remodeling inhibition on the increased LAMP-2 levels at the PM, macrophages were incubated at 4°C with FM4-64 for PM staining. FM4-64 is a lipophilic probe that exhibits low fluorescence in water but fluoresces intensely upon binding the outer leaflet of the PM. After FM4-64 PM biding, the cells were heated to 37°C to follow PM remodeling. For this purpose, we followed the formation of endocytic vesicles over time. The results obtained in Figure 5.8D and E showed that ChA-treated macrophages did not

show any delay in membrane remodeling that could explain the higher levels of LAMP-2 at membrane surface. Thus, these results confirm that the increase in LAMP-2 was due to an increase in lysosome exocytosis rather than a delay in membrane remodeling.

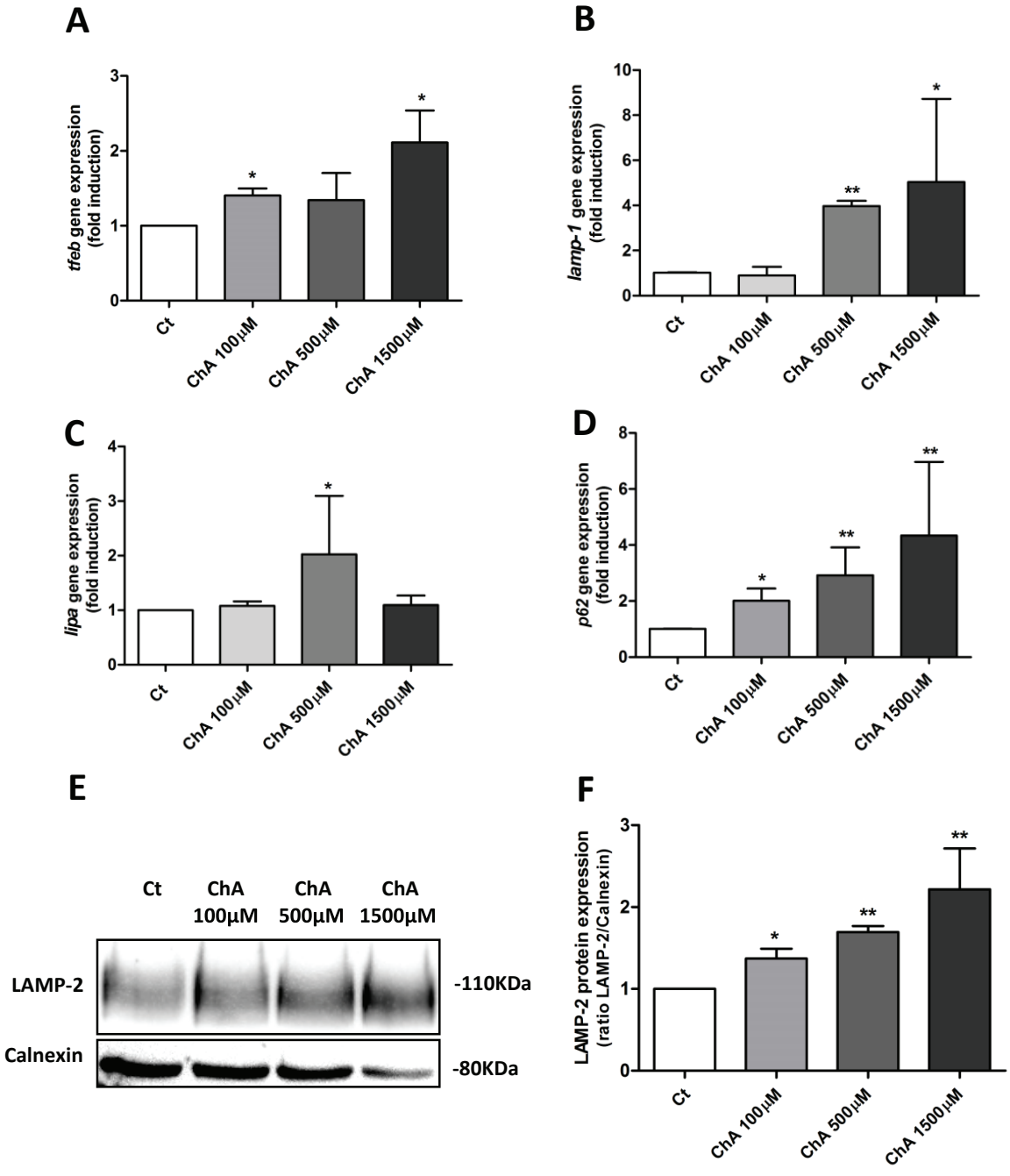

Figure 5.7 | ChA promotes transcriptional activation of lysosomal and autophagy genes as well as an increase in LAMP2 protein levels.

A-C. RAW macrophages were incubated during 72 h with POPC or ChA and the expression of *tfeb* **(A)**, *lamp-1* **(B)**, *lipa* **(C)** and *p62* **(D)** genes was assessed by RT-qPCR. Data were normalized to the endogenous *Hprt* and *Pgk1* genes. The values are mean±SEM expression levels of three independent experiments, each measured in two technical replicates. **E.** Western-blot showing LAMP-2 protein levels in lysates of cells treated with POPC (control) or ChA. Calnexin was used as loading control. **F.** Ratio of LAMP2-Calnexin of quantified bands obtained in **(D)** image shows the mean±SEM. **, p<0.01; *, p<0.05.

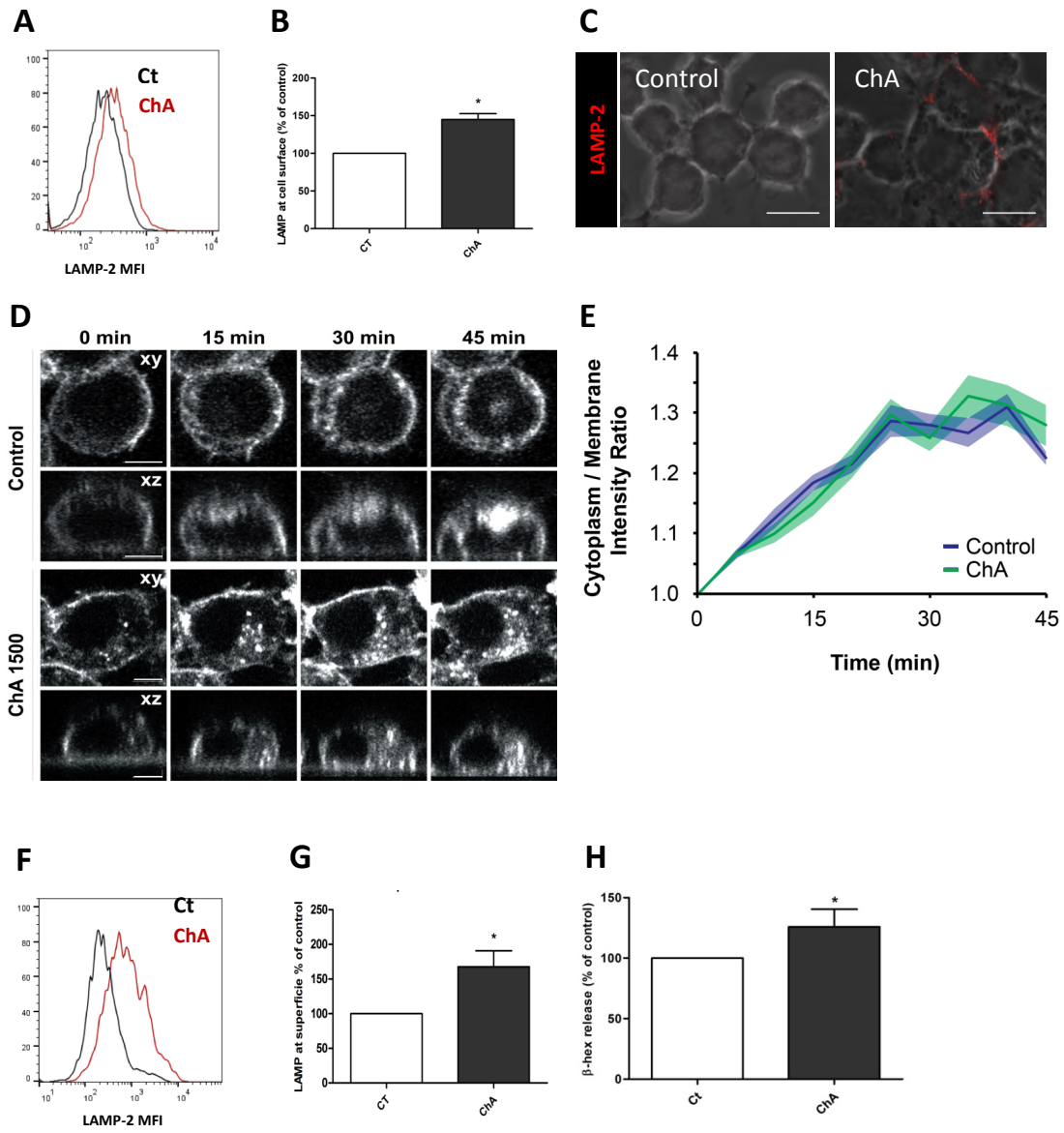

Figure 5.8 | In ChA treated macrophages the peripheral dysfunctional lysosomes are exocytic.

A. Representative histogram of LAMP-2 levels in macrophages treated with 1500 µM ChA for 72 h. x-values indicate the LAMP-2 MFI of the selected cell population. **B.** LAMP-2 levels, quantified by Flow Cytometry, at the cell surface of non-permeabilized macrophages treated with POPC or ChA. The PI-positive cells were excluded. **C.** Representative confocal images of control and ChA-treated cells exhibiting LAMP-2 at the cell surface without permeabilization. The fluorescent images are merged with the corresponding DIC images. **D.** Representative images of FM4-64 fluorescence followed in live cells in function of time. **E.** Single cell analysis of FM4-64 fluorescence in cytosol. Fluorescence was normalized to the time 0 min (FM4-64 pulse). SEM is represented by the color area around the mean line. **F.** Histogram showing LAMP-2 levels at membrane surface of macrophages incubated for 72 h with lipids and stimulated with ionomycin in presence of Ca^{2+}. Quantification are represented in **(G)** and error bars represent SEM (n = 4). **H.** Graph showing percent of β-hexosaminidase (β-hex) release upon ionomycin treatment in presence of Ca^{2+}. Bars, 10 µm. Data represent the mean±SEM of three independent experiments. Statistical significance was assessed by a t-test: *, p<0.05.

To further characterize the exocytic capacity of lysosomes in ChA-treated cells, we evaluated the response of these cells to an exocytic stimulus. It is well established that cell treatment with ionomycin, a Ca^{2+} ionophore, leads to lysosome exocytosis (Rodríguez et al. 1997; Encarnação et al. 2016). Therefore, as expected, ionomycin-treated RAW macrophages present an increased in LAMP-2 median fluorescence intensity (MFI) in the presence of Ca^{2+} compared with untreated cells (Supplementary Figure 5.4). When ChA-loaded macrophages were stimulated with ionomycin in the presence of Ca^{2+}, a 1.67 fold-increase in LAMP-2 at cell

surface in relation to stimulated control cells was observed (Figure 5.8F and G). To validate the increase in lysosome exocytosis in lipidotic macrophages, we evaluated the release of the lysosomal enzyme β-hexosaminidase after ionomycin and Ca^{2+} addition. As shown in Figure 5.8H, a higher level of this lysosomal enzyme was released when cells were exposed to ChA than in control cells. Together these results suggested that the peripheral lysosomes in macrophages treated with ChA were more exocytic than those in control cells.

5.3.7 In ChA-loaded macrophages there is an increase in gene expression of proteins involved in lysosome positioning and exocytosis

In recent years, lysosomal positioning and exocytosis, the mechanisms and their physiological implications, have been extensively studied (Johnson et al. 2016; Encarnação et al. 2016; Sbano et al. 2017; Pu et al. 2016). A correlation between lysosome protein composition and lysosome positioning had been reported. It was demonstrated that the balance between Rab7 and *Arl8b* determines the subcellular localization of lysosomes. The more centrally located lysosomes had considerably higher levels of Rab7 than Arl8b, whereas in the peripheral lysosomes, the inverse relationship between this two small GTPases was observed (Johnson et al. 2016). Taking this into consideration, we measured the gene expression levels of Rab7a and Arl8b. As shown in Figure 5.9A and B, *rab7a* mRNA expression levels were not changed, compared to the non-treated cells, while the expression levels of *arl8b* were higher than in control cells. These results need to be further explored by immunostaining to confirm their intracellular distribution and their levels of protein expression. However, they suggest that ChA, by inducing an increase in Arl8b, could induce lysosome peripheral positioning.

Lysosome exocytosis requires two sequential steps. First, lysosomes are recruited to the cell periphery and then fuse with the PM. To further characterize the trafficking molecular machinery involved in lysosome exocytosis, our group performed an RNAi screen of the Rab proteins to identify the members of this family involved in this process. It was found that Rab3a and Rab10 were the most robust hits. In the absence of these Rabs, Ca^{2+}-dependent lysosomal exocytosis was drastically reduced (Encarnação et al. 2016). Thus, we hypothesized that these Rabs could also be affected in macrophages loaded with ChA. For this purpose, the basal gene expression levels of Rab3a and Rab10 were evaluated. The results depicted in Figure 5.9C and D showed an increase in Rab3a and no significant difference in Rab10 gene expression levels in macrophages incubated with ChA. Rab3a is necessary to anchor the peripheral lysosomes to the cortical actin (Encarnação et al. 2016) and this data is well correlated with the increase in lysosomes at the periphery of ChA-treated cells.

Thus, we have several candidates to explore the mechanism behind the increase in lysosomal exocytosis in atherosclerotic macrophages.

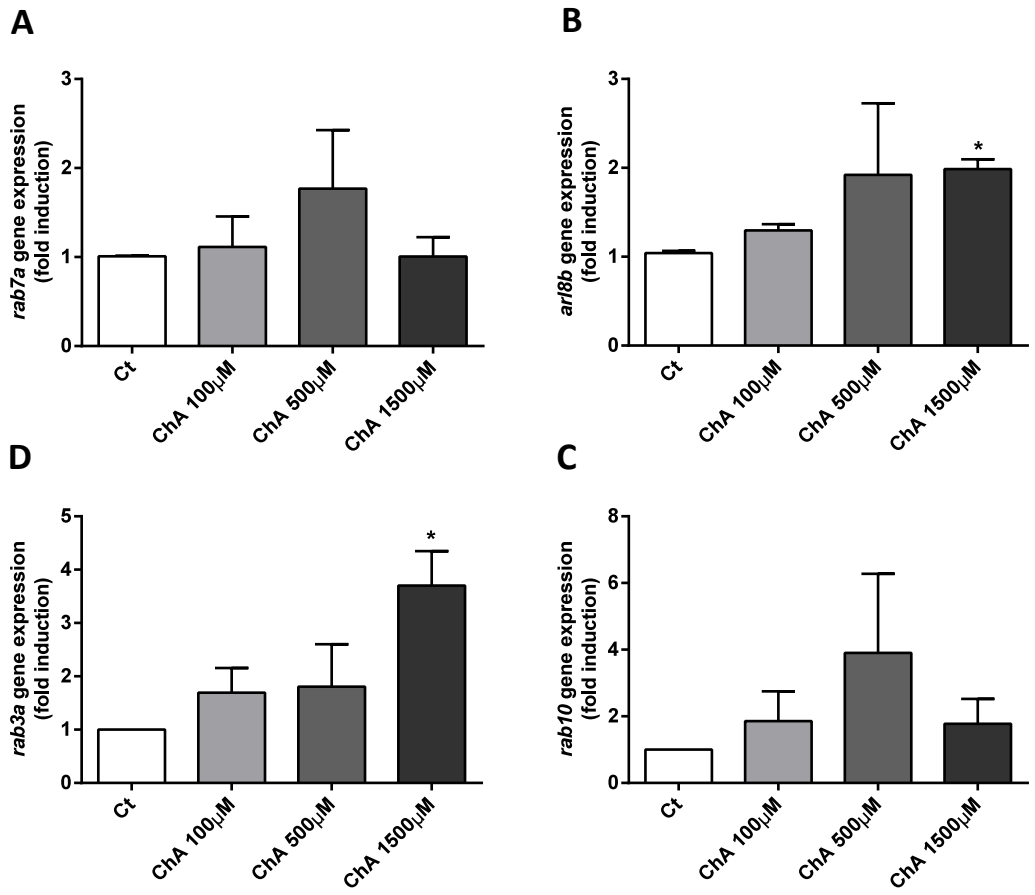

Figure 5.9 | In atherogenic macrophages there is an increase in gene expression of small GTPases involved in lysosome peripheral positioning and exocytosis.

Macrophages were treated for 72 h with ChA. mRNA levels of *rab7a* **(A)**, *arl8b* **(B)**, *rab3a* **(C)**, and *rab10* **(D)**. Gene expression were measured through qRT-PCR. Data were normalized to the endogenous *Hprt* and *Pgk1* genes. The values are mean±SEM expression levels of three independent experiments, each measured in two technical replicates. Statistical significance was assessed by a t-test: *, $p<0.05$.

5.4 DISCUSSION

Lysosomes are fundamental organelles in the processing and clearance of endocytosed material from the extracellular environment, as well as intracellular contents, including dysfunctional organelles and proteins. In atheroma, macrophages are the main cells responsible for the clearance of the Ox-Lp and apoptotic cell debris through efferocytosis. Thus, defects in macrophages' degradative capacity leads to the accumulation of lipids and toxic material, such as cell debris, increasing local inflammation and, consequently, leading to lesion development.

Few reports had linked macrophage dysfunction in atheroma with the final component of the cellular traffic system, the lysosome (Cox et al. 2007; Emanuel et al. 2014; Domingues et al. 2017; Jerome 2006). Previously, our group demonstrated that ChS was sufficient to induce cell lipidosis (Estronca et al. 2012) and lysosome dysfunction in macrophages (Domingues et al. 2017). Here, using a series of complementary experiments, we show that a newly identified cholesteryl hemiester in human plasma (data not published, Chapter 4) - ChA, beyond lysosome

dysfunction also causes an increase in exocytosis of these dysfunctional organelles and this outcome is a new pathological mechanism in atheroma formation.

In RAW and BMDM, ChA induces striking changes in lysosome morphology and positioning. The lysosomes are enlarged and became preferentially positioned at the periphery of the cells. These results are extremely interesting because although lipidotic macrophages share similarities with some lysosomal storage diseases (LSDs), the lysosomes in the latter diseases are normally localized in the perinuclear region of the cells. For example, in Niemann Pick C1 (NPC1), a LSD associated with mutations in *npc1* (encodes a cholesterol exporter), there is accumulation of free cholesterol in lysosomes and these organelles are mainly perinuclear (Sokol et al. 1988; Vanier 2010). Furthermore, it is known that in cholesterol-enriched lysosomal membranes (Rocha et al. 2009), the Rab7 effector oxysterol-binding protein-related protein 1 long (ORP1L), a cholesterol sensor, exists in a closed conformation that is compatible with dynein complex assembly and consequent lysosomes transport towards the minus-end of microtubules.

Lysosomal localization had been related with specific GTPase composition. The balance between Rab7 and Arl8b determines the subcellular localization of lysosomes: more peripheral lysosomes have reduced Rab7 and increased Arl8b density (Johnson et al. 2016). To further characterize the mechanism behind lysosome peripheral position in ChA-treated macrophages, we measured the mRNA levels of the above-mentioned GTPases: Rab7 and Arl8b. There were no significant changes in Rab7a mRNA expression, a small GTPase involved in trafficking of cargo to late endosomes-lysosome. Since lysosomal biogenesis is stimulated in ChA-loaded macrophages, an increase in *tfeb* and autophagic-lysosomal gene expression, as well as overexpression of LAMP-2 protein was observed (Figure 5.7), it was expected an overall increase in gene expression of all lysosomal proteins. However, no change in the levels of Rab7a expression was observed, perhaps indicating that ChA-induced enlarged lysosomes present a lower Rab7a density. This finding is in accordance to the fact that peripheral lysosomes have reduced Rab7 compared with perinuclear lysosomes (Johnson et al. 2016). However, this results need further confirmation and it will be also important to address, in our experimental settings, the role of two Rab7-effectors: Rab-interacting lysosomal protein (RILP) that moves lysosomes towards the microtubule minus-end, and kinesin-1 adaptor protein FYVE and coiled-coil domain-containing 1 (FYCO1) that directs endosome transport towards the cell periphery via the kinesin-1 motor.

In contrast to the Rab7a data, ChA-treated cells express higher levels of Arl8b than control cells. Arl8b, when anchored by the BORC complex, transports lysosomes towards the microtubule minus-end by recruiting kinesin-1 via its effector SKIP/PLEKHM2 (Rosa-Ferreira and Munro 2011; Pu et al. 2015). Thus, the observed Arl8b increase (Figure 5.9B) is in accordance with peripheral lysosome positioning in ChA-treated cells. Since Rab3a or their effectors, synaptotagmin-like protein 4a (Slp4-a) and non-muscle myosin heavy chain IIA are important to keep the lysosomes at the periphery of the cells (Encarnação et al. 2016) we also assessed Rab3a expression. Rab3a expression is also increased in ChA-treated cells (Figure 5.9C) and as for Arl8b this result is well correlated with the increase in the lysosome fraction at the periphery of the cells.

The mechanism involved in the loss of lysosomal function in lipid-loaded cells has been largely study in a LSDs context (reviewed in (Platt, Boland, and van der Spoel 2012)), and more recently in atherosclerosis (Yancey and Jerome 1998; Emanuel et al. 2014; Domingues et al. 2017). Our results also demonstrated a loss of lysosomal function induced by ChA (Figure 5.6 A-D). The diminished proteolytic activity of lysosomes in ChA-treated cells is likely associated to the luminal pH increase which in turn affects the activity of the lysosomal hydrolases, then leading to undigested cargo accumulation and to their enlargement. Moreover, changes in the distribution of cholesterol within membranes can have important consequences and, according to filipin staining there is accumulation of ChA and/or free cholesterol in enlarged lysosomes after ChA-loading (Figure 5.6G). As described already for macrophages loaded with Ox-LDL, cholesterol-crystals or with ChS-LDL, an increase in sterol concentration in lysosomal membranes leads to impairment in V-H^+ATPase, the proton transporter responsible for lysosomal acidification. Thus, lysosomal pH increase leads to a decrease in the hydrolytic capacity of lysosomal enzymes and subsequently to cargo accumulation and lysosomal enlargement (Cox et al. 2007; Emanuel et al. 2014; Domingues et al. 2017; Yancey and Jerome 1998). In our experimental settings, ChA accumulation in the lysosomal membranes is expected to be the major contributor to the loss of V-H^+ATPase function. On the other hand, the Rab7-effector RILP regulates the recruitment and stability of the V1G1 component of the lysosomal V-H^+ATPase (De Luca et al. 2015) and since the peripheral lysosomes have less Rab7, this can also contribute to the reduced acidification and impaired proteolytic activity. Furthermore, acidification loss, via the reduction in V-H^+ATPase activity and an increase in proton leak through lysosomal membranes, was recently associated with peripheral positioning of lysosomes (Johnson et al. 2016).

In LSDs, there has been some vesicular trafficking defects associated with the dysfunctional lysosomes identified (Klein et al. 2009; Choudhury et al. 2002; Puri et al. 1999; Ballabio and Gieselmann 2009). Thus, in ChA-laden macrophages a defect in endocytic trafficking was expected. ChA induced a delay in the transport of cargo targeted to lysosomes for degradation as well as cargo sorting at the early stages of the endocytic pathway. The exact mechanism by which the ChA affects intracellular trafficking is not known. However, amphiphilic Ox-Lp like ChA will be in constant partitioning equilibrium between the vehicle and the membrane of the traffic vesicles, changing their biophysical properties and consequently the activity of transmembrane proteins. Interestingly, it was shown that the traffic defects observed in lipid storage diseases are correlated with membrane lipid composition and the activity of Rab proteins (Puri et al. 1999).

One of the important outcomes of our work is that peripheral dysfunctional lysosomes were more exocytic than the lysosomes in control macrophages. It is known from the literature that only a small fraction of the lysosomes at the periphery of non-secretory cells is exocytic (Jaiswal, Andrews, and Simon 2002). Therefore, it is possible that because ChA-treatment increases the fraction of dysfunctional lysosomes at the periphery of the macrophages, that these organelles are more prone to exocytosis. Since lysosomes are full of lipids and

other undigested cargo, once these organelles fuse with the plasma membrane all the luminal contents are secreted into the extracellular milieu, which in turn can contribute to atherogenesis. Of note, ChA is highly proinflammatory (Chapter 4), which could be related with the increased lysosomes exocytosis as a pathway for cytokine secretion. Exocytosis of secretory lysosomes is one of the identified mechanisms of IL-1β (Andrei et al. 2004), a crucial cytokine in atherosclerosis lesion development (Ridker et al. 2017). Thus, the increase in proinflammatory molecules and toxic material secreted by lysosomes will both contribute to the progression of atherosclerotic lesions. This aspect was never reported in the pathology of atherosclerosis. In conclusion, in our experimental settings, it is possible that once lipid accumulates in the lysosomes, V-H^+ATPase activity decreases, proteolytic activity is reduced, cargo starts to accumulate, culminating in the enlargement of lysosome that become peripheral and more exocytic. These events affect membrane traffic in general and promote lysosomal biogenesis cell reprogramming to overcome the defect in flux (Figure 5.10, working model). However, the mechanism under the preferential positioning of lysosomes in the periphery of macrophages and their exocytic properties requires further characterization through loss- and gain- of function experiments for the known traffic players involved in lysosome positioning. The mechanism behind ChA-induced lysosomal biogenesis is also an important aspect that we will address in the future. Understanding the cellular processes that underlie lysosome dysfunction remains an important area of investigation both scientifically and clinically, serving as the basis for future therapeutics.

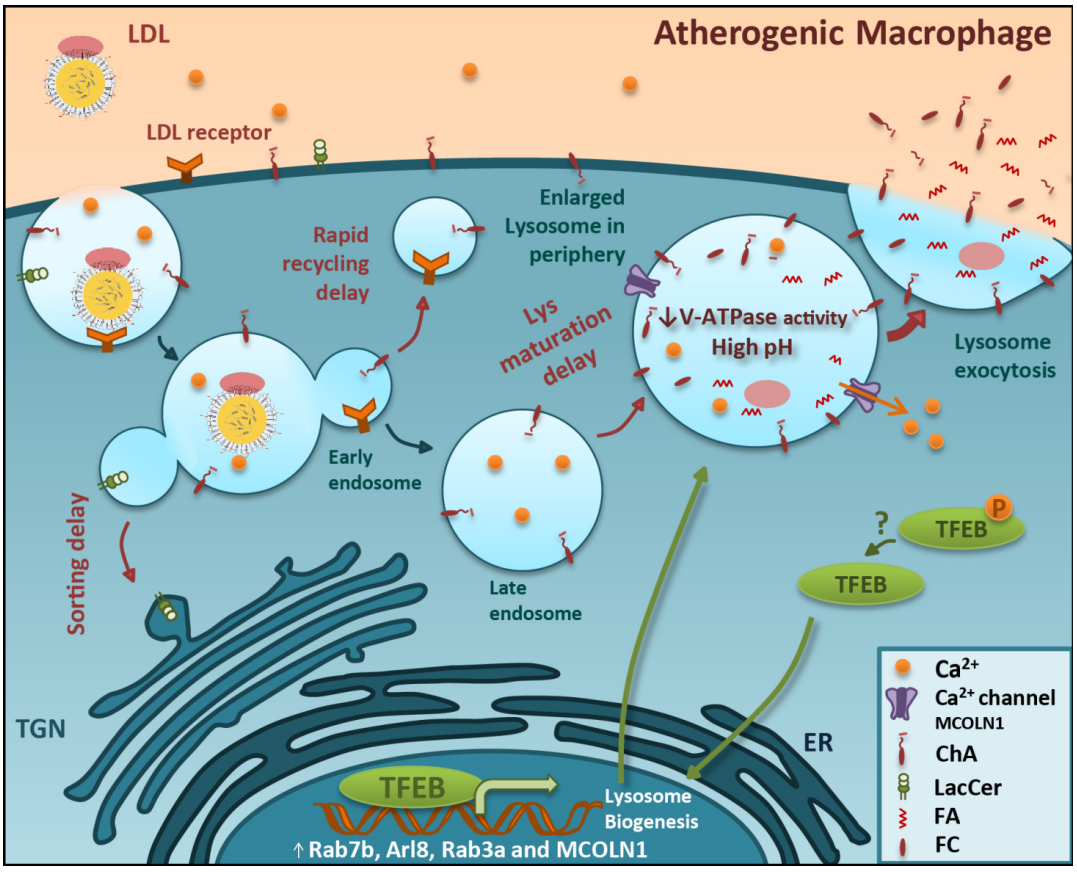

Figure 5.10 | Schematic representation of the trafficking effects and lysosomal dysfunction of ChA-loaded macrophages.

TGN – Trans-Golgi network; ER- endoplasmic reticulum; LacCer – lactosylceramide; FC – free cholesterol; Lys – lysosome.

5.5 REFERENCES

Andrei, Cristina, Paola Margiocco, Alessandro Poggi, Lavinia V Lotti, M R Torrisi, and Anna Rubartelli. 2004. "Phospholipases C and A2 Control Lysosome-Mediated IL-1 Beta Secretion: Implications for Inflammatory Processes." Proceedings of the National Academy of Sciences of the United States of America 101 (26): 9745–50. doi:10.1073/pnas.0308558101.

Ballabio, Andrea, and Volkmar Gieselmann. 2009. "Lysosomal Disorders: From Storage to Cellular Damage." Biochimica et Biophysica Acta - Molecular Cell Research. doi:10.1016/j.bbamcr.2008.12.001.

Canton, Johnathan, and Sergio Grinstein. 2015. "Measuring Lysosomal pH by Fluorescence Microscopy." Methods in Cell Biology 126: 85–99. doi:10.1016/bs.mcb.2014.10.021.

Choudhury, Amit, Michel Dominguez, Vishwajeet Puri, Deepak K. Sharma, Keishi Narita, Christine L. Wheatley, David L. Marks, and Richard E. Pagano. 2002. "Rab Proteins Mediate Golgi Transport of Caveola-Internalized Glycosphingolipids and Correct Lipid Trafficking in Niemann-Pick C Cells." Journal of Clinical Investigation 109 (12): 1541–50. doi:10.1172/JCI200215420.

Cox, Brian E, Evelyn E Griffin, Jody C Ullery, and W Gray Jerome. 2007. "Effects of Cellular Cholesterol Loading on Macrophage Foam Cell Lysosome Acidification." Journal of Lipid Research 48 (5): 1012–21. doi:10.1194/jlr.M600390-JLR200.

Domingues, Neuza, Luís M.B.B. Estronca, João Silva, Marisa R. Encarnação, Rita Mateus, Diogo Silva, Inês B. Santarino, et al. 2017. "Cholesteryl Hemiesters Alter Lysosome Structure and Function and Induce Proinflammatory Cytokine Production in Macrophages." Biochimica et Biophysica Acta - Molecular and Cell Biology of Lipids 1862 (2): 210–20. doi:10.1016/j.bbalip.2016.10.009.

Emanuel, Roy, Ismail Sergin, Somashubhra Bhattacharya, Jaleisa N. Turner, Slava Epelman, Carmine Settembre, Abhinav Diwan, Andrea Ballabio, and Babak Razani. 2014. "Induction of Lysosomal Biogenesis in Atherosclerotic Macrophages Can Rescue Lipid-Induced Lysosomal Dysfunction and Downstream Sequelae." Arteriosclerosis, Thrombosis, and Vascular Biology 34 (9): 1942–52. doi:10.1161/ATVBAHA.114.303342.

Encarnação, Marisa, Lília Espada, Cristina Escrevente, Denisa Mateus, José Ramalho, Xavier Michelet, Inês Santarino, et al. 2016. "A Rab3a-Dependent Complex Essential for Lysosome Positioning and Plasma Membrane Repair." Journal of Cell Biology 213 (6): 631–40. doi:10.1083/jcb.201511093.

Estronca, Luis M B B, Joao C P Silva, Julio L Sampaio, Andrej Shevchenko, Paul Verkade, Alfin D N Vaz, Winchil L C Vaz, and Otilia V Vieira. 2012. "Molecular Etiology of Atherogenesis--in Vitro Induction of Lipidosis in Macrophages with a New LDL Model." PloS One 7 (4): e34822. doi:10.1371/journal.pone.0034822.

Griffin, Evelyn E., Jody C. Ullery, Brian E. Cox, and W. Gray Jerome. 2005. "Aggregated LDL and Lipid Dispersions Induce Lysosomal Cholesteryl Ester Accumulation in Macrophage Foam Cells." Journal of Lipid Research 46 (10): 2052–60. doi:10.1194/jlr.M500059-JLR200.

Hutchins, Patrick M, Ernest E Moore, and Robert C Murphy. 2011. "Electrospray MS/MS Reveals Extensive and Nonspecific Oxidation of Cholesterol Esters in Human Peripheral Vascular Lesions." Journal of Lipid Research 52 (11): 2070–83. doi:10.1194/jlr.M019174.

Jaiswal, Jyoti K., Norma W. Andrews, and Sanford M. Simon. 2002. "Membrane Proximal Lysosomes Are the Major Vesicles Responsible for Calcium-Dependent Exocytosis in Nonsecretory Cells." Journal of Cell Biology 159 (4): 625–35. doi:10.1083/jcb.200208154.

Jerome, W Gray. 2006. "Advanced Atherosclerotic Foam Cell Formation Has Features of an Acquired Lysosomal Storage Disorder." Rejuvenation Research 9 (2): 245–55. doi:10.1089/rej.2006.9.245.

Jerome, W Gray. 2010. "Lysosomes, Cholesterol and Atherosclerosis." Clinical Lipidology 5 (6): 853–65. doi:10.2217/clp.10.70.

Jerome, W Gray, Brian E Cox, Evelyn E Griffin, and Jody C Ullery. 2008. "Lysosomal Cholesterol Accumulation Inhibits Subsequent Hydrolysis of Lipoprotein Cholesteryl Ester." Microscopy and Microanalysis : The Official Journal of Microscopy Society of America, Microbeam Analysis Society, Microscopical Society of Canada 14 (2): 138–49. doi:10.1017/S1431927608080069.

Johnson, Danielle E., Philip Ostrowski, Valentin Jaumouillé, and Sergio Grinstein. 2016. "The Position of Lysosomes within the Cell Determines Their Luminal pH." Journal of Cell Biology 212 (6): 677–92. doi:10.1083/jcb.201507112.

Kamido, H., A. Kuksis, L. Marai, and J.J. Myher. 1995. "Lipid Ester-Bound Aldehydes among Copper-Catalyzed Peroxidation Products of Human Plasma Lipoproteins." Journal of Lipid Research 36 (9): 1876–86. http://www.ncbi.nlm.nih.gov/pubmed/8558076.

Klein, Diana, Afshin Yaghootfam, Ullrich Matzner, Bettina Koch, Thomas Braulke, and Volkmar Gieselmann. 2009. "Mannose 6-Phosphate Receptor-Dependent Endocytosis of Lysosomal Enzymes Is Increased in Sulfatide-Storing Kidney Cells." Biological Chemistry 390 (1): 41–48. doi:10.1515/BC.2009.009.

Libby, Peter, Paul M. Ridker, and Attilio Maseri. 2002. "Inflammation and Atherosclerosis." Circulation 105 (9): 1135–43. doi:10.1161/hc0902.104353.

Luca, M. De, L. Cogli, C. Progida, V. Nisi, R. Pascolutti, S. Sigismund, P. P. Di Fiore, and C. Bucci. 2015. "RILP Regulates Vacuolar ATPase through Interaction with the V1G1 Subunit." Journal of Cell Science 128 (14): 2565–2565. doi:10.1242/jcs.175323.

Luzio, J. Paul, Paul R. Pryor, and Nicholas A. Bright. 2007. “Lysosomes: Fusion and Function.” Nature Reviews Molecular Cell Biology 8 (8): 622–32. doi:10.1038/nrm2217.

Mason, R W, G D Green, and a J Barrett. 1985. “Human Liver Cathepsin L.” The Biochemical Journal 226 (1): 233–41. http://www.pubmedcentral.nih.gov/articlerender.fcgi?artid=1144697&tool=pmcentrez&rendertype=abstract.

Miller, Yury I., and John Y.J. Shyy. 2017. “Context-Dependent Role of Oxidized Lipids and Lipoproteins in Inflammation.” Trends in Endocrinology and Metabolism. doi:10.1016/j.tem.2016.11.002.

Moore, Kathryn J., and Ira Tabas. 2011. “Macrophages in the Pathogenesis of Atherosclerosis.” Cell 145 (3): 341–55. doi:10.1016/j.cell.2011.04.005.

Platt, Frances M., Barry Boland, and Aarnoud C. van der Spoel. 2012. “Lysosomal Storage Disorders: The Cellular Impact of Lysosomal Dysfunction.” Journal of Cell Biology 199 (5): 723–34. doi:10.1083/jcb.201208152.

Pu, Jing, Carlos M. Guardia, Tal Keren-Kaplan, and Juan S. Bonifacino. 2016. “Mechanisms and Functions of Lysosome Positioning.” Journal of Cell Science 129 (23): 4329–39. doi:10.1242/jcs.196287.

Pu, Jing, Christina Schindler, Rui Jia, Michal Jarnik, Peter Backlund, and Juan S. Bonifacino. 2015. “BORC, a Multisubunit Complex That Regulates Lysosome Positioning.” Developmental Cell 33 (2): 176–88. doi:10.1016/j.devcel.2015.02.011.

Puri, V, R Watanabe, M Dominguez, X Sun, C L Wheatley, D L Marks, and R E Pagano. 1999. “Cholesterol Modulates Membrane Traffic along the Endocytic Pathway in Sphingolipid-Storage Diseases.” Nature Cell Biology 1 (6): 386–88. doi:10.1038/14084.

Ridker, Paul M, Brendan M. Everett, Tom Thuren, Jean G. MacFadyen, William H. Chang, Christie Ballantyne, Francisco Fonseca, et al. 2017. “Antiinflammatory Therapy with Canakinumab for Atherosclerotic Disease.” New England Journal of Medicine, NEJMoa1707914. doi:10.1056/NEJMoa1707914.

Rocha, Nuno, Coenraad Kuijl, Rik Van Der Kant, Lennert Janssen, Diane Houben, Hans Janssen, Wilbert Zwart, and Jacques Neefjes. 2009. “Cholesterol Sensor ORP1L Contacts the ER Protein VAP to Control Rab7-RILP-p150Glued and Late Endosome Positioning.” Journal of Cell Biology 185 (7): 1209–25. doi:10.1083/jcb.200811005.

Rodríguez, Ana, Paul Webster, Javier Ortego, and Norma W. Andrews. 1997. “Lysosomes Behave as Ca^{2+}-Regulated Exocytic Vesicles in Fibroblasts and Epithelial Cells.” Journal of Cell Biology 137 (1): 93–104. doi:10.1083/jcb.137.1.93.

Rosa-Ferreira, Cláudia, and Sean Munro. 2011. “Arl8 and SKIP Act Together to Link Lysosomes to Kinesin-1.” Developmental Cell 21 (6): 1171–78. doi:10.1016/j.devcel.2011.10.007.

Sbano, Luigi, Massimo Bonora, Saverio Marchi, Federica Baldassari, Diego L. Medina, Andrea Ballabio, Carlotta Giorgi, and Paolo Pinton. 2017. “TFEB-Mediated Increase in Peripheral Lysosomes Regulates Store-Operated Calcium Entry.” Scientific Reports 7: 40797. doi:10.1038/srep40797.

Schulze, Heike, and Konrad Sandhoff. 2011. “Lysosomal Lipid Storage Diseases.” Cold Spring Harbor Perspectives in Biology 3 (6): 1–19. doi:10.1101/cshperspect.a004804.

Sergin, Ismail, Trent D. Evans, Xiangyu Zhang, Somashubhra Bhattacharya, Carl J. Stokes, Eric Song, Sahl Ali, et al. 2017. “Exploiting Macrophage Autophagy-Lysosomal Biogenesis as a Therapy for Atherosclerosis.” Nature Communications 8: 15750. doi:10.1038/ncomms15750.

Settembre, C., C. Di Malta, V. A. Polito, M. G. Arencibia, F. Vetrini, S. Erdin, S. U. Erdin, et al. 2011. “TFEB Links Autophagy to Lysosomal Biogenesis.” Science 332 (6036): 1429–33. doi:10.1126/science.1204592.

Sokol, J., E. J. Blanchette-Mackie, H. S. Kruth, N. K. Dwyer, L. M. Amende, J. D. Butler, E. Robinson, et al. 1988. “Type C Niemann-Pick Disease. Lysosomal Accumulation and Defective Intracellular Mobilization of Low Density Lipoprotein Cholesterol.” Journal of Biological Chemistry 263 (7): 3411–17. doi:10.1046/j.1365-2141.2000.02536.x.

Still, W.J.S., and P.R. Marriott. 1964. “Comparative Morphology of the Early Atherosclerotic Lesion in Man and Cholesterol-Atherosclerosis in the Rabbit an Electronmicroscopic Study.” Journal of Atherosclerosis Research 4 (5): 373–86. doi:10.1016/S0368-1319(64)80023-5.

Vanier, Marie T. 2010. “Niemann-Pick Disease Type C.” Orphanet Journal of Rare Diseases 5 (1): 16. doi:10.1186/1750-1172-5-16.

Yancey, P G, and W G Jerome. 1998. “Lysosomal Sequestration of Free and Esterified Cholesterol from Oxidized Low Density Lipoprotein in Macrophages of Different Species.” Journal of Lipid Research 39 (7): 1349–61.

Yancey, P G, and W G Jerome. 2001. “Lysosomal Cholesterol Derived from Mildly Oxidized Low Density Lipoprotein Is Resistant to Efflux.” Journal of Lipid Research 42 (3): 317–27.

5.6 SUPPLEMENTAL INFORMATION

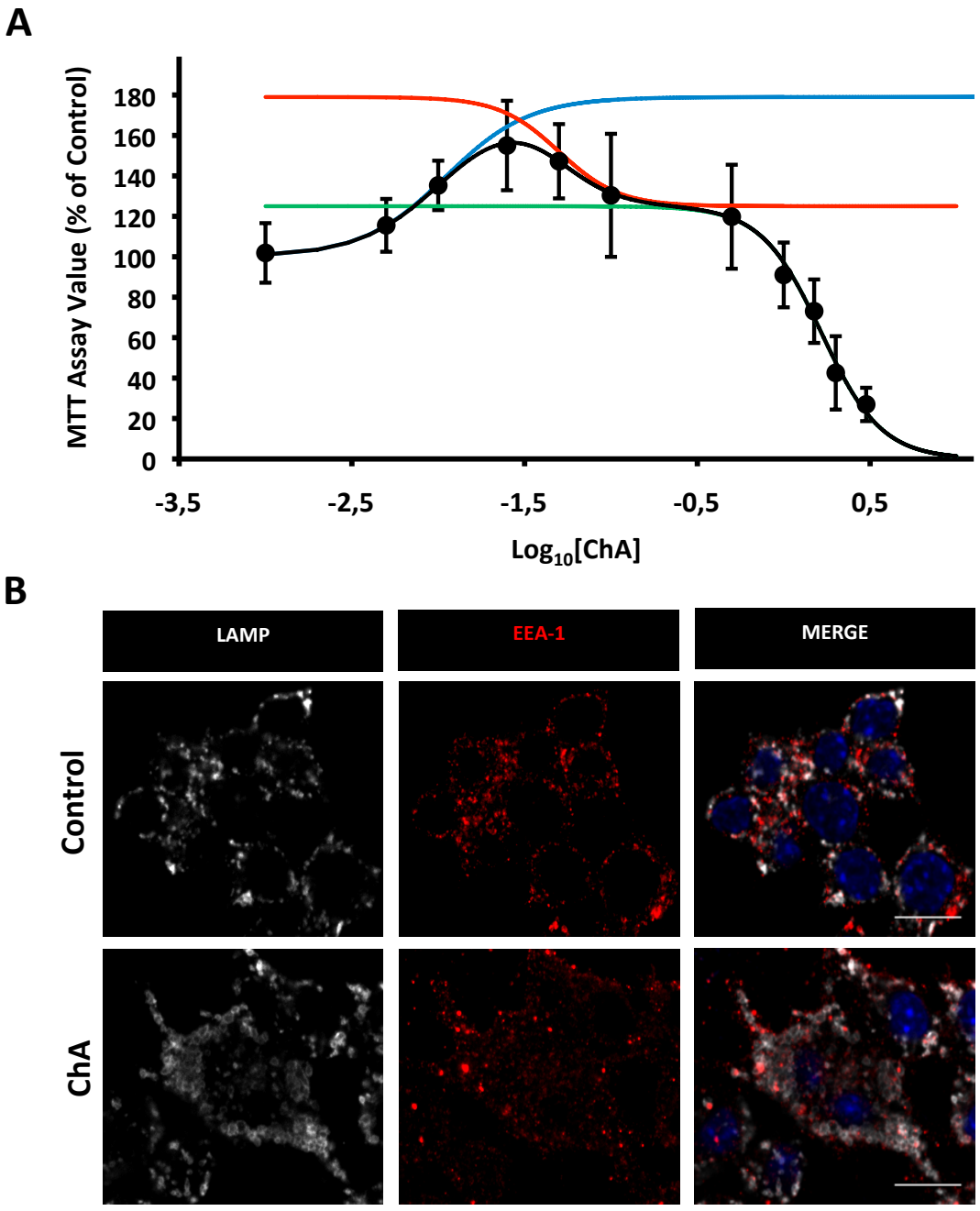

Supplementary Figure 5.1 | Effect of ChA towards RAW cells viability and early endosomes morphology.

A. RAW macrophages were incubated with ChA or with POPC (control) during 72 h and cell viability was evaluated by the MTT assay. The results are present as mean±SEM of four independent experiments **B.** RAW cells incubated with 1500 µM ChA or with POPC (control cells) for 72 h and co-stained for Early Endosomes Antigen-1 (EEA-1, in red) and LAMP (in white). Scale bars, 10 µm.

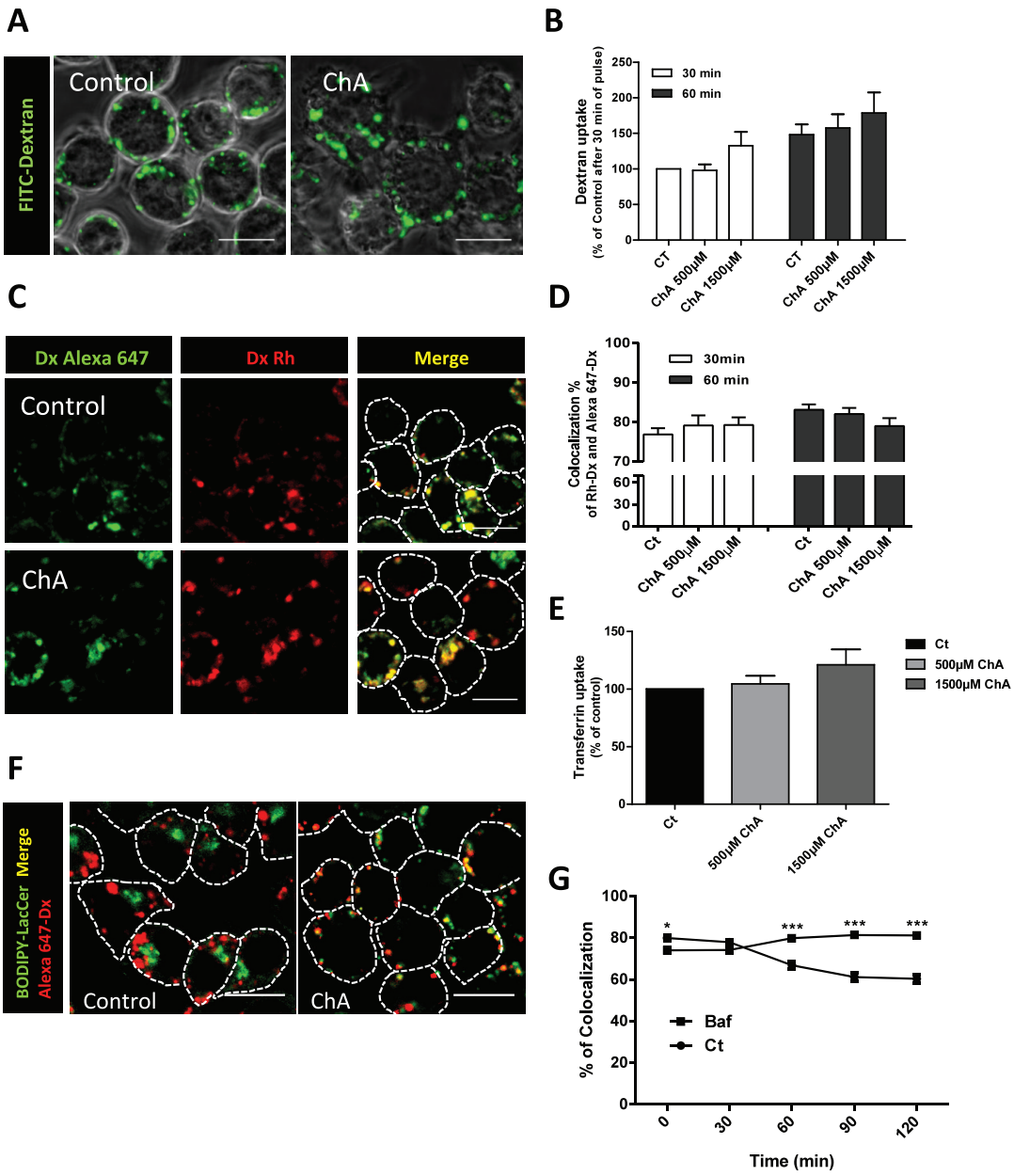

Supplementary Figure 5.2 | ChA does not affect pinocytosis neither transferrin internalization, however it induces a delay in the transport of internalized cargo to the lysosomes. Decrease in lysosomal acidification induces a deffective endosomes sorting to trans-Golgi Network.

A. Effect of ChA on dextran uptake, a fluid phase marker. Representative confocal images of fixed cells incubated for 60 min with FITC–dextran. The fluorescent images are merged with the corresponding DIC images. **B.** RAW macrophages were treated for 72 h with POPC (control) or ChA and loaded with FITC-Dextran for 30 and 60 min and then fixed. Cell fluorescence was measured by Flow Cytometry. **C.** Representative confocal images of live cells. After ChA treatement, lysosomes were labeled with Alexa Fluor 647-dextran. Then the cells were pulsed with Rodhamine (Rh)-dextran for 30 min. **D.** Quantification of colocatization of internalized dextran with lysosomes. The colocalization was quantified by ImageJ software; **E.** Quantification of Rodhamine-transferrin internalization after 15 min of pulse by Flow Cytometry. Bars, 10 µm. Data represent the mean±SEM of three independent experiments. **F.** Representative confocal images of lipid sorting to trans-Golgi network of macrophages treated or untreated with bafilomycin before the pulse with BODIPY-Lactosylceramide (LacCer) for 30 min. Cells were chased for 180 min and imaged. Lysosomes were label with Alexa Fluor 647-dextran; **G.** Quantification of colocalization percentage of internalized BODIPY-LacCer and lysosomes. Bars, 10 µm. Data represent the mean±SEM of three independent experiments; ***, p<0.001.

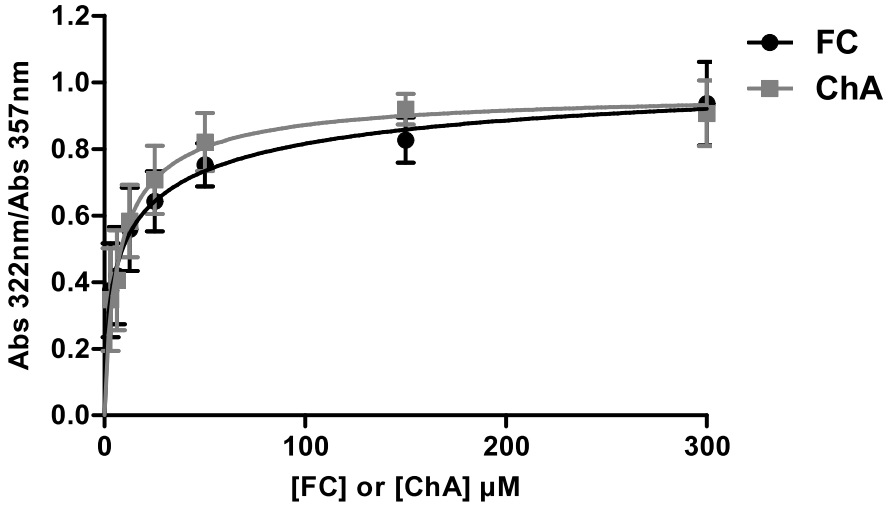

Supplementary Figure 5.3 | Filipin binds to ChA and to free cholesterol (FC) with a similiar binding constant.

Filipin association curve with liposomes of POPC-FC (3.5:6.5) and POPC-ChA (3.5:6.5). The graph shows the absorption intensity ratio (A_{320}/A_{356}) for Filipin as a function of FC (●, black line) or ChA (■, grey line) using Hill equation for theoretical fitting. It was determined that dissociation constant is 95 µM for the Filipin-FC complex and 100 µM for the Filipin-ChA complex, with a Hill coefficient of 1.5 and 1.6, respectively. Data show the mean±SEM of four independent experiments.

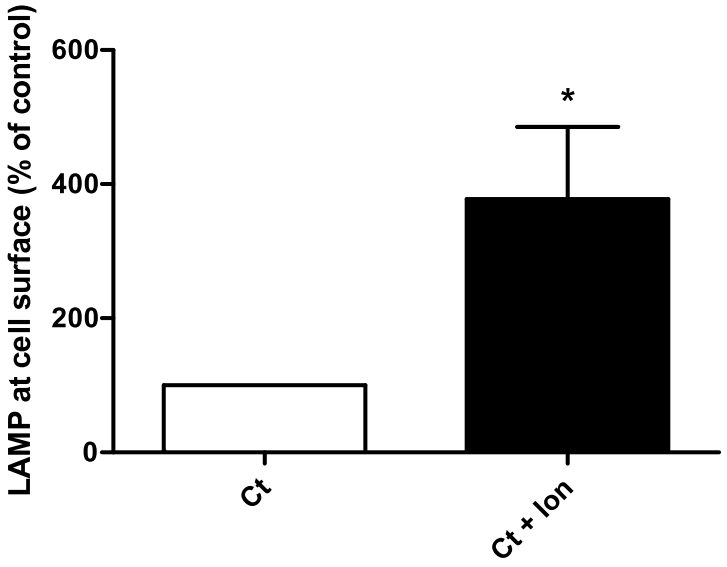

Supplementary Figure 5.4 | Effect of ionomycin and calcium in lysosome exocytosis.

RAW control cells were incubated with 5 µM of Ionomycin and of 4 mM of calcium and the levels of LAMP-2 at membrane surface were measured by Flow Cytometry. The PI-positive cells were excluded. Data represent the mean±SEM of three independent experiments. Statistical significance was assessed by a t-test: *, $p<0.05$.

06 *IN VIVO* PROATHEROGENIC PROPERTIES OF CHOLESTERYL HEMIESTERS

6.1 ABSTRACT

Atherosclerosis is a lipid-driven chronic inflammatory disease of the arterial wall. During atherosclerosis a continuous infiltration of leukocytes into the plaque contributes to enhance the progression of the lesion. Macrophages, one of the best-characterized cells in atheroma formation, are specialized in removing lipids and cellular debris present in the atherosclerotic plaque. A default in the degradative capacity of these cells promotes plaque progression, further exacerbating the inflammatory process. Our group has detected a novel oxidized lipid (Ox-Lp) in human plasma, named ChA that induces lysosomal dysfunction and proinflammatory cytokine release in both mouse macrophages *in vitro* and *ex vivo* human monocytes and macrophages. Here, using zebrafish larvae fed with a diet enriched in ChA as an animal model of atheroma formation, we demonstrate the *in vivo* proatherogenic features of this new Ox-Lp. ChA induces lipid accumulation in the vasculature of zebrafish larvae, with a higher incidence in the bifurcation sites. ChA also promotes the recruitment of neutrophils and macrophages to the vasculature, likely via the increased abundance of adhesion molecules on the endothelial cell (EC) surface. *In vivo* imaging of ChA-loaded macrophages showed morphological alterations in the lysosomes of these cells, which become enlarged, suggesting they are dysfunctional. Additionally, we observed neutrophils and macrophages in close proximity, which it is known to be related with macrophages priming. Then, zebrafish larvae fed with ChA-enriched diet revealed an increase in proinflammatory cytokine expression: IL-1β, IL-6 and TNF-α. Altogether, our findings provide novel evidences on the *in vivo* proatherogenic properties of ChA.

6.2 INTRODUCTION

Atherosclerosis is a chronic inflammatory disease resulting from an imbalance in lipid metabolism, that culminates in the accumulation of lipid-laden macrophages in the arterial intima, and an inefficient immune response (Libby 2012). Interleukin-1β (IL-1β), which plays a critical role in the pathogenesis of atherosclerosis (Sheedy and Moore 2013), and other proinflammatory cytokines, such as tumor necrosis factor (TNF)-α and IL-6, have been associated with the accumulation of cholesterol crystals and/or Ox-Lp in monocyte-derived macrophages (Tedgui 2006; Erridge et al. 2008; Duewell et al. 2010). The secretion of these molecules stimulates endothelial cells (EC) to express adhesion molecules, leading to myeloid cell recruitment to the vascular endothelium and their differentiation into macrophages in the arterial intima.

Inflammation is a very tightly regulated process (Lamkanfi and Dixit 2014) with IL-1β/IL-18 production being regulated by two different pathways. Firstly, IL-1β/IL-18 transcription is triggered

by activation of pattern recognition receptors (PRRs), such as toll-like receptors (TLRs). Then, for IL-1β or IL-18, the second signal for the mature active cytokine release is given through "danger" signals associated with host cell damage (i.e. danger-associated molecular patterns (DAMPs)) (Schroder and Tschopp 2010). In the context of atherosclerosis, this second signal has been associated with lysosomal hydrolase release from dysfunctional lysosomes (Emanuel et al. 2014; Moore and Tabas 2011; Duewell et al. 2010). In the case of IL-1β, one of the main proinflammatory cytokines in atherosclerosis (Ridker et al. 2017), the second signal activates the NOD-like receptor family pyrin domain-containing protein (NLRP)-3. This promotes the cleavage and activation of the protease caspase-1 that processes IL-1 family cytokines, such as IL-1β into their mature form (Guo, Callaway, and Ting 2015). Despite the enormous amount of published data on lipids and inflammation in atherosclerosis, the endogenous priming signal(s) that activate IL-1β transcription prior to inflammasome activation is still not clear.

The autocrine and paracrine action of released IL-1β stimulates the secretion of chemokines that recruit neutrophils to atherosclerotic lesions, independently of other leukocytes (Miller et al. 2006; Rotzius et al. 2010; Nahrendorf and Swirski 2015). The role of neutrophils in the pathophysiology of atherosclerosis has been underappreciated. However, recent work has provided evidence of a fundamentally important role for neutrophils in early and late human and murine atherosclerotic lesions (Döring et al. 2012; Drechsler et al. 2010; Döring, Soehnlein, and Weber 2017; Wantha et al. 2013). Using apolipoprotein E-deficient (*Apoe*$^{-/-}$) mice, Warnatsch and collaborators have reported the accumulation of neutrophil extracellular traps (NETs) near cholesterol crystals and macrophages in atherosclerotic lesions (Warnatsch et al. 2015). Importantly, NETs were able to prime macrophages for cytokine release, activating Th17 cells that further amplify immune cell recruitment to atherosclerotic plaques (Warnatsch et al. 2015).

Cholesteryl hemiesters (ChE) are stable end-products of LDL cholesteryl ester (CE) oxidation. Although ChE precursors had been identified in *in vitro* in oxidized-low density lipoprotein (ox-LDL) and in human lesions (Kobayashi et al. 2001; Hoppe et al. 1997), their role in atherogenesis has been largely unexplored. Our group has been interested in the study of the atherogenic properties of a newly identified member of ChE - ChA, that is increased in the plasma of cardiovascular disease patients (Chapter 4). In our first study to characterize ChE family members as proatherogenic lipids, we observed these lipid species were able to induce an irreversible lipidosis in macrophages, causing cell death (Estronca et al. 2012). Recently, we have demonstrated that long-term treatment of macrophage with ChE induced lysosomal dysfunction and an increase in proinflammatory cytokine release (Domingues et al. 2017). In this thesis, we also demonstrated the proinflammatory features of ChA in human monocytes and macrophages, as well as in murine primary macrophages (Chapter 4). ChA-loaded macrophages showed an increase in lipid accumulation and lysosomal dysfunction, with effects on intracellular trafficking (Chapter 5). Finally, we identified the peripheral positioning of lysosomes with a higher exocytic capacity in ChA-treated macrophages (Chapter 5), which could be related to the proinflammatory features of ChA (Chapter 4), given that one of the described release mechanisms of IL-1β is via secretory lysosomes.

In recent years, a combination of genetic, developmental, and physiological advantages, have allowed zebrafish to emerge as an important *in vivo* tool to study inflammation as well as dyslipidemia (Berg et al. 2016; Fang, Liu, and Miller 2014; Stoletov et al. 2009). Several groups have taken advantage of zebrafish susceptibility to metabolic stress induced by feeding with free cholesterol (FC)-enriched diets to demonstrate several responses that firmly establish the advantages of either adult or larvae zebrafish as compared with mouse models in the dyslipidemia and atherogenesis studies (Yoon et al. 2013; Wang et al. 2013; Progatzky et al. 2014; Stoletov et al. 2009; Fang et al. 2010). Using zebrafish larvae, vascular intimal lipid accumulation was observed after a short exposure to an FC-enriched diet, with accumulated lipids attracted circulating monocytes (Stoletov et al. 2009). Another study using zebrafish larvae also reported an increase in proinflammatory cytokine gene expression upon animal feeding with a high FC-enriched diet (Progatzky et al. 2014). Our group also observed an increase in lipid accumulation and myeloid cell recruitment to the vasculature of these animals when they were fed with cholesteryl hemisuccinate (ChS) (Domingues et al. 2017). Taking all this information into consideration, we decided to evaluate the atherogenic properties of ChA *in vivo* using zebrafish larvae fed with this lipid.

In this work, we showed that ChA induced lipid accumulation and myeloid cell recruitment to the vasculature of zebrafish larvae. Interestingly, we observed different kinetics of neutrophil and macrophage infiltration into the vasculature, with neutrophils appearing earlier than macrophages. The increase in inflammatory cell recruitment was accomplished by an increase in vascular cell adhesion molecule1 (V-CAM1) gene expression. Additionally, macrophages from animals fed with a ChA-enriched diet showed an increase in lipid accumulation and enlarged lysosomes, suggestive of lysosomal dysfunction. Finally, in ChA-fed animals we found higher mRNA expression levels of proinflammatory cytokines: IL-1β, TNF-α and IL-6. Together, our data corroborate the role of neutrophils in plaque development and demonstrate the *in vivo* atherogenic effects of ChA on vascular lipid accumulation and lysosomal dysfunction that triggers inflammation.

6.3 RESULTS

6.3.1 ChA induces lipid accumulation in the vasculature of zebrafish larvae

Zebrafish are a suitable animal model to study lipid metabolism, expressing many of the genes necessary for lipid transport and metabolism, such as the lipoprotein gene microsomal triglyceride transfer protein (MTP) (Marza et al., 2005), FA transport protein (slc27a), acyl-CoA synthetase (acsl) gene families and the putative cholesterol transporter Niemann-Pick C1-Like 1 (Anderson, Carten, and Farber 2011). Additionally, zebrafish larvae are transparent, allowing dynamic and interactive studies on vascular lipid accumulation and inflammation. We have shown in this thesis that ChA is a proinflammatory ligand, and induces lysosomal dysfunction

and cellular lipid accumulation *in vitro* in macrophages. Taking this into account, we explored whether ChA induces vascular lipid accumulation in zebrafish larvae exposed to this lipid.

To evaluate the effects of ChA, zebrafish larvae were provided a diet supplemented with ChA. FC and a normal diet were used as controls. Initially, as in our previous work (Domingues et al. 2017), the toxicity induced by ChA towards zebrafish was assessed. When AB zebrafish larvae (wild type zebrafish) begin to feed freely (on 5 dpf), we administered different molar concentrations of ChA and FC-enriched diets for 10 days. After this period, larvae were counted and the survival was normalized to the numbers obtained with normal diet fed larvae. The results in Figure 6.1A showed that ChA was toxic in the zebrafish in a dose- and time-dependent manner (Supplementary Figure 6.1). For all the tested doses, we also observed higher toxicity of ChA compared with the same molarity of FC. Through the equation of Hill, we determined an ED_{50} of 47 and 80 µmol/g, with the minimum percentage of survival (Ymin) of 9% and 54%, for ChA and FC respectively.

To address if this newly identified ChE could induce vascular lipid accumulation, normal, FC- or ChA-diet was supplemented with a red fluorescent CE analog (BODIPY 542/563 C11) and the caudal vein of larvae were imaged 10 days after feeding, as shown in Figure 6.1B. The concentration of FC used was based on a previously published report (Stoletov et al. 2009), demonstrating that a 4% (W/W) FC-supplemented diet (corresponding to 52 µmol/g) is sufficient to induce lipid accumulation in the larvae caudal vasculature (Stoletov et al. 2009). As shown in Z-projections of the caudal vein of animals fed with normal, FC- or ChA-enriched diets (Figure 6.1C), the appearance of red fluorescent bright spots suggested the accumulation of lipids in the vasculature of the caudal vein. The percentage of lipid structure area per area of caudal vein was quantified (Figure 6.1D) and an increase in the total area of fluorescent structures was found in the positive control - larvae fed with 4 % FC, as well as in animals fed with 3 % (half of the molarity of 4 % FC) and 6 % ChA (the same molarity), in a dose-dependent manner. Interestingly, the 2 % FC-enriched diet, corresponding to the same molarity as 3 % ChA, did not induce an increase in lipid accumulation (Figure 6.1D), suggesting ChA is potentially more atherogenic than FC. Furthermore, the increase in lipid accumulation observed in the vasculature was statistically significantly different in larvae fed for 5 days with ChA compared to the control groups (Supplementary Figure 6.1). These results are in agreement with previous data obtained by our group using another member of the ChE family, ChS (Domingues et al. 2017). To further characterize the lipid accumulation in the vasculature of zebrafish larvae, *fli1:EGFP* larvae, which constitutively express GFP in the vasculature under the control of the *fli1* promoter, were fed with different diets enriched with the lipid tracking probe. We observed that the fluorescence lipid accumulation was subendothelial and localized at sites

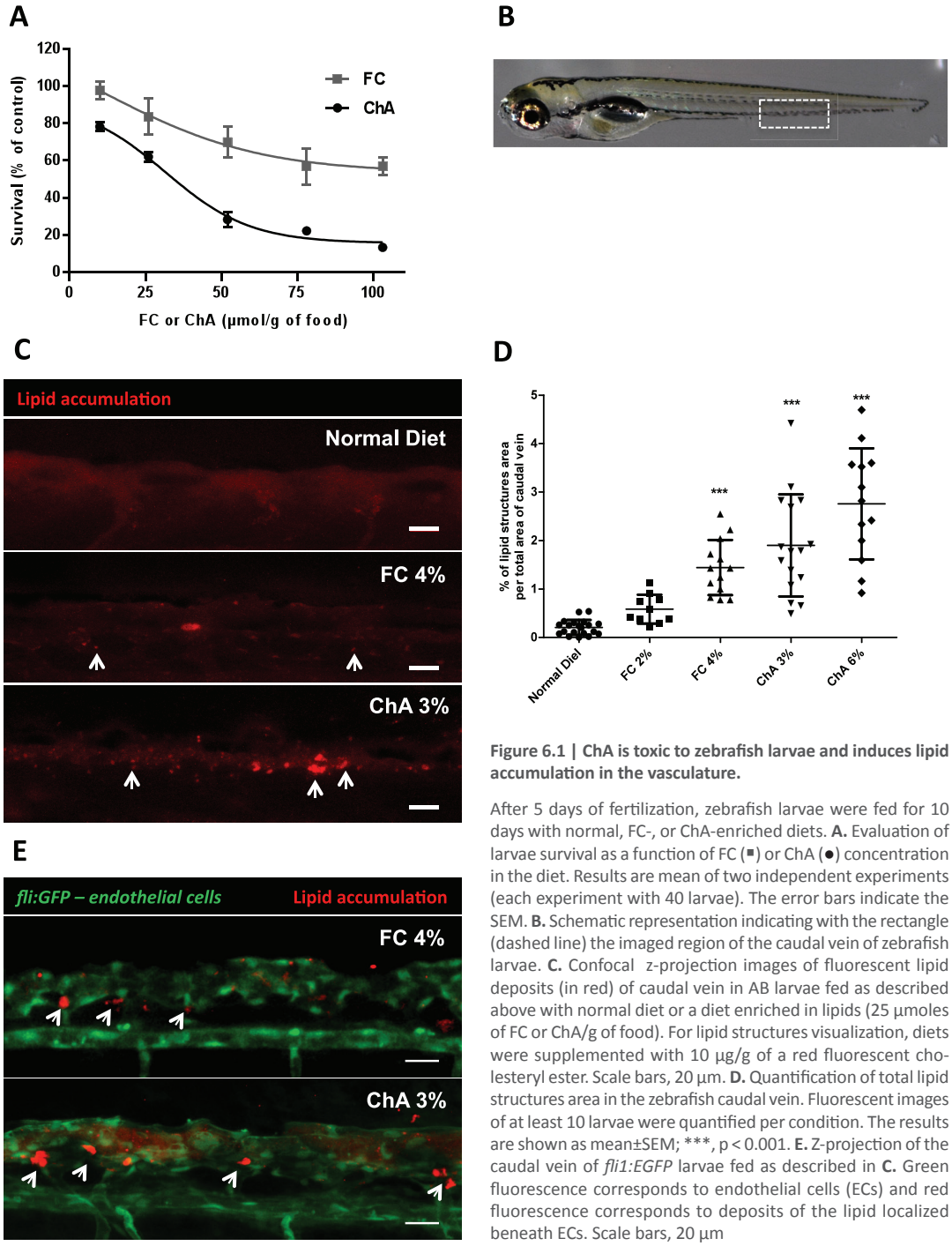

Figure 6.1 | ChA is toxic to zebrafish larvae and induces lipid accumulation in the vasculature.

After 5 days of fertilization, zebrafish larvae were fed for 10 days with normal, FC-, or ChA-enriched diets. **A.** Evaluation of larvae survival as a function of FC (▪) or ChA (●) concentration in the diet. Results are mean of two independent experiments (each experiment with 40 larvae). The error bars indicate the SEM. **B.** Schematic representation indicating with the rectangle (dashed line) the imaged region of the caudal vein of zebrafish larvae. **C.** Confocal z-projection images of fluorescent lipid deposits (in red) of caudal vein in AB larvae fed as described above with normal diet or a diet enriched in lipids (25 µmoles of FC or ChA/g of food). For lipid structures visualization, diets were supplemented with 10 µg/g of a red fluorescent cholesteryl ester. Scale bars, 20 µm. **D.** Quantification of total lipid structures area in the zebrafish caudal vein. Fluorescent images of at least 10 larvae were quantified per condition. The results are shown as mean±SEM; ***, $p < 0.001$. **E.** Z-projection of the caudal vein of *fli1:EGFP* larvae fed as described in **C.** Green fluorescence corresponds to endothelial cells (ECs) and red fluorescence corresponds to deposits of the lipid localized beneath ECs. Scale bars, 20 µm

of blood vessel bifurcation (Figure 6.1E). This subendothelial localization is well correlated with what has been described in humans and mice (Stoletov et al. 2009).

6.3.2 Zebrafish larvae fed with ChA accumulate higher numbers of inflammatory cells than FC-fed larvae in their vasculature

Atherosclerosis is characterized by the subendothelial accumulation of ox-LDL that stimulates the recruitment and activation of inflammatory cells. Therefore, we evaluated if ChA, similar to ChS (Domingues et al. 2017), was sufficient to increase the recruitment of myeloid cells to

the zebrafish larvae vasculature. After 10 days of feeding *pu.1:EGFP* transgenic larvae, whose myeloid cells express GFP, with normal, FC- or ChA-enriched diets, we found an increase in GFP-labelled cell recruitment to the caudal vein of animals fed with 4% FC, and 3% and 6% ChA (visualized in Figure 6.2A and quantified in Figure 6.2B). Since 3% ChA-enriched diet was sufficient to induce lipid accumulation and an increase in myeloid cells recruitment, we proceed our experiment with this concentration of ChE. Furthermore, in response to vascular injury, EC increase the expression of adhesion molecules resulting in the recruitment of inflammatory cells. Next, we measured VCAM-1 levels upon zebrafish larval feeding. This revealed an increase in VCAM-1 gene expression at 2 and 10 days post-feeding (Figure 6.2C and D), which is in agreement with the accumulation of myeloid cells in larvae vascular walls.

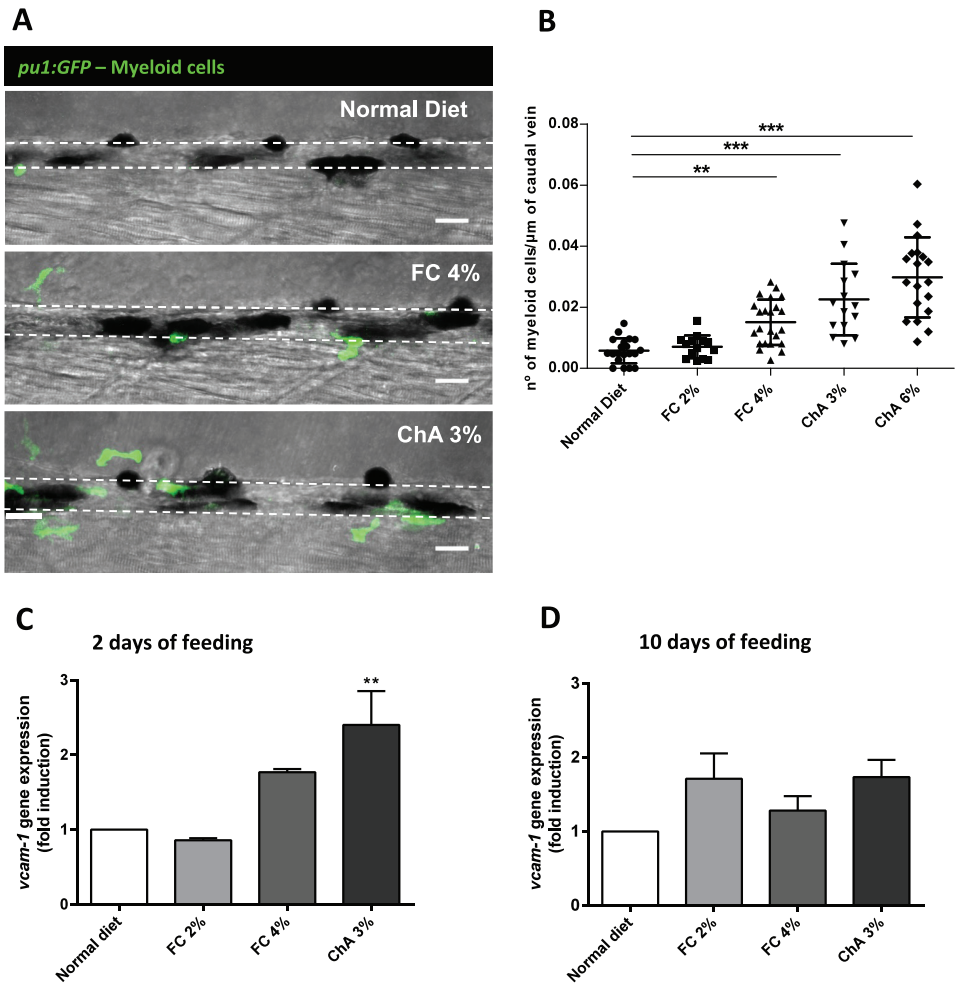

Figure 6.2 | Diet enriched in ChA induces myeloid cell recruitment to the vasculature and an increase in V-CAM1 gene expression.

A. *PU.1:EGFP* larvae were fed with normal, FC- or ChA-enriched diet for 10 days. FC 4% was used as positive control. Merge of GFP-fluorescent cells accumualtion in caudal vein (delineated by dotted lines) and bright field images. Scale, 20 µm. **B.** Quantification of myeloid cells normalized to the total lenght (µm) of of caudal vein analyzed. **C.** and **D.** Quantitative RT-PCR of zebrafish gene expression of V-CAM1 after 2 or 10 days of feeding with normal, FC- or ChA-enriched diet. The experiment was performed in triplicate (n = 20-30 zebrafish larvae per group) and the results are shown as mean±SEM; ** $p < 0.01$; ***, $p < 0.001$.

Neutrophils have been found in mice and humans both in early and advanced atherosclerotic lesions (Ionita et al. 2010; Rotzius et al. 2010; Drechsler et al. 2010), with NETs in close proximity with macrophages (Warnatsch et al. 2015). Zebrafish has been proposed as an well suitable model for neutrophilic inflammation studies (Renshaw and Loynes 2006). As

shown in Figure 6.3A and B and quantified in Figure 6.3C-F, a ChA-enriched diet stimulated an early (day 2) recruitment of neutrophils (green fluorescent cells) and macrophages (red fluorescent cells), while at this time point the recruitment of these cellular populations in FC-fed fish was similar to that of the normal diet. After 10 days of feeding, the induced neutrophil recruitment by FC-enriched diet did not change, whereas in ChA-fed animals, a reduction in neutrophil numbers was observed in the vasculature (Figure 6.3D). In addition, macrophage recruitment in FC and ChA-fed larvae was increased after 10 days of feeding with FC- and ChA-enriched diets, when compared with 2 days post-feeding (Figure 6.3F). Interestingly, we observed a close proximity between neutrophils and macrophages along the vasculature and this outcome will be explored in more detail in future.

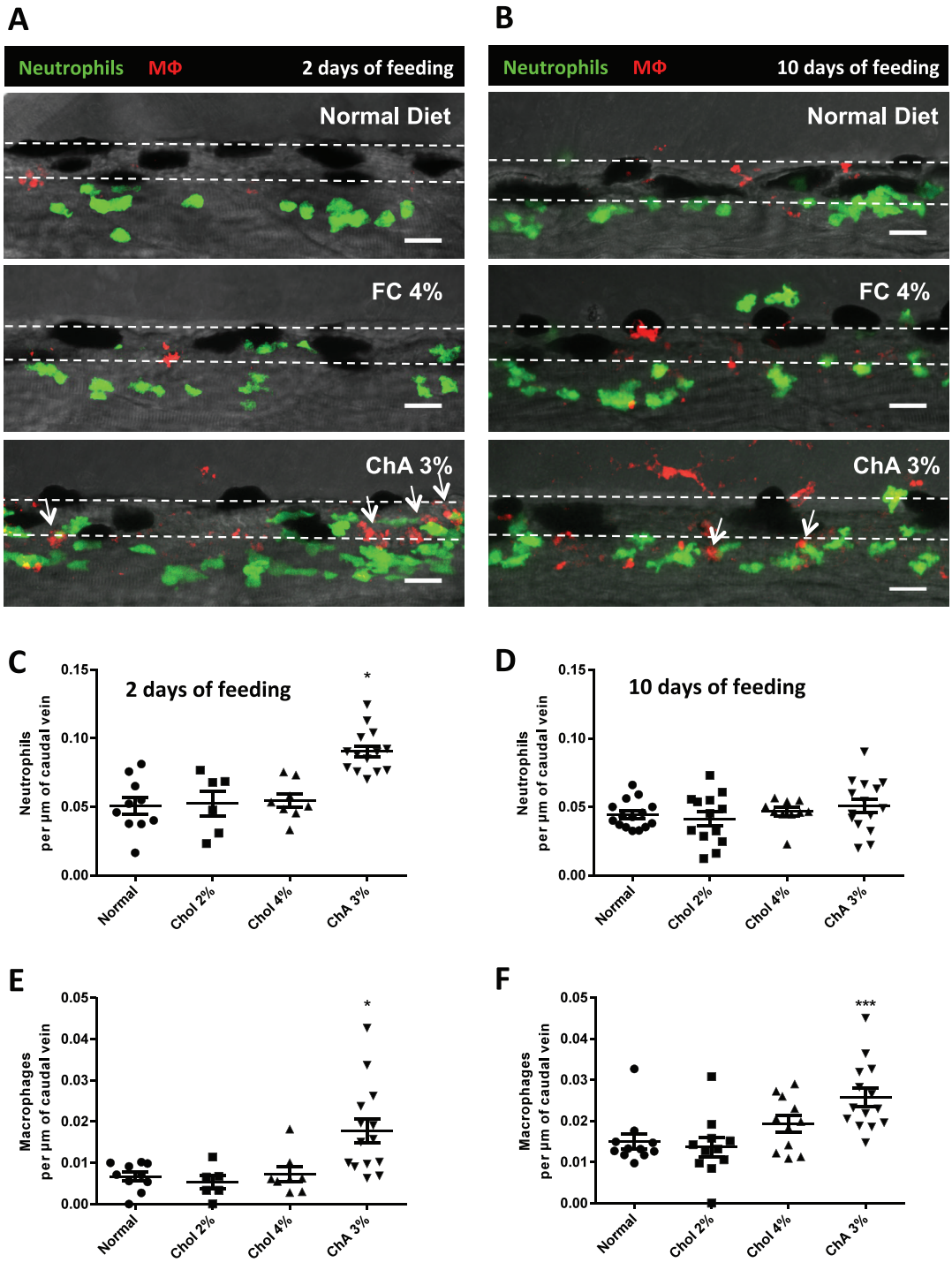

Figure 6.3 | ChA stimulates an early neutrophil and macrophage recruitment.

Descriptive and quantitative analysis of macrophages and neutrophil dynamics with feeding time. ChA stimulates an early neutrophils and macrophages recruitment. Descriptive and quantitative analysis of macropahges and neutrophil behavior with feeding time. **A-B.** Tg *(mpeg.mCherryCAAX SH378, mpx:EGFP i114)* larvae were fed for 2 **(A)** or 10 days **(B)** with normal, FC-or ChA-enriched diet and imaged using confocal microscopy. Z-stacks of fluorescent green (neutrophils) and red (macrophages) cells and the respective bright field were merged. Arrows point the close proximity between neutrophils and macrophages. Dashed lines deliniate caudal vein. Scale 20µm; **C-F.** Quantification of neutrophils (green cells, **C** and **E**) and macrophages (red cells, **D** and **F**) after 2 (**C** and **E**) or 10 days of feeding (**D** and **F**). The results are shown as mean±SEM of two independent experiments (at least 5 larvae per condition were analyzed); *, $p < 0.05$; ***, $p < 0.001$.

6.3.3 Macrophages isolated from ChA fed zebrafish larvae show lipid accumulation and lysosomal enlargement

In Chapters 4 and 5 of this thesis we showed that ChA-treated macrophages present an increase in lipid accumulation, a feature of foam cells, together with an impairment in lysosomal function. We thus questioned the capacity of ChA to induce lipid accumulation in macrophages *in vivo*. After 10 days of feeding, m-Cherry positive macrophages were isolated by fluorescence-assisted cell sorting (FACS) and stained for neutral lipids with BODIPY 493/503. As shown in Figure 6.4A and C, macrophages isolated from larvae fed with ChA presented an increase in neutral lipid accumulation, when compared with larvae fed with FC (2 % and 4 %) enriched or normal diet.

Several studies have correlated changes in lysosomal morphology with a reduction in the degradative function of these organelles (Kieseier, Wisniewski, and Goebel 1997; Emanuel et al. 2014; Jerome et al. 2008). In zebrafish animals, lysosomal dysfunction in macrophages was correlated with an increased susceptibility to *Mycobacterium marinum* infection, by reducing macrophage migration (Berg et al. 2016). Therefore, we considered whether macrophages from ChA-fed animals would show evidence of lysosomal dysfunction. To evaluate lysosomal dysfunction, we measured the lysosomal area in macrophages isolated by FACS from larvae fed with the different regimens. The results shown in Figure 6.4B and C demonstrated an increase in lysosomal size in macrophages isolated from zebrafish larvae fed with a ChA-enriched diet, compared with the controls. To confirm this result, we also evaluated the lysosomal morphology *in vivo*. As observed in *ex vivo* macrophages, lysosomes in the vasculature of zebrafish fed with a ChA-enriched diet presented enlarged lysosomes (Figure 6.4E). Interestingly, lysosomal positioning in macrophages treated with FC and ChA-enriched diet was also different. In animals fed with FC, lysosomes seemed to be clustered in the perinuclear region in FC- loaded macrophages, while lysosomes in macrophages from ChA-fed animals were located more proximal to macrophage edges. Together these findings suggest that ChA induces lipid accumulation and enlargement lysosomal in macrophages recruited to the vasculature of zebrafish larvae. These results corroborate the *in vitro* data using macrophages RAW cell line and primary BMDM shown in the Chapter 5 of this thesis.

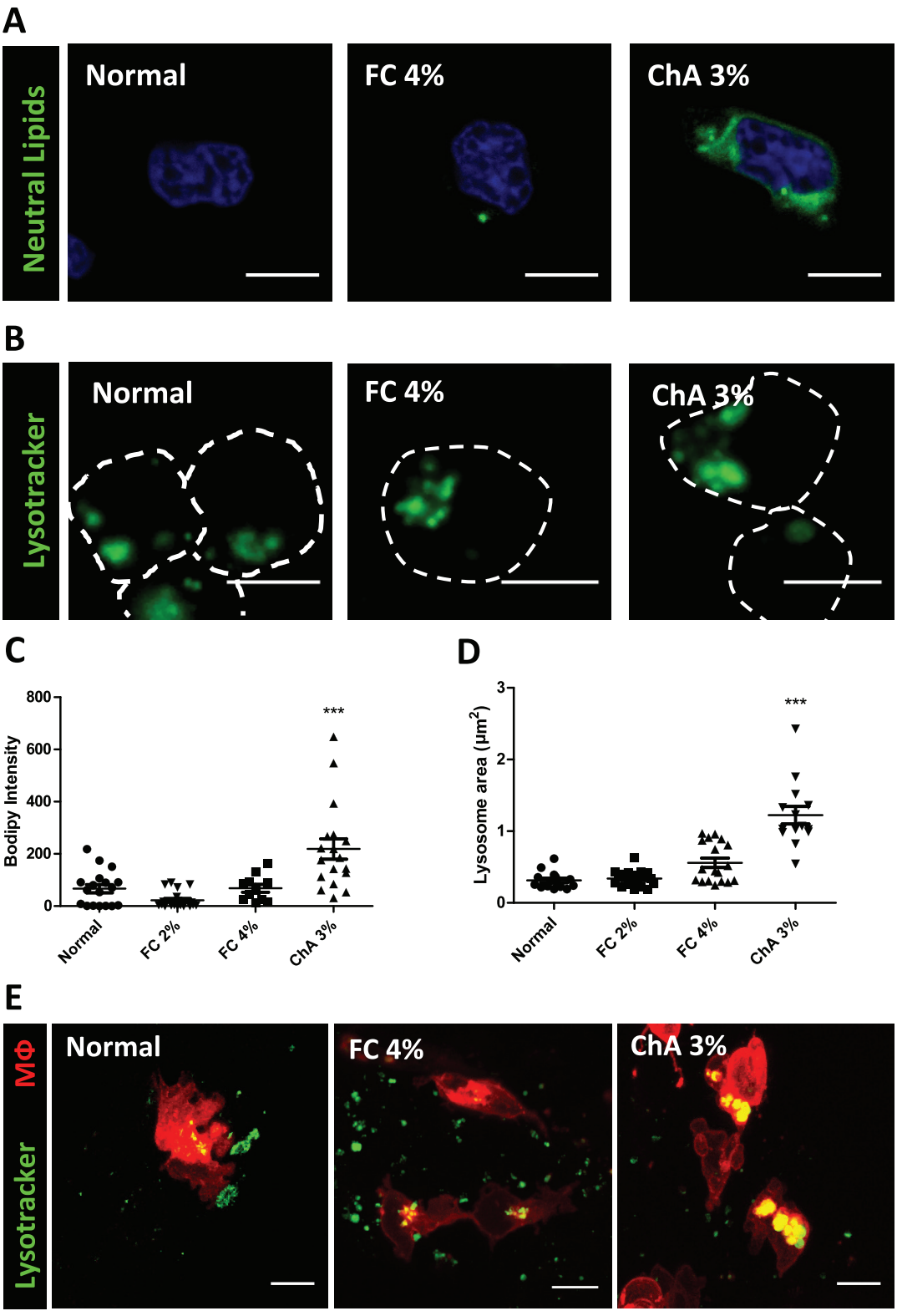

Figure 6.4 | Macrophages from zebrafish larvae fed with ChA exhibit lipid accumulation and lysosome enlargment.

Zebrafish larvae were fed for 10 days with normal, FC- or ChA- enriched diet and macrophages were isolated using cell sorting cytometry (FACS). **A.** Representative images of macrophages stained with BODIPY 493/503 to visualize neutral lipids and DAPI to visualize nuclei. **B.** Lysosomes/acid organelles from macrophages were labeled with lysotracker and cells were imaged by confocal microscopy. Scale bar, 5 µm. **C-D** Quantification of neutral lipid accumulation **(C)** and lysosome area **(D)** on isolated macrophages. The results are the mean±SEM of two independent experiments (analyzed at least 10 cells per condition); ***, $p < 0.01$. **E.** *In vivo* lysosomal imaging of macrophages (m-Cherry) from larvae fed with different diets. Lysosomes were stained with lysotracker (green). Scale bars, 10 µm.

6.3.4 ChA increases the mRNA levels of inflammatory cytokines

Our previous work showed that primary macrophages incubated with ChS and a low dose of LPS demonstrated an increase in proinflammatory cytokine release, which included elevated levels of IL-1β, IL-6 and TNF-α (Domingues et al., 2017). Furthermore, in this thesis we have also shown that ChA increased the release of proinflammatory cytokines in primary monocytes and macrophages of human and mouse origin (Chapter 4). Thus, we next assessed the proinflammatory potential of ChA *in vivo* in the zebrafish model. Initially, by stimulation with LPS, we confirmed the ability of zebrafish larvae at 15 dpf to express cytokines as previously reported (Yoon et al. 2013; Progatzky et al. 2014). An overnight treatment of zebrafish larvae with LPS induced a significantly increase in IL-1β, IL-6 and TNF-α gene expression, as compared to untreated control larvae (Supplementary Figure 6.2B, C and F). Next, we analyzed of these cytokines levels in larvae fed for 2 and 10 days with normal-, FC- and ChA-enriched diets. At 2 days post-feeding, no statistically significant differences were observed in gene expression levels for the proinflammatory cytokines tested (Figure 6.4A, C and E). However, at 10 days post-feeding, the results obtained showed an increase of IL-1β (Figure 6.5B), IL-6 (Figure 6.5D) and TNF-α (Figure 6.5F) gene expression in ChA-fed larvae. These results suggest that proinflammatory cytokine levels were increased in zebrafish larvae when fed with ChA-enriched diet, demonstrating the in vivo proinflammatory properties of ChA.

6.4 DISCUSSION

Since cardiovascular diseases are the leading cause of death worldwide, there is a global effort to develop early diagnostic tools and effective treatments for atherosclerosis, one of the major conditions that increases the risk of a CVD event (Steinberg, Glass, and Witztum 2008; Benedek et al. 2016). The initial events that characterize atherogenesis are: i) activation of EC and consequent recruitment of neutrophils and monocytes; ii) excessive accumulation of Ox-Lp in macrophages and, iii) inflammation that is present through the entire pathological process. This work is an attempt to correlate those early events with the presence of a family of ChE, formed during oxidation of the main cholesteryl esters of the LDL particles found in the arterial intima.

By feeding zebrafish larvae with the ChS, we have been able to reproduce many of the processes involved in early atherogenesis (Domingues et al. 2017). In this study, using a member of the ChE family identified in human plasma – ChA – we observed that zebrafish larvae fed with a ChA-enriched diet showed a decrease in survival accompanied by vascular lipid deposition (Figure 6.1) and myeloid cell accumulation (Figure 6.2). Moreover, we demonstrated that a ChA-rich diet caused an increased in the number of neutrophils and macrophages to accumulate in the vasculature (Figure 6.3) and an increase in proinflammatory cytokine gene expression (Figure 6.5). Moreover, atherosclerosis has been considered a lysosomal storage

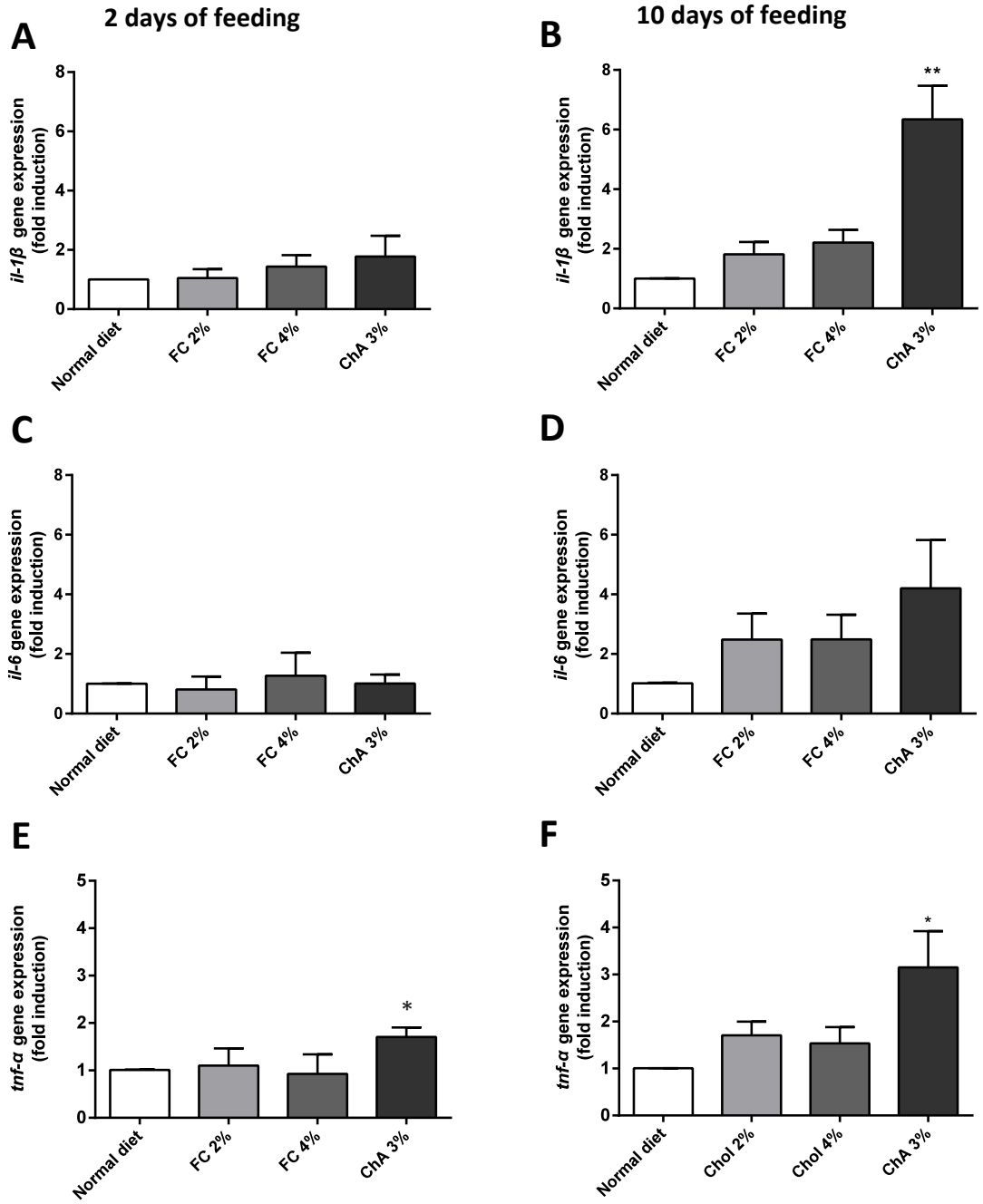

Figure 6.5 | ChA induces a increase in expression of proinflammatory cytokines in a time-dependent manner.

A-F Quantitative RT-PCR of zebrafish gene expression of *IL-1β* (**A** and **B**), *IL-6* (C and D) and *TNF-α* (**E** and **F**) after 2 or 10 days of feeding (left and right column, respectively) with normal, FC- or ChA-enriched diet. The values represent the mean±SEM of three experiment was performed in triplicate (n = 20-30 zebrafish larvae per group); *, $p < 0.05$ **, $p < 0.01$.

disease (Jerome 2006; Emanuel et al. 2014) and, in this work, using zebrafish as an animal model, we also demonstrate lysosome enlargement suggestive of lysosomal dysfunction in macrophages isolated from larvae fed with ChA.

Zebrafish larvae is a suitable animal model to study *in vivo* atherogenic processes and inflammation, with an innate immune response reminiscent with other animal models (Stoletov et al. 2009; Fang, Liu, and Miller 2014; Progatzky et al. 2014; Novoa and Figueras 2012). Using transgenic zebrafish with GFP-labelled EC, we observed an increase in lipid accumulation in

the bifurcations of the caudal vein of larvae fed with ChA (Figure 6.1E), where turbulent blood flow is expected to occur. These results are in agreement with published data in humans and mice, where a higher propensity of lipid-driven disease is observed in the arteries branches with disturbed flow. In these regions, there is an endothelial activation which facilitates the intimal retention of lipoproteins (Tabas, García-Cardeña, and Owens 2015; Ku et al. 1985; Maeda et al. 2007). Our results are also in accordance with the observed lipid accumulation induced by an FC-enriched diet in the zebrafish caudal vein (Stoletov et al. 2009), where the deposits in veins were explained by the direct connectivity system of large arteries and veins in zebrafish at this stage.

As a chronic inflammatory disease, atherosclerosis is defined by an increase in the recruitment of leukocyte cells to the arterial vessel wall, resulting in intimal lesion growth. Activated EC increase the expression of adhesion molecules, such as VCAM-1 (Ley and Huo 2001). Our results show that a ChA-enriched diet induced an increase in VCAM-1 gene expression, which presents a role in the increase of neutrophil and monocyte recruitment along the vessel walls. The role of macrophages in atherosclerosis initiation and development is well characterized (Moore and Tabas 2011; Tabas 2010; Libby, Ridker, and Maseri 2002). In the past decade, the contribution of neutrophils to atheroma initiation and progression has also received growing attention (Döring et al. 2012; Rotzius et al. 2010; Nahrendorf and Swirski 2015; Döring, Soehnlein, and Weber 2017). In summary, it has been shown that neutrophils play an active role in aggravating endothelial dysfunction, recruitment of monocytes to atherosclerotic lesions and in promoting foam cell formation (Döring, Soehnlein, and Weber 2017; Döring et al. 2015; Moreno et al. 2012). The work developed by Warnatsch *et al.* (Warnatsch et al. 2015) reported that neutrophils are responsible for the priming of macrophages through NETs release. In the context of atherosclerosis, extracellular cholesterol crystals were shown to interact with neutrophils triggering the release of NETs, which prime macrophages to produce a precursor form of the inflammatory cytokine IL-1β (pro–IL-1β) (Warnatsch et al. 2015). Thus, the increase in neutrophil numbers in ChA fed animals and the close proximity of these cells with macrophages suggest a possible involvement of NETs in the priming of ChA-loaded macrophages. To validate this hypothesis, these results need to be confirmed in the zebrafish larvae by staining extracellular DNA with Sytox, thus detecting NETs.

The capacity of macrophage lysosomes to digest both exogenous and internally derived cargo, is a key event in the clearance of excessive lipid accumulation and cytotoxic material present in the atherosclerotic plaque (Tabas 2010). Accordingly, lipid-mediated loss of function in macrophage lysosomes has been characterized as a critical event in plaque initiation and progression (Jerome 2010; Emanuel et al. 2014; Domingues et al. 2017). Among several consequences, we highlight the involvement of dysfunctional lysosomes in inflammatory signaling, particularly the inflammasome and IL-1β release (Duewell et al. 2010). Here, we observed a change in lysosomal morphology in macrophage foam cells generated by feeding zebrafish larvae with ChA-enriched diet (Figure 6.4B and E) suggesting a loss-of-function as previously described for other experimental settings (Kinghorn, Asghari, and Castillo-Quan

2017; Jerome et al. 2008; Cox et al. 2007; Domingues et al. 2017; Emanuel et al. 2014) and also described in this thesis (Chapter 5).

Several data have implicated IL-1β in a number of CVDs (reviewed in (Bujak and Frangogiannis 2009)). IL-1β mediates an amplification loop, whereby a single molecule of IL-1β can stimulate many molecules of IL-6 (Libby and Ridker 2006), which in turn lead to the overexpression of other atherothrombosis mediators, such as, the adhesion molecules: intercellular adhesion molecule (ICAM)-1 and VCAM-1 (Takei, Huang, and Lopes-Virella 2001). Here, we extend our understanding of the proinflammatory properties of ChA using a model that delivers lipids through its normal route of ingestion to the blood flow. We found an increase in IL-1β, IL-6 and TNF-α gene expression in larvae fed with a ChA-enriched diet, providing novel evidence of the proinflammatory properties of ChA *in vivo*. Moreover, we were able to, for the first time, monitor time-dependent neutrophil and macrophage infiltration in lipid-injured vasculature and lysosomal morphology changes in live animals. Based on these results, we propose a working model in which neutrophils can prime macrophage, conferring the first signal for transcription of proinflammatory cytokines in ChA-fed animals (Figure 6.6). When ChA is internalized by macrophages, it induces lysosome dysfunction that is responsible for the second signal, which leads to inflammasome assembly and proteolytic activation of immature cytokines (Chapter 4). Nevertheless, more experiments need to be performed to confirm our hypothesis regarding the inflammasome involvement in zebrafish activated macrophages. Through the use of inhibitors, it will be crucial to evaluate the effect of NLRP3/caspase-1 and cathepsins on IL-1β gene expression and release, confirming the lysosomal role in atherosclerosis development.

We conclude that ChA, identified to be increased in the plasma of human CVD, is able to induce *in vivo* features observed in early stages of atherogenesis. Through the feeding of zebrafish larvae with ChA-enriched diet, we offered a new experimental approach to study the initial mechanisms underlying atherogenesis.

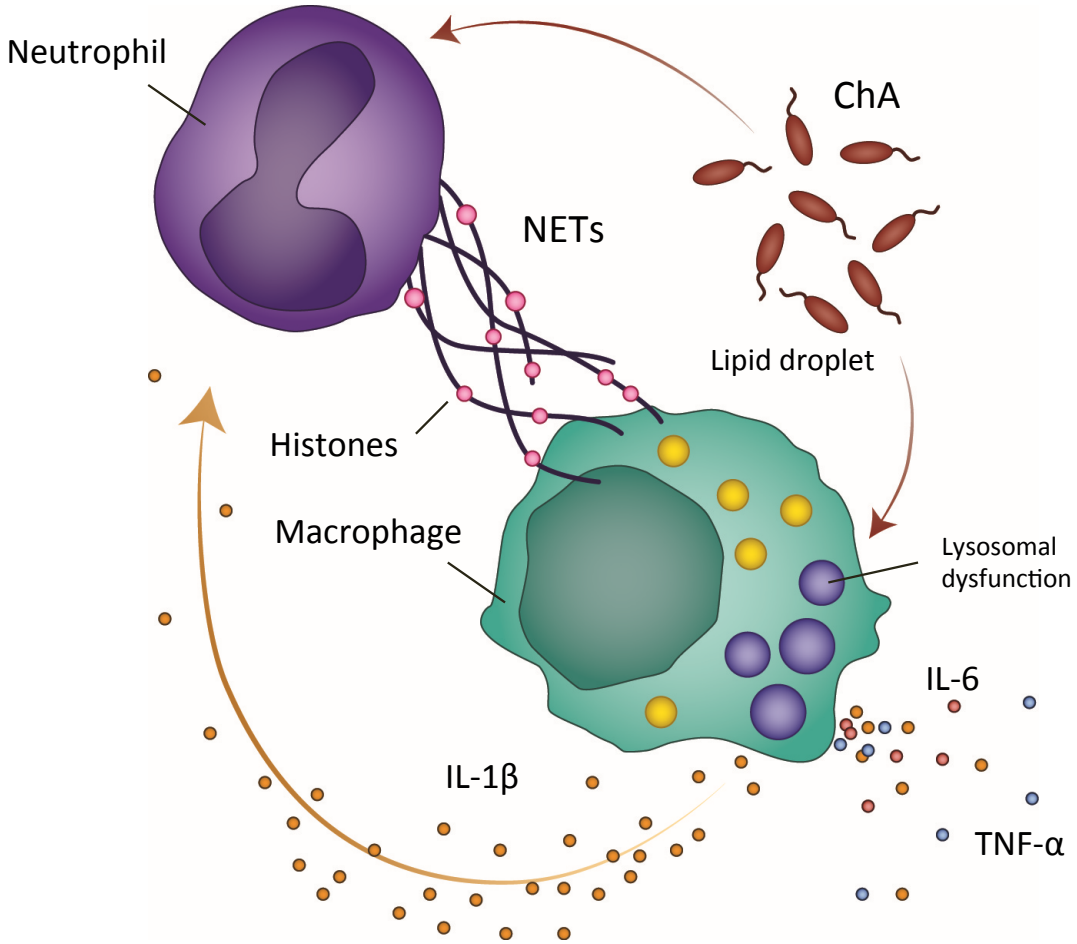

Figure 6.6 | Putative mechanism behind atherosclerotic macrophages activation under ChA presence

ChA accumulates in arterial intima, promoting the recruitment of innate immune cells, neutrophils and macrophages. In arterial intima, ChA-activates neutrophils to secret neutrophil extracellular traps (NETs) which are responsible for macrophage priming. In primed macrophages, ChA induces lysosomal dysfunction, confering then the second signal necessary for IL-1β secretion mediated by inflammasome activation. IL-1β can initiate a propagation loop of the inflammation, increasing the macrophages secretion of IL-6 and TNF-α. This working model was also based in the findings of Warnatsch *et al*. 2015.

6.5 REFERENCES

Anderson, Jennifer L., Juliana D. Carten, and Steven A. Farber. 2011. Zebrafish Lipid Metabolism: From Mediating Early Patterning to the Metabolism of Dietary Fat and Cholesterol. Methods in Cell Biology. Vol. 101. doi:10.1016/B978-0-12-387036-0.00005-0.

Benedek, Theodora, Pál Maurovich-Horváth, Péter Ferdinandy, and Béla Merkely. 2016. "The Use of Biomarkers for the Early Detection of Vulnerable Atherosclerotic Plaques and Vulnerable Patients. A Review." Journal Of Cardiovascular Emergencies 2 (3). doi:10.1515/jce-2016-0017.

Berg, Russell D., Steven Levitte, Mary P. O'Sullivan, Seónadh M. O'Leary, C. J. Cambier, James Cameron, Kevin K. Takaki, et al. 2016. "Lysosomal Disorders Drive Susceptibility to Tuberculosis by Compromising Macrophage Migration." Cell 165 (1): 139–52. doi:10.1016/j.cell.2016.02.034.

Bujak, Marcin, and Nikolaos G. Frangogiannis. 2009. "The Role of IL-1 in the Pathogenesis of Heart Disease." Archivum Immunologiae et Therapiae Experimentalis. doi:10.1007/s00005-009-0024-y.

Cox, Brian E, Evelyn E Griffin, Jody C Ullery, and W Gray Jerome. 2007. "Effects of Cellular Cholesterol Loading on Macrophage Foam Cell Lysosome Acidification." Journal of Lipid Research 48 (5): 1012–21. doi:10.1194/jlr.M600390-JLR200.

Domingues, Neuza, Luís M.B.B. Estronca, João Silva, Marisa R. Encarnação, Rita Mateus, Diogo Silva, Inês B. Santarino, et al. 2017. "Cholesteryl Hemiesters Alter Lysosome Structure and Function and Induce Proinflammatory Cytokine Production in Macrophages." Biochimica et Biophysica Acta - Molecular and Cell Biology of Lipids 1862 (2): 210–20. doi:10.1016/j.bbalip.2016.10.009.

Döring, Yvonne, Maik Drechsler, Oliver Soehnlein, and Christian Weber. 2015. "Neutrophils in Atherosclerosis: From Mice to Man." Arteriosclerosis, Thrombosis, and Vascular Biology 35 (2): 288–95. doi:10.1161/ATVBAHA.114.303564.

Döring, Yvonne, Maik Drechsler, Sarawuth Wantha, Klaus Kemmerich, Dirk Lievens, Santosh Vijayan, Richard L. Gallo, Christian Weber, and Oliver Soehnlein. 2012. "Lack of Neutrophil-Derived CRAMP Reduces Atherosclerosis in Mice." Circulation Research 110 (8): 1052–56. doi:10.1161/CIRCRESAHA.112.265868.

Döring, Yvonne, Oliver Soehnlein, and Christian Weber. 2017. "Neutrophil Extracellular Traps in Atherosclerosis and Atherothrombosis." Circulation Research. doi:10.1161/CIRCRESAHA.116.309692.

Drechsler, Maik, Remco T A Megens, Marc Van Zandvoort, Christian Weber, and Oliver Soehnlein. 2010. "Hyperlipidemia-Triggered Neutrophilia Promotes Early Atherosclerosis." Circulation 122 (18): 1837–45. doi:10.1161/CIRCULATIONAHA.110.961714.

Duewell, Peter, Hajime Kono, Katey J. Rayner, Cherilyn M. Sirois, Gregory Vladimer, Franz G. Bauernfeind, George S. Abela, et al. 2010. "NLRP3 Inflammasomes Are Required for Atherogenesis and Activated by Cholesterol Crystals." Nature 466 (7306): 652–652. doi:10.1038/nature09316.

Emanuel, Roy, Ismail Sergin, Somashubhra Bhattacharya, Jaleisa N. Turner, Slava Epelman, Carmine Settembre, Abhinav Diwan, Andrea Ballabio, and Babak Razani. 2014. "Induction of Lysosomal Biogenesis in Atherosclerotic Macrophages Can Rescue Lipid-Induced Lysosomal Dysfunction and Downstream Sequelae." Arteriosclerosis, Thrombosis, and Vascular Biology 34 (9): 1942–52. doi:10.1161/ATVBAHA.114.303342.

Erridge, Clett, Simon Kennedy, Corinne M. Spickett, and David J. Webb. 2008. "Oxidized Phospholipid Inhibition of Toll-Like Receptor (TLR) Signaling Is Restricted to TLR2 and TLR4: Roles for CD14, LPS-Binding Protein, and MD2 as Targets for Specificity of Inhibition." Journal of Biological Chemistry 283 (36): 24748–59. doi:10.1074/jbc.M800352200.

Estronca, Luis M B B, Joao C P Silva, Julio L Sampaio, Andrej Shevchenko, Paul Verkade, Alfin D N Vaz, Winchil L C Vaz, and Otilia V Vieira. 2012. "Molecular Etiology of Atherogenesis--in Vitro Induction of Lipidosis in Macrophages with a New LDL Model." PloS One 7 (4): e34822. doi:10.1371/journal.pone.0034822.

Fang, Longhou, Richard Harkewicz, Karsten Hartvigsen, Philipp Wiesner, Soo Ho Choi, Felicidad Almazan, Jennifer Pattison, et al. 2010. "Oxidized Cholesteryl Esters and Phospholipids in Zebrafish Larvae Fed a High Cholesterol Diet: Macrophage Binding and Activation." Journal of Biological Chemistry 285 (42): 32343–51. doi:10.1074/jbc.M110.137257.

Fang, Longhou, Chao Liu, and Yury I. Miller. 2014. "Zebrafish Models of Dyslipidemia: Relevance to Atherosclerosis and Angiogenesis." Translational Research. doi:10.1016/j.trsl.2013.09.004.

Guo, Haitao, Justin B Callaway, and Jenny P-Y Ting. 2015. "Inflammasomes: Mechanism of Action, Role in Disease, and Therapeutics." Nature Medicine 21 (7): 677–87. doi:10.1038/nm.3893.

Hoppe, G, a Ravandi, D Herrera, a Kuksis, and H F Hoff. 1997. "Oxidation Products of Cholesteryl Linoleate Are Resistant to Hydrolysis in Macrophages, Form Complexes with Proteins, and Are Present in Human Atherosclerotic Lesions." Journal of Lipid Research 38 (7): 1347–60.

Ionita, Mihaela G., Pleunie Van Den Borne, Louise M. Catanzariti, Frans L. Moll, Jean Paul P M De Vries, Gerard Pasterkamp, Aryan Vink, and Dominique P V De Kleijn. 2010. "High Neutrophil Numbers in Human Carotid Atherosclerotic Plaques Are Associated with Characteristics of Rupture-Prone Lesions." Arteriosclerosis, Thrombosis, and Vascular Biology 30 (9): 1842–48. doi:10.1161/ATVBAHA.110.209296.

Jerome, W Gray. 2006. "Advanced Atherosclerotic Foam Cell Formation Has Features of an Acquired Lysosomal Storage Disorder." Rejuvenation Research 9 (2): 245–55. doi:10.1089/rej.2006.9.245.

Jerome, W Gray. 2010. "Lysosomes, Cholesterol and Atherosclerosis." Clinical Lipidology 5 (6): 853–65. doi:10.2217/clp.10.70.

Jerome, W Gray, Brian E Cox, Evelyn E Griffin, and Jody C Ullery. 2008. "Lysosomal Cholesterol Accumulation Inhibits Subsequent Hydrolysis of Lipoprotein Cholesteryl Ester." Microscopy and Microanalysis : The Official Journal of Microscopy Society of America, Microbeam Analysis Society, Microscopical Society of Canada 14 (2): 138–49. doi:10.1017/S1431927608080069.

Kieseier, B C, K E Wisniewski, and H H Goebel. 1997. "The Monocyte-Macrophage System Is Affected in Lysosomal Storage Diseases: An Immunoelectron Microscopic Study." Acta Neuropathol. http://www.ncbi.nlm.nih.gov/entrez/query.fcgi?cmd=Retrieve&db=PubMed&dopt=Citation&list_uids=9341937.

Kinghorn, KerriJ, AmirM Asghari, and JorgeIván Castillo-Quan. 2017. "The Emerging Role of Autophagic-Lysosomal Dysfunction in Gaucher Disease and Parkinson's Disease." Neural Regeneration Research 12 (3): 380. doi:10.4103/1673-5374.202934.

Kobayashi, K, E Matsuura, Q Liu, J Furukawa, K Kaihara, J Inagaki, T Atsumi, et al. 2001. "A Specific Ligand for beta(2)-Glycoprotein I Mediates Autoantibody-Dependent Uptake of Oxidized Low Density Lipoprotein by Macrophages." Journal of Lipid Research 42 (5): 697–709. http://www.ncbi.nlm.nih.gov/pubmed/11352976.

Ku, D. N., D. P. Giddens, C. K. Zarins, and S. Glagov. 1985. "Pulsatile Flow and Atherosclerosis in the Human Carotid Bifurcation. Positive Correlation between Plaque Location and Low Oscillating Shear Stress." Arteriosclerosis, Thrombosis, and Vascular Biology 5 (3): 293–302. doi:10.1161/01.ATV.5.3.293.

Lamkanfi, Mohamed, and Vishva M. Dixit. 2014. "Mechanisms and Functions of Inflammasomes." Cell. doi:10.1016/j.cell.2014.04.007.

Ley, Klaus, and Yuqing Huo. 2001. "VCAM-1 Is Critical in Atherosclerosis." Journal of Clinical Investigation. doi:10.1172/JCI13005.

Libby, Peter. 2012. "History of Discovery : Inflammation in Atherosclerosis." Arterioscler Thromb Vasc Biol. 32 (9): 2045–51. doi:10.1161/ATVBAHA.108.179705.History.

Libby, Peter, and Paul M. Ridker. 2006. "Inflammation and Atherothrombosis. From Population Biology and Bench Research to

Clinical Practice." Journal of the American College of Cardiology. doi:10.1016/j.jacc.2006.08.011.

Libby, Peter, Paul M. Ridker, and Attilio Maseri. 2002. "Inflammation and Atherosclerosis." Circulation 105 (9): 1135–43. doi:10.1161/hc0902.104353.

Maeda, Nobuyo, Lance Johnson, Shinja Kim, John Hagaman, Morton Friedman, and Robert Reddick. 2007. "Anatomical Differences and Atherosclerosis in Apolipoprotein E-Deficient Mice with 129/SvEv and C57BL/6 Genetic Backgrounds." Atherosclerosis 195 (1): 75–82. doi:10.1016/j.atherosclerosis.2006.12.006.

Miller, Lloyd S., Ryan M. O'Connell, Miguel A. Gutierrez, Eric M. Pietras, Arash Shahangian, Catherine E. Gross, Ajaykumar Thirumala, Ambrose L. Cheung, Genhong Cheng, and Robert L. Modlin. 2006. "MyD88 Mediates Neutrophil Recruitment Initiated by IL-1R but Not TLR2 Activation in Immunity against Staphylococcus Aureus." Immunity 24 (1): 79–91. doi:10.1016/j.immuni.2005.11.011.

Moore, Kathryn J., and Ira Tabas. 2011. "Macrophages in the Pathogenesis of Atherosclerosis." Cell 145 (3): 341–55. doi:10.1016/j.cell.2011.04.005.

Moreno, Juan Antonio, Almudena Ortega-Gómez, Sandrine Delbosc, Nathalie Beaufort, Emmanuel Sorbets, Liliane Louedec, Marina Esposito-Farèse, et al. 2012. "In Vitro and in Vivo Evidence for the Role of Elastase Shedding of CD163 in Human Atherothrombosis." European Heart Journal 33 (2): 252–63. doi:10.1093/eurheartj/ehr123.

Nahrendorf, Matthias, and Filip K. Swirski. 2015. "Neutrophil-Macrophage Communication in Inflammation and Atherosclerosis." Science 349 (6245): 237–38. doi:10.1126/science.aac7801.

Novoa, Beatriz, and Antonio Figueras. 2012. "Zebrafish: Model for the Study of Inflammation and the Innate Immune Response to Infectious Diseases." Advances in Experimental Medicine and Biology 946: 253–75. doi:10.1007/978-1-4614-0106-3_15.

Progatzky, Fränze, Navjyot J. Sangha, Nagisa Yoshida, Marie McBrien, Jackie Cheung, Alice Shia, James Scott, et al. 2014. "Dietary Cholesterol Directly Induces Acute Inflammasome-Dependent Intestinal Inflammation." Nature Communications 5: 5864. doi:10.1038/ncomms6864.

Renshaw, SA, and CA Loynes. 2006. "A Transgenic Zebrafish Model of Neutrophilic Inflammation." Blood… 108 (13): 3976–78. doi:10.1182/blood-2006-05-024075.The.

Ridker, Paul M, Brendan M. Everett, Tom Thuren, Jean G. MacFadyen, William H. Chang, Christie Ballantyne, Francisco Fonseca, et al. 2017. "Antiinflammatory Therapy with Canakinumab for Atherosclerotic Disease." New England Journal of Medicine, NEJMoa1707914. doi:10.1056/NEJMoa1707914.

Rotzius, Pierre, Sebastian Thams, Oliver Soehnlein, Ellinor Kenne, Chi-Nan Tseng, Niklas K Björkström, Karl-Johan Malmberg, Lennart Lindbom, and Einar E Eriksson. 2010. "Distinct Infiltration of Neutrophils in Lesion Shoulders in ApoE-/- Mice." The American Journal of Pathology 177 (1): 493–500. doi:10.2353/ajpath.2010.090480.

Schroder, Kate, and Jurg Tschopp. 2010. "The Inflammasomes." Cell. doi:10.1016/j.cell.2010.01.040.

Sheedy, Frederick J, and Kathryn J Moore. 2013. "IL-1 Signaling in Atherosclerosis: Sibling Rivalry." Nature Immunology 14 (10). Nature Publishing Group: 1030–32. doi:10.1038/ni.2711.

Steinberg, Daniel, Christopher K. Glass, and Joseph L. Witztum. 2008. "Evidence Mandating Earlier and More Aggressive Treatment of Hypercholesterolemia." Circulation. doi:10.1161/CIRCULATIONAHA.107.753152.

Stoletov, Konstantin, Longhou Fang, Soo Ho Choi, Karsten Hartvigsen, Lotte F. Hansen, Chris Hall, Jennifer Pattison, et al. 2009. "Vascular Lipid Accumulation, Lipoprotein Oxidation, and Macrophage Lipid Uptake in Hypercholesterolemic Zebrafish." Circulation Research 104 (8): 952–60. doi:10.1161/CIRCRESAHA.108.189803.

Tabas, Ira. 2010. "Macrophage Death and Defective Inflammation Resolution in Atherosclerosis." Nature Reviews Immunology 10 (2): 117. doi:10.1038/nri2675.

Tabas, Ira, Guillermo García-Cardeña, and Gary K. Owens. 2015. "Recent Insights into the Cellular Biology of Atherosclerosis." Journal of Cell Biology 209 (1): 13–22. doi:10.1083/jcb.201412052.

Takei, a, Y Huang, and M F Lopes-Virella. 2001. "Expression of Adhesion Molecules by Human Endothelial Cells Exposed to Oxidized Low Density Lipoprotein. Influences of Degree of Oxidation and Location of Oxidized LDL." Atherosclerosis 154 (1): 79–86. doi:S0021-9150(00)00465-2 [pii].

Tedgui, A. 2006. "Cytokines in Atherosclerosis: Pathogenic and Regulatory Pathways." Physiological Reviews 86 (2): 515–81. doi:10.1152/physrev.00024.2005.

Wang, Zemin, Yun Mao, Taixing Cui, Dongqi Tang, and Xing Li Wang. 2013. "Impact of a Combined High Cholesterol Diet and High Glucose Environment on Vasculature." PLoS ONE 8 (12). doi:10.1371/journal.pone.0081485.

Wantha, Sarawuth, Jean Eric Alard, Remco T A Megens, Anne M. Van Der Does, Yvonne Döring, Maik Drechsler, Christine T N Pham, et al. 2013. "Neutrophil-Derived Cathelicidin Promotes Adhesion of Classical Monocytes." Circulation Research 112 (5): 792–801. doi:10.1161/CIRCRESAHA.112.300666.

Warnatsch, A., M. Ioannou, Q. Wang, and V. Papayannopoulos. 2015. "Neutrophil Extracellular Traps License Macrophages for Cytokine Production in Atherosclerosis." Science 349 (6245): 316–20. doi:10.1126/science.aaa8064.

Yoon, Yina, Jihye Yoon, Man-Young Jang, Yirang Na, Youngho Ko, Jae-Hoon Choi, and Seung Hyeok Seok. 2013. "High Cholesterol Diet Induces IL-1β Expression in Adult but Not Larval Zebrafish." PloS One 8: e66970. doi:10.1371/journal.pone.0066970.

6.6 SUPPLEMENTAL INFORMATION

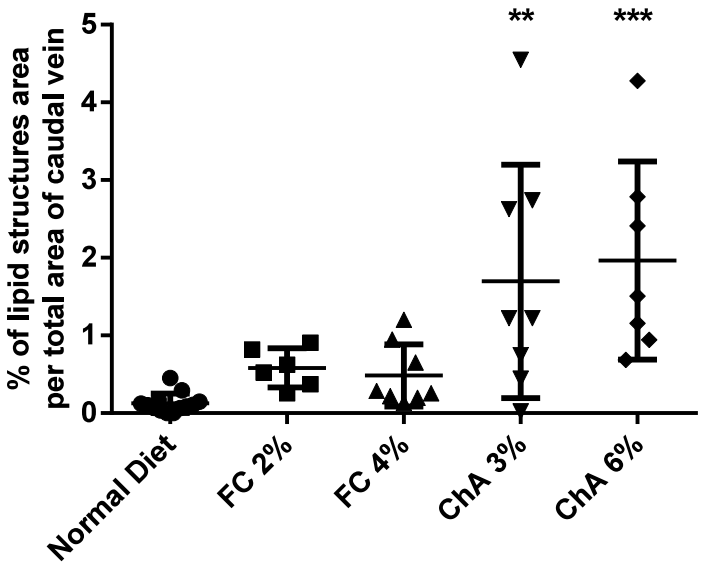

Supplementary Figure 6.1 | ChA induces accumulation of lipid in the vasculature earlier than free cholesterol.

After 5 days of feeding with normal, FC-, or ChA-enriched diets, AB zebrafish larvae were imaged by confocal microscopy and total lipid deposits area was quantified in zebrafish caudal vein. Fluorescent images of at least 6 larvae were quantified. The results are shown as mean±SEM; **, $p < 0.01$; ***, $p < 0.001$.

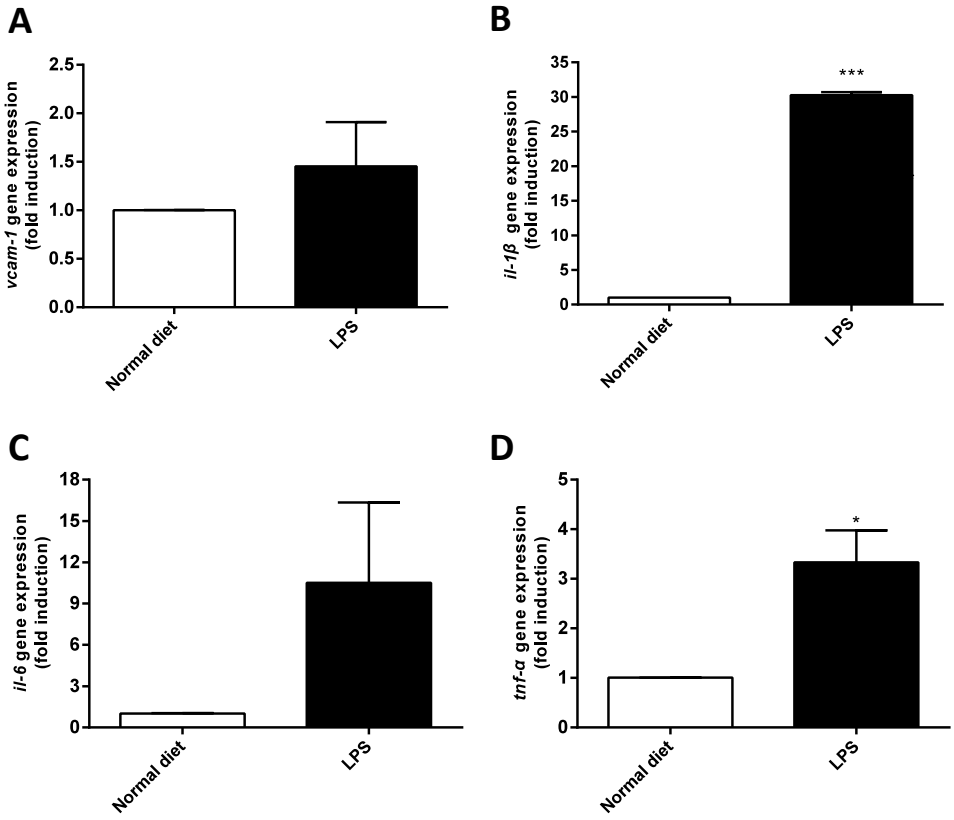

Supplementary Figure 6.2 | LPS induces an increase in proinflammatory cytokines and adhesion molecules gene expression.

A-D Quantitative q-PCR of zebrafish gene expression of V-CAM1 **(A)**, IL-1β **(B)**, IL-6 **(C)** and TNF-α **(D)** after 18 h of LPS incubation in embryonic medium. The experiments were performed in triplicate (n = 20-30 zebrafish larvae per group) and the results are shown as mean±SEM; *, $p < 0.05$; ***, $p < 0.001$.

07 CONCLUSION AND FUTURE WORK

At the time of this study, there are no analytical techniques that can efficiently predict the existence of atheroma unstable plaques. With this work, we have contributed to the identification of a family of lipids that can predict the amount of atheromata and/or the existence of unstable plaques. Indeed, we observed an increased level of ChE in the plasma of patients with an ASCVD. ChE are the most table oxidized products derived from the previously detected oxo-CE in ''core-aldehydes''. Oxo-CE are present in atherosclerotic lesions and are resistant to hydrolysis upon internalization by macrophages (Hoppe, Ravandi, Herrera, Kuksis, & Hoff, 1997; Kobayashi et al., 2001). With lesional development, the increase in the oxidizing environment, or via the action of intracellular aldehyde oxidizing systems, they will become completely oxidized to ChE of the corresponding bi-acids. Then, being amphiphilic molecules, they may be expected to partition between the lipid environment in which they are formed, cell membranes, the (intra- and extracellular) aqueous phase, translocate readily across cellular membranes and into serum components. Thus, the detection of ChE in human plasma in our clinical study can potentially indicate an increased oxidative environment, characteristic of advanced atheroma plaques. The observed correlation between increased ChE in human plasma and the prevalence of ASCVD becomes stronger when we demonstrated, through different *in vitro* and *in vivo* approaches, the robust atherogenic features of these lipids. By exposing macrophages to a single lipid of the ChE family or by providing a ChE-enriched diet to zebrafish larvae, we were able to induce: i) lipid accumulation in lipidotic foam cells and in the vasculature of zebrafish larvae; ii) macrophage malfunction, with reduced efferocytic and decreased lysosomal degradative capacity; iii) inflammation, by increasing the inflammatory markers in monocytes and macrophages, as well as an increase in inflammatory cell recruitment to the vasculature of zebrafish larvae and an increase in proinflammatory gene expression.

The first evidence of the atherogenic properties of ChE were obtained through the study of macrophages loaded with ChS, which it is a natural product of CE oxidation but was only detected in human plasma as a minor fraction of total ChE. Through acute exposure to ChS, we observed an irreversible macrophage lipidosis with a consequent induced cell death (Estronca et al., 2012). The results in Chapter 3 had provided further clues regarding the proatherogenic properties of ChS. In RAW 264.7 macrophages at sub-toxic conditions, long-term incubation with ChS induced lysosomal dysfunction, with a decrease in lysosomal degradative capacity. In primary BMDM, ChS induced an increase in pro-inflammatory cytokine (IL-1β, IL-6, TNF-α) release. Additionally, in zebrafish larvae on a ChS-enriched diet, the number of myeloid cells infiltrating the vasculature was significantly higher than in the animals fed with the control diets. Thus, before the identification of the most abundant ChE in human plasma- ChA, we already had solid data affirming the biological importance of ChE on atherosclerosis. As expected, several cellular and *in vivo* effects were shared by both ChE. However, some important differences were observed, namely: i) ChA induced LDL aggregation, making it necessary to alter the delivery vehicle; ii) *in vitro*, ChA was less toxic then ChS, however in *in vivo* system the opposite effect was verified; iii) ChS induces irreversible lipid accumulation in RAW cells yet with ChA, we only observed irreversibility

using BMDM primary cells; finally, iv) the effects induced by ChA on cellular trafficking were more pronounced. Some of these effects can be explained by the small chemical difference between these two lipids, demonstrating the complexity of atherogenic lipid milieu. However, to better understand some of the above-mentioned differences, the identification and quantification of the accumulated lipid species in ChA-loaded macrophages will be crucial. With this quantitative lipidomic analysis, we will be able to evaluate the macrophage degradative capacity on ChA metabolism.

Circulating and the lesional early recruited monocytes are one of the first immune cells to be stimulated by ChE. Studies in bone marrow transplantation models in atherosclerosis-prone mice indicate that an "inflammatory" ($LY6C^{high}$) monocyte subset is readily recruited into the arterial intimal layer (Rahman, Murphy, & Woollard, 2017; Swirski et al., 2006). Thus, we evaluated the phenotypical changes induced in these cells upon ChA treatment. Human monocytes loaded with low doses of ChA revealed different phenotypical alterations in monocyte surface receptors. The levels of HLA-DR were reduced in ChA-treated monocytes compared with surface expression in control monocytes. Decreased expression of HLA-DR on monocytes has been correlated with altered immune status in patients with a systemic inflammatory response syndrome (SIRS) (Kim et al., 2010) and with adverse prognosis on different pathologies (Berry et al., 2011; Gadd et al., 2016; Hershman, Cheadle, Wellhausen, Davidson, & Polk, 1990; Sachse, Prigge, Cramer, Pallua, & Henkel, 1999). ChA-loaded monocytes also showed a decreased level of the monocyte scavenger receptor CD163 and increased mannose receptor CD206, both markers of alternative activated monocytes (Etzerodt & Moestrup, 2013; Weinberg et al., 2016). Furthermore, the cytokine profile of ChA-loaded monocytes revealed an increase in IL-1β, IL-6 and IL-10. Based on these findings, we concluded that these monocyte alterations characterize a unique ChA-induced monocyte activated phenotype with an increased capacity for IL-1β release and ROS production. These inflammatory outcomes are likely to be correlated and contribute to the development of an inflammatory status that can trigger and perpetuate atheroma development. To further investigate the observed monocyte phenotype, we will in future evaluate the phagocytic capacity of monocytes after lipid treatment. Another important future experiment is to define the monocyte subset resulting from ChA-treatment. By exposing human monocytes $CD14^{low/high}$ or peripheral blood mononuclear cells (PBMC) to ChA, we will be able to evaluate the different subset population of the stimulated monocytes in terms of CD14 and CD16 expression.

The consequences of activated monocytes in the context of atherosclerosis are poorly understood. However, we can predict that these activated cells can enhance the inflammatory environment in arterial intima, stimulating neighbouring cells – SMCs, DC, neutrophils and EC, to secrete inflammatory and chemotactic molecules that can contribute to lesional inflammatory development. In addition, monocytes can develop an activated macrophage phenotype depending on the microenvironment stimulus. The effect of different ox-LDL and Ox-Lp on monocyte differentiation into macrophages was already performed (Hayden et al., 2002; Seo, Yang, Yoo, & Choi, 2015). The published data demonstrated that the inflammatory

status of the resulting macrophage is dependent on the lipid species and the oxidation stage of each molecule. Here, we investigated the effect of ChA on monocyte differentiation into macrophages. Human monocytes differentiated in the presence of ChA revealed a profile of surface markers different from controls, with an increase in HLA-DR and CD206 levels, and increased cytokine production: IL-1β, IL-6 and IL-10. This unique inflammatory phenotype was also verified in differentiated murine macrophages. ChA-loaded BMDM also presented increased pro- and anti-inflammatory cytokines, and an increase in antioxidant gene expression. Although our lipid-loaded macrophage phenotype did not fit with any of the described macrophage phenotypes, we observed some similarities with M2b macrophages, that also express IL-1β, IL-6, TNF-α and IL-10, although the observed surface markers profile of this subtype is different (Anderson, Gerber, & Mosser, 2002; Ohlsson et al., 2014). On the other hand, a similarity is seen with M2a, as the profile in surface markers is similar with ChA-induced macrophages, but in this case the two subsets present distinctly different cytokine profiles (Ohlsson et al., 2014; Roszer, 2015). Finally, ChA-loaded macrophages resemble Mox and Mhem phenotypes, due to the expression of Hmox-1 gene (Chinetti-Gbaguidi, Colin, & Staels, 2014; Kadl et al., 2010; Naito, Takagi, & Higashimura, 2014). The M1 and M2 macrophage phenotypes described in the literature are extremes of an inflammatory spectrum. However, in an *in vivo* system, a broad spectrum of different and rapidly evolving macrophage phenotypes is expected to exist. Thus, considering the obtained results and the macrophage phenotypes described in the literature, we can conclude that ChA induced a novel intermediate inflammatory macrophage phenotype.

TLRs are key players in the pathogenesis of inflammatory conditions including CVD. TLR4 is highly expressed in lipid-rich and atherosclerotic plaques and in *tlr4*$^{-/-}$ mice, atherosclerosis-associated inflammation is diminished (den Dekker, Cheng, Pasterkamp, & Duckers, 2010; Lee, Scanga, Bachelder, Chen, & Snapper, 2007). Several reports have demonstrated that TLR4 present a crucial role on Ox-Lp internalization and signaling cascades, the latter in an NF-κB dependent manner (S. H. Choi et al., 2009, 2013; S. H. Choi, Sviridov, & Miller, 2017; Fang et al., 2010; Stewart et al., 2010). In ChA-loaded *tlr4*$^{-/-}$ macrophages, the depletion of this receptor did not inhibit foam cell formation (data not shown), suggesting an alternative internalization pathway. However, we observed that ChA induced an inflammatory response dependent on TLR4 signaling. Furthermore, the activation of TLR4 by ChA primes macrophages to increase the expression of NLRP3 inflammasome components, including IL-1β and can also be responsible for the increase in TNF-α, as well as the expression and release of other cytokines, (Hoareau et al., 2010; Lin, Kong, Wu, Yang, & Ji, 2015; Miller et al., 2005). This latter effect still needs to be confirmed in ChA-loaded macrophages, by measuring the other cytokine expressed and released in *tlr4*$^{-/-}$ macrophages. Interestingly, besides the direct priming of macrophages by ChA, we also have shown a potential role for neutrophils in macrophage priming in zebrafish larvae fed with a ChA-enriched diet (Chapter 6).

Metabolic shifts in response to macrophage activation have been intensively studied in the last few years (Kelly & O'Neill, 2015; O'Neill, Kishton, & Rathmell, 2016; O'Neill & Pearce,

2016; Van den Bossche, O'Neill, & Menon, 2017). An inflammatory stimulus induces a specific immune response accompanied by a unique metabolic shift that will supply the energetic demands necessary for the cellular response (Van den Bossche et al., 2017). LPS-stimulated TLR4 induces a glycolytic metabolic shift (Kelly & O'Neill, 2015) and a truncated TCA cycle, impairing mitochondrial respiration. In addition, TLR4 activation by LPS was shown to induce macrophage proliferation (Wang, Zhu, Huang, Li, & Zhu, 2013). A cellular increase in proliferative capacity is also associated with aerobic glycolysis (Feron, 2009; Hsu & Sabatini, 2008). Taking these findings into account and the observed TLR4 requirement for IL-1β release (Chapter 4), we investigated the role of this receptor in the metabolic shift and the proliferative capacity of ChA-loaded macrophages. Indeed, we observed that glucose and glutamine consumption and mitochondrial respiration in ChA-loaded cells were dependent on TLR4. These results suggested a metabolic reprogramming of macrophages upon ChA inflammatory stimulation. However, the proliferative capacity of macrophages was independent of this receptor, and consequently, independent of the metabolic reprogramming and inflammatory stimulus. Besides TLR4, we already evaluated several possible molecular targets that could be involved in the increased proliferative capacity of ChA-loaded macrophages: Nrf-2, TNF-α, ROS, HIF-1α and myelocytomatosis viral oncogen (Myc) (data not shown), all of them involved in cell proliferation (Arana et al., 2012; H. K. Choi, Kim, Jhon, & Lee, 2011; L. Liu et al., 2016; Murakami & Motohashi, 2015; Parameswaran & Patial, 2010). Unfortunately, we were not yet able to dissect the molecular mechanism behind macrophage proliferation in the presence of ChA. Considering previously published data, PKCδ can be a potential future candidate for having a role in ChA-induced macrophage proliferation. Macrophage proliferation in ox-LDL-loaded macrophages has been associated with the activation of PKCδ. Deletion of PKCδ specifically in myeloid cells in *Apoe*$^{-/-}$ mice accelerated atherosclerosis and splenomegaly by inducing proliferation and decreasing apoptosis of macrophages in the arterial wall and in the spleen (Li et al., 2017). Thus, PKCδ is a possible target to investigate, however we are planning to perform RNAseq to understand and correlate all the phenotypes observed in ChA-treated macrophages.

As mentioned before, each macrophage phenotype presents an imprinted metabolism. In ChA-loaded macrophages some pieces are still missing to establish the exact metabolic prolife, however, our findings already suggest a novel metabolic pathway. We observed an increase in glucose consumption and an increase in lactate production, without an increase in the glycolytic rate. In addition, hyperpolarization of mitochondria in ChA-treated macrophages was also shown and it is in agreement with data from LPS-stimulated macrophages (Mills et al., 2016). However, glycolytic LPS-loaded cells present a decrease in OXPHOS, whereas in ChA-loaded macrophages we observed an increase. As discussed before, at equilibrium, ChA will be incorporated into all cellular membranes, not only in lysosomes, as we demonstrated in this work, but also in mitochondrial membranes. The physico-chemical alteration of membranes can lead to the proton leak observed in mitochondria from ChA-loaded macrophages. Macrophages then increase the mitochondrial respiration to compensate for this loss in protons, inducing an excessive increase in mitochondrial potential and an increase in basal respiration and ATP

production. Furthermore, we hypothesized that the TCA cycle in ChA-loaded cells is impaired. A broken TCA cycle can then stimulate glutamine oxidation to overcome the missing metabolites and proceed with the cycle. Thus, glutaminolysis can be a key metabolic pathway behind the immune metabolic reprogramming induced by ChA. Now, it is crucial to evaluate mitochondrial respiration blocking glutaminolysis as well as lactate production and subsequently analyze the cytokine secretion in these macrophages. With this set of experiments we will be able to dissect how ChA shapes macrophage metabolism to modulate the immune cell response. This experience will be crucial in lipid-loaded macrophages since little is known about the interplay between metabolic reprogramming and immunity in this context.

In this work, we provide several lines of evidence that characterize atherosclerosis as a lysosomal storage disease. In lysosomal storage diseases, intracellular trafficking events were reported (Ballabio & Gieselmann, 2009). In sulfatide storing kidney cells, both endocytosis of the mannose-6-phosphate receptor and the transferrin receptor were enhanced in these cells, due to an increase in the endosomal receptor pool. However, despite this increase in the endocytic capacity, their recycling rate was reduced (Klein et al., 2009). These data are in accordance with a general increase in the endocytic capacity of ChA-treated macrophages and the observed delay in endosome recycling and sorting (Chapter 3 and 5). Furthermore, pH neutralization of endocytic vesicles, by inhibition of V-H^+ATPase with bafilomycin A, slowed the recycling of the transferrin-receptor to PM, affected the sorting to TGN and delayed the cargo delivery to lysosomes (Clague, Urbé, Aniento, & Gruenberg, 1994; Johnson, Dunn, Pytowski, & McGraw, 1993; Presley, Mayor, McGraw, Dunn, & Maxfield, 1997; Sillence, 2013). Thus, the trafficking delay in the investigated endocytic pathways in ChA-loaded macrophages (transferrin recycling, lactosylceramide sorting and the delivery of endocytosed cargo to lysosomes) can be a consequence of the observed pH increase of the endocytic vesicles. Furthermore, in lysosomal lipid storage diseases and in atherosclerosis, lysosomal dysfunction associated with the increase in lysosomal pH has been also reported (Emanuel et al., 2014; Jerome, Cox, Griffin, & Ullery, 2008; Platt, Boland, & van der Spoel, 2012; Puri et al., 1999). Through the removal of excess cholesterol in lysosomal membranes from lipid-laden macrophages, normal lysosomal function and trafficking was reestablished (Cox, Griffin, Ullery, & Jerome, 2007; Puri et al., 1999). However, in the context of atherosclerosis little is known regarding the effect of atherogenic lipids on the molecular mechanism underlying trafficking defects. Thus, our study advances the knowledge of cellular trafficking in this field, showing the affected endocytic pathways and the molecular targets involved in lipidotic macrophages malfunction.

In addition to lysosomal role in the degradation and recycling processes of cells, lysosomes are also involved in a secretory pathway. Lysosomal exocytosis is classified as an “unconventional secretion” pathway, which also includes the fusion of multi-vesicular bodies (MVBs) (exosome release), autophagosomes, autolysosomes, and early endosomes to the plasma membrane (Nickel & Rabouille, 2009; Samie & Xu, 2014). Furthermore, exocytosis of secretory lysosomes (lysosome-related organelles) has been implicated in several physiological

processes such as cellular migration, immune cell response and PM repair (Andrews, 2002; Bossi & Griffiths, 2005; Y. Liu, Zhou, & Zhu, 2012; Reddy, Caler, & Andrews, 2001). These lysosomes are generally found in cells that are derived from the haematopoietic lineage, as in macrophages (Blott & Griffiths, 2002). The role of secretory lysosomes in macrophages is still poorly understood, and the role of these lysosomes in the context of atherosclerosis awaits elucidation. IL-1β secretion has been correlated with lysosome secretion and secretory autophagy (Andrei et al., 2004; Murray & Stow, 2014). Pro-caspase-1 and pro-IL-1β were shown to be targeted in part to specialized secretory lysosomes and their externalization of the mature forms were accompanied by lysosomal proteins (Andrei et al., 2004). Secretory autophagy may also contribute transiently to the acute release of IL-1β in activated macrophages, via a pathway that is mediated by Atg5, the inflammasome, the Golgi reassembly stacking protein 55 (GRASP55) and Rab8a (Dupont et al., 2011). Thus in ChA-loaded macrophages, to further study the increase in the exocytic lysosomes pool, we will assess the origin of these organelles by co-immunostaining of the mentioned markers and LAMP-proteins. Moreover, the secretion of peripheral lysosomes will also increase the secretion of undigested cellular components. In turn, the increase in extracellular toxic compounds can increase the inflammatory status of macrophages and the lesion environment. Thus, in the near future, we will also investigate the effect of exocytosis inhibition on the inflammatory process, by evaluating its effect on cytokines release upon ChA macrophage stimulation.

Here in this study, we identified several potential molecular targets that can be related to the increase in the secretory pool of lysosomes induced by macrophage ChA-loading: Rab7, Rab3a, Arl8 and even TFEB. Since the increase in lysosomal secretion in immune cells is associated with an increase in the inflammatory condition (Marks, Heijnen, & Raposo, 2013; Murray & Stow, 2014), the correlation of these two events on lipid-loaded macrophages will be an important discovery and advance our understanding of the cellular mechanisms operating during atherosclerosis. In LPS-stimulated BMDM the depletion of Rab8a reduced the autophagic secretion, but not the synthesis of IL-1β (Dupont et al., 2011). Thus, in the next step, we aim to genetically manipulate the mentioned targets and measure cytokine release and lysosomal exocytosis upon ChA macrophage treatment. With this experiment, we will be able to understand how atherogenic lipids reprogram macrophage trafficking in response to the inflammatory stimulus. Finally, facing the obtained results, our ultimate goal is to apply the main findings on zebrafish animal model. Can we reduce the ChA-induced inflammatory effect on zebrafish by reducing the secretory capacity of macrophages? Answering this question will certainly originate new strategies for the development of therapeutic approaches in atherosclerosis diseases.

In conclusion, the presented work provided important tools for the early diagnostic of unstable atheroma plaques, together with new insights into the molecular and cellular etiology of atherosclerosis disease, as well as a pre-clinical model for the study of atherosclerosis diseases.

7.2 REFERENCES

Anderson, C. F., Gerber, J. S., & Mosser, D. M. (2002). Modulating macrophage function with IgG immune complexes. Journal of Endotoxin Research, 8(6), 477–481. https://doi.org/10.1179/096805102125001118

Andrei, C., Margiocco, P., Poggi, A., Lotti, L. V, Torrisi, M. R., & Rubartelli, A. (2004). Phospholipases C and A2 control lysosome-mediated IL-1 beta secretion: Implications for inflammatory processes. Proceedings of the National Academy of Sciences of the United States of America, 101(26), 9745–50. https://doi.org/10.1073/pnas.0308558101

Andrews, N. W. (2002). Lysosomes and the plasma membrane: Trypanosomes reveal a secret relationship. Journal of Cell Biology. https://doi.org/10.1083/jcb.200205110

Arana, L., Gangoiti, P., Ouro, A., Rivera, I.-G., Ordoñez, M., Trueba, M., … Gomez-Muñoz, A. (2012). Generation of reactive oxygen species (ROS) is a key factor for stimulation of macrophage proliferation by ceramide 1-phosphate. Experimental Cell Research, 318(4), 350–60. https://doi.org/10.1016/j.yexcr.2011.11.013

Ballabio, A., & Gieselmann, V. (2009). Lysosomal disorders: From storage to cellular damage. Biochimica et Biophysica Acta - Molecular Cell Research. https://doi.org/10.1016/j.bbamcr.2008.12.001

Berry, P. A., Antoniades, C. G., Carey, I., McPhail, M. J. W., Hussain, M. J., Davies, E. T., … Vergani, D. (2011). Severity of the compensatory anti-inflammatory response determined by monocyte HLA-DR expression may assist outcome prediction in cirrhosis. Intensive Care Medicine, 37(3), 453–460. https://doi.org/10.1007/s00134-010-2099-7

Blott, E. J., & Griffiths, G. M. (2002). Secretory lysosomes. Nat Rev Mol Cell Biol, 3(2), 122–131. https://doi.org/10.1038/nrm732

Bossi, G., & Griffiths, G. M. (2005). CTL secretory lysosomes: Biogenesis and secretion of a harmful organelle. Seminars in Immunology. https://doi.org/10.1016/j.smim.2004.09.007

Chinetti-Gbaguidi, G., Colin, S., & Staels, B. (2014). Macrophage subsets in atherosclerosis. Nature Reviews Cardiology, 12(1), 10–17. https://doi.org/10.1038/nrcardio.2014.173

Choi, H. K., Kim, T. H., Jhon, G. J., & Lee, S. Y. (2011). Reactive oxygen species regulate M-CSF-induced monocyte/macrophage proliferation through SHP1 oxidation. Cellular Signaling, 23(10), 1633–1639. https://doi.org/10.1016/j.cellsig.2011.05.017

Choi, S. H., Harkewicz, R., Lee, J. H., Boullier, A., Almazan, F., Li, A. C., … Miller, Y. I. (2009). Lipoprotein accumulation in macrophages via toll-like receptor-4-dependent fluid phase uptake. Circulation Research, 104(12), 1355–1363. https://doi.org/10.1161/CIRCRESAHA.108.192880

Choi, S. H., Sviridov, D., & Miller, Y. I. (2017). Oxidized cholesteryl esters and inflammation. Biochimica et Biophysica Acta - Molecular and Cell Biology of Lipids, 1862(4), 393–397. https://doi.org/10.1016/j.bbalip.2016.06.020

Choi, S. H., Yin, H., Ravandi, A., Armando, A., Dumlao, D., Kim, J., … Miller, Y. I. (2013). Polyoxygenated cholesterol ester hydroperoxide activates TLR4 and SYK dependent signaling in macrophages. PLoS ONE, 8(12). https://doi.org/10.1371/journal.pone.0083145

Clague, M. J., Urbé, S., Aniento, F., & Gruenberg, J. (1994). Vacuolar ATPase activity is required for endosomal carrier vesicle formation. Journal of Biological Chemistry, 269(1), 21–24.

Cox, B. E., Griffin, E. E., Ullery, J. C., & Jerome, W. G. (2007). Effects of cellular cholesterol loading on macrophage foam cell lysosome acidification. Journal of Lipid Research, 48(5), 1012–21. https://doi.org/10.1194/jlr.M600390-JLR200

den Dekker, W. K., Cheng, C., Pasterkamp, G., & Duckers, H. J. (2010). Toll like receptor 4 in atherosclerosis and plaque destabilization. Atherosclerosis. https://doi.org/10.1016/j.atherosclerosis.2009.09.075

Dupont, N., Jiang, S., Pilli, M., Ornatowski, W., Bhattacharya, D., & Deretic, V. (2011). Autophagy-based unconventional secretory pathway for extracellular delivery of IL-1β. The EMBO Journal, 30(23), 4701–4711. https://doi.org/10.1038/emboj.2011.398

Emanuel, R., Sergin, I., Bhattacharya, S., Turner, J. N., Epelman, S., Settembre, C., … Razani, B. (2014). Induction of lysosomal biogenesis in atherosclerotic macrophages can rescue lipid-induced lysosomal dysfunction and downstream sequelae. Arteriosclerosis, Thrombosis, and Vascular Biology, 34(9), 1942–1952. https://doi.org/10.1161/ATVBAHA.114.303342

Estronca, L. M. B. B., Silva, J. C. P., Sampaio, J. L., Shevchenko, A., Verkade, P., Vaz, A. D. N., … Vieira, O. V. (2012). Molecular etiology of atherogenesis--in vitro induction of lipidosis in macrophages with a new LDL model. PloS One, 7(4), e34822. https://doi.org/10.1371/journal.pone.0034822

Etzerodt, A., & Moestrup, S. K. (2013). CD163 and Inflammation: Biological, Diagnostic, and Therapeutic Aspects. Antioxidants & Redox Signaling, 18(17), 2352–2363. https://doi.org/10.1089/ars.2012.4834

Fang, L., Harkewicz, R., Hartvigsen, K., Wiesner, P., Choi, S. H., Almazan, F., … Miller, Y. I. (2010). Oxidized cholesteryl esters and phospholipids in zebrafish larvae fed a high cholesterol diet: Macrophage binding and activation. Journal of Biological Chemistry, 285(42), 32343–32351. https://doi.org/10.1074/jbc.M110.137257

Feron, O. (2009). Pyruvate into lactate and back: From the Warburg effect to symbiotic energy fuel exchange in cancer cells. Radiotherapy and Oncology. https://doi.org/10.1016/j.radonc.2009.06.025

Gadd, V. L., Patel, P. J., Jose, S., Horsfall, L., Powell, E. E., & Irvine, K. M. (2016). Altered peripheral blood monocyte phenotype

and function in chronic liver disease: Implications for hepatic recruitment and systemic inflammation. PLoS ONE, 11(6). https://doi.org/10.1371/journal.pone.0157771

Hayden, J. M., Brachova, L., Higgins, K., Obermiller, L., Sevanian, A., Khandrika, S., & Reaven, P. D. (2002). Induction of monocyte differentiation and foam cell formation in vitro by 7-ketocholesterol. Journal of Lipid Research, 43(1), 26–35. Retrieved from http://www.ncbi.nlm.nih.gov/pubmed/11792719

Hershman, M. J., Cheadle, W. G., Wellhausen, S. R., Davidson, P. F., & Polk, H. C. (1990). Monocyte HLA-DR antigen expression characterizes clinical outcome in the trauma patient. British Journal of Surgery. https://doi.org/10.1002/bjs.1800770225

Hoareau, L., Bencharif, K., Rondeau, P., Murumalla, R., Ravanan, P., Tallet, F., … Festy, F. (2010). Signaling pathways involved in LPS induced TNFalpha production in human adipocytes. Journal of Inflammation (London, England), 7, 1. https://doi.org/10.1186/1476-9255-7-1

Hoppe, G., Ravandi, a, Herrera, D., Kuksis, a, & Hoff, H. F. (1997). Oxidation products of cholesteryl linoleate are resistant to hydrolysis in macrophages, form complexes with proteins, and are present in human atherosclerotic lesions. Journal of Lipid Research, 38(7), 1347–1360.

Hsu, P. P., & Sabatini, D. M. (2008). Cancer cell metabolism: Warburg and beyond. Cell, 134(5), 703–707. https://doi.org/10.1016/j.cell.2008.08.021

Jerome, W. G., Cox, B. E., Griffin, E. E., & Ullery, J. C. (2008). Lysosomal cholesterol accumulation inhibits subsequent hydrolysis of lipoprotein cholesteryl ester. Microscopy and Microanalysis : The Official Journal of Microscopy Society of America, Microbeam Analysis Society, Microscopical Society of Canada, 14(2), 138–49. https://doi.org/10.1017/S1431927608080069

Johnson, L. S., Dunn, K. W., Pytowski, B., & McGraw, T. E. (1993). Endosome acidification and receptor trafficking: bafilomycin A1 slows receptor externalization by a mechanism involving the receptor's internalization motif. Molecular Biology of the Cell, 4(12), 1251–66. https://doi.org/10.1091/mbc.4.12.1251

Kadl, A., Meher, A. K., Sharma, P. R., Lee, M. Y., Doran, A. C., Johnstone, S. R., … Leitinger, N. (2010). Identification of a novel macrophage phenotype that develops in response to atherogenic phospholipids via Nrf2. Circulation Research, 107(6), 737–746. https://doi.org/10.1161/CIRCRESAHA.109.215715

Kelly, B., & O'Neill, L. A. (2015). Metabolic reprogramming in macrophages and dendritic cells in innate immunity. Cell Research, 25(7), 771–784. https://doi.org/10.1038/cr.2015.68

Kim, O. Y., Monsel, A., Bertrand, M., Coriat, P., Cavaillon, J.-M., & Adib-Conquy, M. (2010). Differential down-regulation of HLA-DR on monocyte subpopulations during systemic inflammation. Critical Care (London, England), 14(2), R61. https://doi.org/10.1186/cc8959

Klein, D., Yaghootfam, A., Matzner, U., Koch, B., Braulke, T., & Gieselmann, V. (2009). Mannose 6-phosphate receptor-dependent endocytosis of lysosomal enzymes is increased in sulfatide-storing kidney cells. Biological Chemistry, 390(1), 41–48. https://doi.org/10.1515/BC.2009.009

Kobayashi, K., Matsuura, E., Liu, Q., Furukawa, J., Kaihara, K., Inagaki, J., … Koike, T. (2001). A specific ligand for beta(2)-glycoprotein I mediates autoantibody-dependent uptake of oxidized low density lipoprotein by macrophages. Journal of Lipid Research, 42(5), 697–709. Retrieved from http://www.ncbi.nlm.nih.gov/pubmed/11352976

Lee, K. S., Scanga, C. A., Bachelder, E. M., Chen, Q., & Snapper, C. M. (2007). TLR2 synergizes with both TLR4 and TLR9 for induction of the MyD88-dependent splenic cytokine and chemokine response to Streptococcus pneumoniae. Cellular Immunology, 245(2), 103–110. https://doi.org/10.1016/j.cellimm.2007.04.003

Li, Q., Park, K., Xia, Y., Matsumoto, M., Qi, W., Fu, J., … King, G. L. (2017). Regulation of Macrophage Apoptosis and Atherosclerosis by Lipid-Induced PKCδ Isoform Activation. Circulation Research, 121(10), 1153–1167. https://doi.org/10.1161/CIRCRESAHA.117.311606

Lin, X., Kong, J., Wu, Q., Yang, Y., & Ji, P. (2015). Effect of TLR4/MyD88 signaling pathway on expression of IL-1 ?? and TNF- ?? in synovial fibroblasts from temporomandibular joint exposed to lipopolysaccharide. Mediators of Inflammation, 2015. https://doi.org/10.1155/2015/329405

Liu, L., Lu, Y., Martinez, J., Bi, Y., Lian, G., Wang, T., … Wang, R. (2016). Proinflammatory signal suppresses proliferation and shifts macrophage metabolism from Myc-dependent to HIF1 α -dependent. Proceedings of the National Academy of Sciences, 113(6), 1564–1569. https://doi.org/10.1073/pnas.1518000113

Liu, Y., Zhou, Y., & Zhu, K. (2012). Inhibition of Glioma Cell Lysosome Exocytosis Inhibits Glioma Invasion. PLoS ONE, 7(9). https://doi.org/10.1371/journal.pone.0045910

Marks, M. S., Heijnen, H. F. G., & Raposo, G. (2013). Lysosome-related organelles: Unusual compartments become mainstream. Current Opinion in Cell Biology. https://doi.org/10.1016/j.ceb.2013.04.008

Miller, Y. I., Viriyakosol, S., Worrall, D. S., Boullier, A., Butler, S., & Witztum, J. L. (2005). Toll-like receptor 4-dependent and -independent cytokine secretion induced by minimally oxidized low-density lipoprotein in macrophages. Arteriosclerosis, Thrombosis, and Vascular Biology, 25(6), 1213–1219. https://doi.org/10.1161/01.ATV.0000159891.73193.31

Mills, E. L., Kelly, B., Logan, A., Costa, A. S. H., Varma, M., Bryant, C. E., … O'Neill, L. A. (2016). Succinate Dehydrogenase Supports Metabolic Repurposing of Mitochondria to Drive Inflammatory Macrophages. Cell, 167(2), 457–470.e13. https://doi.org/10.1016/j.cell.2016.08.064

Murakami, S., & Motohashi, H. (2015). Roles of Nrf2 in cell proliferation and differentiation. Free Radical Biology and Medicine, 88(Part B), 168–178. https://doi.org/10.1016/j.freeradbiomed.2015.06.030

Murray, R. Z., & Stow, J. L. (2014). Cytokine secretion in macrophages: SNAREs, Rabs, and membrane trafficking. Frontiers in

Immunology. https://doi.org/10.3389/fimmu.2014.00538

Naito, Y., Takagi, T., & Higashimura, Y. (2014). Heme oxygenase-1 and anti-inflammatory M2 macrophages. Archives of Biochemistry and Biophysics. https://doi.org/10.1016/j.abb.2014.09.005

Nickel, W., & Rabouille, C. (2009). Mechanisms of regulated unconventional protein secretion. Nature Reviews Molecular Cell Biology, 10(2), 148–155. https://doi.org/10.1038/nrm2617

O'Neill, L. A. J., Kishton, R. J., & Rathmell, J. (2016). A guide to immunometabolism for immunologists. Nature Reviews Immunology. https://doi.org/10.1038/nri.2016.70

O'Neill, L. A. J., & Pearce, E. J. (2016). Immunometabolism governs dendritic cell and macrophage function. The Journal of Experimental Medicine, 213(1), 15–23. https://doi.org/10.1084/jem.20151570

Ohlsson, S. M., Linge, C. P., Gullstrand, B., Lood, C., Johansson, Å., Ohlsson, S., … Hellmark, T. (2014). Serum from patients with systemic vasculitis induces alternatively activated macrophage M2c polarization. Clinical Immunology, 152(1–2), 10–19. https://doi.org/10.1016/j.clim.2014.02.016

Parameswaran, N., & Patial, S. (2010). Tumor necrosis factor-α signaling in macrophages. Critical Reviews in Eukaryotic Gene Expression, 20(2), 87–103. https://doi.org/10.1016/j.bbi.2008.05.010

Platt, F. M., Boland, B., & van der Spoel, A. C. (2012). Lysosomal storage disorders: The cellular impact of lysosomal dysfunction. Journal of Cell Biology, 199(5), 723–734. https://doi.org/10.1083/jcb.201208152

Presley, J. F., Mayor, S., McGraw, T. E., Dunn, K. W., & Maxfield, F. R. (1997). Bafilomycin A1 treatment retards transferrin receptor recycling more than bulk membrane recycling. Journal of Biological Chemistry, 272(21), 13929–13936. https://doi.org/10.1074/jbc.272.21.13929

Puri, V., Watanabe, R., Dominguez, M., Sun, X., Wheatley, C. L., Marks, D. L., & Pagano, R. E. (1999). Cholesterol modulates membrane traffic along the endocytic pathway in sphingolipid-storage diseases. Nature Cell Biology, 1(6), 386–388. https://doi.org/10.1038/14084

Rahman, M. S., Murphy, A. J., & Woollard, K. J. (2017). Effects of dyslipidaemia on monocyte production and function in cardiovascular disease. Nature Reviews Cardiology. https://doi.org/10.1038/nrcardio.2017.34

Reddy, A., Caler, E. V., & Andrews, N. W. (2001). Plasma membrane repair is mediated by Ca2+-regulated exocytosis of lysosomes. Cell, 106(2), 157–169. https://doi.org/10.1016/S0092-8674(01)00421-4

Roszer, T. (2015). Understanding the mysterious M2 macrophage through activation markers and effector mechanisms. Mediators of Inflammation. https://doi.org/10.1155/2015/816460

Sachse, C., Prigge, M., Cramer, G., Pallua, N., & Henkel, E. (1999). Association between reduced human leukocyte antigen (HLA)-DR expression on blood monocytes and increased plasma level of interleukin-10 in patients with severe burns. Clinical Chemistry and Laboratory Medicine : CCLM / FESCC, 37(3), 193–8. https://doi.org/10.1515/CCLM.1999.036

Samie, M. A., & Xu, H. (2014). Lysosomal exocytosis and lipid storage disorders. Journal of Lipid Research, 55(6), 995–1009. https://doi.org/10.1194/jlr.R046896

Seo, J. W., Yang, E. J., Yoo, K. H., & Choi, I. H. (2015). Macrophage differentiation from monocytes is influenced by the lipid oxidation degree of low density lipoprotein. Mediators of Inflammation, 2015. https://doi.org/10.1155/2015/235797

Sillence, D. J. (2013). Glucosylceramide modulates endolysosomal pH in Gaucher disease. Molecular Genetics and Metabolism, 109(2), 194–200. https://doi.org/10.1016/j.ymgme.2013.03.015

Stewart, C. R., Stuart, L. M., Wilkinson, K., van Gils, J. M., Deng, J., Halle, A., … Moore, K. J. (2010). CD36 ligands promote sterile inflammation through assembly of a Toll-like receptor 4 and 6 heterodimer. Nature Immunology, 11(2), 155–161. https://doi.org/10.1038/ni.1836

Swirski, F. K., Pittet, M. J., Kircher, M. F., Aikawa, E., Jaffer, F. A., Libby, P., & Weissleder, R. (2006). Monocyte accumulation in mouse atherogenesis is progressive and proportional to extent of disease. Proceedings of the National Academy of Sciences of the United States of America, 103(27), 10340–5. https://doi.org/10.1073/pnas.0604260103

Van den Bossche, J., O'Neill, L. A., & Menon, D. (2017). Macrophage Immunometabolism: Where Are We (Going)? Trends in Immunology. https://doi.org/10.1016/j.it.2017.03.001

Wang, L., Zhu, R., Huang, Z., Li, H., & Zhu, H. (2013). Lipopolysaccharide-induced toll-like receptor 4 signaling in cancer cells promotes cell survival and proliferation in hepatocellular carcinoma. Digestive Diseases and Sciences, 58(8), 2223–2236. https://doi.org/10.1007/s10620-013-2745-3

Weinberg, J. B., Volkheimer, A. D., Rubach, M. P., Florence, S. M., Mukemba, J. P., Kalingonji, A. R., … Mwaikambo, E. D. (2016). Monocyte polarization in children with falciparum malaria: Relationship to nitric oxide insufficiency and disease severity. Scientific Reports, 6. https://doi.org/10.1038/srep29151